

Durham E-Theses

Edge emission and exciton recombination in cadmium sulphide

D. S. Orr

How to cite:

Orr, D. S. (1970) Edge emission and exciton recombination in cadmium sulphide. Doctoral thesis, Durham University.

Use policy

The full-text may be used and/or reproduced, and given to third parties in any format or medium, without prior permission or charge, for personal research or study, educational, or not-for-profit purposes provided that:

- a full bibliographic reference is made to the original source
- a <https://etheses.durham.ac.uk/id/eprint/8867/> is made to the metadata record in Durham E-Theses
- the full-text is not changed in any way

The full-text must not be sold in any format or medium without the formal permission of the copyright holders.

Please consult the [full Durham E-Theses policy](#) for further details.

EDGE EMISSION AND EXCITON RECOMBINATION

IN CADMIUM SULPHIDE.

by

D. S. Orr, B.Sc..

Presented in candidature for the degree of

Doctor of Philosophy

of the University of Durham.



ACKNOWLEDGEMENTS

The author wishes to thank the Ministry of Defence (Naval Department) for financial support during the course of this research and Professor D.A. Wright for permitting the use of his laboratory facilities. He is indebted to Dr. J. Woods for his excellent supervision and guidance. He would also like to thank the other members of the group for their stimulating interest and discussions, the members of the departmental workshop for their work in the construction and adaptation of the apparatus, and Miss Carole Gyll, Miss Delia Pettit and his wife for their assistance in the final preparation of the thesis.

ABSTRACT

The Stokes (U.V.) and anti-Stokes (A.S.) photo-excited emissions of large, doped and undoped CdS single crystals, grown under controlled partial pressures of cadmium and sulphur, at liquid helium temperatures were examined to establish a correlation between the crystal growth conditions and the spectral distribution of the green edge and exciton emissions. Anti-Stokes excitation spectra were also obtained.

Two longitudinal optical phonon assisted series constituted the green emission. The "high energy series" (H.E.S.) was attributed to the recombination of free electrons with holes bound to acceptors some 0.17eV above the valence band, the "low energy series" (L.E.S.) to a distant-pair recombination process involving electrons bound to donors some 0.03eV below the conduction band and holes bound to the same acceptor. The mean separation between the donors and acceptors was about 100 Å. Only the L.E.S. was observed in A.S. excited green emission.

The I_1 and I_2 bound excitons which dominated the blue emissions are associated with exciton recombination at neutral acceptors and neutral donors respectively. I_2^* emission, associated with excitons bound to neutral donors losing some of their recombination energy in raising the donor electron to an excited state of the donor, was observed and used to evaluate a donor ionisation energy of 0.026eV. Blue emission was excited by A.S. radiation in several crystals and ascribed tentatively to I_2^* emission.

A model is developed to explain the variation of the emission characteristics with crystal growth conditions. A cadmium vacancy-donor impurity complex is suggested as the acceptor involved in the green and I_1 exciton emissions, with the hole in an excited state of

the complex, and as the centre through which the two-step A.S. excitation process proceeds. Sulphur vacancy-acceptor impurity complexes and donor impurities are suggested to explain the donors associated with the L.E.S. and I_2 emissions.

CONTENTS

	<u>Page</u>
Chapter 1. Properties of cadmium sulphide	1.
Chapter 2. Recombination processes responsible for the "Band Edge Emission" of CdS	19.
Chapter 3. Emission spectroscopy : experimental apparatus and procedure	42.
Chapter 4. Stokes excited edge emission of undoped cadmium sulphide	55.
Chapter 5. Anti-Stokes excited edge emission of undoped cadmium sulphide	81.
Chapter 6. Edge emission of doped cadmium sulphide crystals	95.
Chapter 7. Anti-Stokes excitation spectroscopy	109.
Chapter 8. Conclusion and discussion	117.

CHAPTER 1

PROPERTIES OF CADMIUM SULPHIDE

1.1 Introduction

Cadmium sulphide is a II-VI compound which normally crystallises in the wurtzite structure. The lattice of wurtzite crystals consists of two interpenetrating hexagonally packed lattices, one containing the anions (S^{--}), and the other the cations (Cd^{++}). The interatomic distance between the cadmium ion and its four tetrahedrally arranged nearest sulphur neighbour ions is 2.52 Å. The lattice parameters are $a=4.1368$ Å and $c=6.7163$ Å(1). CdS is also found in the cubic, zincblende phase, but it is not so common (2).

The investigation of the exciton spectra of CdS by Thomas and Hopfield (3, 4) established that the extrema of the principal band edges were at the same point, $k=0$, in the Brillouin zone. The generally accepted values for the forbidden energy gap at temperatures of 300°K (room), 77°K (liquid nitrogen) and 4.2°K (liquid helium) are 2.43, 2.52 and 2.582 eV respectively (3, 5).

In its intrinsic form, pure stoichiometric cadmium sulphide is an insulator at room temperature, with resistivities greater than 10^{10} ohm. cm. However, native lattice defects and foreign impurity atoms greatly affect the electrical and optical properties of the material. The forms that these imperfections take, and their influence on some of the properties, is discussed below ^{and is} followed by an account of the evaluation of the band structure. This is followed by a summary of the principal properties and applications of CdS.

1.2 Imperfections in CdS

The introduction of Group VII; halogen impurities (with the exception of fluorine which tends to form complexes with other chemical

impurities ^{or} native defects) into high resistivity n-type CdS produces low resistivity n-type material (6). Shallow donor levels some 0.03eV below the conduction band are formed when these impurities substitute for sulphur atoms. Group IIIb (In, Ga, Al) impurities substitute for cadmium atoms producing similar donor levels which are generally accompanied by compensating acceptor levels (7). Shallow donor levels may be found in CdS due to a deficiency of sulphur, which results either in the formation of cadmium interstitials or sulphur vacancies. Group Ib, (Cu, Ag, Au) and group Vb impurities form acceptor levels about one electron volt above the valence band (8). Cadmium vacancies will produce similar levels. The concentration of donors is generally greater than that of acceptors, and since the holes cannot be thermally ionised from these deep acceptors at room temperatures, p-type CdS cannot be produced. Woods and Champion (9) demonstrated p-type conduction in highly copper doped CdS, however this was probably due to conduction in an impurity band.

The effect of imperfections on the optical and electronic properties of CdS may be summarised as follows.

- (1) Levels within the band gap may provide alternative radiative recombination paths and centres for free electrons and holes, other than free exciton recombination. The resulting "edge emission" and "infra-red emission" of CdS will be discussed in Chapter two and section 1.5.1.
- (2) Optical absorption attributable to donor-acceptor-associates is introduced (10), and will be discussed in Section 1.5.1.
- (3) Since cadmium sulphide is generally n-type, donors will increase and acceptors decrease the dark conductivity.
- (4) Free carriers which have been created by photons with less than band gap energy via imperfection levels lead to the photoconductive

response being extended to the long wavelength side of the absorption edge. Alternatively, the electrons and holes may recombine producing "Anti-Stokes" luminescence, which will be discussed in Chapter two.

(5) The imperfections which act as recombination centres reduce the photoconductive efficiency, whereas those centres that have a large cross section for capture of photo-excited holes but a small one for the capture of electrons after capturing the holes, may increase the sensitivity by increasing the free electron lifetime.

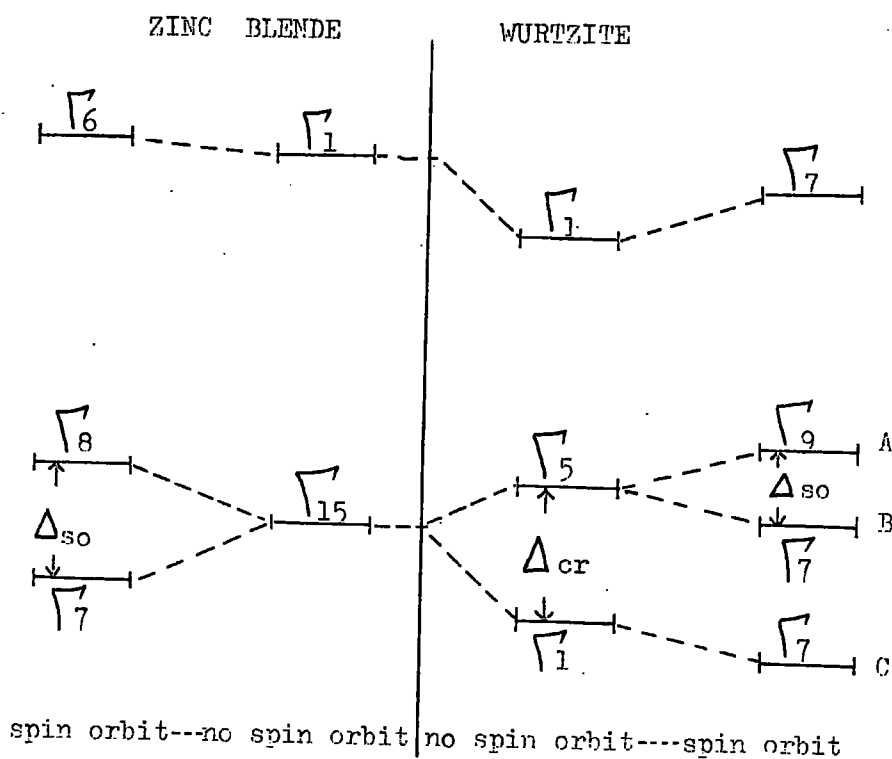
(6) Imperfections may trap free carriers for a time before they can be thermally freed. Thus they effectively reduce the carrier mobility, and the speed of response of the photoconductivity is reduced.

1.3 Band Structure of CdS

The conduction band of cadmium sulphide may be considered to originate from the 5s atomic levels of the cadmium ions and the valence band from the 3p atomic levels of the sulphur ions. Utilising the similarities of the crystallographic lattices and the iso-electronic nature of many of the materials, Herman (11) developed a semi-empirical method of deducing the band structure of zinc-blende materials from those of the diamond type materials, germanium and silicon. Birman (12) noticed that in a direction parallel to the c-axis, the electronic states of the wurtzite lattice may be considered equivalent to the zinc-blende states in the (111) direction, provided that a small hexagonal crystal field perturbation is taken into account.

Figure 1.1 illustrates the extrema of the three doubly degenerate valence bands (A, B and C) and the conduction band of the wurtzite structure at $k=0$. The diagram illustrates the combined effects of "spin orbit" (so) and "crystal field" (cr) perturbations on the simplest zinc-blende case (13). The selection rules (14) governing the allowed

Figure 1.1. The band structure and selection rules for the zinc blende and wurtzite structures at $\underline{k} = 0$;



Selection Rules.

Zinc blende ; No polarisation.

Wurtzite (no spin orbit) ; $\underline{E} // \underline{c}$ $\Gamma_1 - \Gamma_1$

$\underline{E} \perp \underline{c}$ $\Gamma_5 - \Gamma_1$

Wurtzite (spin orbit) ; $\underline{E} // \underline{c}$ $\Gamma_7 - \Gamma_7$

$\underline{E} \perp \underline{c}$ $\Gamma_7 - \Gamma_7$

$\Gamma_2 - \Gamma_7$

transitions between the various symmetry representations are shown for the electric vector of the photon parallel and perpendicular to the c-axis of the wurtzite crystal.

Experimental evidence supporting this model was provided by Thomas and Hopfield (3). Three exciton series were observed in reflection measurements on CdS which could be associated with electrons in the conduction band and with holes in the three valence bands, according to the selection rules arising from the symmetry requirements. The group theory calculations performed by Balkanski and Des Cloiseaux (15) produced a band structure model which supported Birman's symmetry representation.

High resolution transmission spectra of selected CdS single crystals obtained by Thomas and Hopfield (16) showed deviations from the exciton binding energies, reduced masses and band gaps predicted by the "spherical hydrogenic" model. The deviation of the wurtzite lattice from cubic symmetry results in an alteration of the constant energy surfaces of the valence and conduction bands from the spherical shape effected in the cubic case. Possible toroidal (17) and ellipsoidal (18, 12, 13) energy surfaces and multi-valley band structures (15) have been suggested by various authors. All three, and or intermediate cases are possible in principle in the same crystal within different temperature ranges. In all experimental work, the valence bands are assumed to have their extrema at $\underline{k}=0$, since this is the simplest case and does not invalidate the results. The problem is then to establish the shape of the conduction band.

Dutton (19), and Thomas et al (20) explained their measurements of the absorption of CdS single crystals in terms of direct exciton plus phonon processes rather than via indirect absorption, although Balkanski

and Des Cloiseaux (21) reported indirect absorption spectra in support of their many valley model (15). Hopfield and Thomas (4), however, showed that this interpretation was incorrect, and provided further support for their single ellipsoidal model using magneto-optical measurements of the exciton spectrum. Zook and Dexter (22) interpreted their measurements of the magneto resistivity tensors of CdS in terms of a single valley model at temperatures above 77°K, with the possibility of a toroidal system below 77°K in which the extrema lie close to $\underline{k}=0$. They also emphasised the difficulties of interpreting such results because of crystal inhomogeneity and contact effects, and suggested that Masumi's (23) results may have been similarly affected. Masumi had supported the many valley model.

The single valley model for the conduction band is strongly supported by electron effective mass (m_e^*) measurements. Piper and Halsted (24) measured the temperature dependence of the Hall constant and Hall mobility of semi-conducting n-type CdS. Interpreting their results in terms of a simple hydrogen-like model for the donor level, they obtained an effective mass for an electron of $0.19m_e$, where m_e is the free electron mass. Piper and Marple (25) measured the contribution of free electrons to the infra-red absorption of CdS, obtaining an average value of the electron effective mass of $(0.22 \pm 0.01)m_e$. The electron effective mass was measured parallel ($m_e^{*//}$) and perpendicular ($m_e^{*\perp}$) to the c-axis in one crystal at room temperature. The ratio $\frac{m_e^{*\perp}}{m_e^{*//}} = 1.08 \pm 0.04$ gave a measure of the anisotropy of the conduction band which agrees with that observed by Thomas and Hopfield (4) from their measurements of the magneto-optical splitting of the exciton emission. Thomas and Hopfield found $m_e^{*c} = (0.204 \pm 0.010)m_e$ to be isotropic to within 5%. The effective masses of the holes in the valence band parallel ($m_h^{*//}$) and perpendicular ($m_h^{*\perp}$) to the c-axis were found to be

$(5.0 \pm 0.5) m_e$ and $(0.7 \pm 0.1) m_e$ respectively.

The 5% anisotropy in the electron effective mass was confirmed by Baer and Dexter (26) and Sawamoto (27) in cyclotron resonance measurements performed at microwave frequencies. The piezoelectric-phonon interaction (28) was used to account for the 15% reduction in the electron effective mass as measured by cyclotron resonance compared with previous measurements. Baer and Dexter observed only one resonance absorption at each orientation, which they attributed to electrons, and which is consistent with the single ellipsoidal model. The electron effective masses determined at 4.2°K, with the crystal c-axis parallel and perpendicular to the magnetic field were $(0.171 \pm 0.003) m_e$ and $(0.162 \pm 0.003) m_e$ respectively. Sawamoto did not measure the angular dependence, but confirmed the value of $0.17 m_e$ for cyclotron electron mass as well as observing another resonance absorption, which he attributed to holes. His value of $0.81 m_e$ is in agreement with the value for m_h^* obtained by Thomas and Hopfield (4).

The single valley model for the conduction band of CdS, with anisotropy of the order of a few percent, is generally accepted. Thus a simple single valley model is a good approximation. The values for the separation of the A and B, and the B and C valence bands are 0.016 and 0.057 eV respectively, at 4.2°K and $k=0$, as determined by Thomas and Hopfield (3).

1.4 Electrical Properties

1.4.1 Introduction

At any fixed temperature above absolute zero, the electrical conductivity of a material is determined by the number of charge carriers available for conduction, and their mobility. The temperature dependence of the mobility over a given temperature range gives an indication of the carrier scattering mechanisms operating within the

material over that range. The principal scattering mechanisms affecting the carrier mobility are briefly described below, followed by an account of the effect of the absorption of radiation upon the conductivity. A description of the acoustoelectric effect and of electron spin resonance studies in cadmium sulphide completes the section.

1.4.2 Mobility

Table 1.1 summarises the temperature dependence of mobility for the principal scattering mechanisms which may operate within a material.

(1) Lattice scattering. Charge carriers travelling through a crystal at a temperature above absolute zero have their mobility reduced by interactions with the thermal vibrations of the lattice. The lattice can vibrate in both acoustic and optical modes. In covalent elemental semiconductors, such as germanium and silicon, acoustic mode lattice scattering is the dominant mechanism, becoming increasingly important as the temperature increases. Optical mode lattice scattering is the principal mechanism in ionic crystals. The movement of the different constituent atoms of a compound semiconductor causes dipoles in the crystal that can interact with the carriers, resulting in polar mode lattice scattering. Lattice vibrations in piezoelectric materials give rise to electric fields which result in the piezoelectric scattering of carriers.

(2) Impurity scattering. Neutral impurities can give rise to scattering effects in crystals, however the theory is uncertain and indicates only a slight temperature dependence. Charged impurities can produce large scattering effects. The density of impurities determines the importance of the process compared with other competing mechanisms. The temperature dependence of impurity scattering, see Table 1.1,

Table 1.1. The temperature dependence of mobility for the principal carrier scattering mechanisms in a crystal.

Scattering Mechanism	Dependence of mobility on T and m^*	Reference
Lattice : optical mode	$(T^{-1/2}) (\exp (\theta/T) - 1)$ θ is the equivalent temperature of the optical phonons.	38
: acoustic mode	$(T^{-3/2}) (m^{*5/2})$	37
: polar mode	$(\exp T) (m^{*3/2})$	39
: piezoelectric mode	$(T^{-1/2}) (m^{*3/2})$	32
Impurity : neutral	Uncertain slight temperature dependence	40
: charged	$(T^{3/2}) (m^{*1/2})$	41
Dislocation : charged	Linear temperature dependence	30

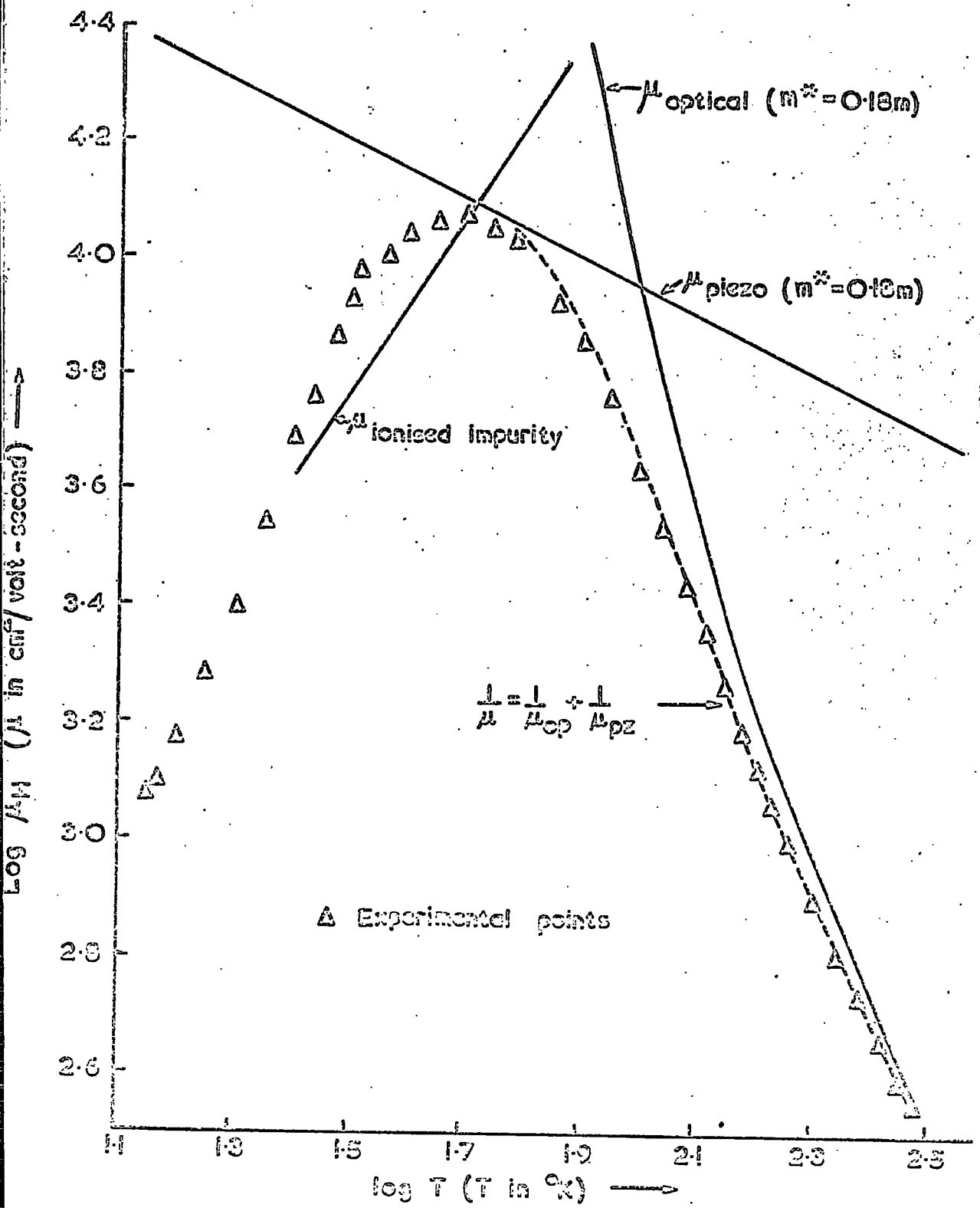
indicates how this process becomes particularly important at lower temperatures, when lattice scattering decreases.

(3) Carrier-carrier scattering. When the effective mass of holes is larger than that of electrons, electron - hole collisions can reduce the electron mobility showing a similar dependence to charged impurity scattering. Electron - electron scattering is more complicated and particularly in the case of cadmium sulphide, can generally be neglected. However at very high current densities, carrier - carrier scattering can become important.

(4) Dislocation scattering. For dislocation densities greater than 10^9 cm^{-2} , the effect on mobility should theoretically become apparent (29). The temperature dependence of mobility for charged dislocation scattering was found to be linear by Read (30).

The temperature variation of the Hall mobility of cadmium sulphide had been attributed to optical and acoustic mode lattice scattering by Kröger et al (7), and optical plus impurity scattering by Miyazawa et al (31) before Hutson (32) pointed out the importance of piezoelectric mode scattering. Piper and Halstead (24), Zook (33), and Fujita et al. (34) found progressively better agreement between experimental and theoretical mobility versus temperature curves when optical and piezoelectrical mode scattering only were considered, using Hutson's ^{improved} ~~improving~~ values of the piezoelectrical constants. The apparent absence of impurity scattering is probably due to the neutralisation of the compensated acceptors by the trapped holes. Figure 1.2 shows the temperature dependence of the Hall mobility in n-type CdS, illustrating the onset of ionised impurity scattering (35).

Spear and Mort (36) measured the drift mobility of electrons and holes in CdS using short pulses of electron beam excitation to create



G. 1-2. The temperature dependence of the Hall mobility in n-type CdS.

free carriers. The electron mobility varied from sample to sample, being of the order of $300 \text{ cm}^2 \text{ V}^{-1} \text{ sec.}^{-1}$, in agreement with other room temperature values. The hole mobility was found to be between 10 and $18 \text{ cm}^2 \text{ V}^{-1} \text{ sec.}^{-1}$.

1.4.3 Photoconductivity

The absorption of radiation by a photoconductor creates free electrons and or holes which contribute to the electrical conductivity of the material until they are trapped or recombine. Photons with an energy greater than the band gap energy of the crystal create equal numbers of free electrons and holes. Lower energy photons may liberate electrons or holes from centres lying within the band gap of the material, extending the spectral response of the photoconductivity to longer wavelengths. In pure, perfect CdS, the electron and hole lifetimes of photoexcited carriers are short, of the order of microseconds. By the introduction of suitable imperfections, the crystal may be made more "photosensitive", and the electron lifetime increased to milliseconds while the hole lifetime is decreased to nanoseconds.

The centres that give rise to high photosensitivity are compensated acceptors, produced by impurities such as copper, or cadmium vacancies resulting in levels some 1.1 eV above the valence band. These centres are known as "Class II centres", following the nomenclature of Rose (42), with an effective negative charge in thermal equilibrium. Their capture cross-section for free holes is some 10^4 to 10^6 times greater than their subsequent capture cross-section for a free electron. In "pure" insensitive material, recombination centres known as "Class I centres" are present. These produce a small majority carrier lifetime, since they have an approximately equal capture cross-section for electrons as for holes. ("Class III centres" are defined as having larger capture cross-sections for electrons than holes).

The centres described so far have been introduced as recombination centres. The Class II centres may, under certain conditions of illumination and temperature, be regarded as hole "traps". A centre acts as a trap when there is a greater probability that the carrier, associated with the centre, be thermally excited back to its respective band. The centre acts as a recombination centre when it is more probable that a carrier of the opposite sign recombines with the first carrier at that centre. The term "demarcation level" has been introduced by Rose, its significance is that when it coincides with the energy level of a centre, there is an equal probability of the centre acting as a trap or a recombination centre. Thus in Figure 1.3(a), the hole demarcation level (H.D.L.), which is always in the lower half of the band gap, is below the Class I centres, so that they act as recombination centres. In Figure 1.3(b), Class II centres have been introduced, but the H.D.L. is above them, so they act only as hole traps, and do not sensitise the material. In Figure 1.3(c), the H.D.L. is below the Class II centres which now act as sensitising recombination centres. As the H.D.L. slowly passes through the level corresponding to the Class II centres as the light intensity is increased or the temperature decreased, the photo-current-intensity relation become superlinear. This effect is used to determine the depth of the Class II centres. Figure 1.3(d) illustrates how the simultaneous irradiation of CdS with infra-red and the pumping excitation may be used to quench the photoconductivity. Holes are liberated from the Class II centre by the infra-red (1), and travel via the valence band (2) recombining with electrons at the Class I centres (3 and 4). At 300°K, infra-red quenching of the photoconductivity of CdS is effected in two spectral bands with maxima at wavelengths of 0.92 and 1.45 microns. The 1.45 micron band is not present at 77°K. To explain these results, two

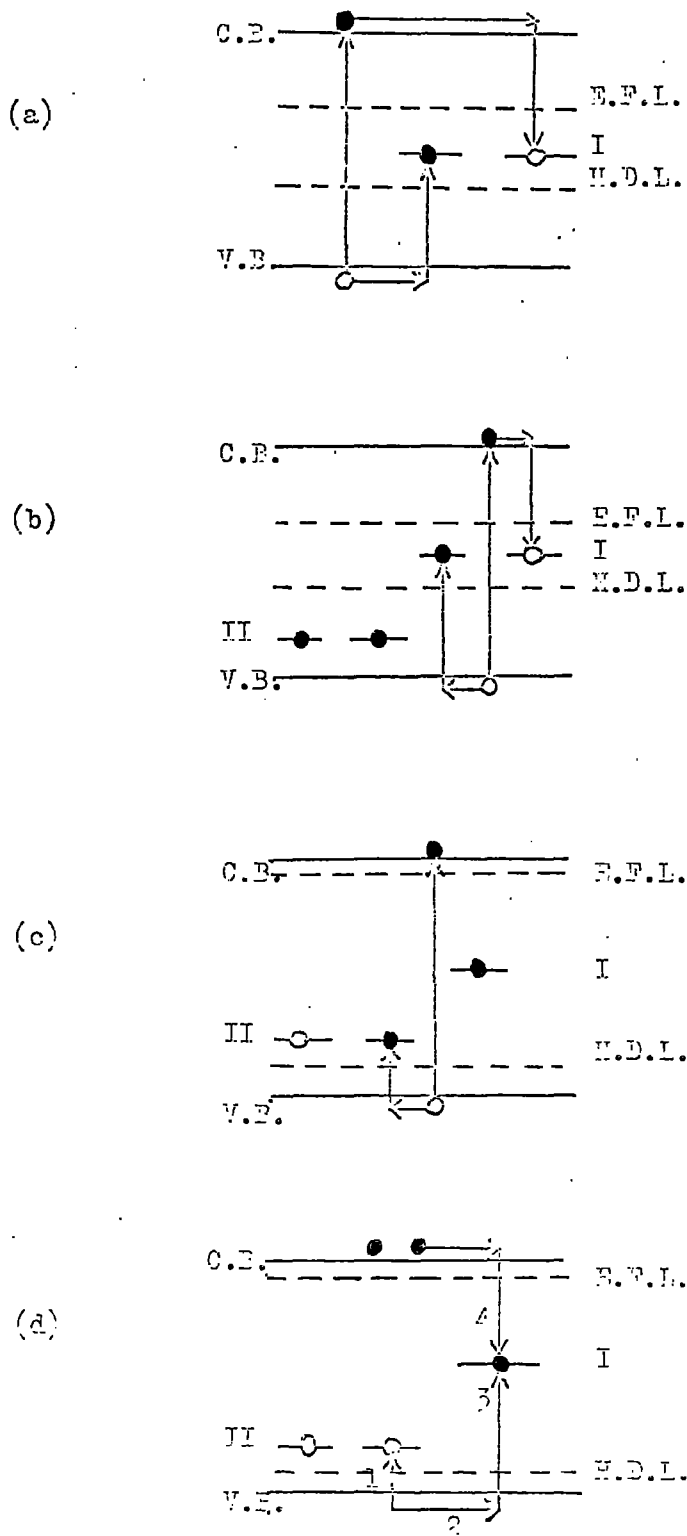


Figure 1.3. Imperfection sensitisation of photoconductivity by class I and II centres.

E.F.L. - electron Fermi level.

H.D.L. - hole demarcation level.

● electrons ○ holes.

levels some 1.1 and 0.2 eV above the valence band are suggested (5).

The number of electron traps is usually much greater than that of sensitising centres. It is generally accepted that there are at least six prominent traps in CdS crystals (43, 44). The density, and possibly the existence of some of these traps shows a strong dependence upon the preparative conditions of the crystal, its physical history and photochemical reactions as described by Woods and Nicholas (45). The technique of thermally stimulated conductivity (TSC) is used to evaluate the energy depths, capture cross sections, and densities of the traps. (The method consists essentially of observing the changes in the conductivity while the traps are being emptied by raising the temperature at a linear rate). A single discrete set of traps gives rise to a maximum in the TSC. The trap density can then be determined from the area under that portion of the TSC curve (48). The following is a list of the six electron trapping levels most commonly reported for CdS. The depth is the energy of the level below the conduction band in electron volts; (a) 0.05, (b) 0.15, (c) 0.25, (d) 0.41, (e) 0.63 and (f) 0.83. Woods and Nicholas assigned the a and b levels to isolated sulphur vacancies, the c level to a complex association of sulphur vacancies, the d and f levels to a complex association of sulphur and cadmium vacancies in nearest neighbour sites and the e levels to a complex of associated cadmium vacancies. Cowell and Woods (46) have shown that one 0.63 eV trap may be created photochemically from two 0.85 eV traps, and suggest that the centre responsible for the 0.63 eV trap is an association of two cadmium vacancies, while the 0.85 eV trap is an association of a cadmium and sulphur vacancy, confirming the assignments of Woods and Nicholas.

Photoexcitation may also lead to a change in the mobility of the

carriers as a result of change in the number or the charge of the scattering centres, or the onset of two carrier conductivity. The change in the charge of scattering centres by the addition or removal of electrons or holes causes a change in mobility which may be used to evaluate the effective charge, the energy depth and the scattering cross-section of the imperfection centre. Bube and Macdonald (49) have given a detailed account of the evaluation of the properties of CdS using such "photoHall" data. Onuki and Hase (50) measured the a.c. photoHall effect in CdS under d.c. illumination as a function of wavelength. They interpreted the mobility decrease for excitation wavelengths below 0.53 microns in terms of two carrier effects. Assuming an electron mobility of $225 \text{ cm}^2 \text{ V}^{-1} \text{ sec}^{-1}$, they calculated the hole mobility to be $38 \text{ cm}^2 \text{ V}^{-1} \text{ sec}^{-1}$, a value comparable to those obtained by Spear and Mort (36) in their drift mobility experiments.

Park and Reynolds (51) observed maxima in the spectral response of the photoconductivity, using ^{polarized} ~~polarized~~ light, of CdS at 4.2 and 77°K. The maxima corresponded to the maxima observed in the absorption coefficient. This indicates that the initial absorption of photons with the exciton energy leads to the formation of intrinsic excitons, associated with transitions involving the A, B, and C valence bands of CdS. The excitons then dissociate into current carriers, and contribute to the photoconductivity so that maxima appear in the spectral response of the photoconductivity. The dissociation may occur either by interaction with an impurity centre or by absorption or emission of phonons. The energies corresponding to those of an exciton plus multiple longitudinal optical phonon energies give rise to minima, which have been observed by Park and Langer (51), in the spectral response at high energies.

1.4.4 Acousto-electric Effect

Crystals of CdS obey Ohm's law at applied fields up to the order of

1000 $V.cm^{-1}$. Above a threshold voltage, when the electron drift velocity exceeds the phase velocity of acoustic waves (which may originate from thermal vibrations within the crystal), travelling wave amplification of the acoustic waves can take place because of the strong piezo-electric interaction in CdS. (53, 54, 55). The acoustic waves are reflected at the ends of the crystal, and the crystal may break into self-sustained oscillations if the round trip gain exceeds unity (56). The acousto-electric current associated with the amplification or oscillations subtracts from the d.c. current, as energy is transferred from the applied field to ultrasonic energy, resulting in deviations from Ohm's law. The acoustic flux causes a non-uniform electric field distribution, so that above the threshold there exists a region of high electric field near the anode in samples that have uniform low-field properties (57, 58). Brillouin scattering, involving the scattering of light by phonons, has demonstrated the involvement of acoustic domains (59).

Hutson et. al. (60) attached quartz transducers to the ends of a CdS crystal. Radio frequency pulses applied to the input transducer produced pulses of ultrasonic waves which travelled through the CdS to the output transducer. Drift fields were applied to the crystal via indium contacts. Ultrasonic gain of 38 db at 45 Mc/s was achieved for drift fields higher than a critical field of about $700 V.cm^{-1}$. At the critical field, the electron drift velocity equalled the appropriate shear wave velocity of sound. Losses occurring in the transducers were so great that there was no overall amplification of the r.f. signal. It is hoped to use evaporated films of CdS as transducers (61), which have a greater efficiency at higher frequencies than mechanically applied quartz transducers.

1.4.5 Electroluminescence

Electroluminescence of CdS single crystals under d.c. fields, using

ohmic contacts, has been known since 1952 (62). More recently, CdS MOS diodes have been used to investigate the emission (63). The diodes were of the In-CdS-SiO_x-Au configuration, with the In contact as the cathode. At 77°K, using fields of the order of 50 V.cm⁻¹, luminescence appeared close to the anode. Blue, green and infra-red components were observed. As the current density was increased, the blue component became more dominant. The blue emission has been assigned to the radiative annihilation of an exciton bound to a neutral acceptor, assisted by acoustic and optical phonons (64). The green emission has been attributed to the donor-acceptor pair recombination process. These recombination processes are described in detail in Chapter 2.

1.4.6 Electron Spin Resonance

Electron spin resonance has been employed as a technique to investigate the properties of defects in CdS. Brailsford and Woods (65) found a correlation between their "D" line and the intensity of the L.E.S. green edge emission and the I₂ bound exciton emission observed in the photoluminescence of their crystals. Both these luminescent processes are associated with shallow donor levels. They associated the D line with a sulphur vacancy centre. They suggested that the line which they denoted as "A" was associated with a cluster of four nearest-neighbour cadmium vacancies which forms an acceptor some 0.7 eV above the valence band. Centres arising from sulphur and cadmium vacancies have also been reported by Morigaki and Hoshina (66), to explain the variations observed in the ESR signal under different conditions of illumination. The electron transfer processes which they proposed may be explained, with reference to figure 1.4, as follows:

- (a) Band gap radiation excites free electrons and holes : 1
- (b) Electrons are trapped by sulphur vacancies : 3, or by electrons traps : 2.
- (c) Holes are trapped by cadmium vacancies : 6.

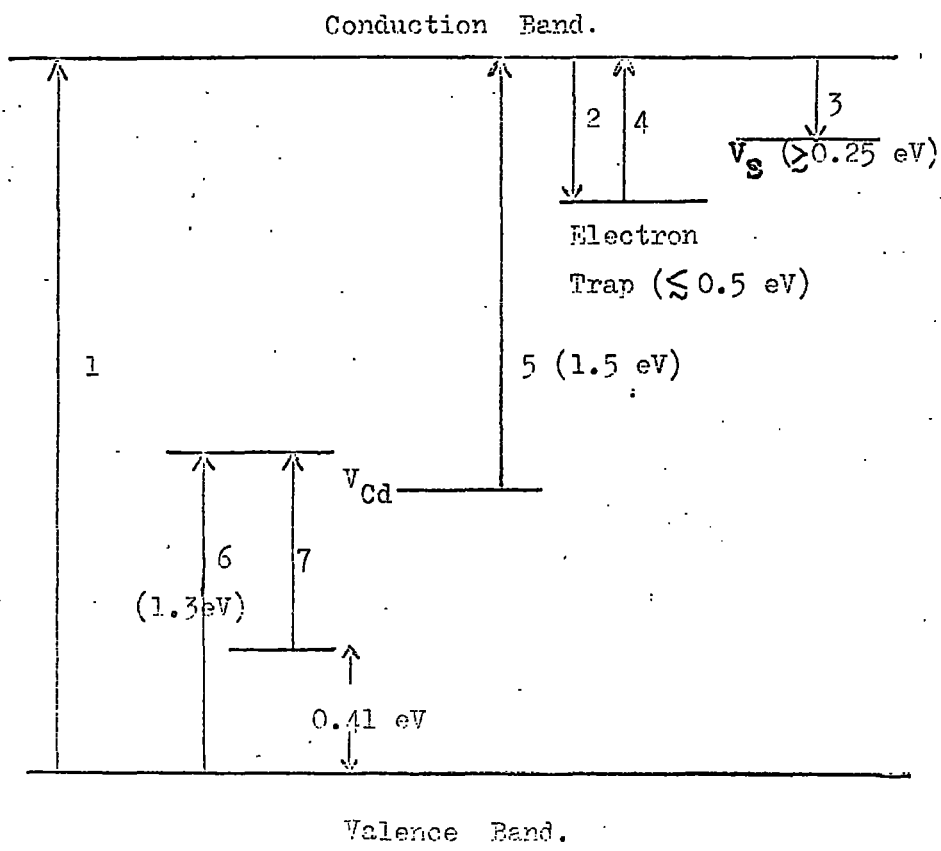


Figure 1.4. The energy level diagram and transitions proposed by Morigaki and Koshina to explain their electron spin resonance results.

- (d) Holes can be excited by 0.95 micron radiation from the cadmium vacancies to the valence band : 6, reverse of (c).
- (e) After mechanisms (a) and (d), radiation of energy greater than 1.5 eV excites electrons from cadmium vacancies into the conduction band : 5; which are subsequently trapped by sulphur vacancies : 3.
- (f) After mechanisms (a) and (c), 1.4 micron radiation can raise holes trapped in the cadmium vacancies to excited states : 7.
- (g) After mechanisms (a) and (b), electron transfer from electron traps to sulphur vacancies can occur via the conduction band. This required excitation by radiation with an energy greater than or of the order of 0.5 eV : 4 and 3.

It is normally assumed that a simple sulphur vacancy would have two trapped electrons, which would most probably result in a diamagnetic system. It is possible that the levels described result from the formation of donor-acceptor complexes. Thus the cadmium vacancy complex may be an associated of a cadmium vacancy with a singly ionisable donor on a near-neighbour site. This concept is expanded in the discussion chapter.

1.5 Optical Properties of CdS

The absorption, transmission, reflection and emission spectra of cadmium sulphide may be divided into "edge" and "infra-red" components. The characteristics of the edge emission are the subject of this thesis, and so the optical properties associated with processes near the fundamental edge are considered in greater detail in chapter two. The characteristics of the "infra-red" properties are described below.

1.5.1 Infra-red Emission and Absorption

Bryant and Cox (67) observed three luminescent emission bands with maxima at 1.6, 1.8 and 2.05 microns. They attributed the emission to the radiative recombination of an electron, from an energy level 0.7 eV above

the highest valence band (0.83 eV above the highest valence band when unoccupied), with holes in the three valence bands of CdS. Bryant and Cox (68) also observed emission bands with maxima at 0.73 to 0.78 microns and 1.06 microns. These emission bands required band gap light for their excitation, whereas the three longer wavelength bands could not be excited by band gap light, but required light in the range 0.6 to 1.05 or 1.3 to 1.65 microns. They showed that the excited state responsible for the 0.73 to 0.78 micron emission could be changed, by heat treatment under broad band illumination, into the complex centre which is at the same time the 0.73 to 0.78 and the 1.06 micron ground state and the 1.5 to 2.2 micron excited state. The proposed energy level scheme and transitions are shown in figure 1.5.

Cox et. al. (69) have explained the infra-red emission in terms of a cadmium vacancy and defect configuration containing copper atoms. It is suggested that the centre giving rise to the levels denoted X in figure 1.5 is a cadmium vacancy, and that the 0.78 and 1.06 micron emissions arise from transitions from the copper impurity centre to the levels of the cadmium vacancy. The 1.5 to 2.2 micron emission may be explained in terms of transitions within the energy levels of the vacancy or from the levels to the valence band. Cowell and Woods (46) have suggested that the centre responsible for the level denoted X in figure 1.5 is associated with a defect consisting substantially of sulphur vacancies, since the 1.06 micron emission was decreased as crystals were treated in increasing pressures of sulphur vapour.

Maxima in the absorption coefficient of CdS in the infra-red have been attributed to intrinsic defects. The energy level scheme and the maxima of corresponding transitions and their assignments suggested by Boyn (70) to explain his infra-red absorption measurements are shown in figure 1.6. The maxima denoted by E, G and H were associated, according

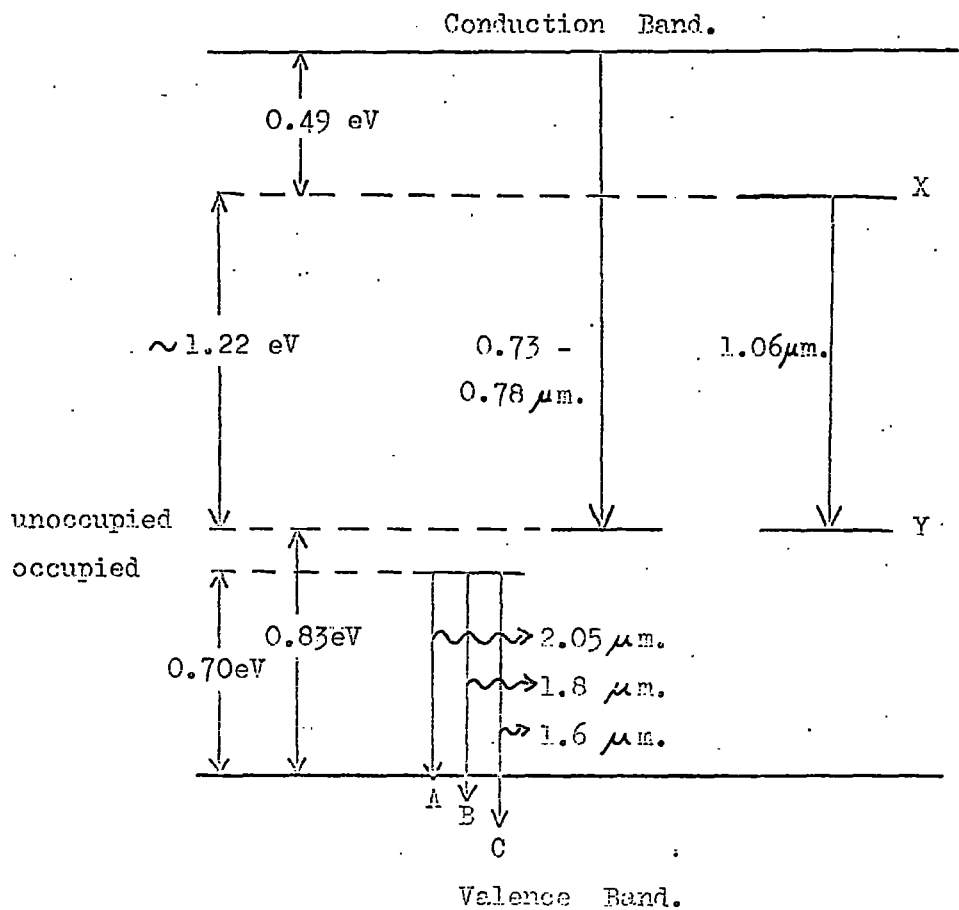
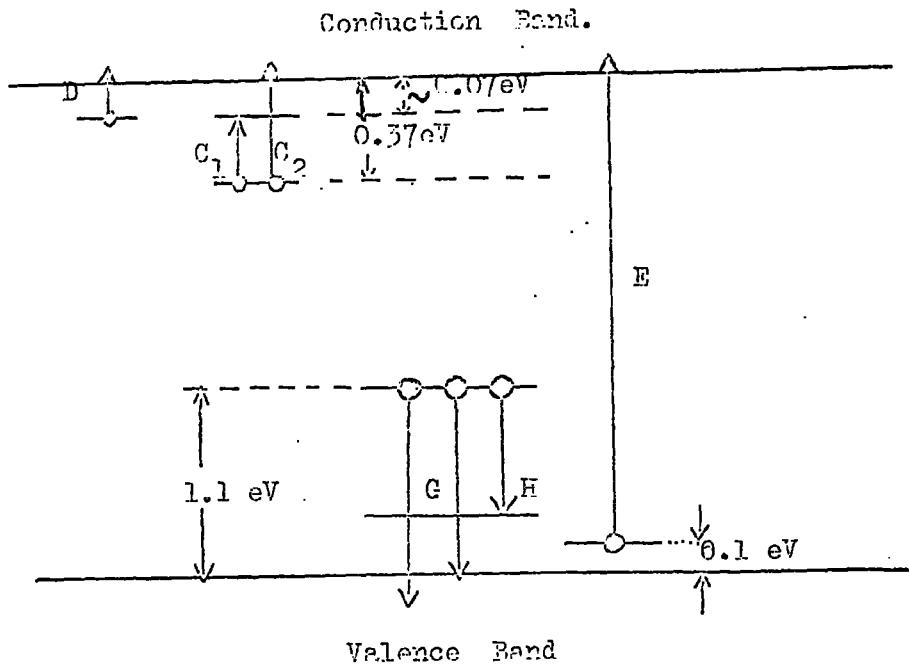


Figure 1.5. The energy level diagram and transitions proposed by Bryant and Cox to explain their infra-red emission results.



Band	Peak position (eV)	Assignment
A ₁	1.995] v _{Cd} ^D
A ₂	2.15	
B(many)	1.25 - 1.84	Cd ₁ A
C ₁	0.32] Cd ₁
C ₂	0.4	
D	< 0.15] v _{Cd}
E	≈ 2.4] v _{Cd}
G	1.53] v _{Cd}
H	0.8] v _{Cd}

Figure 1.6. The energy level scheme and the nature of the corresponding transition with their assignments suggested by Tegen to explain his infrared absorption results.

to Boyn, with the energy levels of cadmium vacancies. The energy levels above the valence band are in reasonable agreement with those associated with infra-red emission. The maxima associated with the levels C and D were attributed to cadmium interstitials. The A and B bands were associated with transitions within donor-acceptor associates. He suggested that a cadmium vacancy associated with a donor on a lattice site was responsible for the A band, in agreement with the assignment made by Goede (71) to explain the 2.0 eV emission band. Boyn suggests that the strong polarisation of the B bands indicates that the associated complex is an aggregate of cadmium interstitials with acceptors on lattice sites.

Most studies of the infra-red properties of CdS have been carried out at temperatures close to 30°K. As the temperature is decreased, the intensity of the infra-red emission is generally reduced and the edge emission becomes more intense. The infra-red processes, involving largely cadmium vacancies and donor-acceptor associates, are probably closely linked with the edge emission processes. It is hoped to explain the characteristics of the edge emission reported in this thesis in terms of transitions involving these or similar centres.

1.6 Conclusion

Many of the electrical and optical properties of CdS described in this chapter may be explained in terms of centres with approximately equal energy separation from the valence or conduction band. It is becoming generally accepted that these levels are associated in some way with intrinsic defects. Evidence of association between intrinsic defects and impurity centres is also suggested to explain certain properties.

It is necessary to study the defect centres involved in the hope that an understanding of the relationship between the observed physical properties and the defect centres will lead to improvements in the

preparation of the material and hence the possible applications of CdS. These applications involve both bulk and thin film material. Bulk material is more important in the study of the defect centres.

CH. I

REFERENCES

1. See W. L. Roth (1967) "Phys. and Chem. of II-VI Compounds" Chapter 3 (N. Holland).
2. M. Bujatti (1967) Phys. Letters, 24, 36.
3. D. G. Thomas and J. J. Hopfield (1959) Phys. Rev. 116, 573.
4. D. G. Thomas and J. J. Hopfield (1961) Phys. Rev. 122, 35.
5. D. Curie (1963) "Luminescence in Crystals" (Methuen).
6. See H. H. Woodbury (1967) "Phys. and Chem. of II-VI Compounds" Chapter 5 (N. Holland).
7. F. A. Kröger, H. J. Vink and J. Volger (1955) Phys. Res. Rep. 10, 39.
8. F. A. Kröger, H. J. Vink and J. van der Boomgaard (1954)
Z. Phys. Chem. 203, 1.
9. J. Woods and J. A. Champion (1959) J. Elect. and Control. 7, 243.
10. R. Boyn (1968) Phys. Stat. Sol. 29, 307.
11. F. Herman (1955) J. Electronics 1, 103.
12. J. L. Birman (1959) Phys. Rev. 155, 1493.
13. J. L. Birman (1959) Phys. Rev. Lett. 2, 157.
14. G. Dresselhaus (1955) Phys. Rev. 100, 580.
15. M. Balkanski & J. Des Cloiseaux (1960) J. Phys. Rad. 21, 825; 22, 41.
16. D. G. Thomas and J. J. Hopfield (1961) Phys. Rev. 124, 657.
17. R. C. Cassella (1959) Phys. Rev. 114, 1514.
R. C. Cassella (1960) Phys. Rev. Lett. 5, 371.
18. J. J. Hopfield (1960) J. Phys. Chem. Solids 15, 97.
19. D. Dutton (1958) Phys. Rev. 112, 785.
20. D. G. Thomas, J. J. Hopfield and M. Power (1960) Phys. Rev. 119, 570.
21. M. Balkanski and J. Des Cloiseaux (1960) Proc. Conf. Electronic Processes in Solids (Berlin).

CH. I

22. J. D. Zook and R. N. Dexter (1963) Phys. Rev. 129, 1980.
23. T. M. Masumi (1959) J. Phys. Soc. Japan 14, 47.
24. W. W. Piper & R. E. Halsted (1960) Proc. Int. Conf. on
Semiconductor Physics (Prague).
25. W. W. Piper & D. F. T. Marple (1961) J. Appl. Phys. 32, 2237.
26. W. S. Baer & R. N. Dexter (1964) Phys. Rev. 135, A.1388.
27. K. Sawamoto (1964) J. Phys. Soc. Japan 19, 318.
28. G. D. Mahan & J. J. Hopfield (1964) Phys. Rev. Letts. 12, 241.
29. D. H. Dexter & F. Seitz (1952) Phys. Rev. 86, 964.
30. W. T. Read (1955) Phil. Mag. 46, 111.
31. H. Miyazawa, H. Maeda & H. Tomishima (1959) J. Phys. Soc. Japan 14, 41.
32. A. R. Hutson (1958) J. Phys. Chem. Solids 8.
A. R. Hutson (1960) Phys. Rev. Letters 4, 505.
A. R. Hutson (1961) J. Appl. Phys. 32, 2287.
33. D. Zook (1964) Phys. Rev. 136, 869.
34. H. Fujita, K. Kobayashi, T. Kawai & K. Shiga (1965) J. Phys. Soc.
Japan 20, 109.
35. M. A. Subham, Ph.D. Thesis (1969) Dunelm.
36. W. E. Spear & J. Mort (1963) Proc. Phys. Soc. 81, 130.
37. J. Bardeen & W. Shockley (1950) Phys. Rev. 80, 72.
38. F. J. Morinz, J. P. Maita (1954) Phys. Rev. 94, 1525.
39. H. Ehrenreich (1957) J. Phys. Chem. Solids 2, 131.
40. N. Sclar (1956) Phys. Rev. 104, 1559.
41. H. Brooks (1955) Advan. Electron. Electron Phys. 7, 156.
42. A. Rose (1957) Prog. in Semiconductors 2, 1.
43. R. H. Bube (1964) J. Appl. Phys. 35, 586.
44. K. H. Nicholas & J. Woods (1964) Brit. J. Appl. Phys. 15, 783.
45. J. Woods & K. H. Nicholas (1964) Brit. J. Appl. Phys. 15, 1361.

CH. I

46. T. A. T. Cowell & J. Woods (1969) Brit. J. Appl. Phys.
(J. Phys. D.) 2, 2,1053.
48. See R. H. Bube (1967) "Phys. Chem. of II-VI Compounds"
Chapter 13 (North Holland).
49. R. H. Bube & H. E. Macdonald (1961) Phys. Rev. 121, 473.
50. M. Onuki & N. Hase (1965) J. Phys. Soc. Japan 20, 171.
51. Y. S. Park & D. C. Reynolds (1963) Phys. Rev. 132, 2450.
52. Y. S. Park & D. L. Langer (1964) Phys. Rev. Letters 13, 392.
53. R. W. Smith (1962) Phys. Rev. Letters 9, 87.
54. A. R. Hutson (1962) Phys. Rev. Letters 9, 296.
55. D. L. White (1962) J. Appl. Phys. 33, 2547.
56. J. H. McFee (1963) J. Appl. Phys. 34, 1548.
57. J. H. McFee & P. K. Tien (1966) J. Appl. Phys. 37, 2754.
58. H. J. Fossum & A. Rannestad (1967) J. Appl. Phys. 38, 5177.
59. A. Ishida & Y. Inuishi (1969) J. Phys. Soc. Japan 26, 957.
60. A. R. Hutson, J. H. McFee & D. L. White (1961) Phys. Rev. Letts. 7, 237.
61. N. F. Foster (1965) Proc. I.E.E.E. 53, 1400; (1967) J. Appl.
Phys. 38, 49.
62. K. W. Boer & U. Kummel (1952) Z. Phys. Chem. 200, 193.
63. J. H. Yee & G. A. Condas (1968) Sol. State Electr. 11, 419.
64. H. J. Hensch (1968) Phys. Stat. Sol. 28, 255.
65. J. R. Brailsford & J. Woods (1968) J. Phys. C. (Proc. Phys. Soc.)
2, 1213.
66. K. Morigaki & T. Hoshina (1968) J. Phys. Soc. Japan 24, 120.
67. F. J. Bryant & A. F. J. Cox (1965) Brit. J. Appl. Phys. 16, 463.
68. F. J. Bryant & A. F. J. Cox (1965) Brit. J. Appl. Phys. 16, 1065.
69. A. F. J. Cox, W. E. Hagston & C. J. Radford (1968) Phys. C.
(Proc. Phys. Soc.) 2, 1746.
70. R. Bayn (1968) Phys. Stat. Sol. 29, 307.
71. O. Goede (1968) Phys. Stat. Sol. 28, K. 167.

CHAPTER 2

RECOMBINATION PROCESSES RESPONSIBLE FOR THE "BAND EDGE EMISSION" OF CdS

2.1 Introduction

The term band edge emission is loosely employed to describe radiative recombination processes occurring within several tenths of an electron-volt of the band gap energy. These processes become predominant in the recombination spectra observed in crystals at low temperatures and under strong excitation conditions. The edge emission of cadmium sulphide excited by 3650 Å radiation at liquid helium temperatures consists of two major components described as the "green" and the "blue" emission (1).

The blue edge emission has been shown to be due to the emission of radiation associated with the recombination or annihilation of free and bound excitons. The green edge emission has been associated with the recombination of free electrons and of electrons bound to donors with holes bound to acceptors. The recombination processes suggested to account for the components of the blue and green emissions are described in this chapter.

At very high excitation intensities, crystals of suitable geometry may be made to "lase". The suggested lasing transitions of CdS are briefly summarised at the end of the chapter. Anti-Stokes excited edge emission is also described.

2.2 Blue Edge Emission

Radiative recombination associated with the recombination or annihilation of "free" and "bound" excitons has been shown to be responsible for the blue edge emission of CdS. Consequently the properties and characteristics of excitons in CdS are described below.

2.2.1 Free Excitons

The free exciton may be thought of as an excited state of the crystal comprised of an electron and hole in orbit about one another. The recombination of the electron and hole may result in the emission of a photon with an energy equal to the band gap energy less the binding energy of the exciton, E_{ex} . Similarly, a photon with an energy $E_G - E_{ex}$ may be absorbed to create a free exciton, where E_G is the band gap energy. By analogy to the hydrogen atom,

$$E_{ex} = 13.6 \frac{\mu}{m_0 \epsilon_s^2 n^2}, \text{ (eV)}$$

where ϵ_s is the low frequency dielectric constant, which is required to scale the 13.6 eV ionisation energy of the hydrogen atom to the crystal lattice environment of the exciton. Since the electron and hole are of roughly comparable mass, m_e^* and m_h^* , respectively, a reduced mass μ , where $1/\mu = (1/m_e^* + 1/m_h^*)$, must be used. m_0 is the electron rest mass, n is an integer, $n = 1$ for the ground state energy. The concepts of free excitons have been derived from absorption and transmission measurements which are described below.

Thomas and Hopfield (2) studied the reflection spectra from CdS crystals at 4.2°K. Densitometer traces are shown in figures 2.1 (a) and (b). In addition to the parent transitions A, B, and C involving the three valence bands, the structure A' and B' was observed. The polarisation properties of A' and B' indicate that they are associated with the transitions A and B respectively. The energy separations between A-A' and B-B' are identical and equal to 0.021 eV. It is reasonable to assume that A and B correspond to the ground state excitons associated with the first and second valence bands respectively. The weaker transitions A' and B' result from the n=2 state of the parent transitions. If the excitons are hydrogen-like, an estimate of the binding energy can be made, e.g. $E_{ex} = 4/3 \times 0.021 = 0.028$ eV.

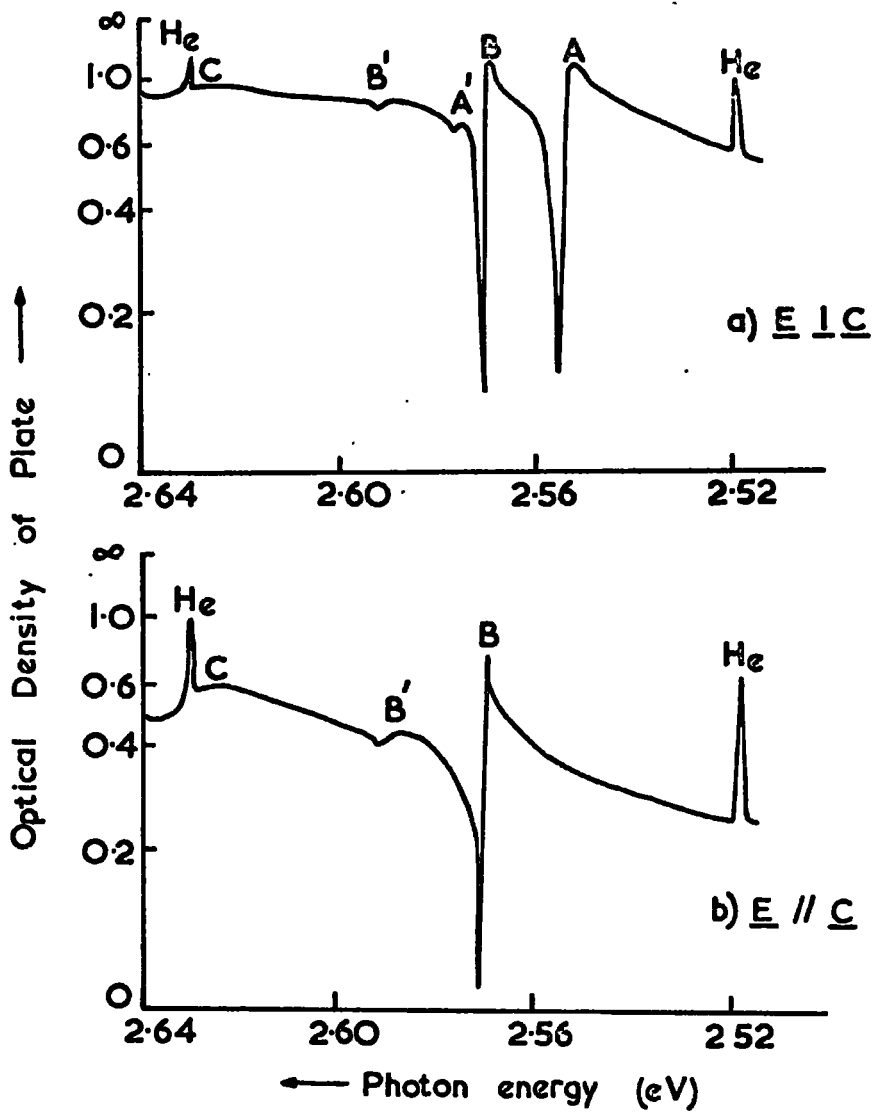


FIG. 2.1. Microdensitometer recordings of the reflection spectra of CdS at 4.2°K for light polarised parallel and perpendicular to the c axis. Helium calibration lines indicate the resolution used.

Using this value for the binding energy and the expression (5)

$$G = \frac{2\pi^2 e^4 \mu}{h^2 \epsilon_s^2}$$

where e is the electronic charge and h is Planck's constant, the reduced exciton mass was calculated giving a value of 0.18. From the analyses of their reflection data, Thomas and Hopfield deduced many of the parameters relating to the band structure of CdS (see figure 2.2) as follows:

$$E_G - E_{\text{exA}} = 2.554 \text{ eV.}$$

$$E_G - (E_B - E_A) - E_{\text{exB}} = 2.570 \text{ eV.}$$

$$E_G - (E_C - E_A) - E_{\text{exC}} = 2.632 \text{ eV.}$$

E_{exA} represents the binding energy of exciton A and similarly for B and C. Assuming $E_{\text{exA}} = E_{\text{exB}}$ then $E_A - E_B = 0.016 \text{ eV}$, with $E_{\text{exA}} = 0.028 \text{ eV}$, the band gap is $E_G = 2.582 \text{ eV}$. In order to determine $(E_C - E_A)$ it was necessary to compute E_{exC} which was done using a quasi cubic model based on the similarity between the wurtzite and zincblende structures. The values obtained were $E_{\text{exC}} = 0.026 \text{ eV}$ and $(E_A - E_C) = 0.073 \text{ eV}$.

To interpret the exciton spectra fully in wurtzite crystals, it is necessary to account for the interaction between excitons and the electric polarisation waves in the crystal. Excitons contribute to the dielectric constant of the crystal and so are closely related to quantised waves of electric polarisation with which an electromagnetic field interacts strongly (6). In the wurtzite lattice, it is possible to classify the polarisation waves as purely transverse or purely longitudinal when \underline{K} (the exciton wave vector) is in the principal directions (i.e. \parallel or \perp to the c axis). However, light not propagating in a principal direction can interact with "mixed" longitudinal - and - transverse excitons (4). Transmission spectra of CdS at 1.8°K enabled Hopfield and Thomas (3) to establish the energies of the

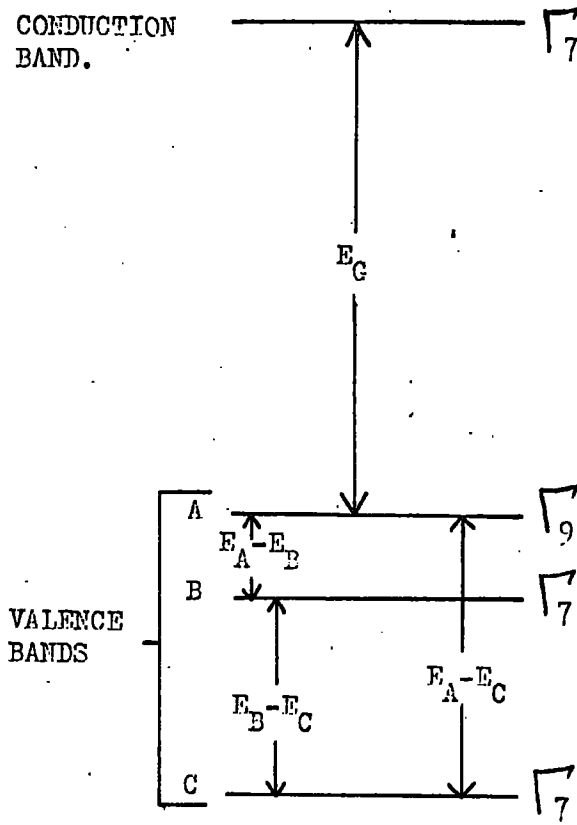


Figure 2.2. The energy band structure of CdS at $k = 0$. The levels A, B and C refer to the hole bands from which the excitons causing the reflections A, B and C arise. The band symmetry is given to the right.

intrinsic exciton absorption bands of CdS, see table 2.1. Zeeman effect studies have shown that the line just below $1S_T$ is the $1S$ state with Γ_6 symmetry, formed with electron and hole spins parallel (the antiparallel configuration gives $1S_T$ and has the Γ_5 symmetry). The energy difference between the Γ_5 and Γ_6 states is thought to arise, in part, from the configurational mixing of the Γ_5 states of series A and B and, in part, from the long range electrostatic interaction of Γ_5 . Although the Γ_6 transition is dipole forbidden, it could be observed as a "forbidden" transition because momentum is supplied by the exciton-creating radiation. The line seen just above $1S_T$ was identified as the associated nearly-longitudinal exciton $1S_L$. These three excitons belonging to the $n = 1$, A series, Γ_6 , Γ_{5T} and Γ_{5L} are the principal free excitons occurring in CdS. For a discussion of the other excitons, see reference 7.

The radiative recombination of a free exciton at the exciton "resonant" energy and of the exciton with the simultaneous emission of one or more longitudinal optical (L.O.) phonons have been definitively identified (8). Gross et. al. (9) carried out detailed experimental investigation of the shape of the emission peaks for a range of temperatures. This has renewed interest in the theoretical aspects of intrinsic exciton emission. The theoretical work is now very briefly summarised.

Hopfield (6) introduced the quantum-mechanical concept of "polariton" states which are the eigenstates of the interacting exciton-photon system or stationary states of the coupled exciton-plus-photon fields. Near exciton resonance energies, excitons and photons cannot be treated as independent entities. Polariton waves propagate through the crystal with "apparent absorption" resulting from the scattering of these waves to other polariton states by crystal imperfections. This

Line identification	Photon energy (eV)
Series A. n = 1, S ₆	2.5524
S _T	2.5537
S _L	2.55455
n = 2, P ₀	2.57508
P _{±1} ; S _L	2.57575
n = 3, D _{±2}	2.57977
n = 4, P, D	2.58094
Series B. n = 1, S _T	2.5686
S _T	2.5687
n = 2,	2.59085

The S, P and D refer to the hydrogenic states of the exciton.

Subscripts T and L refer to transverse or longitudinal

character. The wavefunctions, p, are defined as

$p_{\pm 1} \equiv p_x \pm ip_y$ and $p_0 \equiv p_z$, where p_x transforms like x etc.,

with $z \parallel c$, and $p_{\pm 1}$ and p_0 corresponding to states with ± 1

and 0 units of angular momentum about the c-axis.

Table 2.1. The energies of the intrinsic exciton absorption bands observed in CdS at 1.8 °K.

interpretation is in contrast with the more familiar interpretation where the absorption is said to have occurred after the radiant energy (photons) has transformed into excitons. The contribution of the scattering of polaritons by acoustical phonons to absorption was evolved by Tait and Weiher (10). These authors later (11) showed that the first longitudinal optical (L.O.) phonon replica of the free exciton of CdS at 77°K, i.e. the emission band approximately 0.038 eV below the exciton resonance energy E_{exA} , is due to the inelastic scattering of polaritons. Figure 2.3 shows the dispersion curve for polaritons, see appendix 2.1. The solid curve gives the energy of the polaritons and the dashed curves give the energies of the uncoupled photons and excitons. The first phonon replica, and perhaps the simultaneous creation of two, three, etc, L.O. phonons, is explained by the inelastic scattering of polaritons above the knee of the lowest lying polariton branch (at (a)) to states below the knee (at (b)) with the simultaneous creation of L.O. phonons. The emission band close to the resonance energy is also due primarily to the scattering of polaritons by L.O. phonons. Segall and Mahan (12) calculated the properties of the spectra of the free exciton emission for direct gap compound semiconductors using an interacting exciton-phonon system, however they found it necessary to pay particular attention to polariton effects at high (about 77°K) temperatures.

2.2.2 Bound Excitons

Thomas and Hopfield (13) observed lines to the low energy side of the intrinsic (free) excitons of CdS and interpreted them in terms of "bound" excitons, following the suggestion of Lampert (14) that the centres may be described as states analogous to H_2 , H_2^+ and H^- . The excitons are bound to ionised or neutral defects, and the coulombic

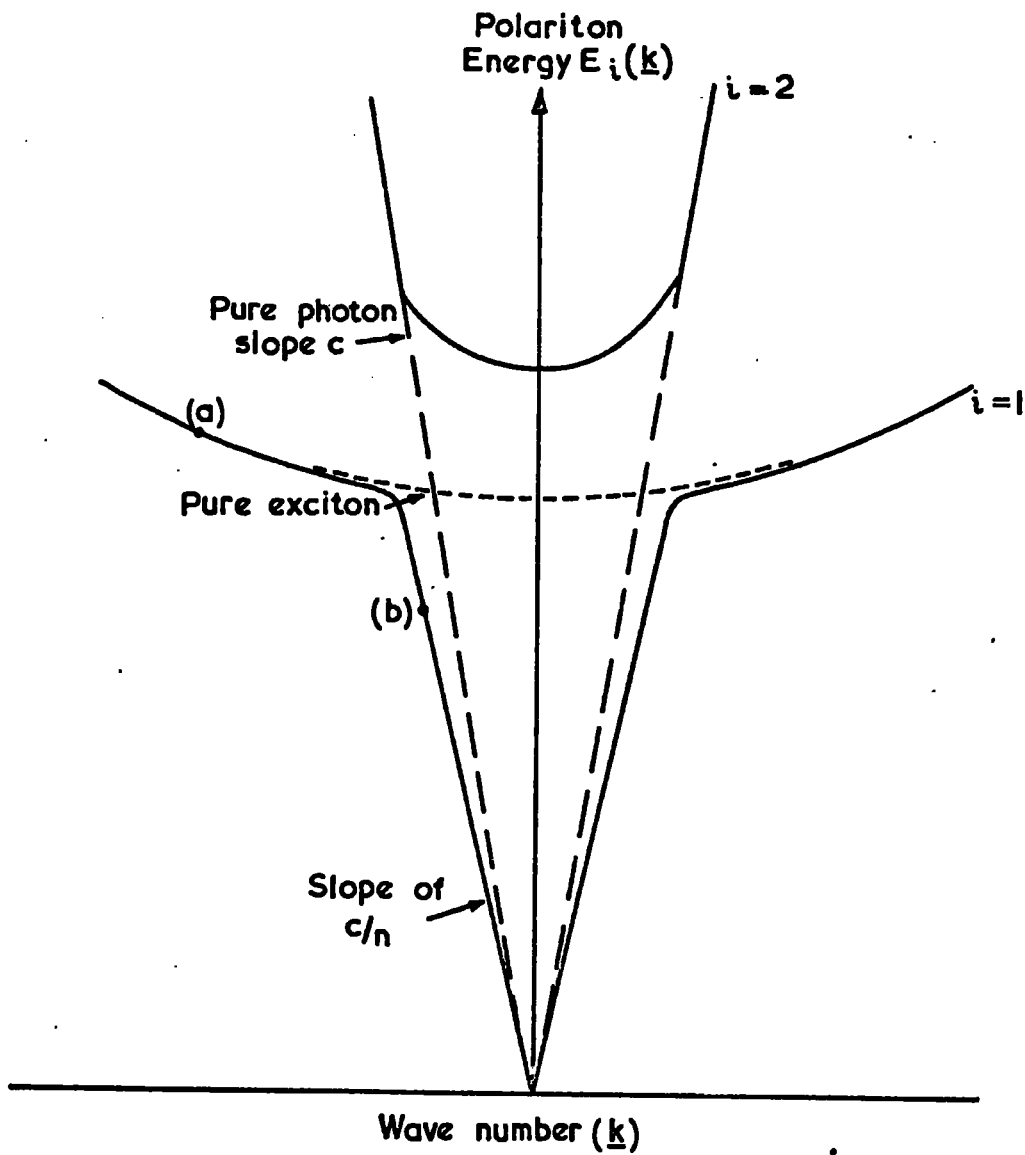


Figure 2.3. The polariton energy diagram.

energy of the environment of the defect disturbs the energy of the exciton. Only the lowest states of the complexes were considered and the theory includes models of complexes which can be formed using holes from either of the top two valence bands. In considering transitions involving bound excitons formed from holes in the top (A) valence band, the g value of the electron is isotropic while the g value of the hole has the form $g = g_{1/2} \cos \theta$, where θ is the angle between the c -axis of the crystal and the direction of the magnetic field. Transitions involving bound excitons formed from holes in the second (B) valence band are more energetic by the energy separation between the top two valence bands. In the case of the neutral donor associated with band B, the transitions are unpolarised. The other bound exciton complexes associated with band B can be identified utilising the Zeeman effect.

The principal lines observed in the absorption and emission spectra reported by Thomas and Hopfield were designated I_1 and I_2 . The characteristics of the behaviour of these lines in a magnetic field and the conclusions drawn from the observations are shown in table 2.2. From the zero g value for the ground state and the one unpaired electronic particle, it was concluded that the complex associated with the I_1 line is an exciton bound to a neutral acceptor site. The characteristics of the I_2 line indicated that the complex is an exciton bound to a neutral donor site.

A line at 4861.7 Å, designated I_3 , was detected in absorption only. The behaviour of this line in a magnetic field was different from that of I_1 and I_2 . At zero field, only the high energy component was observed. At approximately 10 KG and with $c \perp H$, the low energy component appeared, which when extrapolated back to zero field, showed that the line is zero field split. No thermalisation was observed for absorption with $c \perp H$ indicating that the ground state is a singlet

Exciton	I_1 (4868.5 Å)	I_2 (4867.15 Å)
Observation		
$\underline{c} \perp \underline{H}$	Doublet, splitting shows $g_e = -1.76$	
At arbitrary \ominus	4 lines, shows g_h anisotropic.	
Magnetic field splitting w.r.t. \ominus	Linear, shows one unpaired electronic particle.	
Absorption spectra at $\underline{c} \perp \underline{H}$	No thermalisation, thus zero g value for ground state.	High energy component more intense, thus electron in ground state.
" at $\underline{c} \parallel \underline{H}$	4 lines.	No splitting, thus g values of excited and ground states are equal.

Table 2.2. The characteristics of the behaviour of the I_1 and I_2 bound exciton lines in a magnetic field.

($g=0$) state. The zero field splitting arises from an exchange interaction between an unpaired electron and an unpaired hole in the upper state. Such an interaction can occur in lines resulting from an exciton bound to ionised donors or acceptors. The small binding energy of the exciton to the centre suggests that the complex is an exciton bound to an ionised donor.

Thomas and Hopfield found that I_1 and I_2 decreased in intensity while I_3 increased when the lines were observed in absorption while the sample was simultaneously illuminated with infra-red radiation. The infra-red radiation was of an appropriate energy to ionise the acceptors preferentially. It was concluded that the free holes then ionised the donors, so that the population of neutral centres was decreased while that of the ionised centres increased, confirming the identification of the complexes.

Reynolds and Litton (15) observed the I_3 line in the emission of CdS crystals at about 1°K , with two components in zero magnetic field. Zeeman measurements were in good agreement with the corresponding absorption measurements. Reynolds and Litton also observed a strong emission line, denoted I_5 (4869.14 \AA), which they attributed, using Zeeman measurements, to a transition involving an exciton bound to a neutral acceptor site. The same authors later attributed this line to an exciton bound to a neutral donor (16), following the suggestion of Handelman and Thomas (17).

In the spectral range 6 to 8 meV below the intrinsic exciton line, numerous sharp lines have frequently been observed and referred to as I_2 lines (13). These lines all behave very similarly in a magnetic field.

Following the nomenclature of Handelman and Thomas and the other

authors mentioned above, the major emission lines in the blue edge emission of CdS at 4.2°K, and their assignments, are listed in table 2.3. It now remains to describe the nature of the defects to which the excitons become bound.

The intensity of the emission of the I_1 exciton may be decreased by annealing the crystal in cadmium vapour and increased by annealing in vacuum. This suggests that the acceptor associated with I_1 is a cadmium vacancy, which is expected to have two holes in its ground state. The I_1 line sometimes appears as a closely spaced doublet (15). Thomas et. al. (18) studied the emission of doped crystals of CdS and concluded that to explain the doublet nature and the singly ionisable nature of the centre responsible for the I_1 bound exciton complex, it was reasonable to suppose that the double acceptor vacancy is associated with a singly charged donor. For the low energy line (4888.75 Å, 2.53527 eV), it was suggested that the donor was a chlorine ion substituted on a nearest neighbour site to the cadmium vacancy. (In fact, any halogen impurity produced the same emission line). The proposal for the higher energy line (4888.40 Å, 2.53545 eV) was that it was associated with a complex in which the donor was an aluminium ion say substituted on a cadmium site. It was found that the orientation of neither Cl nor Al ion affected the symmetry properties of the line, and both lines showed the same Zeeman splitting pattern. Thomas et. al. also observed lines which they associated with excitons bound to the isolated halogen and aluminium donors. These they denoted I_{2Cl} and I_{2Al} corresponding to lines at 4869.4 Å (2.5453 eV) and 4869.95 Å (2.5450 eV), respectively.

Handelman and Thomas (17) performed various heat treatments on

Line	Wavelength (\AA)	Energy (eV)	Binding Energy (eV)	Centre
I_1	4888.5	2.53595	0.018	Neutral Acceptor
I_{2A}	4867.15	2.5471	0.007	Neutral Donor
I_{2B} (I_5)	4869.1	2.5460	0.008	Neutral Donor
I_{2C}	4870.2	2.5455	0.008	Neutral Donor
I_3	4861.66 4862.25	2.54984 2.54953	~ 0.003	Ionised Donor

N.B. The subscripts A, B and C do not refer to the three valence bands of CdS.

Table 2.3. The principal emission lines associated with the bound excitons of CdS at 4.2 $^{\circ}$ K.

CdS crystals and observed the resultant effects upon the photoluminescence. Their results implied that the I_{2C} line (4870.2 Å) is associated with a sulphur vacancy. It is perhaps worthwhile remarking that the many I_2 lines may be associated with different acceptors associated with the sulphur vacancy. This suggestion is expanded in the discussion chapter.

2.2.3 Vibrational Spectra of Bound Exciton Complexes

Lampert (14) pointed out that in addition to the gross energy level or electronic level scheme of the H_2^+ complex, there will exist a fine structure for each electronic level similar to the vibrational-rotational level scheme of H_2^+ . This type of spectrum was observed in the emission of selected CdS platelets at 1.2°K by Reynolds et. al. (19) and Collins et. al. (20). The following points confirm the interpretation:

- (1) A series of converging levels fitted a standard vibrational-electronic term scheme. There was also a series of rotational lines.
- (2) The line intensity distributions conformed to a Boltzmann distribution at a temperature in reasonable agreement with the actual temperature of measurement.
- (3) The level schemes extrapolated to known exciton states. In fact two series were evolved. The band head for the series that converged to the Γ_5 free exciton (4853 Å) was the 4861.7 Å, I_3 lines described by Thomas and Hopfield (13). The band head for the series that converged to the Γ_6 free exciton (4857 Å) was at 4865.08 Å. Since the energy difference between the band heads of the two series was the same as the energy difference between the convergence limits of the two series, it was suggested that the 4865.08 Å line is due to the Γ_6 exciton associated with the

I_3 complex.

2.2.4 "Excited States" of Bound Exciton Complexes.

Reynolds et. al. (16) reported the observation of "excited states" of bound exciton complexes. Using a Zeeman analysis of the emission, they were able to identify the emission maxima at 4907.15, 4908.7, 4912.4, 4915.32 and 4916.5 Å with what they called the "excited states" of the I_3 and I_{2C} (4870.2 Å) excitons.

The emission maxima are associated with the emission of a photon which has originated from the annihilation of an I_{2C} or I_3 bound exciton, but which has lost some energy before being emitted in exciting the neutralising electron of the donor from the ground state to an excited state of the donor. Using a simple hydrogenic model for the donor, it is easy to see that the photon will have lost $3/4 E_D$ eV in exciting the neutralising electron from the ground state ($n=1$) to the first excited state ($n=2$) of the donor, where E_D is the ionisation energy of the donor. Similarly it would lose $8/9 E_D$ and $15/16 E_D$ in exciting the electron to the $n=3$ and $n=4$ excited states respectively.

A value of $E_D=0.026$ eV provided good agreement between the observed and calculated "excited states" of the I_{2C} and I_3 excitons. This agrees with previously reported donor ionisation energies in CdS, see for example (18). An electron effective mass of 0.18 times the electron rest mass gave a good theoretical fit to the experimental data of the magnetic field splitting of the lines. No emission attributable to the "excited states" of neutral acceptors has been observed.

2.2.5 Phonon Replicas of Bound Excitons

Thomas and Hopfield (13) noted that, at energies less than that corresponding to the I_1 lines, a number of fluorescent lines are observed in CdS at 1.6°K which are described as phonon replicas of the

I_1 and I_2 transitions. Exciton recombination occurring with the simultaneous emission of phonons is suggested by the facts that (a) some of the lines occur at known phonon intervals and (b) at low temperatures there is no absorption corresponding to the emission. The spectrum could be accounted for using the following phonon energies: Longitudinal Optical (L.O.) = 0.0377eV, Transverse Optical (T.O.) = 0.0344eV and Transverse Acoustic (T.A.) = 0.0206 eV. The assignment of T.O. and T.A. phonons was tentative.

The co-operation of I_1 with low-energy acoustic phonons was seen as a small peak about 0.001 eV below I_1 , which tailed out to the peaklet I_1 - TA, which presumably marked the energy of acoustic phonons at the zone boundary. Similar effects were observed on the low energy side of the I_1 - LO peak. With the I_1 line, phonon co-operation was much greater than for the I_2 line. This is probably due to the greater binding energy of the I_1 complex. No co-operation with low energy acoustic phonons was seen with the I_2 lines, while the relative intensities of the LO phonon replicas of I_2 were much less than those of the I_1 exciton.

To observe bound exciton emission, without what may be termed excessive phonon co-operation, it is generally accepted that the CdS crystal be maintained at 20°K or lower (21). At temperatures above about 20°K, the majority of the excitons remain free, and intrinsic exciton emission is observed.

2.3.1 Green Edge Emission

In CdS, the green emission can contain two phonon-assisted series. The higher energy of the two series has its zero-order phonon component centred on about 5140 Å. This series will be denoted H.E.S., standing for "high energy series". The lower energy series has its zero-order component located at about 5170 Å, and will be denoted L.E.S., for "low energy series". The basic recombinations process suggested for

the green emission has been disputed, and the reader is referred to the survey by Reynolds et. al. (1). The essentials of the presently accepted models are discussed below.

Hopfield (22) was able to fit a Poisson distribution to the heights of the maxima of the phonon components of the green edge emission of CdS recorded by Klick (23). (This procedure has been used on results obtained during the course of this thesis, and the reader is referred to chapter four for details of the application). The mean of the Poisson distribution was found to be 0.87. This suggests that for every hundred photons emitted, there are 87 phonons emitted, and that the number of phonons emitted per photon is described by a Poisson distribution. According to Hopfield the mean number of phonons determined by this fitting process provides (a) a measure of the mass of the heavy carrier if recombination of free carriers occurs or (b) a measure of the radius of the trapped carrier if the recombination process involves a trapped carrier. The mass required for the heavy particle is about $5 m_e$ if the green emission is due to a free electron to free hole transition or to exciton recombination in the field of an impurity. In view of this, Hopfield concluded that a trapped carrier was involved, and its orbiting radius was 11 \AA , which is consistent with the model. However, whether the hole or the electron was trapped was not resolved.

Spear and Bradberry (24) showed that their measurements of the intensity of the green emission of CdS as a function of temperature and excitation could be predicted if the radiative recombination took place between a free electron and a hole trapped at a class II type centre situated 0.13 to 0.15 eV above the valence band. Photoconductive measurements and other experiments verified the existence of that centre. Spear and Bradberry thereby confirmed the postulate

of Pedrotti and Reynolds (25) that the transition of a free electron to bound hole explains the single green series at 77°K . Pedrotti and Reynolds noted that as the temperature was reduced below 77°K , the " 77°K series" decreased in intensity, while at about 30°K , a second series appeared, which we have already introduced as the L.E.S. The " 77°K series" became the H.E.S. at liquid helium temperatures. A transition between a bound electron and a bound hole was postulated to explain the L.E.S. The electrons become ionised at elevated temperatures, while the holes are bound to the same acceptors in both processes. Thus the H.E.S. dominates at 77°K while the L.E.S. dominates at 4.2°K .

The model so far is that:

- (1) The H.E.S. is due to the recombination of free electrons with holes bound to acceptors some 0.14 eV above the valence band.
- (2) The L.E.S. is due to the recombination of electrons bound to donors, some 0.023 eV below the conduction band, with holes bound to the same 0.14 eV acceptors.
- (3) The replicas at lower energies result from the simultaneous emission of one or more longitudinal optical phonons.
- (4) The large width of the individual components of the emission may be associated with acoustic lattice vibrations, the influence of imperfections on the binding energy of the trapped hole, or lifetime broadening (22). The explanation of the L.E.S. recombination process has been modified by the concept of distant-pair recombination which is treated in the following section.

2.3.2 Light from Distant Pairs

Crystals of gallium phosphide frequently show remarkable photoluminescent spectra at temperatures below 20°K . Immediately to the low energy side of the bound exciton emission, a large number of very sharp lines are seen, which are more closely spaced at lower energies, and

eventually merge into a broad band, which is replicated at lower energies by phonon emission. The lines can be explained in terms of the recombination of an electron trapped at a donor with a hole trapped at an acceptor which is separated by a distance r from the donor (26). When r is large compared to the radii of the donors and acceptors, the energy of the photon emitted, $E(r)$, is given by

$$E(r) = E_G - (E_A + E_D) + \frac{e^2}{4\pi\epsilon_s\epsilon_0 r}$$

where E_G is the band gap energy, E_A and E_D are the acceptor and donor binding energies respectively, e is the electronic charge and ϵ_s is the low frequency dielectric constant. The final term is due to the coulombic interaction of the donors and acceptors. Numerous discrete lines occur because the donors and acceptors are substituted on lattice sites so that r can only assume certain discrete values. It has been shown that by doping with different donors and acceptors which can substitute on either the Ga or P sub-lattices, different values for E_A and E_D and hence different line spectra can be obtained. Using the equation, the value of $(E_A + E_D)$ for a particular pair of impurities can be derived. The broad emission is typical of "edge emission" observed in many II - VI compounds at low temperatures. The broad emission is clearly associated with the pair lines for it also shifts when $(E_A + E_D)$ is varied. The r values associated the peak of the broad emission are 50 - 150Å, which suggests that the distant pairs may merge to a continuum. Little information can be derived about these pairs from simple spectra obtained under continuous (D.C.) excitation.

Since the lifetime of the pairs is expected to vary with r , it was anticipated that a study of the spectral distribution during the

decay of the broad band emission would be instructive. Thomas et al.

(27) developed the theory and applied the results to GaP and CdS.

Colbow (28) extended the measurements on CdS, and made measurements

using the technique of "time resolved spectroscopy" at different

temperatures. Thomas ~~et~~^{et} al. (18) extended the measurements on CdS

at 4.2°K by observing the spectral distribution of the emission after

a 0-4 nanosecond delay using pulsed electron beam excitation. The

major conclusions of their work are as follows:

(1) The spectra observed at long times (50 microseconds) after the flash consists of sharp peaks, at shorter times (10 - 100 nanoseconds) the peaks occur at shorter wavelengths and are broader on the high energy side, see figure 2.4. This is because at large separations a variation in r changes the energy very little, while at smaller separations a change in r has a profound effect, yet lifetime is affected equally by a given Δr no matter what the value of r . Hence if a certain range of lifetimes is being examined, which is achieved by observing, for a short time, the spectra after a time t , for small t there will be considerable coulombic broadening, but at longer times there will be less broadening. (It was necessary to use the shape of the spectra observed at long times, when there is little coulombic broadening, to calculate the line shape constants for the evaluation of theoretical line shapes for GaP because no account of acoustic phonon co-operation or broadening of the line due to other impurities could be included in the evaluation).

(2) Colbow studied the decay of photoconductivity and the intensity of the H.E.S. and of the L.E.S. at 4.2°K. He concluded that (a) the free electron concentration varied as $n(t) = n_0 t^{-0.20}$ after excitation,

(b) The H.E.S. decayed as $t^{-1.2}$, which on the basis of a free to bound transition, implies that the product of the free electron concentration -

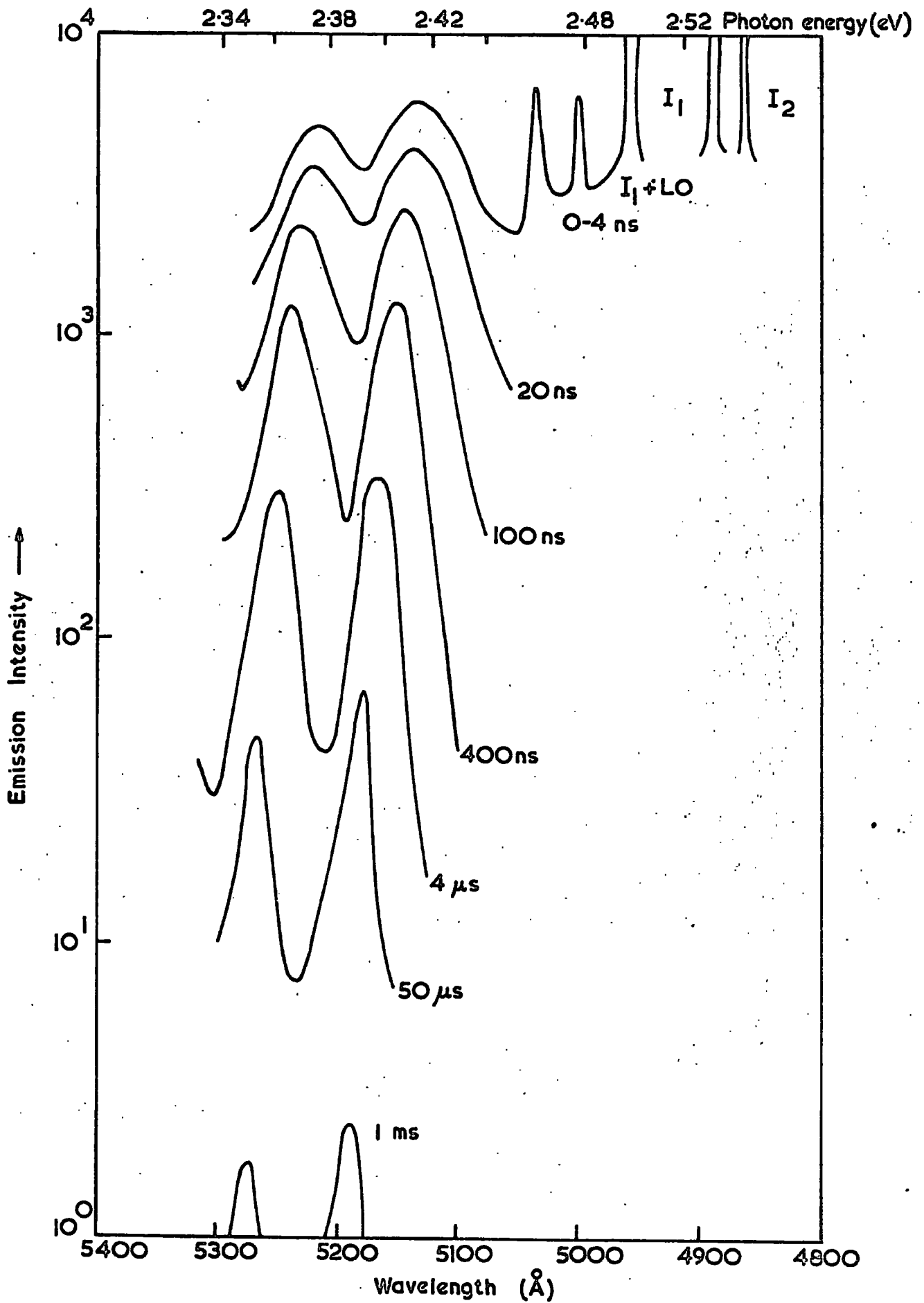


FIG. 2-4. Time decay spectra of CdS at 4.2°K excited by pulsed electron beam apparatus.

$n(t)$ - and neutral acceptor concentration - $N_a(t)$ - decays as $n(t) N_a(t) = M t^{-1.2}$, with M a constant, (c) At short times after excitation, the L.E.S. decays as $t^{-1.0}$, which on the interpretation of a bound to bound transition is equivalent to the decay of the neutral acceptors. This is consistent with (a) and (b) since $1.2 - 1.0 = 0.2$, i.e. the neutral acceptor decay index leaves the free electron decay index when subtracted from the free-to-bound decay index. To explain the large photoconductivity observed at low temperatures and relatively long times after excitation, Colbow postulated a deep trap for holes which is not active in the edge recombination process.

(3) The binding energy of the acceptor determined by Colbow was 169.6 ± 0.4 meV. The binding energy of the donor was 30.5 ± 0.5 meV. The donors and acceptors responsible for the L.E.S. emission were separated by about 127 \AA after 10^{-4} seconds and 199 \AA after 0.1 seconds. Colbow also attributed what may be called "ripples" on the emission bands of both series and their LO phonon replicas to the emission and absorption of transverse optical phonons with an energy of 5.5 meV. This was not confirmed by Thomas et. al.

The effects of the distant pair recombination process observed in spectra excited by continuous excitation, and other characteristics of these spectra, are now described.

(1) Since the transition probability for radiative recombination tends to decrease with increasing separation r , the spontaneous lifetime of a pair increases with increasing r , and so a shift in the maximum of the emission should be observed when the intensity of the excitation is changed. That is, as the intensity of excitation is increased, the low energy pairs (i.e. pairs at larger r) would be occupied by holes and electrons first, and then the higher energy pairs would be filled. Thus as the intensity of excitation is increased, the observed emission

should shift to higher energy. This has been observed by Condas and Yee (29) and Orr et. al. (30). From the shift of the maxima per order of magnitude change in the intensity of excitation, Orr et. al. were able to show that r must be of the order of 100 \AA , in agreement with Colbow's value of mean pair separations. (This is demonstrated in Chapter four).

(2) Because of the spectral shift with intensity of excitation, it is difficult to evaluate the binding energy of the donors and acceptors involved in the recombination process. It was also observed, by Handelman and Thomas (17), that the position of the two series varied as layers of the crystal were removed, which was probably not associated with changes in the nature of the centres. It is suggested that there is a range of possible values for the zero phonon maxima of the two series. The range for the H.E.S. is about $5135 \pm 15 \text{ \AA}$, while the L.E.S. is about $5175 \pm 15 \text{ \AA}$.

(3) Kingston et. al. (31) observed five series in the green emission of CdS, with zero phonon peaks at 5128, 5140, 5163, 5179 and 5234 \AA , at 4.2°K . They proposed the existence of two acceptors, separated by 0.006 eV, to explain the multiplicity of the series. They also suggested that bound-to-bound transitions were involved, but were unable to demonstrate any shift with variation of excitation intensity. Nyberg and Colbow (32) were more convincing in their demonstration of the observation of free-to-bound and bound-to-bound recombination radiation associated with a new acceptor level 0.131 eV above the valence band, which they attributed to a nitrogen impurity.

Summary

The current explanation of the green edge emission of undoped CdS excited by continuous "band gap" radiation is now summarised. A wide variety of spectral curves may be expected depending upon the crystal

used and the intensity of excitation. Even in the same crystal, different surface preparation techniques may result in variations in the proportion of incident radiation absorbed, which in turn affects the spectral emission (32, 33). Usually at 4.2°K , the L.E.S. dominates (zero phonon maximum within the $5175 \pm 15 \text{ \AA}$ range), however some crystals can be found which show almost exclusively the H.E.S. (zero phonon maximum within the $5135 \pm 15 \text{ \AA}$ range). Generally both series occur together. The shift of the L.E.S. to lower energies as the excitation intensity is decreased confirms the explanation in terms of a donor-acceptor pair (bound-to-bound) recombination process. The ionisation energy of the donor is about 0.03 eV , while that of the acceptor is some 0.17 eV . The H.E.S. shows little, if any, shift with excitation intensity which is consistent with the emission arising from a free-to-bound transition, in which holes are bound to the same acceptors as in the L.E.S. recombination process. It has been suggested by Thomas et. al. (18), that any shift observed in the H.E.S. may be due to changes in the electric fields within the crystals arising from the variation of the degree to which the compensating donors and acceptors are neutralised.

Since in CdS there must always be at least as many donors as there are acceptors due to autocompensation (see discussion chapter), the prominence of the H.E.S. at 4.2°K is difficult to explain. Colbow's postulate of a deep hole trap to explain the large photoconductivity at low temperatures at relatively long times after flash excitation (28) means that there is probably a high free electron concentration at all times under continuous excitation. This may possibly explain the occurrence of the H.E.S. in the emission of CdS below about 40°K .

The variation from crystal to crystal, of the intensity of the green edge emission may be correlated with the intensity of the I_1 bound

exciton (17, 30). It seems very probable that the same acceptor is involved in both the I_1 and the edge emission. The nature of the donors is rather more open to discussion, and may be associated with both impurities and native defects probably sulphur vacancies (17, 18, 30).

2.4 Edge Emission Excited by Anti-Stokes Radiation

The observation of green edge emission excited by photons with energies less than the band gap energy (anti-Stokes (A.S.) radiation) was reported for CdS at 77°K by Halstead et. al. (34). This effect has been seen in doped and undoped CdS, and in other II-VI materials at 4.2°K, by Broser and Broser-Warminsky (35). The excitation mechanism suggested is a two step process across the band gap using an ~~intermediary~~ ^{intermediate} level. This level has been attributed to copper since it was found in crystals which showed the effect and because the effect can be optimised by preparing CdS with a minimal donor impurity and stoichiometric compensation by the copper (36). The preparative conditions implied that the copper is largely present as $Cu_{Cd}^0, 3d^9$, (i.e. substituted on a cadmium site, with no charge excess with respect to the lattice and with nine 3d electrons) in the unilluminated state. Condas and Yee (37) have questioned the role of copper as the centre responsible for the ~~intermediary~~ ^{intermediate} level since their crystals, with an impurity content of the order of 10^{17} atoms cm^{-3} , contained no detectable copper. Brown et. al. (38) suggest a model in which the centres normally associated with deep centre luminescence are associated with the excitation process and are involved in the recombination process. (This will be amplified in the discussion chapter.)

The L.E.S. generally dominates the green emission of CdS at 4.2°K excited by A. S. radiation (37), however the H.E.S. has been observed in selected crystals (38). The spectral shift of the series as the

intensity of excitation is varied confirms that the same recombination process is responsible for the A.S. excited emission as for the "band gap" excited emission. The absence of a shift of the H.E.S. confirms the free-to-bound nature of the transition. The absorption coefficients corresponding to the "red" (A.S.) and "band gap" excitations are of the order of 1 and 10^5 cm^{-1} respectively (39, 7). Possibly as a consequence, the donor-acceptor pairs involved in the A.S. excited L.E.S. tend to be more distant than those involved in the band gap excited emission, and the A.S. excited L.E.S. tend to have sharper, narrower peaks (38). Above about 40°K the H.E.S. becomes the dominant emission process.

Blue edge emission has been observed in CdS at liquid helium temperatures excited by A.S. radiation (38). The precise nature of the recombination process remains in dispute, however it appears that either the I_2 bound exciton or the free exciton or a contribution from both types, together with L.O. phonon co-operation, may be responsible for the emission. This will be discussed later in this thesis.

2.5 Lasing Transitions of CdS

Light amplification by stimulated emission of radiation has been observed using sample cavities cut from thin platelets of CdS (typically a few microns thick, up to 0.5 mm wide and 1 to 2 mm long), with micro-second pulsed electron beam excitation (up to 60 KV at 20 mA over a 0.5 mm diameter) impinging on the larger platelet face, normal to the c-axis. The spectral emission occurs in the blue region of the edge emission. There are basically two types of CdS laser, which may be termed intrinsic and extrinsic.

Benoit & la Guillaume et. al. (40) distinguished three processes which can lead to lasing action in intrinsic CdS below 77°K .

(a) The annihilation of a free exciton with the emission of a photon and an L.O. phonon, which has only a weak gain.

(b) The interaction of two free excitons resulting in an exciton with no momentum (which is then able to be emitted as a photon since a photon has no momentum - conservation of momentum), and one exciton. The emission line is 27 meV below the free exciton line, which implies that the photon gives up this energy before being emitted. The energy released would ionise the remaining exciton and create an electron hole pair. This process has medium gain.

(3) A free exciton interacts with an electron and transfers its momentum to it. As a result, the exciton may become a photon. This is a high gain process.

Litton and Reynolds (41) showed that the two extrinsic laser lines of CdS, which they called I_{8p} (4896 Å) and I_1 (4888 Å), are associated. Using conventional U.V. excitation of CdS platelets at 1.2°K, they made the following observations and conclusions:

- (a) The two lines had identical Zeeman splitting and hole g values.
- (b) The intensity of the I_{8p} line increased at the expense of the I_1 line as the concentration of excess cadmium was increased from crystal to crystal.
- (c) They confirmed that the I_1 line is a bound exciton-neutral complex.
- (d) They observed discrete lines between the I_1 and I_{8p} peaks. They assigned these lines and I_{8p} to near neighbour donor acceptor pairs, suggesting that the acceptor involved in I_1 was associated with donors arising from cadmium interstitials or sulphur vacancies. The lines also showed Zeeman splitting and g values identical to that of I_1 .

Crystals which had been heavily doped with cadmium no longer showed the I_1 line or the intermediate lines, but did show the I_{8p} line and a line at 4869 Å which Litton and Reynolds assigned to the I_5 complex. The authors did not investigate any of the characteristics associated with donor- acceptor pair recombination. It would be more self-consistent if

the 4869 Å line had in fact been assigned to the I_{20} complex, which Handelman and Thomas (17) suggested was a sulphur vacancy. (The authors differed from Hurwitz (42) in the value of the wavelength they observed for the I_{8p} laser line). It is possible then that the I_{8p} complex is in fact associated with a cadmium ^{interstitial} interstitial. This is not ruled out by Zeeman measurements, as there is some doubt as to whether the I_{8p} line is associated with a neutral acceptor or a neutral donor. This would not preclude the possibility of donor-acceptor pairs at lower cadmium doping levels.

The extrinsic process appears to be more efficient than the intrinsic ones in obtaining amplification. Hurwitz (43) observed lasing with 11 KeV electrons in CdS crystals grown under excess cadmium conditions. The electron beam was pulsed with 50 - 200 nano-second pulses at a repetition rate of 60 cycles per second. The maximum attainable output power (about 350 watts) and efficiency (overall power efficiency about 27%) remained essentially constant over the temperature range 4.2 to 110°K, while the threshold current rose slowly (50 to 80 microamps). With further increase in temperature, the threshold current rose very rapidly with a corresponding decrease in efficiency until at 250°K the laser threshold was at 22mA, 60 KeV, the maximum capacity of the gun. CdS lasing at room temperature had been observed by Nicoll (44).

2.6 Conclusion

The edge emission of cadmium sulphide consists of the "blue" and "green" components. The blue emission is associated with the recombination or annihilation of intrinsic or free excitons and bound excitons. The free exciton emission is presently being used to analyse the mechanisms associated with the excited states of crystals. The study of the bound exciton emission, which may be analysed in terms of

"hydrogen-molecule complexes", provides information about the nature of imperfections in CdS. The green emission, at temperatures below about 40°K, is associated with two, phonon assisted series known as the high energy (H.E.S.) and low energy (L.E.S.) series. Above 40°K, the L.E.S. disappears. The H.E.S. is attributed to the recombination of free electrons with holes bound to acceptors some 0.17 eV above the valence band. The L.E.S. is attributed to a distant donor-acceptor pair mechanism, involving donors some 0.03 eV below the conduction band and the same acceptors as those involved in the H.E.S. The intensity of the I_1 , neutral acceptor bound exciton, and the green emission are affected by heat treatment in cadmium vapour, indicating that the acceptor involved in the recombination process is associated with a cadmium vacancy. The donors involved in the edge emission are associated with native or impurity defects. The donor-acceptor associate model is now being tentatively applied to the centres involved in edge emission.

Edge emission may be excited in various ways. Time resolved spectroscopy - involving "flash" excitation - is the most efficient method of determining the ionisation energies of donors and acceptors associated with the green edge emission. Continuous band-gap (U.V.) excitation is used to study the exciton components and the variation of the green emission from crystal to crystal. Electron-beam excitation can cause CdS to lase. Anti-Stokes excitation excites green and blue emission and should prove useful as a tool to investigate the levels lying in the middle of the band-gap.

APPENDIX 2.1

The Lorentz model of excitons considers the exciton as an oscillator, consisting of a particle of mass m_e , negative charge e , vibrating about some equilibrium position, with a natural frequency ω_0 , at which a positive charge of equal magnitude is fixed. The dynamical behaviour of the excitons under the influence of electromagnetic wave (wavelength $2\pi/\omega$) leads to the dispersion curves for the longitudinal (L) and transverse (T) waves, see figure A2.1 (a) ("Excitons", D. L. Dexter and R. S. Knox, 1965 Interscience Tracts on Physics and Astronomy No. 25). The introduction of the notion that the oscillators or excitons may be coupled results in a curving of the ω_0 curve of figure A2.1 (a) which is analogous to the curvature of an exciton band, see figure A2.1 (b).

Thus a photon, P_0 entering the crystal may become either a polariton P_1 or P_1' , which correspond to photons to which different refractive indices ($n = c/\omega$), but the same frequency can be assigned. Thus if the P_0 photons produce approximately equal numbers of P_1 and P_1' polaritons, and if P_1 and P_1' are not scattered, these two excitations of the crystal may optically interfere with one another. Hopfield and Thomas (1963, Phys. Rev. 132, 563) showed that this "spatial dispersion" affects the reflection spectrum of CdS in a region of strong dispersion. The Lorentz model predicts 100% reflectivity for incident photons between ω_0 and ω_L because there are no modes of the system available in this energy range, see figure A2.1 (a). Spatial dispersion introduces allowed modes, with the curvature of the exciton band leading to an exciton effective mass of $1.80 m_e$, and reduces the peak reflection to 65%.

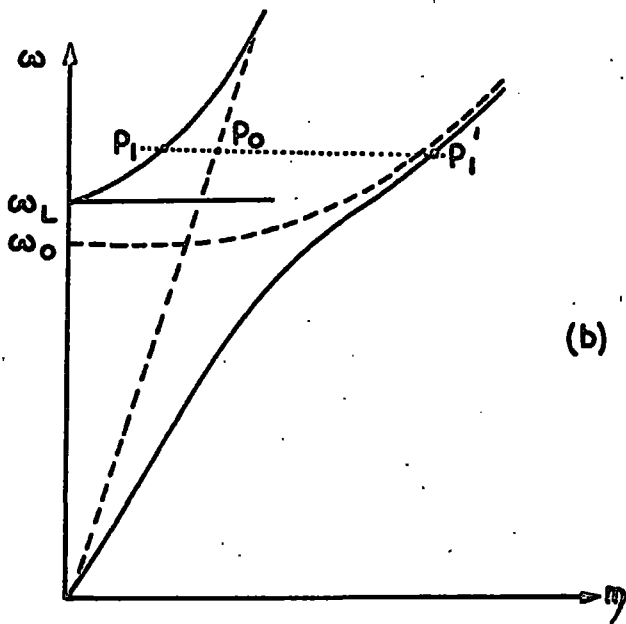
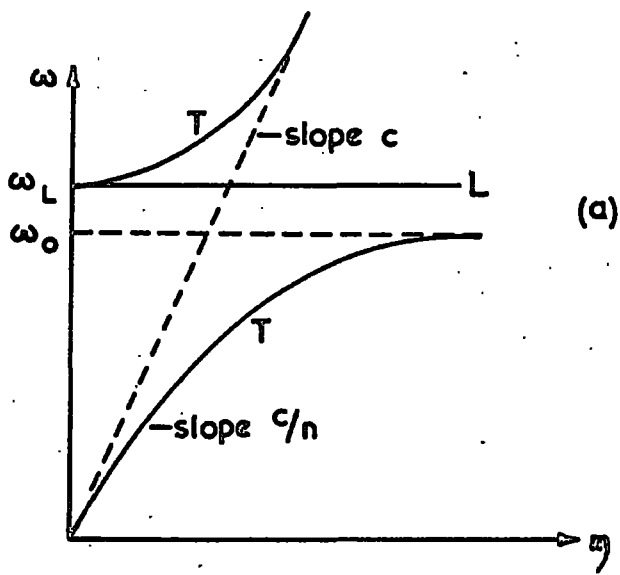


FIG. A2.1. Dispersion curves for (a) the simple Lorentz type exciton-photon interaction, and (b) the effect of spatial dispersion.

CHAPTER 2

REFERENCES

- 1 D. C. Reynolds, C. W. Litton & T. C. Collins (1965) Phys. Stat. Sol. 2, 645 & 12, 3.
- 2 D. G. Thomas & J. J. Hopfield (1959) Phys. Rev. 116, 573.
- 3 D. G. Thomas & J. J. Hopfield (1961) Phys. Rev. 122, 35.
- 4 D. G. Thomas & J. J. Hopfield (1960) J. Phys. Chem. Solids 12, 276.
- 5 R. J. Elliott (1957) Phys. Rev. 108, 1384.
- 6 J. J. Hopfield (1958) Phys. Rev. 112, 1555.
- 7 B. Segall & D. T. F. Marple (1967) Ch. 7 "Phys. & Chem. of II - IV Compounds", Aven & Prener.
- 8 C. E. Bleil & I. Broser (1964) Proc. Int. Conf. on Phys. of Semiconductors p. 897.
C. E. Bleil (1966) J. Phys. Chem. Solids 27, 1631.
- 9 E. Gross, S. Permogorov & B. Razbrin (1966) J. Phys. Chem. Solids 27, 1647.
- 10 W. C. Tait & R. L. Weiher (1968) Phys. Rev. 166, 769.
- 11 W. C. Tait & R. L. Weiher (1969) Phys. Rev. 178, 1404.
- 12 B. Segall & G. D. Mahan (1968) Phys. Rev. 171, 935.
- 13 D. G. Thomas & J. J. Hopfield (1962) Phys. Rev. 128, 2135.
- 14 M. A. Lampert (1958) Phys. Rev. Letters 1, 450.
- 15 D. C. Reynolds & C. W. Litton (1963) Phys. Rev. 132, 1023.
- 16 D. C. Reynolds, C. W. Litton & T. C. Collins (1968) Phys. Rev. 174, 845.
- 17 E. T. Handelman & D. G. Thomas (1965) J. Phys. Chem. Solids 26, 1261.
- 18 D. G. Thomas, R. Dingle & J. D. Cuthbert (1967) Proc. Int. Conf. on Phys. of Semiconductors p. 863.
- 19 D. C. Reynolds, C. W. Litton & R. G. Wheeler (1964) Proc. Int. Conf. on Phys. of Semi conductors p. 739.
- 20 T. C. Collins, C. W. Litton & D. C. Reynolds (1964) Proc. Int. Conf. on Phys. of Semiconductors p. 745.

CHAPTER 2

- 21 D. G. Thomas & J. J. Hopfield (1962) J. Appl. Phys. 33, 3243.
- 22 J. J. Hopfield (1959) J. Phys. Chem. Solids 10, 110.
- 23 C. C. Klick (1951) J. Opt. Soc. Amer. 41, 816.
- 24 W. E. Spear & G. W. Bradberry (1965) Phys. Stat. Sol. 8, 649.
- 25 L. S. Pedrotti & D. C. Reynolds (1960) Phys. Rev. 120, 1664.
- 26 J. J. Hopfield, D. G. Thomas & M. Gershenzon (1963) Phys. Rev. Letters 10, 162.
- 27 D. G. Thomas, J. J. Hopfield & K. Colbow (1964) Proc. Int. Conf. on Phys. of Semiconductors p. 67.
- 28 K. Colbow (1966) Phys. Rev. 141, 742.
- 29 G. A. Condas & J. H. Yee (1966) App. Phys. Letters 9, 188.
- 30 D. S. Orr, L. Clark & J. Woods (1968) Brit. J. Appl. Phys. (J. Phys. D.) 2, 1609.
- 31 D. L. Kingston, L. C. Greene & L. W. Croft (1968) J. Appl. Phys. 39, 5949.
- 32 D. W. Nyberg & K. Colbow (1967) Can. J. Appl. Phys. 45, 3333.
- 33 D. W. Nyberg & K. Colbow (1967) Can. J. Appl. Phys. 45, 2833.
- 34 R. E. Halsted, E. F. Apple & J. S. Prener (1959) Phys. Rev. Letters 2, 420.
- 35 I. Broser & R. Broser-Warminsky (1962) "Luminescence of Organic and Inorganic Materials" (Kallman & Spruch) p. 402.
- 36 R. E. Halsted, E. F. Apple, J. S. Prener & W. W. Piper (1961) Proc. Int. Conf. on Phys. of Semiconductors p. 776.
- 37 G. A. Condas & J. H. Yee (1967) J. Appl. Phys. 38, 3457.
- 38 M. R. Brown, A. F. J. Cox, D. S. Orr, J. M. Williams and J. Woods (1969) to be published.
- 39 R. Boyn (1968) Phys. Stat. Sol. 29, 307.
- 40 C. Benoit à la Guillaume, J. M. Debever & F. Salvan (1969) Phys. Rev. 177, 567.

CHAPTER 2

- 41 C. W. Litton & D. C. Reynolds (1967) Proc. Int. Conf. on Phys. of Semiconductors p. 694.
- 42 C. E. Hurwitz (1966) Appl. Phys. Letters 9, 420.
- 43 C. E. Hurwitz (1967) Proc. Int. Conf. on Phys. of Semiconductors p. 682.
- 44 F. H. Nicoll (1967) Appl. Phys. Letters 10, 69.

CHAPTER 3

EMISSION SPECTROSCOPY : EXPERIMENTAL APPARATUS AND PROCEDURE

3.1 Introduction

Under continuous band gap excitation a wide variety of edge emission spectra may be observed, depending upon the cadmium sulphide crystal used, and the intensity of excitation. One of the purposes of this work has been to examine the photo-excited edge emission of large CdS single crystals at liquid helium temperatures in an attempt to establish a correlation between the crystal growth conditions and the spectral distribution of the edge emissions. This chapter describes the material preparation, the cryostat, the optical apparatus and the experiments performed to analyse the "green" and "blue" CdS edge emissions.

3.2 Material Preparation

The cadmium sulphide crystals studied during the course of this research were grown in the Department of Applied Physics, Durham University, by Dr. L. Clark and Dr. K. Burr. This section serves as a brief description of the method of growth for the purpose of discussing the results of the thesis. The details of the growth technique and the crystal properties have already been fully described (1).

Initial purification, by an argon flow technique, of British Drug Houses "Optran" grade or Derby Luminescents "electronic" grade material was used to obtain the CdS charge for the preparation of the large single crystals. The vertical furnace arrangement, and a typical quartz glass tube used in the large crystal growth technique are shown in figure 3.1. A procedure of evacuation, baking and flushing with argon was used to remove volatile impurities from the tube.

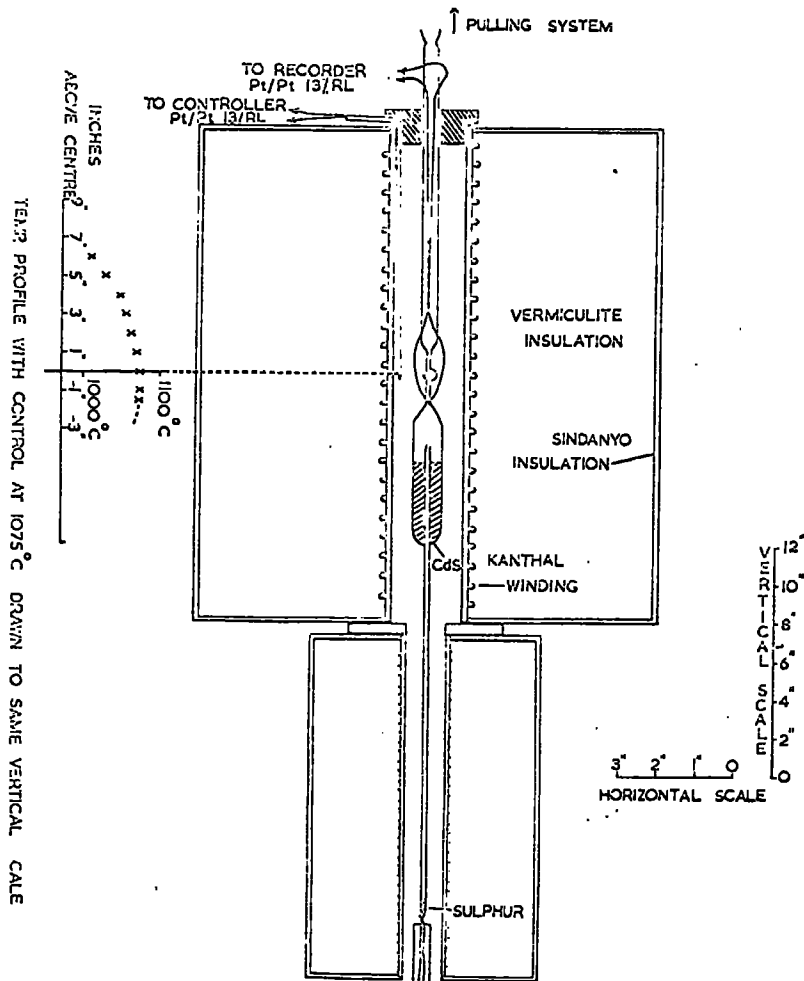


Figure 3.1. Furnace arrangement shown with a growth tube in the initial position.

The procedure was repeated when the excess of sulphur or (cadmium); the first component of the charge, had been placed in the tube. The final component was the purified CdS. Any deliberate dopant was generally mixed with the 30 gms. of CdS before it was added to the tube. After several hours further evacuation to 10^{-6} torr, the tube was sealed from the vacuum system and inserted in the furnace in the position indicated in figure 3.1.

The excess sulphur (or cadmium) sublimed from the upper vessel into the cooler reservoir as the furnace system warmed up. The tube was pulled through the furnace system when the temperatures were stable. As a result the temperature gradient effectively moved across the growth chamber and led to the vapour transport of the CdS from the charge to the upper point of the tube, where the boule formed. The reservoir was maintained at a steady temperature to ensure a constant elemental partial pressure during growth. The pull was usually stopped when about half the charge had sublimed. The crystals were either cooled rapidly by removing the tube from the furnace system or, more usually, were cooled slowly over a period of some 70 hours, which resulted in the boules containing less strain. The changes in the physical properties of the "doped" crystals, compared with those of "pure" crystals grown under the same temperature conditions, confirmed that transport of the dopant from the charge to the boule had taken place.

3.3 Sample Preparation

Cadmium sulphide crystals which had been cut and polished needed to be etched before any green edge emission was observed under ultraviolet excitation at liquid nitrogen temperatures. It was not necessary to treat the cleaved face of a crystal in any way before

luminescence was observable under the same conditions. Samples of "as grown" crystals were obtained by cleaving the boule and selecting a crystal from the central volume of the boule, thus avoiding the strain and damage produced by cutting and polishings, and avoiding contamination from the growth tube wall. It was necessary to etch samples which had been given a post growth treatment in a chromic acid solution at 80°C for several minutes to obtain observable luminescence. Cleaving the crystals meant that the sample geometry was irregular, although the size of all crystals was approximately the same, 5 to 10 by 2 to 5 by 1 to 3 mms.

3.4 The Cryostat

The all metal helium cryostat, shown diagrammatically in figure 3.2, was manufactured by The Oxford Instrument Co. Ltd., and has been modified slightly. The essential features are:

- (1) 1.3 litre capacity liquid helium pot.
- (2) 2 litre capacity liquid nitrogen jacket.
- (3) Two carbon resistors, mounted on a thin stainless steel tube, for use as depth indicators in the liquid helium pot.
- (4) The facility for electrical connections to be made to the sample from outside the cryostat.
- (5) Demountable copper sample holder, copper (liquid nitrogen temperature) radiation shield, and outer vacuum walls surrounding the tail.
- (6) One centimetre diameter, optically flat silica windows in the demountable outer vacuum wall.
- (7) Sample maintained under vacuum.

A conventional vacuum system, incorporating an ES 150 rotary pump and an EO 1 oil diffusion pump (manufactured by Edwards High Vacuum Limited), was used to evacuate the cryostat. Provision was made for the helium exhaust gas to be recovered, alternatively, the contents of the helium pot could be evacuated using the rotary pump.

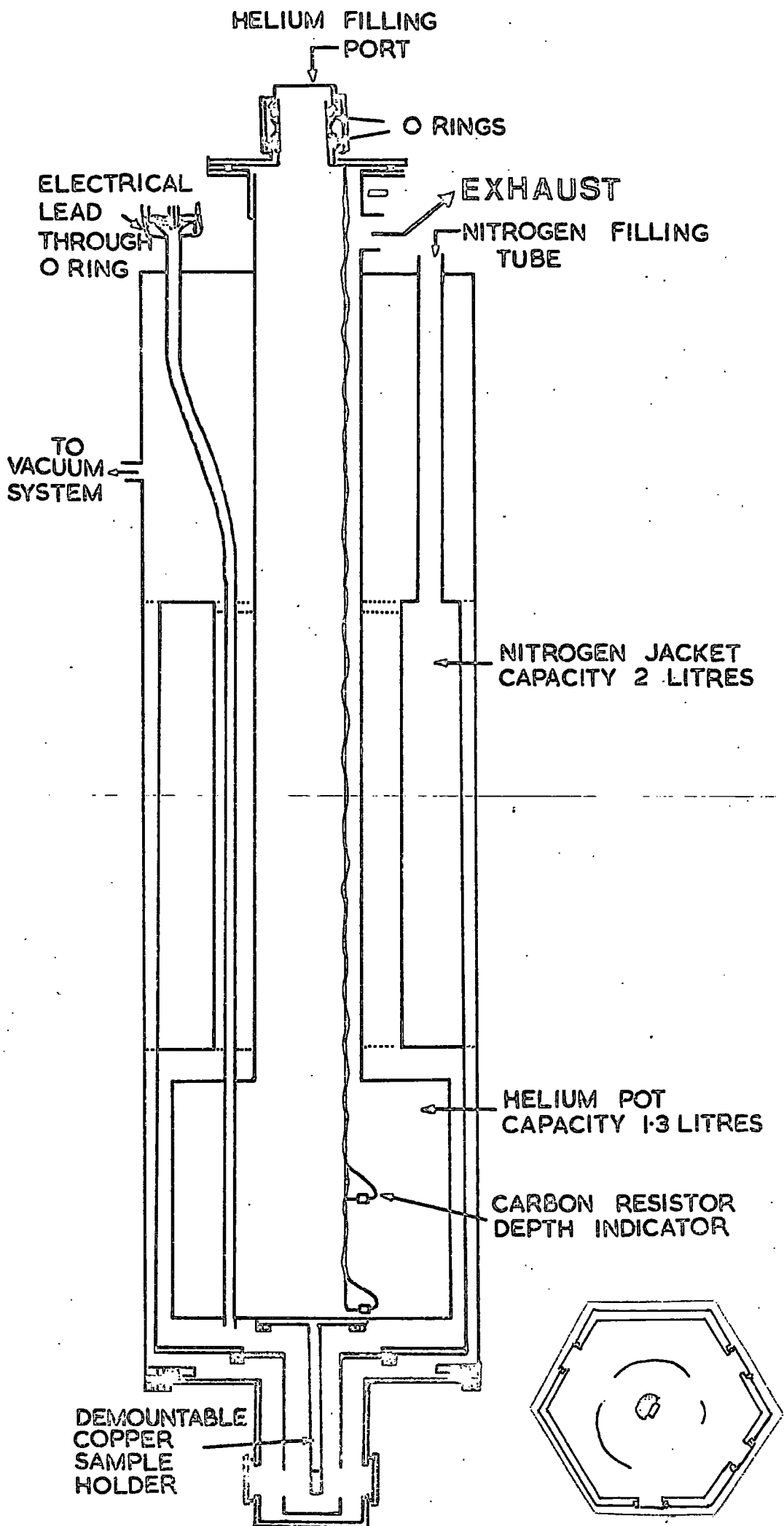


Figure 3.2. Diagram of the metal helium cryostat.

Indium was used to attach the cadmium sulphide samples to the cold copper finger. The cold finger was detached from the cryostat and heated until the indium, covering the sample area, was molten. The heating was then stopped, and the crystal placed on the indium just before it resolidified. The indium provided a good electrical and thermal contact between the crystal and the cryostat. Nyberg and Colbow (2) reported that heating CdS crystals for a few seconds in a nitrogen or air ambient to the point where the crystal turned red produced green edge emission bands, which they associated with nitrogen acceptor levels 0.131 eV above the valence band. No similar series have been observed in the emission spectra observed during the course of this research. It was assumed that the effect of any accidental "heat treatment" upon the samples during the course of mounting upon the copper block was probably very small.

Monitoring the resistance of the carbon radio resistors gave an indication of the temperature of the helium pot, and greatly assisted the estimation of the stage reached during the transfer of liquid helium. A 0.03At % Fe-Au versus chromel thermo-couple (material manufactured by Johnson Matthey Metal Limited) was used to measure the temperature of the crystal under the various illuminations used during the course of the research. With liquid helium in the helium pot, and the thermocouple reference junction in liquid helium, the temperature recorded with and without incident U.V. radiation was 8 to 10°K, rising to 23 to 25°K under OR2 excitation, and falling to 12 to 14°K when two HAL filters were added to the OR2 exciting beam. With liquid nitrogen in the helium pot, and the reference junction in liquid nitrogen, the temperatures recorded under the same excitation conditions were 80, 89 and 81°K respectively. The thermocouple was attached to the face of the crystal upon which the radiation was incident, so that the temperatures

recorded - particularly in the case of excitation via OR2 filters when a high proportion of infra-red radiation was present - were probably the highest that the crystal would experience.

3.5 Photo-excitation

Stokes and anti-Stokes excited emission spectra were recorded for the majority of crystals studied. This section describes the equipment used to produce the different excitation conditions, and the arrangement to excite and collimate the emission.

Stokes excitation was provided by a 500 watt mercury lamp filtered by two Chance glass OX 1A filters to pass 3650 \AA radiation. Data, supplied by Engelhard Hanovia lamps on one of their 100 watt medium pressure mercury arc tubes (arc length 1.85 inches, tube diameter 12 mm), indicates that the total radiative flux was 25.2 watts when the electrical input was 108.5 volts at 1.08 amps, that is 100 watts input. Assuming a linear relationship, the radiative output of the 500 watt lamp, underrun at approximately 90 volts, 5 amps, stabilised d.c., should be approximately 110 watts. Table 3.1 shows the percentage of the radiant energy emitted in the region of the transmission of the OX 1A filters, and the effect of two filters on the emission. The total percentage of the emitted radiant energy which is transmitted by two OX 1A's is the sum of the fourth column, and is 8.28%, being largely composed of the 3650 \AA transition (8.04%). Thus the radiant energy which was available to be focussed onto the crystal was of the order of 9 watts.

Anti-Stokes excitation was provided by a 50 watt tungsten microscope lamp filtered by a Chance glass OR1 or OR2 or a 7700 \AA interference filter (bandwidth 150 \AA at half height). Where the general terms red or A.S. (anti-Stokes) excitation are used, the incident radiation was provided by the tungsten lamp filtered by the OR2 filter. The same

Wavelength (\AA)	Emission of mercury lamp. (%)	Transmission through one OXLA. (%)	Transmission through two OXLA's. (%)
4358	13.34	1	0.0013
4045	7.51	10	0.0751
3650	16.40	70	8.0360
3341	1.36	30	0.1224
3130	9.20	7	0.0444

Table 3.1. The effect of OXLA filters on the percentage of the radiant energy emitted by the mercury lamp in the ultra-violet region of the spectrum.

effects were observed using the OR1 filter, however the green emission intensity was reduced by approximately 10% with this excitation. The emission intensity was reduced by a factor of the order of one hundred when the 7700Å interference filter replaced the OR2 filter. This meant that the luminescence excited by the 7700Å filter was below the limit of detection in some crystals. Figure 3.3 shows the transmission characteristics of some filters used in the excitation and detection of CdS edge emission. Assuming that the microscope lamp had a luminous efficiency of 10 lumens per watt input; then there were 500 lumens of radiant power emitted in the visible spectrum. This is approximately 0.8 watts. Bearing in mind that the shape of the spectral distribution of a tungsten lamp, the radiation transmitted by the OR2 filter between 0.62 and 0.74 microns would be approximately 75% of the visible output, i.e. 0.6 watts. This portion of the spectrum is probably largely responsible for the A.S. excitation of the green edge emission (see Chapter 7 on Excitation Spectroscopy). Thus a conservative estimate of the radiant energy available to be focussed onto the crystal in the form of A.S. excitation is 0.6 watts.

The arrangement used to excite and collimate the luminescence into the Optica spectrophotometer is shown in figure 3.4. Window "one" was used when the sample was to be irradiated with U.V.. Single beam A.S. radiation - OR2 irradiation - was focussed onto the crystal via window "two". The sample could be simultaneously irradiated by an auxiliary beam, through window "one", provided by a second filtered tungsten source, using 1.205 or 0.953 micron (150Å bandwidth at half peak) interference filters or a 1 mm thick slice of silicon.

A set (50, 30, 10 and 1% transmission) of neutral density gelatin filters (manufactured by Barr and Stroud Limited) was used to vary the intensity of the excitation. The transmission characteristics of the neutral filters showed a "flat topped" response in the region

T (%) Transmission percent

I_B Intensity of breakthrough (arbitrary units)

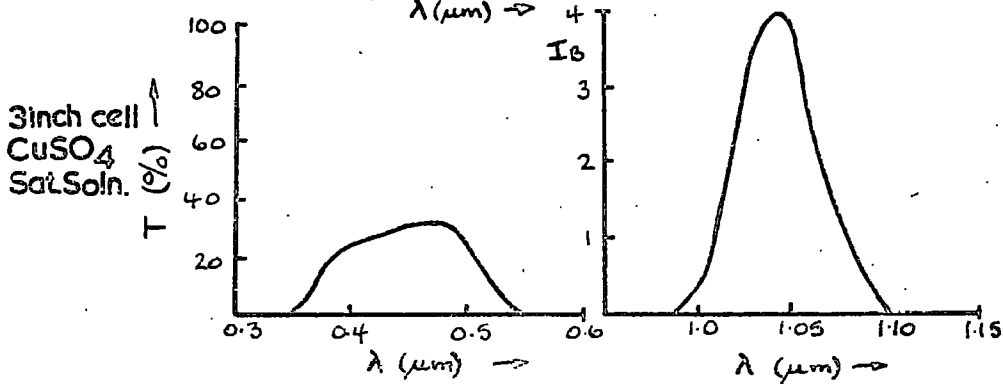
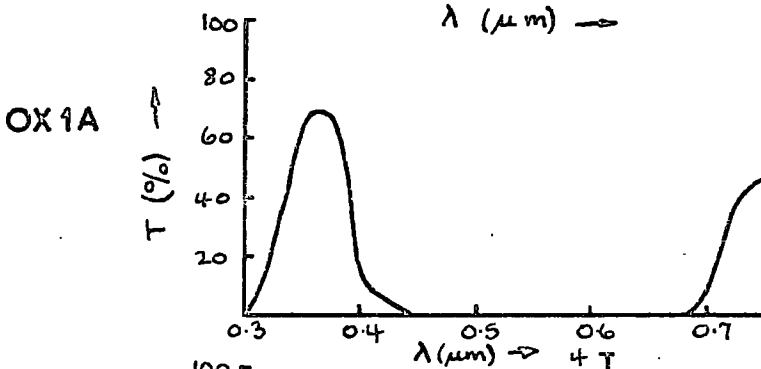
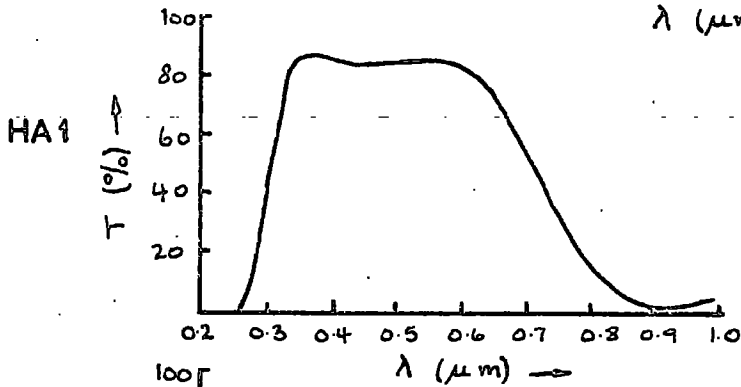
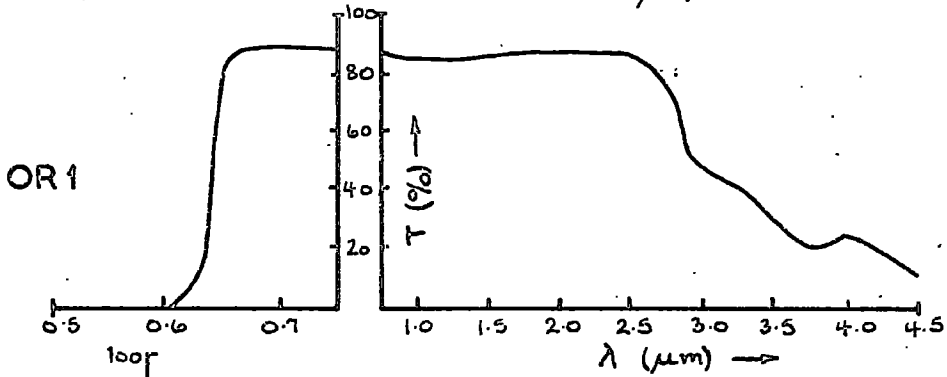
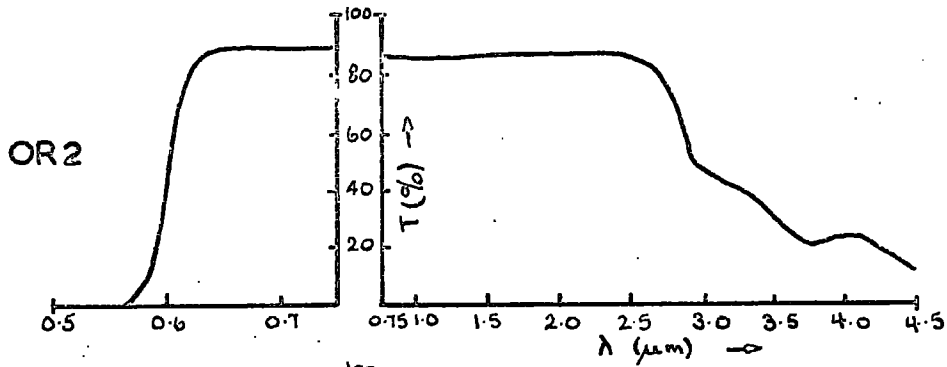


FIG. 3-3. Transmission characteristics of the colour filter glasses used and of a three inch cell containing a saturated solution of copper sulphate.

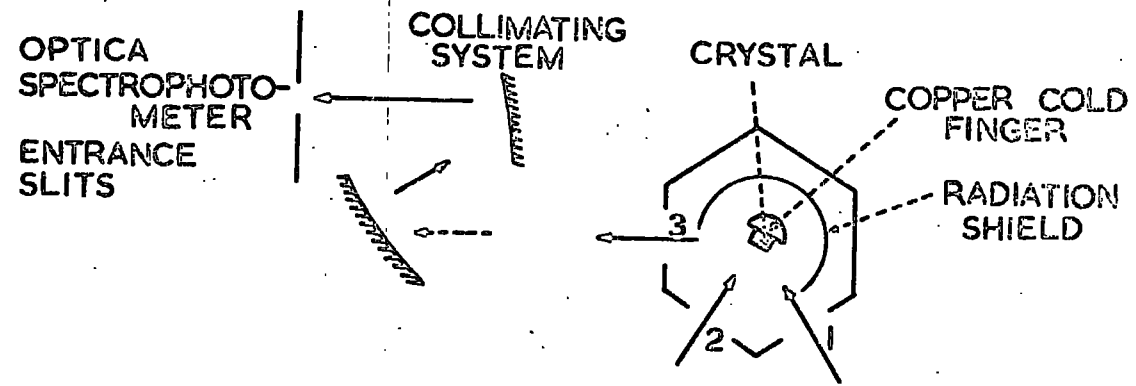


FIG. 3-4. Diagrammatic representation of the arrangement of the cryostat and optical collimation system.

~0.34 to 2.6 microns. (Optica absorption measurements showed the following characteristics:

Filter	3650Å value	IR value (different detector)	6200 Å value
50%	52.5%	45%	50%
30%	35%	25%	30%
10%	12%	7%	10%)

3.6 Optica CF 4N1

The Optica CF 4N1 is a double beam, recording, grating spectrophotometer, principally designed as an absorption measuring instrument, and has a workable spectral range of 0.135 to 3.200 microns. As an emission measuring instrument, the spectral range is reduced by the response of the detectors. The Optica proved to be a reliable and swift means of determining the relative intensity of the various components of the edge emission of CdS single crystals.

For absorption spectroscopy, two sources were provided; a hydrogen lamp for the 0.135 to 0.450 micron range and a tungsten lamp for the 0.32 to 3.20 micron range. A rotatable wheel was mounted over the input aperture of the monochromator. The wheel contained a selection of filters for the suppression of the higher spectral orders of the gratings, and stray light. No filters were necessary when the hydrogen lamp was used, nor in the visible region. However, when the tungsten lamp was used, or when analysing emission spectra, the appropriate filter had to be inserted. These were:

- F 1 A blue filter for the 0.32 - 0.40 micron range
- F2 A red filter for the 0.62 - 1.20 micron range
- F3 An infra-red filter for the 1.2 - 1.8 micron range
- F4 An infra-red filter for the 1.8 - 3.1 micron range

The monochromator was of the Littrow type, with two interchange-

able plane gratings as the dispersive elements. For the ultraviolet and visible regions (0.185 to 1.000 microns), a 600 lines/mm ruled grating with a dispersion of $16\text{\AA}/\text{mm}$ was provided. For the near infrared region (0.9 to 4.0 microns), a 300 lines/mm ruled grating with a dispersion of $32\text{\AA}/\text{mm}$ was used. The grating could be changed by turning a handle on the monochromator. The focal lengths of the common collimator was 0.8 meters, and its diameter 80mm. The wavelength scale followed a helical path on a disc rigidly attached to the wavelength drive unit.

The light leaving the monochromator entered the double beam system, a unit rigidly bolted to the monochromator. A lens, the only lens in the instrument, condensed the light onto a system of mirrors, see figure 3.5. A rotating mirror and a fixed mirror in each beam passed the light through the reference and sample cells alternatively, at 18 cycles per second. The single detector always saw the light from the two cells along the same optical path. For absorption measurements, this system avoided any necessity to compensate for the spectral response of the detector, the spectral emission of the source and any absorption due to sample holders or containers - provided that a matched pair of containers were always used. An induction generator, connected with the rotating axis of the mirrors, provided an electrical signal to a relay which switched the two measured and amplified detector signals. The ratio was displayed on the Honeywell chart recorder.

The slit width of the monochromator was servo controlled by the reference signal level, so that the output from the detector due to radiation which had passed through the reference cell was kept at a constant value. When switched to the "single beam mode" for the study of an emission spectrum focussed onto the monochromator input aperture,

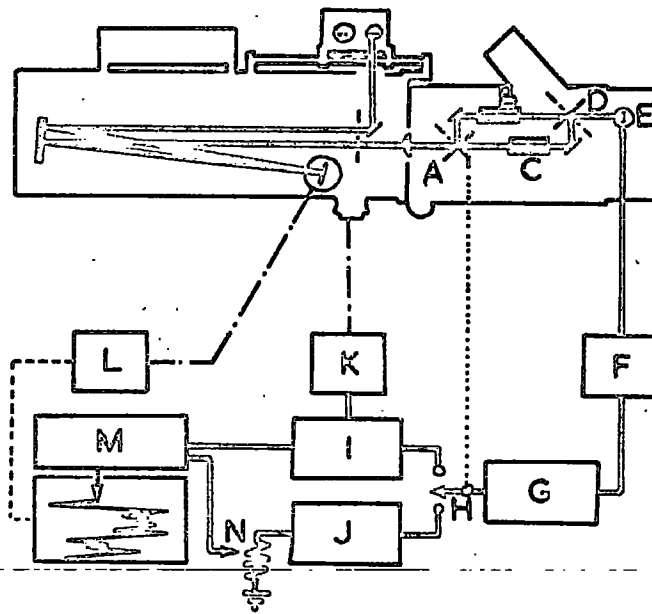


FIG. 3-5. Block diagram of the Optical spectrophotometer

- | | |
|-------------------|--------------------|
| A Rotating mirror | H Commutator |
| B Reference cell | I Reference Demod. |
| C Sample cell | J Sample Demod. |
| D Rotating mirror | K Slit Servo |
| E Detector | L Wavelength drive |
| F Pre-amplifier | M Pen recorder |
| G Amplifier | N 100% adjust |

an independent electrical reference signal replaced that provided by the reference beam on the detector. Thus a constant reference level was provided, and the ratio system of recording was preserved; whilst the servocontrol of the slit system was no longer required. The slits were set to suit the intensity of light being studied, and the bandwidth or resolution required.

An RCA type 1P28 (9 stage, S-5 response) photomultiplier was the detector provided for the 0.2 to 0.62 micron range. A Kodak Ektron lead sulphide detector was provided for the 0.62 to 3.2 micron range. The spectral sensitivities of these detectors are shown in figure 3.6, notice the difference in the scale of the two characteristics. A transistorised E.H.T. stabilised power unit, which incorporated six push-buttons (noted P.V. 1 to 6) to provide sensitivity variation, supplied 850 volts to the photomultiplier. Figures 3.7 shows the effect of the P.V. setting for a constant monochromator slit width, and the effect of the slit variation for a constant P.V. setting, upon an incident emission spectrum signal (i.e. the instrument operating in the single beam mode). The y-axis, or "factor" was obtained by dividing the recorder deflection at the variable P.V. or slit setting by the deflection obtained at P.V.6 or slits 1 respectively. These "factors" were used, where necessary, to estimate the intensity of the emission components of different crystals relative to the standard P.V.6, slits 1. Throughout the course of these recorded experiments, the "time constant" of the system was set at "normal", and the amplifier "gain" at 6 (in the range 0 - 10). These settings were used to keep the noise at a reasonable level whilst maintaining a pen response in keeping with the spectra being studied.

Synchronous motors were used to drive both the paper advance of the recorder and the grating - wavelength scale system. Since the

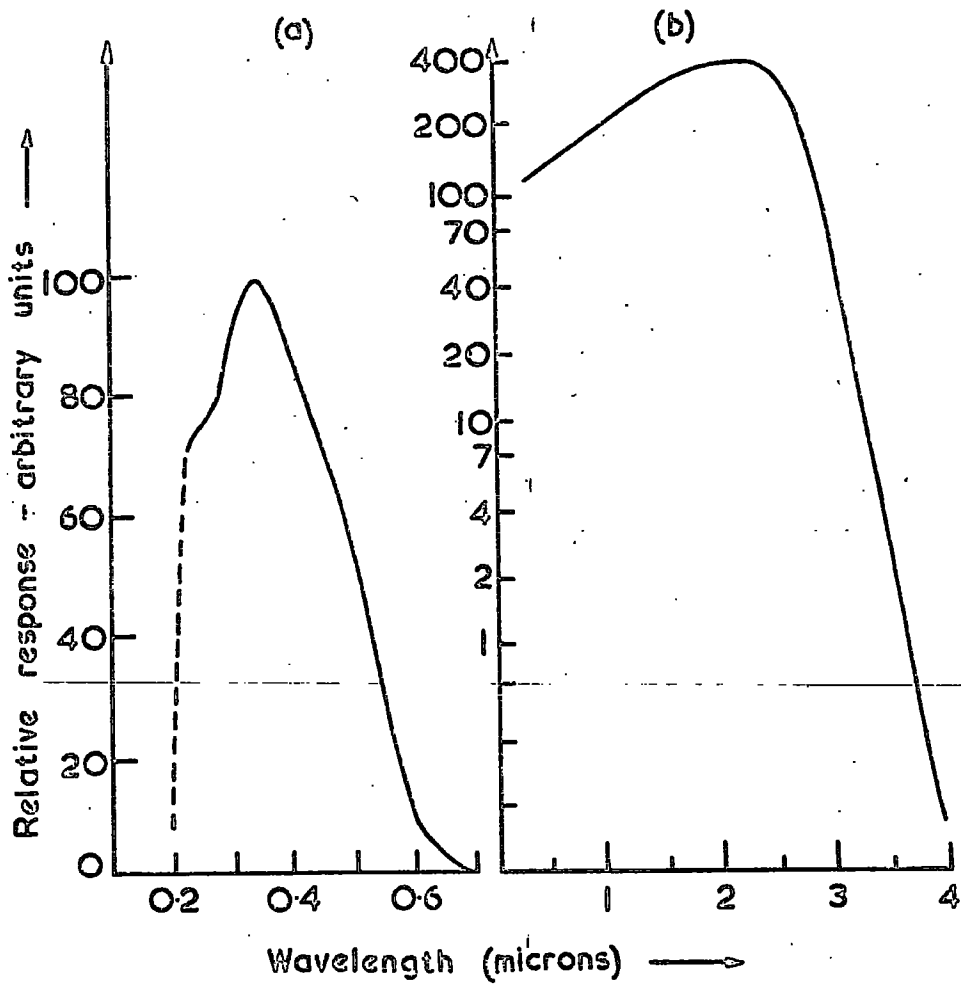


FIG. 3-6. Spectral sensitivity characteristics of (a) Type 1P28 (S-5 Response) photomultiplier and (b) Kodak Ektron PbS detector.

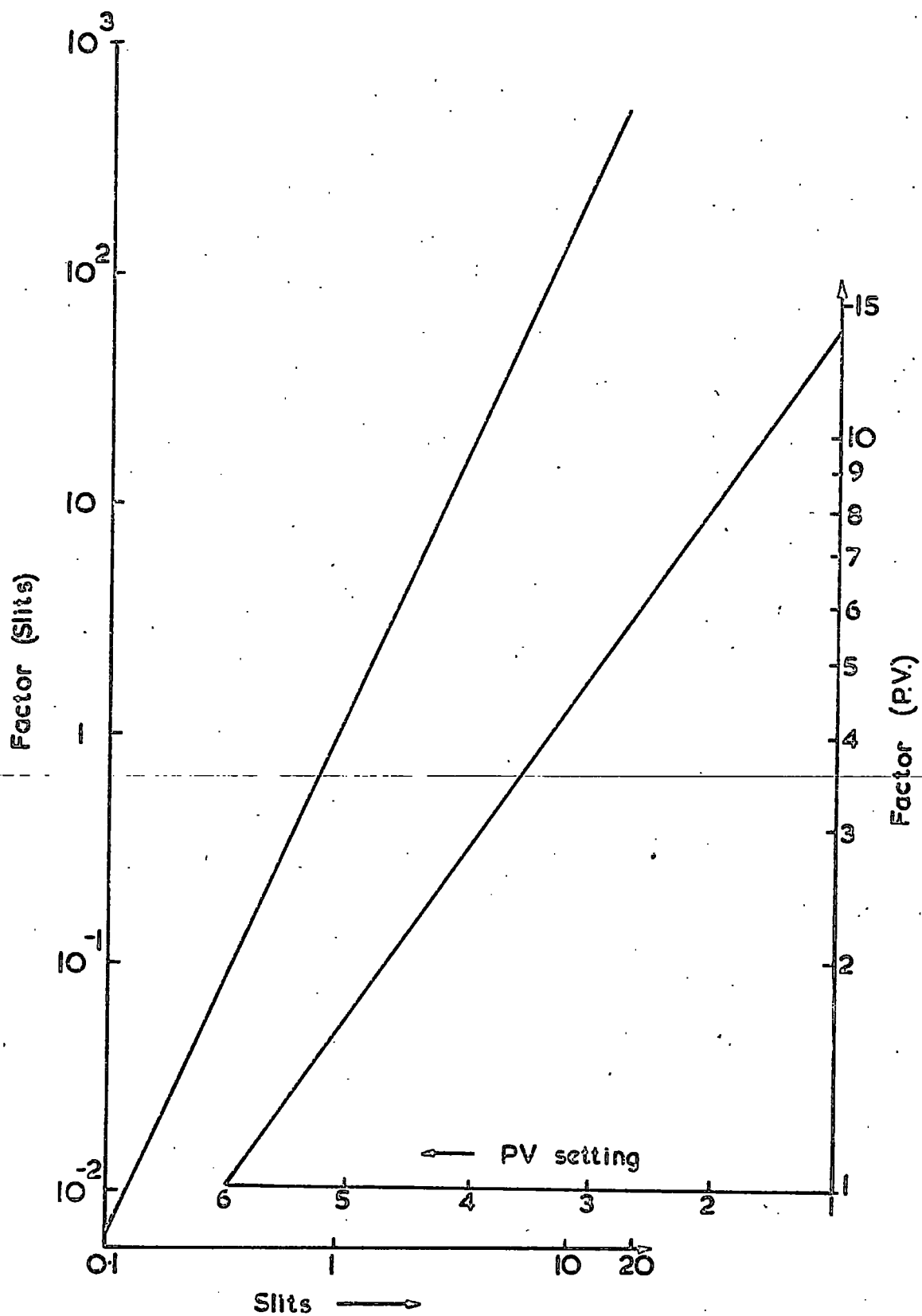


FIG. 37. "Correction factors" used to convert the intensity of the emission to the standard of P.V.1, Slits 1. (Slits 1 \equiv Bandwidth 3.2 Å)

dispersion of a grating is linear, the wavelength analysis of the paper record was simple. The wavelength scan speeds were approximately 0.5, 1 and 2 Å per second, or with another motor; 3, 6 and 12 Å per second. The chart speeds available were 2, 4, 6 and 8 inches per minute. The 2 inches per minute chart speed used in conjunction with the slower wavelength drive motor was found to give good, reproducible records of the green edge emission spectra.

The emission spectra of cadmium, sodium, mercury, helium and neon discharge tubes in the spectral range of particular interest (0.48 to 0.56 microns) were recorded using the Optica. The wavelengths were on average 5 ± 1 Å higher than the accepted values for the emission lines. The emission lines were reproducible to within one to two Angstroms. Thus the Optica was useful as an instrument to investigate the edge emission under different excitation conditions, and to differentiate between the various exciton lines. To obtain more accurate wavelength measurements, it was necessary to use the Bausch and Lomb spectrograph.

3.7 Bausch and Lomb Spectrograph

A model 12 Bausch and Lomb 1.5 metre grating spectrograph, was used to record the emission spectra. The spectral ranges 0.45 to 0.70 microns and 0.225 to 0.35 microns were covered by the first and second orders of the grating, with dispersions of approximately 10 and 5 Å/mm respectively. The instrument is shown diagrammatically in figure 3.8(a).

The slit system incorporated four components:

- i) A simple shutter, manually operated.
- ii) A step-filter-field lens, which focussed incoming radiation onto the grating. Three light transmission values (6, 25 and 100% transmission) were available for quantitative analysis. Rotating the lens through a right angle allowed full 100% transmission, the normal working position.

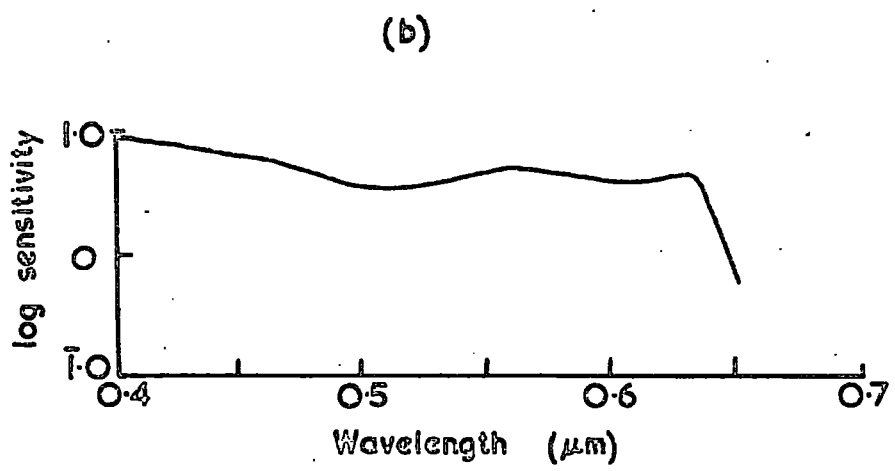
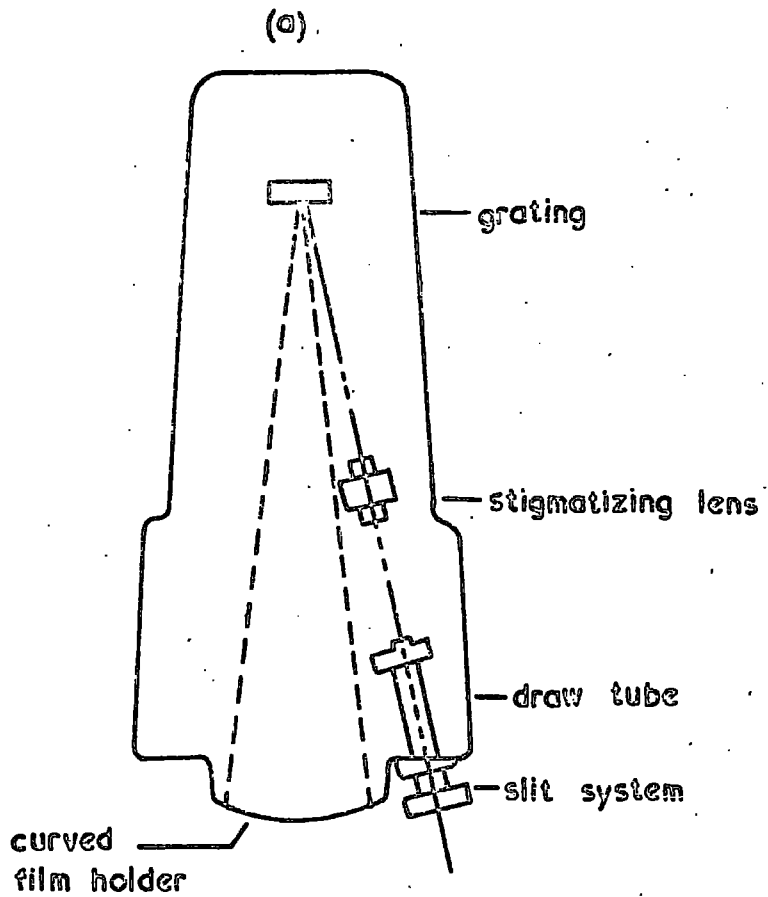


FIG. 3-8. (a) Diagram of the Bausch and Lomb 1.5 m grating spectrograph.
 (b) Spectral response of Kodak "Tri-X" Pan film.

- iii) A Hartmann slide which controlled the height of the spectrum recorded on the film. A sliding fish tail could be used to vary the height of the spectrum from 1.0 to 15 mm. Alternatively, a diagonal slit in the slide, providing a fixed spectral height of 1.5 mm, could be moved across the input aperture allowing eleven exposures to be made on the same film. This latter system was normally used, since it reduced the interference of the calibration lines with the spectrum being investigated.
- iv) A fixed slit assembly providing three fixed slit widths of 10, 32 and 60 microns which could be inserted into the optical path as required. A second, "Durham-made" slit assembly, slit width 0.5mm, was sometimes used for the investigation of weak spectral emissions which did not require such high resolution.

The light travelled through the field lens, the Hartmann slide, and the slit, down a draw tube, which reduced scattered light, through a "stigmatizing" lens, and onto a grating (635.3 grooves per mm). The "stigmatizing" lens corrected for the astigmatism which is associated with any Rowland circle spectrograph. The radiation was diffracted onto the film which was held in a specially curved cassette, such that the dispersion remained linear along the length of the film. Kodak "Tri-X" Pan 35mm film was used to record the spectra. The spectral response of this film, shown in figure 3.8(b), is substantially uniform over the spectral range of interest. Undiluted "Microdol-X" in a tank was used to develop the films, which were then rinsed and fixed in "Kodafix" before a final thirty minute wash.

The same arrangement was used to collimate the luminescence as that shown in figure 3.4. In cases of weak spectral emission, the

luminescence, excited via window "one", was collected via window "two". This meant that the full face of the crystal was "seen", rather than the edge, and so more light could be collected. The exposure required to obtain a measureable image intensity depended upon the alignment and the focussing of the image on the slits, and upon the nature of the spectra. Weak emission due to the excitons was more easily distinguished from the background than that of weak broad emission due to green edge recombination.

3.8 Analysis of Results

A Hilger and Watts Microdensitometer was used to analyse the films. A helium discharge tube provided calibration lines, and allowed measurement of the dispersion for each film. The optical density of the film was monitored by measuring the light transmitted by the film. The light was focussed onto the film, and collected on the other side by a microscope objective arrangement; which focussed the transmitted light onto an adjustable slit system in front of a selenium cell. The output from the cell, was displayed on a galvanometer. The slit width was adjusted to be as narrow as possible whilst still providing a measureable signal level, and was maintained constant throughout the scanning of a film. The most convenient slit width was found to be about 0.8mm. A screw system was used to move the table on which the films were clamped, thus passing the film across the field of view of the objective. The screw was turned by hand, the distance traversed was read off a drum, and the film density was obtained from the galvanometer deflection.

The spectrographic results which are discussed later are presented in terms of wavelength versus the galvanometer deflection observed. To obtain any form of comparison between crystals, it would be necessary

(1) to ensure that the focussing and alignment of the collimation system was maximised for each sample. This is possible when using the Optica with a meter output, but very difficult with the spectrograph.

(2) to correct for the logarithmic response of the film, the slit width of the spectrograph and the response and slit width of the microdensitometer.

(3) to allow for the possibility of variations in developing effectiveness.

Since the narrowest bandwidth of the spectrograph was approximately equal to the reported apparent linewidth of the bound exciton emission lines, (3), no measurements of the linewidth of any exciton spectra were made.

The chart output of the Optica provided a record of the emission intensity per unit wavelength interval versus wavelength. The sensitivity of the photomultiplier fell only by about 50% of its value at 0.48 microns by the time it was in the 0.56 micron region. It was not necessary to correct the chart output of the Optica for the response of the photomultiplier because no comparison of the intensities of the green edge and exciton emission was required. The results from the Optica are therefore presented without correction. The peak heights obtained from the charts were corrected to the 'standard setting' of P.V.6, slits 1, as described in the section concerning the Optica, in order to compare the intensities of the components of the different crystals. The peak intensities of the satellite phonon peaks of the green edge emission were corrected for the photomultiplier response prior to the evaluation of the distribution of the number of emitted photons per photon.

References

- (1) L. Clark and J. Woods (1968) *J. Crystal Growth* 3, 4, 127.
- (2) D. W. Nyberg and K. Colbow (1969) *Can. J. Phys.* 45, 3333.
- (3) D. G. Thomas and J. J. Hopfield (1962) *Phys. Rev.* 128, 2135.

CHAPTER 4

STOKES EXCITED EDGE EMISSION OF UNDOPED CADMIUM SULPHIDE

4.1 Introduction

The edge emission of undoped cadmium sulphide excited by Stokes (ultra-violet) radiation was studied at liquid helium and liquid nitrogen temperatures. The crystals were grown under controlled partial pressures of the constituent elements, as described in Chapter three. At liquid nitrogen temperatures, longitudinal optical (L.O.) phonon assisted free exciton and green edge emission was observed. As the temperature was reduced, the intensity of the emission generally increased. At liquid helium temperatures bound exciton recombination and two green edge emission series could be detected in the majority of crystals.

It was found that the relative intensities of the major components of the U.V. excited emission at liquid helium temperatures could be correlated with the conditions under which crystals were grown, provided that the starting charge was of a consistent, good quality. The Optica spectrophotometer was used to determine these basic trends, while the Bausch and Lomb grating spectrograph was used to make a more detailed study of the components of interesting spectra.

In this chapter, a brief description of the characteristics of the edge emission at liquid nitrogen temperatures is followed by a description of the characteristics at liquid helium temperatures, and their dependence upon crystal growth conditions. Recorded observations of some individual crystals are presented as illustrations of the characteristics. Unless otherwise specified, the measurements were recorded by the Optica, and are presented uncorrected for possible wavelength variation or photomultiplier response. When two recordings have been superimposed in the same figure, the emission intensities

are not directly comparable where the term "Emission intensity (arbitrary units)" is used. "Relative emission intensity" means that the curves may be compared directly. The characteristics of the edge emission of crystals supplied by A.E.I. Limited and Hull University, which were much the same as those of crystals grown at Durham, are briefly described. Table 4.3 outlines the features of the emission characteristics illustrated in the figures of this chapter.

4.2 Edge Emission Characteristics at Liquid Nitrogen Temperatures

The "blue" and "green" components (1) of the U.V. excited edge emission of a crystal (No. 180) grown under an excess of cadmium pressure of approximately one atmosphere are shown in figure 4.1. This illustrates the form of the edge emission of CdS at liquid nitrogen temperatures. The blue edge emission contained emission "lines" which were broad compared with the sharp bound exciton lines which are observed at liquid helium temperatures. The major "blue" maxima were observed at approximately 4888 and 4950Å, and are attributed to the zero and first longitudinal optical (L.O.) phonon replicas of the emission which accompanies the annihilation of a free exciton. These results are in agreement with the maximum of 4883Å observed by Voigt and Spiegelberg (4) which they associated with a zero phonon replica of an exciton transition having the highest energy point of the distribution of the emission at 2.543eV (4875Å). As the intensity of the excitation was varied, the height of the first L.O. component of the blue emission varied as I^n , where I is the excitation intensity and n the index. Figure 4.2 shows the excitation intensity dependence of the height of the first L.O. component, the value of the index (n) obtained was 1.5 ± 0.1 .

The first maximum in the spectral distribution of the green emission occurred at 5164 Å. Replicas of this first component were observed on the low energy side of the emission, see figure 4.1. The separation of the

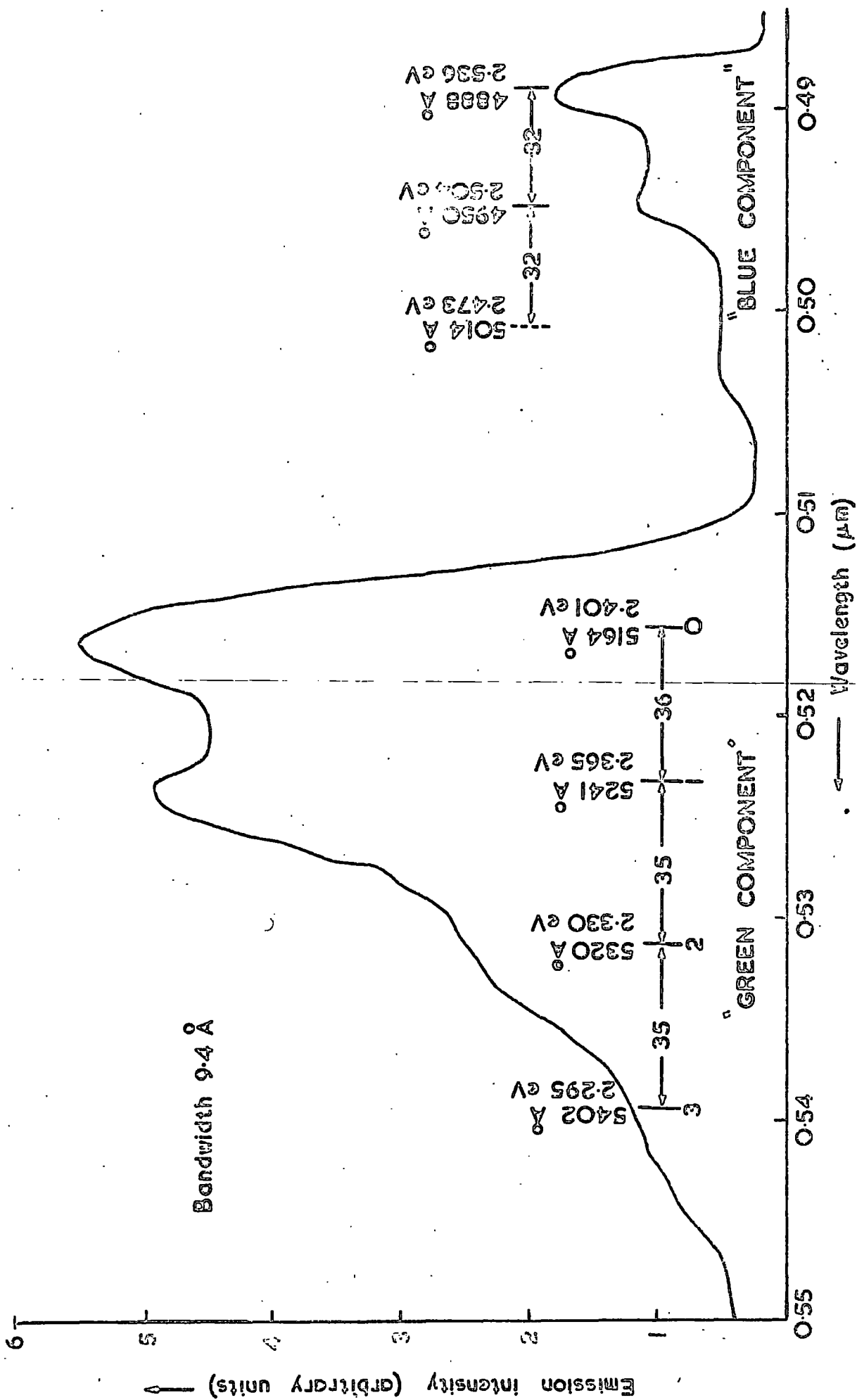


FIG. 41. The S.E.D. of the "blue" and "green" components of the edge emission of CdS at 80°K excited by U.V. radiation

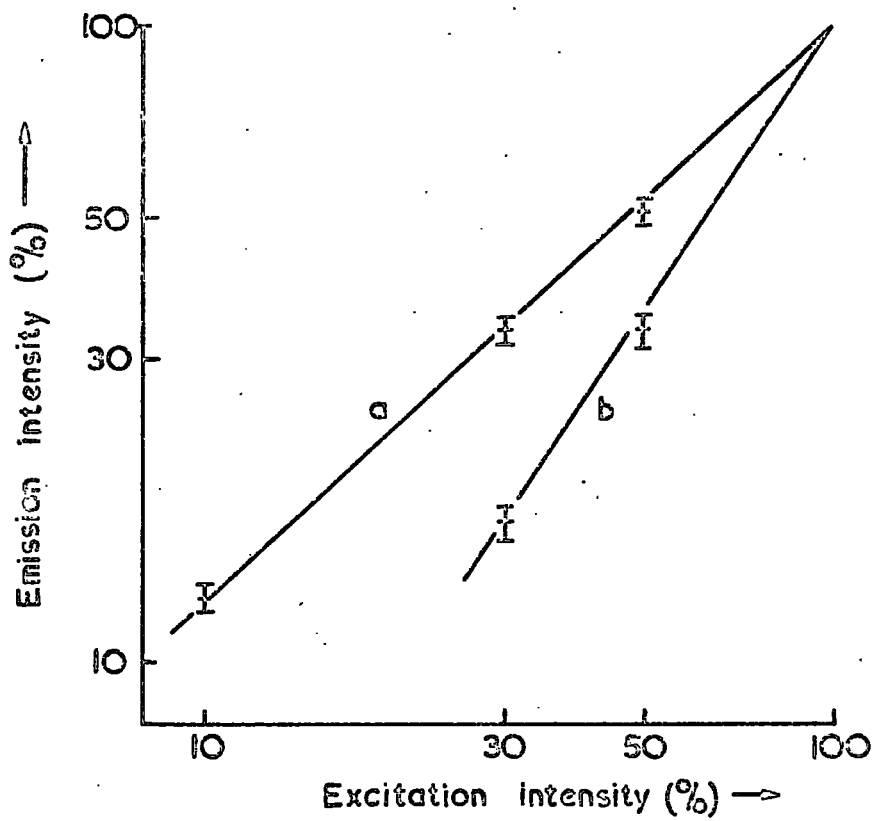


FIG.4.2. The dependence of the intensity of a) the green emission and b) the blue emission of CdS at 80°K upon the intensity of the UV. radiation.

components was about 35 meV, which is approximately equal to the L.O. phonon energy of 38 meV. The green edge emission at liquid nitrogen temperatures has been attributed to phonon assisted recombination between free electrons and holes bound to acceptor levels some 0.14 (2) to 0.17 (3) eV above the valence band. This "Schön-Klasens" (5 & 6) model is supported by the photoconductivity and luminescence measurements of Spear and Bradberry (7). Variation of the intensity of excitation by two orders of magnitude did not lead to any displacement in the wavelengths of the maxima. However the height of the zero phonon component of the green edge emission varied as I^n , where I is the excitation intensity and n was, typically, 0.93 ± 0.04 , see figure 4.2.

The broad nature of the edge emission at liquid nitrogen temperatures made the precise measurement of the maxima of the components difficult. For example, the values of the L.O. phonon energy obtained for the green and blue components, see figure 4.1, were different. The widths at half height of the green emission components at liquid nitrogen temperatures were approximately twice those at liquid helium temperatures. As a result, the spectra could not be readily resolved into separate phonon components, and no attempt was made to fit any mathematical form of distribution to the heights of the phonon components. The value of 5164 \AA for the first maximum of the green edge emission leads to a value of $(2.57 - 2.40) = 0.17 \text{ eV}$ for the separation of the acceptor level from the valence band, assuming the band gap is 2.57 eV at liquid nitrogen temperatures. This provides close agreement with Colbows (3) value of the acceptor energy of the 0.17 eV.

4.3.1 Edge Emission Characteristics at Liquid Helium Temperatures

The edge emission of cadmium sulphide excited by 3650 \AA radiation

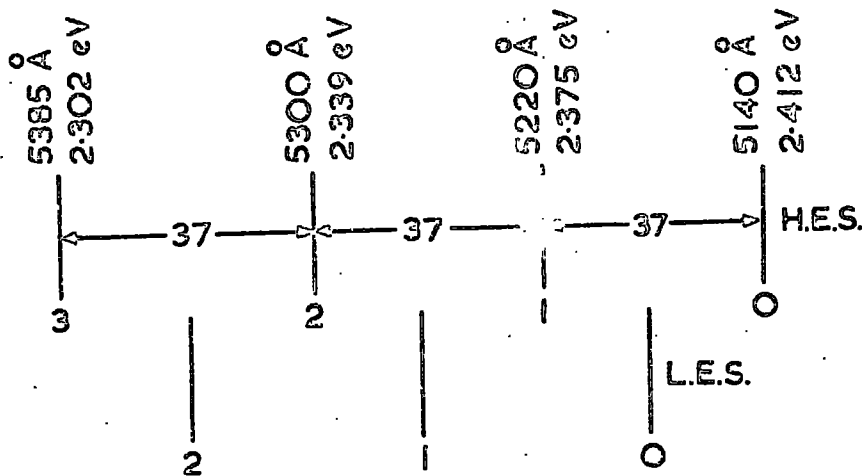
at liquid helium temperatures consists of two major components described as the "green" and the "blue" emission (1). The green emission can contain two L.O. phonon assisted series. The higher energy series has its zero phonon component at 5140 \AA , whereas the lower energy series has its zero order component at 5170 \AA . The high energy series (H.E.S.) has been assigned to recombination between free electrons and holes bound to acceptor levels some 0.17 eV above the valence band (3). The low energy series is due to the distant pair recombination of electrons bound to shallow donors and holes bound to the acceptors (3). The "blue" emission is attributed to the annihilation of free and bound excitons, and their phonon replicas. From Zeeman effect studies of the I_1 (4889 \AA) and I_2 (4867 \AA) exciton lines, Thomas and Hopfield (8) identified I_1 and I_2 with the annihilation of excitons bound to neutral acceptors and donors respectively.

Edge emission components were identified by comparing their wavelengths with the reported values. The behaviour of these components under different excitation conditions and the variations of the spectra from crystal to crystal suggest that these assignments were correct. With the exception of one sample, the I_2 emission could not be resolved using the Optica. However with the Bausch and Lomb spectrograph, it was possible to demonstrate that the I_2 emission often contained several components. The components of the I_2 emission may be correlated with I_{2A} (4867.2 \AA neutral donor, doublet nature), I_{2B} or I_5 (4869.1 \AA neutral donor) and I_{2C} (4870.2 \AA neutral donor) emission (8, 9, 10). Although the I_3 (4861.7 \AA ionised donor) emission was not observed, it is sufficiently far removed from the I_2 exciton to have been resolved by the Optica. In conclusion therefore, the " I_2 emission" recorded by the Optica is essentially an integration of the

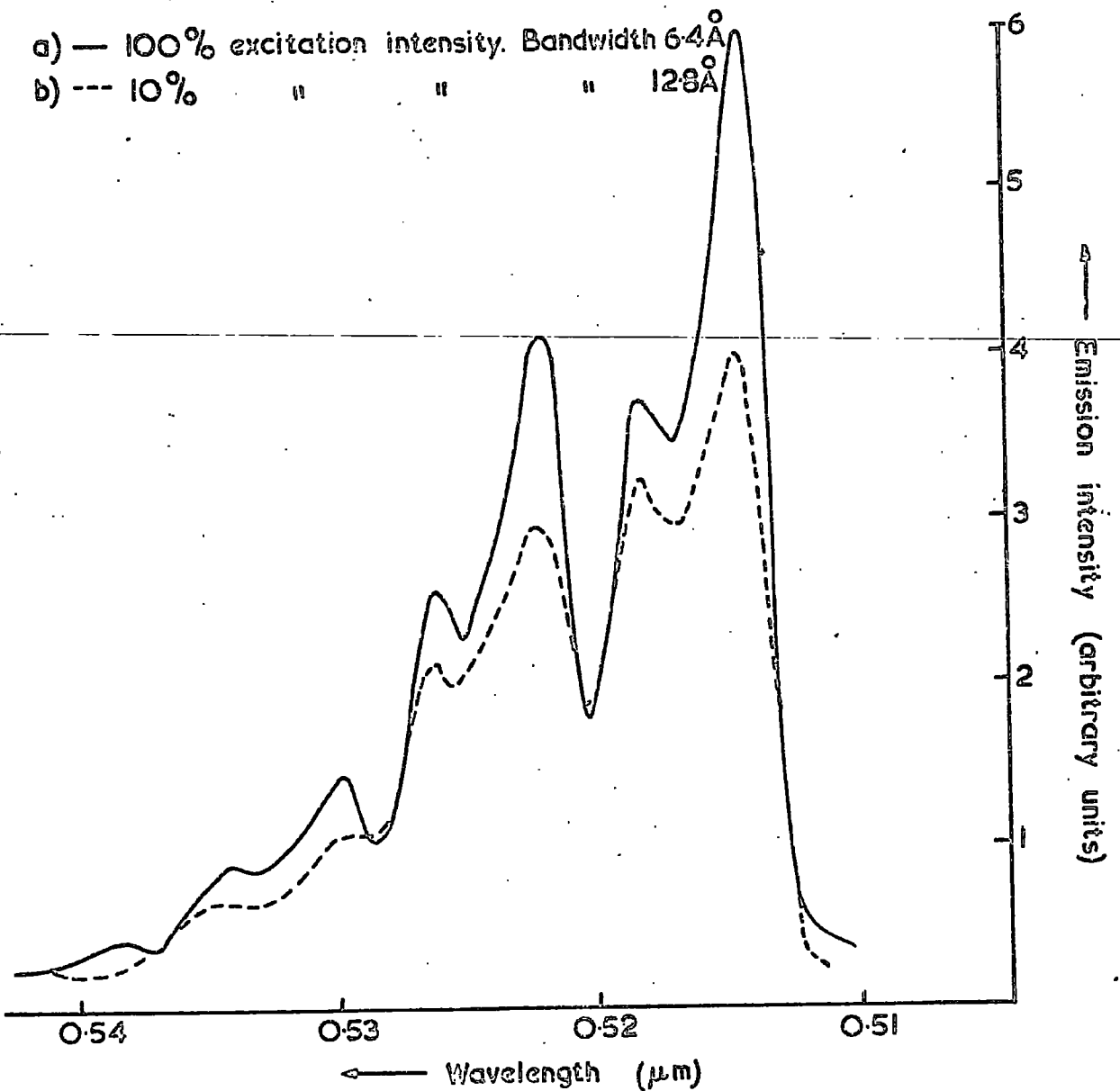
emission of all the excitons bound to neutral donors. The green edge emission components were more readily resolved.

4.3.2 Green Edge Emission

Figures 4.3 and 4.4 show clearly the presence of the two series in the green edge emission of U.V. excited cadmium sulphide at liquid helium temperatures. In figure 4.3 the intensity of the H.E.S. was greater than that of the L.E.S., The zero order phonon component of the H.E.S. was observed at about 5140 \AA , with repeated components at lower energies with energy spacing of 37 meV. Similarly in figure 4.4, where the intensity of the L.E.S. was greater than that of the H.E.S., the zero order phonon component, at about 5188 \AA , was repeated at lower energies with spacings of 37 meV. This repetition is associated with the simultaneous emission of a longitudinal optical phonon (11). The spacings are in agreement with the values for the L.O. phonon energy in CdS obtained from infra red reflectivity measurements (12). The maximum of the zero phonon component of the L.E.S. in figure 4.3 was at approximately 5180 \AA , while the first maximum of the H.E.S. in figure 4.4 was at approximately 5141 \AA . It will become evident, as further results are presented, that the positions of the maxima of the zero order phonon components of the green edge emission of undoped and doped crystals were not observed at one fixed wavelength, but fell within a range of wavelengths. The maxima of the zero order phonon components which lay within the range 5135 to 5155 \AA were assigned to the H.E.S., while those within the range 5170 to 5200 \AA were assigned to the L.E.S. recombination processes. Handelman and Thomas (9) made the same assignments having observed similar variations in the position of maxima. These authors also reported that there was no change in the relative intensities of the H.E.S. and L.E.S. at temperatures of



a) — 100% excitation intensity. Bandwidth 64Å
 b) - - - 10% " " " 128Å



G.4.3. The S.E.D. of the green emission excited by a) 100% and b) 10% intensity U.V. radiation, illustrating the two series

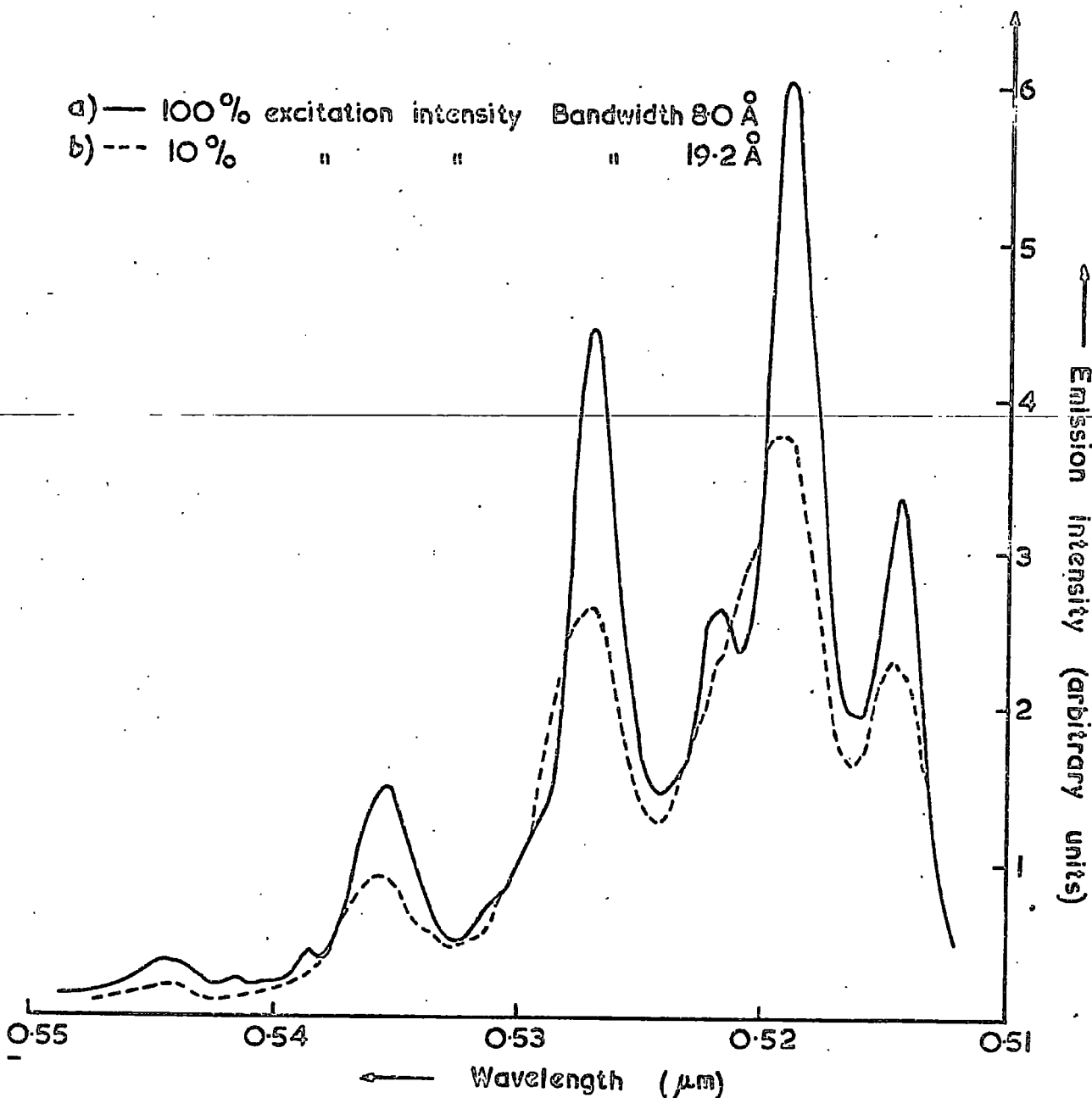
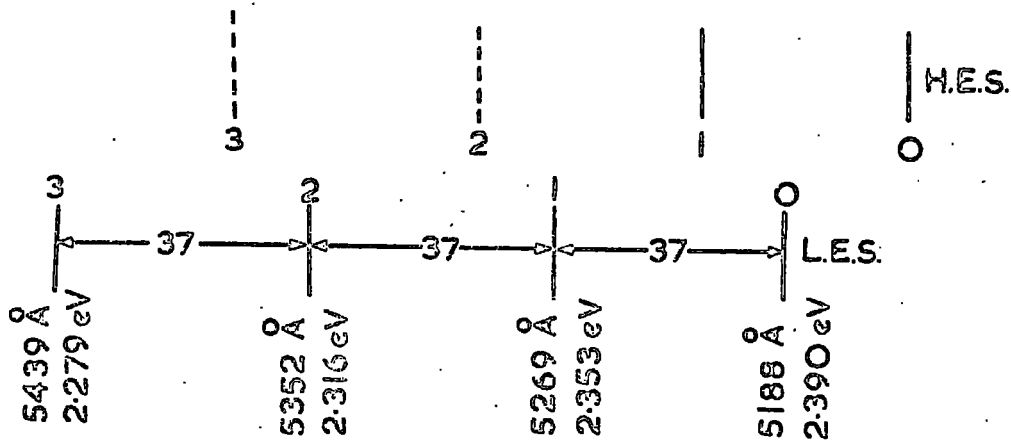


FIG. 4-4. The S.E.D. of the green emission excited by (a) 100% and (b) 10% intensity U.V. radiation, illustrating the two series.

20, 4.2 and 1.6°K, when both series were simultaneously present in a crystal.

Two spectra have been superimposed in figures 4.3 and 4.4, to illustrate the effect of the variation of the intensity of excitation, using neutral density filters, upon the position of the maxima. The L.E.S. was observed to shift towards longer wavelengths as the excitation intensity was reduced. This is more obvious in figure 4.4 than figure 4.3. The shift is illustrated more clearly in figure 4.5 which shows the spectral distribution of the L.E.S. dominated green edge emission of a CdS crystal under 100 and 0.1% U.V. excitation. Figure 4.6 shows the shift with excitation intensity of the energy of the maximum of the zero phonon component of the L.E.S. emission of the crystal of figure 4.5. The gradient of the best fit obtained for this crystal, the solid line of figure 4.6, was equal to 2.2 meV per order of magnitude change in the excitation intensity. The shift in the maximum of the zero phonon component of the L.E.S. emission averaged over five undoped crystals was 2.2 ± 0.4 meV per order of magnitude change in the excitation intensity. This error was used to obtain the dashed lines of figure 4.6. The estimated experimental error of three points lay within the calculated error of the mean.

Since the H.E.S. was never found without a substantial L.E.S. component at liquid helium temperatures, it was difficult to determine whether there was any wavelength shift of the H.E.S. series with excitation intensity. The zero phonon maximum of the green emission of crystal number 78, grown at 1150°C under a "controlled" cadmium pressure of 0.3mm which showed the highest H.E.S. to L.E.S. intensity ratio, was observed to shift from 5150 to 5157 to 5164 Å as the excitation intensity was reduced from 100 to 10 to 1%. The asymmetry

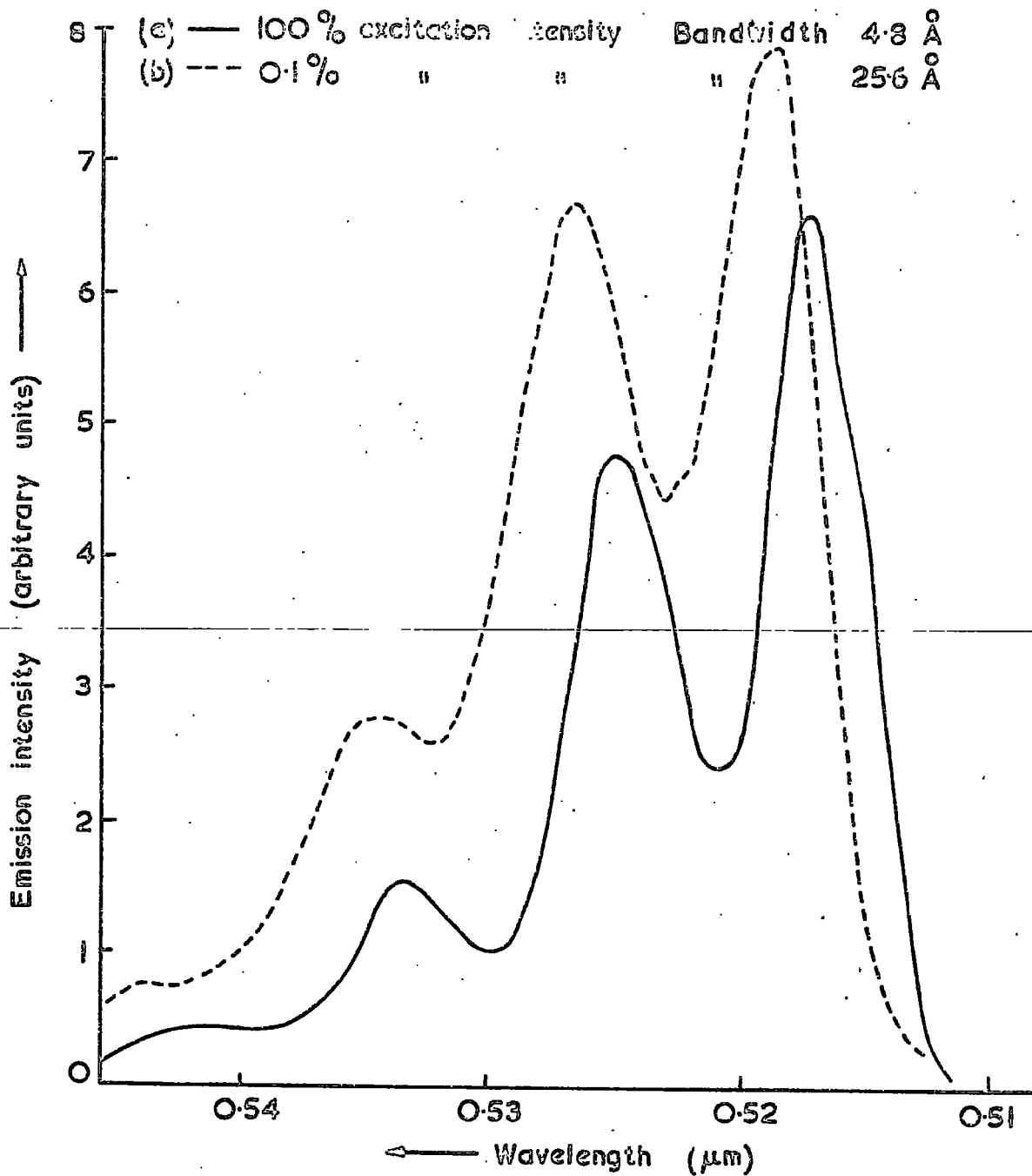


FIG. 4.5. The S.E.D. of the green emission excited by (a) 100% and (b) 0.1% intensity radiation, illustrating the "J shift."

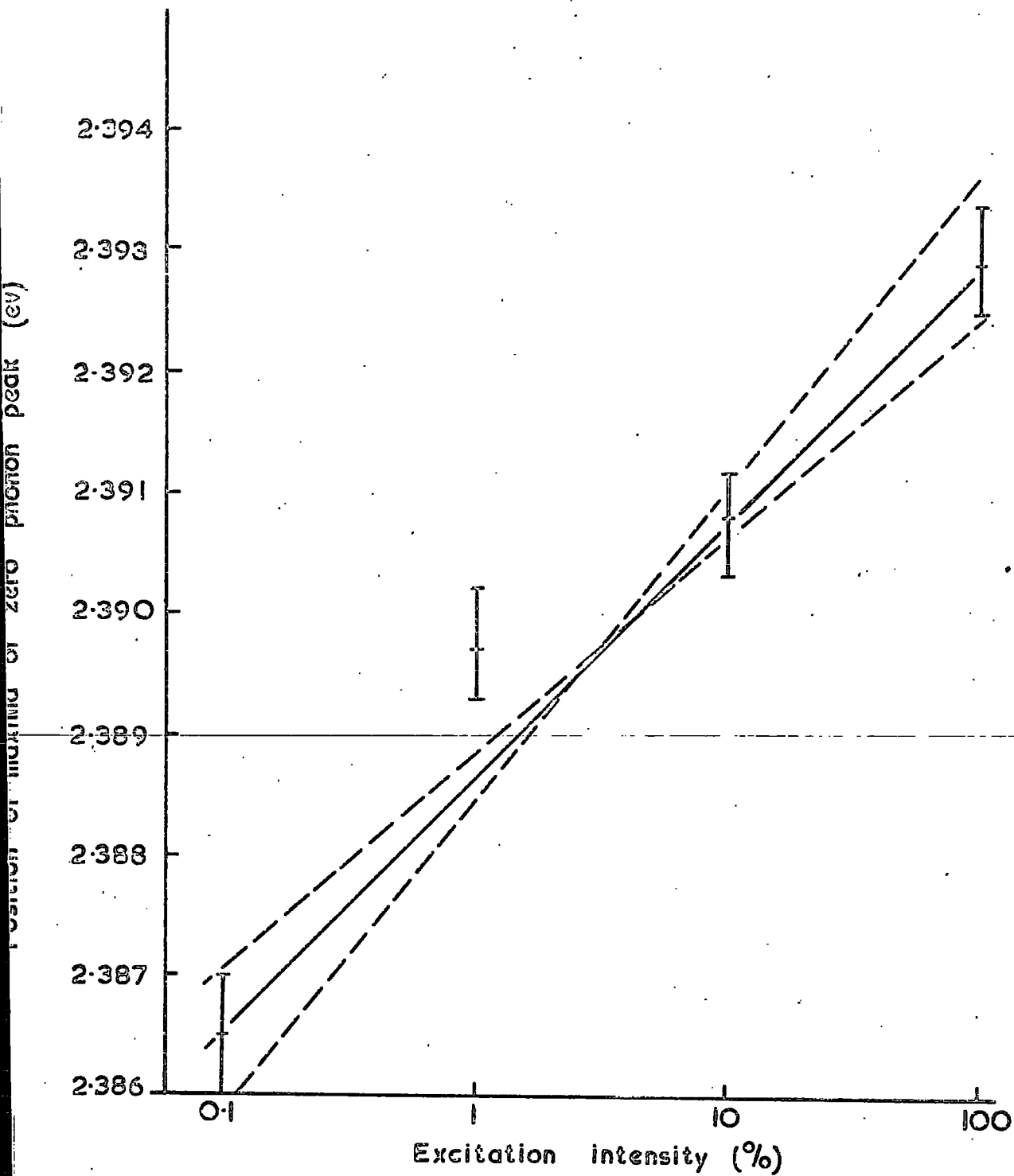


FIG. 4.6. The dependence of the energy of the maximum of the zero phonon component of the L.E.S. emission upon the intensity of the UV excitation.

of the zero phonon component indicated that there was some L.E.S. emission present. Anti-Stokes excitation, which was found to excite the emission of the L.E.S. alone in all crystals (see chapter five), confirmed that the L.E.S. recombination mechanism was operative in this crystal. The observed shift could possibly be explained by the L.E.S. to H.E.S. intensity ratio increasing as the excitation intensity decreased. The resultant envelope would then appear to shift towards longer wavelengths as the relative size of the L.E.S. increased, and shifted to longer wavelengths, while the H.E.S. remained constant. The dependence of the height of the zero phonon component upon the excitation intensity was higher than average in this crystal, i.e. $n = 0.75 \pm 0.01$. This could be explained if the first maximum is an envelope of the first maxima of the two series.

The maximum of the zero phonon component of the H.E.S. shown in figure 4.3 was shifted slightly to longer wavelengths as the excitation intensity reduced. This, once again, may be interpreted as the influence of the L.E.S. upon the observed emission. Since there was no shift with variation of excitation intensity of the green edge emission at liquid nitrogen temperatures, and as the H.E.S. recombination process at liquid helium temperatures was the same as that at the higher temperature (this was confirmed by monitoring the emission maxima as the crystal was cooled to liquid helium temperatures) it was concluded that there was little shift of the H.E.S. as the excitation intensity was varied.

The heights of the maxima of the zero phonon components of the spectra obtained under different intensities of excitation were corrected to the "standard" of intensity, (see chapter on Experimental apparatus and procedure). Figure 4.7 shows the relationship between the corrected emission intensity and the excitation intensity. 100% emission was that obtained when no neutral density filter was inserted in the exciting beam.

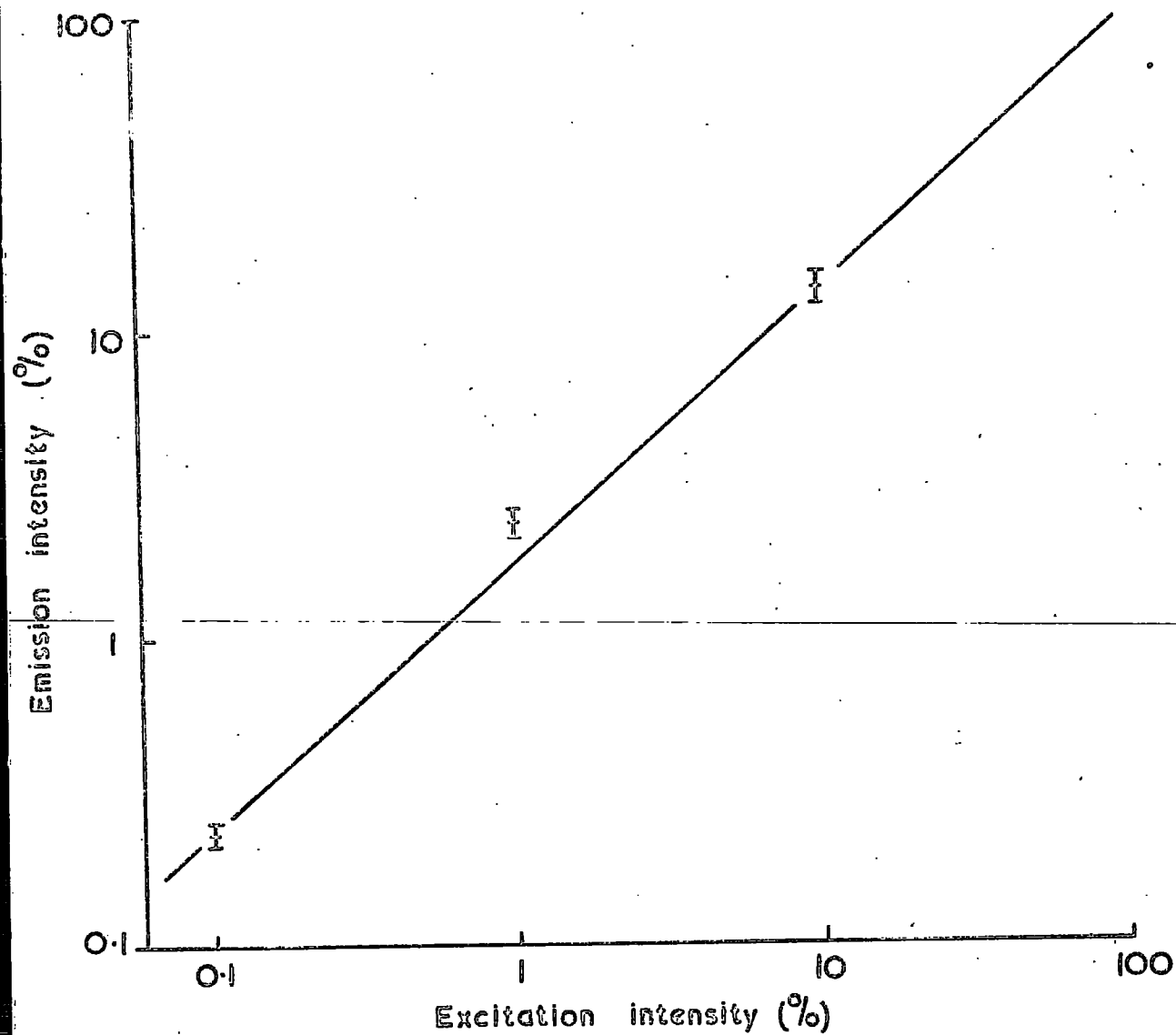


FIG.4.7 The dependence of the intensity of the zero phonon maxima of the green edge emission upon the intensity of the U.V. radiation.

The experimental values are those obtained from crystal No. 68 used in compiling figures 4.5 and 4.6. The "1% excitation intensity" points in figures 4.6 and 4.7 were both rather low compared with the other points, indicating that there may have been a systematic error. The value obtained for the intensity dependence index, n , for the crystal was 0.86 ± 0.02 . The mean value of n for the green edge emission, averaged over seven undoped crystals, was 0.85 ± 0.04 .

A Poisson distribution, for a fixed mean number of emitted phonons \bar{N} , was fitted to the heights of the maxima of the phonon components of the green edge emission. Hopfield (13) showed that the transition probability for a multi-phonon process, $P(m)$, is described by a Poisson distribution,

$$P(m) = (\bar{N}^m / m!) \exp(-\bar{N}),$$

where m is the number of phonons, and \bar{N} the mean number of emitted phonons "per event". The measured heights of the L.O. phonon components of the green edge emission were corrected for photomultiplier response and converted from the units recorded directly by the Optica, i.e. emission intensity per unit wavelength interval, to number of photons emitted per unit energy interval. (Multiplying by a factor of $(\text{wavelength})^2 + 1.24$, where the energy of the photon is in electron volts and the wavelength in microns, converted the wavelength interval to an energy interval. Multiplying by a further factor $(\text{wavelength}) + 1.24$ converted the "emission intensity" into "number of emitted photons".) The corrected heights were normalised so that the height of the zero phonon component ($m=0$) was unity. The normalised values obtained for the "100% excitation intensity" spectrum of the green edge emission of figure 4.5 (crystal No. 68) are compared with the values of $\bar{N}^m / m!$ in table 4.1. The value of \bar{N} is simply the normalised height of the first L.O. phonon component of the emission,

Table 4.1.

A comparison of the experimental and the theoretical phonon component heights, indicating a Poisson distribution having a mean $\bar{N} = 0.82$.

Number of Phonons (m)	Measured peak height (normalised)	Theoretical peak height $\frac{\bar{N}^m}{m!}$ for $\bar{N} = 0.82$
0	1.00	1.00
1	0.82	0.82
2	0.31	0.34
3	0.10	0.09

and was fixed for the evaluation of $\bar{N}^m/m!$ for any one crystal. The agreement between the measured and calculated heights, with \bar{N} equal to 0.82 for this crystal, indicates that the probability of a multiphonon emission process is described by a Poisson distribution.

Values of \bar{N} obtained for other crystals ranged between the extremes of 0.78 and 1.00. The mean of the mean of the distribution was 0.86 ± 0.02 , averaged over eleven crystals. The analysis included green emission spectra which were dominated by the H.E.S.

Discussion

Hopfield (13) developed a theory of the transition probability for a multi-phonon process involving recombination where one of the carriers is trapped at a level with a binding energy greater than the energy of the L.O. phonon. The result obtained was that the Poisson distribution described in the previous section should be observed. Fitting this distribution to the measurements of the peak heights of the edge emission determined by Klick (14), Hopfield found that $\bar{N} = 0.87$ for CdS at 4.2°K . In order to check the theory and the model, he calculated the radius "a" of the bound state corresponding to $\bar{N} = 0.87$, assuming that the charge distribution of the trapped carrier could be approximated by a Gaussian, then

$$\bar{N} = \frac{e^2}{a} \left(\frac{1}{2\pi} \right)^{\frac{1}{2}} \left(\frac{1}{E_{L.O.}} \right) \left(\frac{1}{n^2} - \frac{1}{\epsilon_0} \right)$$

where e is the electronic charge, $E_{L.O.}$ the energy of the longitudinal optical phonon, n the optical index of refraction and ϵ_0 the static dielectric constant. Substituting $\bar{N} = 0.87$, the value of a for CdS was found to be approximately 11 \AA , or approximately two lattice constants. In k space, this is approximately one-sixth of the distance from the centre to the edge of the Brillouin zone. Hopfield pointed out that the value of a obtained, and hence the limited k space extension of the

trapped carrier seemed to be consistent with the original assumption of near cubic symmetry for the trapping potential well which requires that the component wave functions for the trapped particle must be contained in a small part of the Brillouin Zone. He also felt that a mean radius of 22 \AA or $2a$ was not inconsistent with the binding energy of the trapped carrier.

The value of $\bar{N} = 0.86$ which was obtained from the results described in the present work for the H.E.S. and L.E.S. of the green edge emission and the corresponding value of a , approximately 11 \AA , are in excellent agreement with the values obtained by Hopfield. This indicates that at least one trapped carrier is involved in the recombination processes associated with the high and low energy series. The shift of the L.E.S. to lower energies with decreasing excitation intensity indicates that the emission was due to the phonon assisted recombination of an electron bound to a donor with a hole bound to a distant acceptor (15). The magnitude of the shift agrees with that observed by Thomas, Dingle and Cuthbert (19). The observation of the Poisson distribution of the phonon series, and the comparison of the positions of the maxima with those of other works (3), lead to the conclusion that the H.E.S. is due to the phonon assisted recombination of free electrons with holes bound to acceptors. The same acceptor level was probably involved in both recombination mechanisms (3). Assuming that the models are correct, that the same acceptor levels are involved in both mechanisms, that the values of 5140 and 5180 \AA are representative of those obtained for the maxima of the zero order phonon components of the H.E.S. and L.E.S. respectively, and that the band gap energy of CdS at liquid helium temperatures is 2.5826 eV (16), the acceptor and donor binding energies obtained by simple subtraction of values are 0.170 and 0.018 eV , respectively. The value of the acceptor binding energy is in agreement with that deduced by Colbow (3).

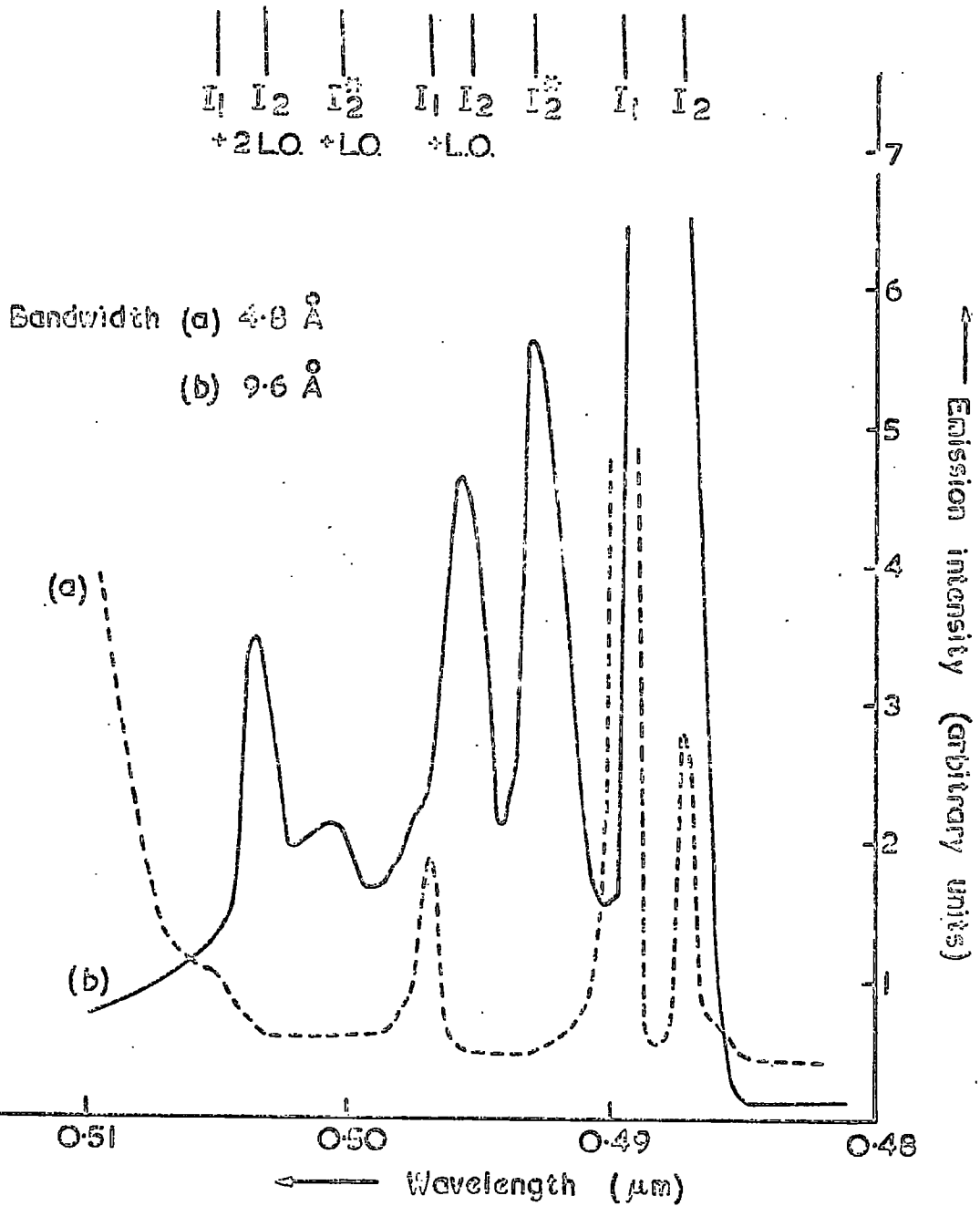
However, in the evaluation of the donor binding energy, no allowance was made for the Coulombic energy component which arises from the attraction between the bound hole and bound electron, and the value of 0.018 eV compares unfavourably with Colbow's value of 0.0305 eV.

To evaluate the effect of the Coulombic term, consider the relationship between the various energies involved. The energy, E_B , of the zero phonon component of the L.E.S., bound to bound transition is described by $E_B = E_G - (E_A + E_D) + E_C$, where E_G , E_A , and E_D are the band gap, acceptor and donor energies, respectively. E_C is the Coulombic term appropriate to a donor acceptor separation r , where $E_C = \frac{e^2}{4\pi\epsilon_0\epsilon_r}$. If the dielectric constant is taken as 10.33 (17), $r = 1.39/E_C$, where r is in \AA and E_C in eV. The problem is to determine r . It was observed that the L.E.S. shifted 2.2 eV to lower energy per order of magnitude decrease in the excitation intensity. Any change in E_B , dE_B , must be due to a change dE_C in E_C , since E_G , E_A and E_D remain constant under different intensities of excitation. Thus $dE_B = dE_C = 1.39dr/r^2$. For $dE_B = 2.2 \text{ meV}$, $dr \approx r^2 10^{-3} \text{\AA}$. dr represents the change in the mean separation of the donor acceptor pairs through which the recombination is proceeding when the excitation intensity is changed by one order of magnitude. If $r \sim 10 \text{\AA}$, $dr \sim 0.1 \text{\AA}$; such a small change in r could not encompass a sufficient number of donors and acceptors to account for the change in the luminescent intensity. If $r \sim 1000 \text{\AA}$, $dr \sim 1000 \text{\AA}$, which would imply that the luminescent intensity should saturate with increasing excitation intensity; this is not observed. It follows therefore that r must be of the order of 100\AA , when $dr \sim 10 \text{\AA}$, an estimate which is in agreement with Colbow's (3) conclusions. Thus a value for E_C of 0.014 eV was used as a correction for the Coulombic interaction, giving a value of E_D of 0.032 eV, which agreed more closely with Colbow's value of $0.0305 \pm 0.0005 \text{ eV}$.

Thus the conventional spectra obtained under continuous excitation could be analysed to provide a measure of the binding energies of the donors and acceptors involved in the green edge emissions. However, the variation in the position of the maxima of the series from crystal to crystal where the positions were expected to be the same, and through the depth of the crystal in the work of Handelman and Thomas (9), indicates that precise measurement of binding energies can only be obtained using some other method. Time resolved spectroscopy is undoubtedly the best method of determining accurately any differences in the level or levels responsible for the green edge emission in CdS, for example see the paper of Colbow (3). It is however reassuring to note the agreement between the estimates of r , E_A and E_D determined by the two methods.

4.3.3 Blue Edge Emission

Figure 4.8 illustrates the components and the phonon replicas which comprise the blue edge emission spectrum of two different CdS crystals at liquid helium temperatures, as recorded by the Optica. The major components of the curves a and b, I_2 and I_1 respectively, were deliberately allowed to drive the pen off-scale in order to show more clearly the phonon replicas. The spectrum of figure 4.8(a) was dominated by the I_1 exciton emission, with the maximum at about 4897 Å recorded by the Optica, and the first and second L.O. phonon replicas at about 4970 and 5050 Å respectively. The I_2 exciton maximum was observed at about 4873 Å in this crystal, which was grown under excess sulphur pressure. The spectrum of figure 4.8(b) was dominated by the I_2 exciton emission, with its first and second L.O. phonon replicas at about 4954 and 5034 Å respectively. The presence of I_1 exciton emission in this crystal (No. 172), which was grown under excess cadmium pressures, was evident as a slight shoulder on the long wavelength side

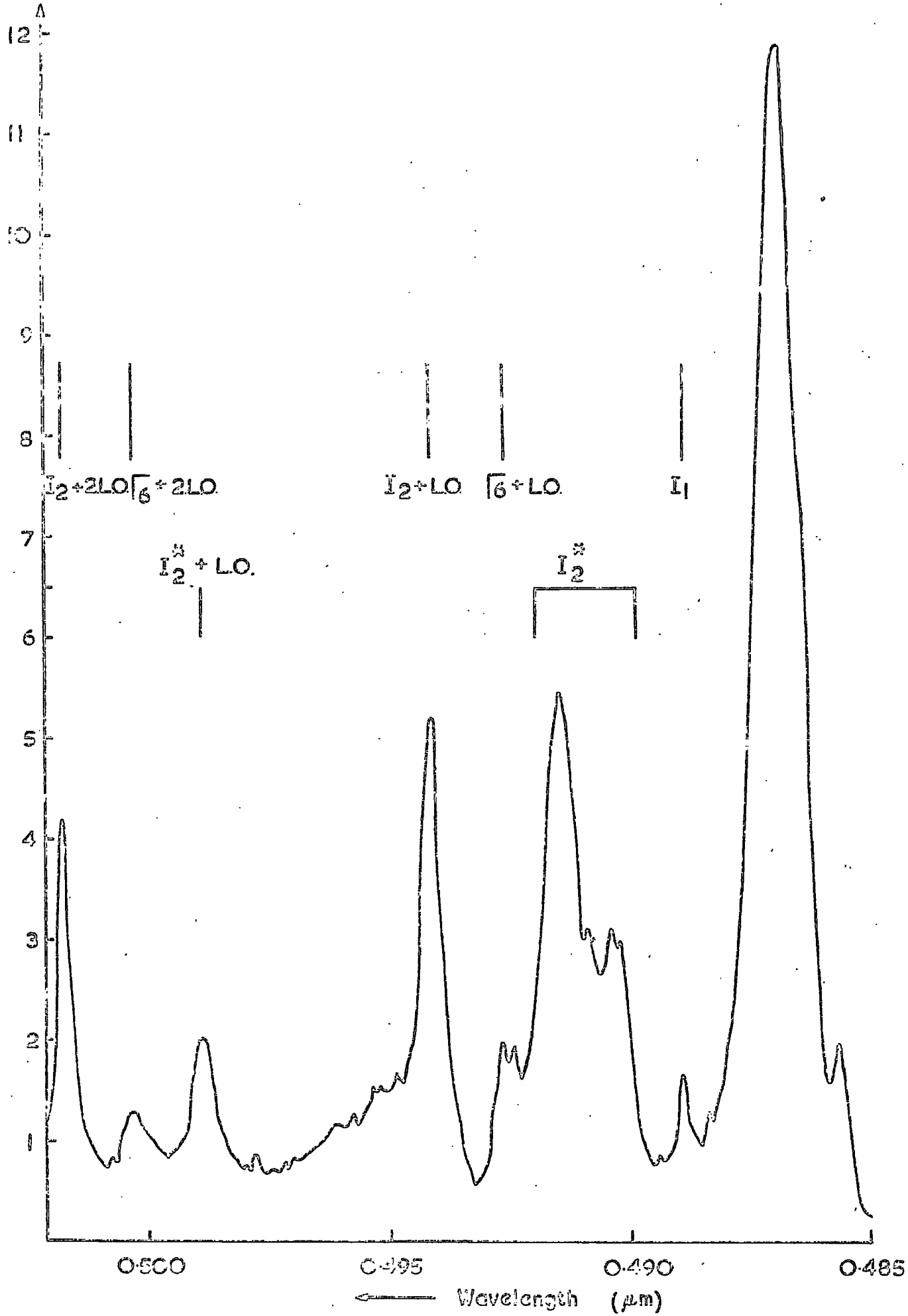


3.4.8. The SED of the blue emission excited by UV. radiation of
 (a) a crystal grown under an excess pressure of sulphur, and
 (b) a crystal grown under an excess pressure of cadmium.

of the I_2 , $I_2 + \text{L.O.}$ and $I_2 + 2\text{L.O.}$ emissions. The emission maxima at about 4930 \AA , designated I_2^* , was tentatively ascribed to the "excited states" of the excitons bound to neutral donors (10).

Any precise measurement of the wavelengths of the maxima of the emission components was extremely difficult with the Optica because of the error in the wavelength drive, the large bandwidth required to obtain a measurable signal and the speed of response of the instrument. Increasing the bandwidth of the instrument resulted in the broadening of the emission so that individual components became lost in a single unresolved "band". The spectrographic measurement of the emission spectrum of the crystal used to obtain figure 4.8(b) confirmed the assignment of the I_2 emission, the presence of I_1 emission and the tentative assignment of the I_2^* emission, see figure 4.9. The " I_2 peak", which spanned the wavelength range from 4850 to 4880 \AA , was shown to contain the following separate components: the Γ_6 free exciton (4857 \AA), the Γ_6 exciton associated with the I_3 complex or another neutral donor line (called here I_{2D}) (4865 \AA), the I_{2A} exciton (4867 \AA) and the I_{2B} (alternatively I_5) or I_{2C} exciton (4870 \AA). The I_1 emission was resolved from the " I_2 composite peak", and was located at 4889 \AA . The first and second L.O. phonon replica of the Γ_6 free exciton were observed at about 4827 and 5004 \AA , respectively. The first and second L.O. phonon replicas of the " I_2 composite peak" were observed at about 4942 and 5019 \AA respectively. I_2^* and $I_2^* + \text{L.O.}$ emissions were observed at about 4910 and 4990 \AA . The fine structure of the I_2^* emission will be discussed at the end of this section. The wavelengths and energies of the components of the major maxima and their assignments are displayed in table 4.2.

The comparison of the observations made with the Optica spectrophotometer with those of the Bausch and Lomb spectrograph confirmed that the identification of the emissions at about 4897 and 4873 \AA , as



G.4.9. The S.E.D. of the blue emission excited by UV radiation, recorded by the spectrograph.

Table 4.2. The positions of the emission maxima of figure 4.9, their assignment and an indication of the accuracy of the assignments. $E_D = 0.026$ eV.

Maximum Wavelength (Å)	Energy eV	Assignment	Energy of Assignment (assuming $E_D=0.026$ eV)
4865	2.54807	I_{2D} or I_3 (Γ_6)	
4870	2.54546	I_{2B} (i.e. I_5) or I_{2C}	
4867	2.54703	I_{2A}	
4857	2.55227	Γ_6 free exciton	
4889	2.53556	I_1	
4902.6	2.52853	$I_{2D} - \frac{3}{4} E_D$	2.52857
4904.3	2.52765	$I_{2A} - \frac{3}{4} E_D$	2.52753
4909	2.52523	$I_5 - \frac{3}{4} E_D$	2.52610
		$I_{2D} - \frac{8}{9} E_D$	2.52496
		$I_{2A} - \frac{8}{9} E_D$	2.52392
4916	2.52169	$I_5 - \frac{8}{9} E_D$	2.52235
		$I_{2D} - \frac{15}{16} E_D$	2.52370
		$I_{2A} - \frac{15}{16} E_D$	2.52266
4925	2.51708	$I_5 - \frac{15}{16} E_D$	2.52109
		Γ_{5L} (free exciton) + L.O.	
4927	2.51601	Γ_6 (free exciton) + L.O.	
4942	2.50863	" I_2 peak" + L.O.	
4989	2.48459	"4916 Å peak" + L.O.	
5004	2.47729	Γ_6 + 2 L.O.	
5019	2.47014	" I_2 peak" + 2 L.O.	

recorded by the Optica, to the recombination of excitons at neutral acceptors (I_1) and neutral donors (I_2), respectively, was correct. No facilities for the measurements of the Zeeman splitting of these lines, which would have been desirable, were available to confirm the assignments. The agreement between the spectrographically observed emission maxima and the previously reported values was assumed to be sufficient to verify the conclusions. Similarly, the agreement between the observed and expected maxima of the energies of the I_2^* emission was assumed to be satisfactory verification of the assignments, see table 4.2, and discussion following. The fact that the emission maxima at about 4920 and 5000 Å (I_2^* and $I_2^* + \text{L.O.}$), as recorded by the Optica, were only observed in crystals with a strong I_2 component, confirmed the assumption that they were in some way associated with the I_2 emission.

The I_1 exciton coupled much more strongly with both the optical and acoustic branch phonons than the I_2 excitons. This is in accord with the fact that excitons are more tightly bound to the acceptor centres than to the donor centres (8). In two samples, the first L.O. phonon replica of I_1 was more intense than the zero order line. The value of the L.O. phonon energy obtained from the replicas of the blue edge emission was in agreement with that obtained from green edge measurements, i.e. it was 37 ± 1 meV. Acoustic phonon wings were seldom observed with I_2 , whilst I_1 was generally accompanied by a low energy acoustic wing. The L.O. phonon replicas of I_2 were some hundred times less intense than the zero order exciton emission, which often meant that they were not observed.

Variation of the intensity of excitation, using neutral filters produced no measurable wavelength shift of the components of the blue edge emission. The intensity of the exciton emission was more dependent than the intensity of the green edge emission upon the

intensity of the exciting radiation. Figure 4.10 shows the dependence of the emission intensity of the zero phonon replica of the I_2 exciton upon the excitation intensity. The index (n) obtained for the intensity dependence of the I_2 emission of this crystal (No. 80) was 1.41 ± 0.05 . The mean of the values of n obtained for both major exciton components, (the zero phonon components of I_1 and I_2), averaged over five undoped crystals was 1.4 ± 0.1 . The rapid intensity dependence and the necessity to increase the bandwidth of the detector to obtain a measureable spectrum made the measurement rather difficult.

Discussion

The assignment of the emission at about 4897 and 4873 Å, recorded by the Optica, to I_1 (neutral acceptor) and I_2 (neutral donor) exciton emission was confirmed by the spectrographic analysis of the emission spectra from the same samples. Also, the intensity of the components of the green edge emission tended to confirm the assignments. This will be described more fully in the next section, however to illustrate the point, consider figure 4.8. In figure 4.8(a), the spectrum is seen to rise sharply at about 5100 Å, due to the very strong green edge emission. The I_1 exciton emission dominated the blue edge emission of this crystal. However in figure 4.8 (b), where the I_2 exciton emission was very much greater than that of the I_1 exciton, there was no rise near 5100 Å, and in fact the green edge emission was very weak.

Emission maxima lying between 4900 and 4920 Å have been reported by Yee and Condas (18) and Reynolds, Litton and Collins (10) with conflicting explanations of the recombination process. Yee and Condas observed peaks at 4906.0(a), 4913.3 (b) and 4922.6 Å(c) superimposed on a broad background, and suggested either that the emission was due to an impurity pair process with average donor to acceptor separations

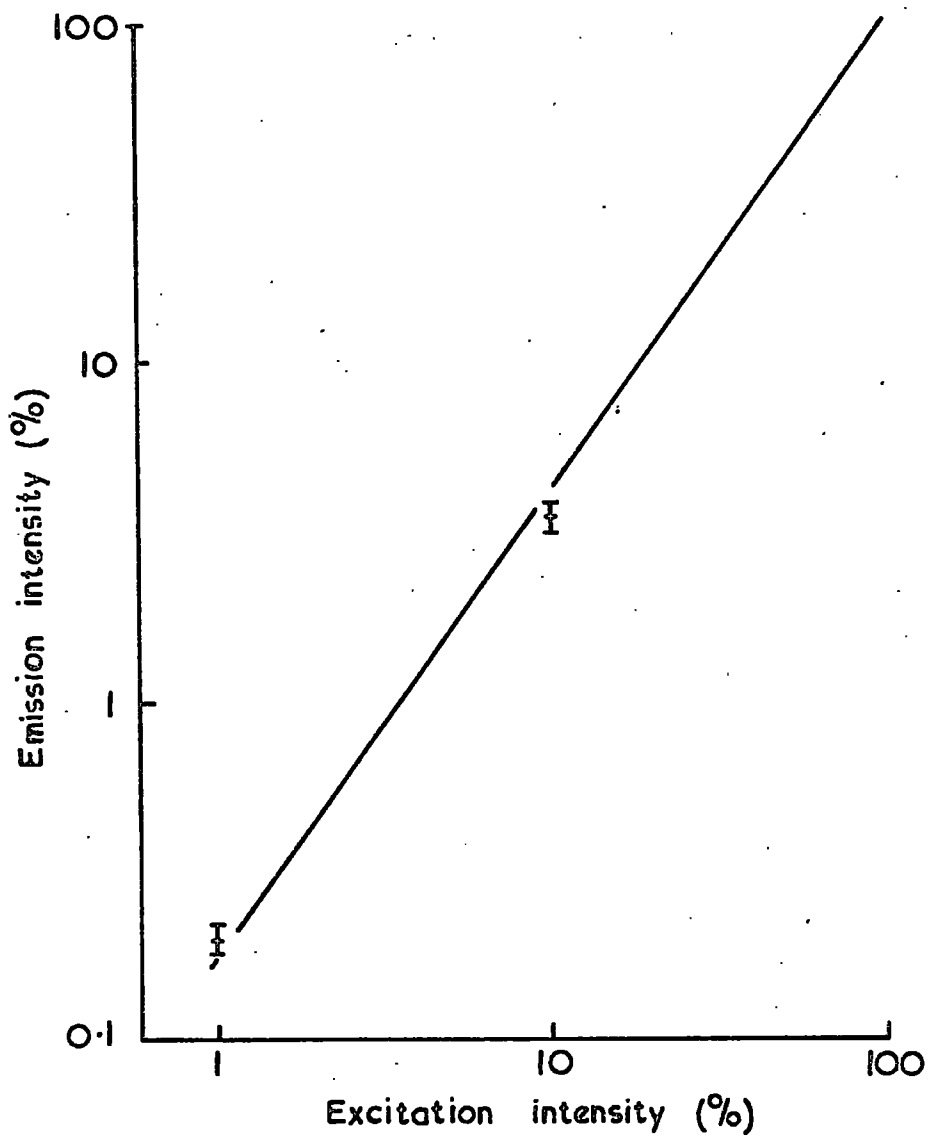


FIG. 4-10. The dependence of the intensity of the I₂ exciton upon the intensity of the U.V. radiation.

of 12.27, 12.60 and 12.94 Å for a, b, and c respectively, or that (a) was the $L0_2$ (0.0214 eV), (b) the $T0_3$ (0.0236 eV) and (c) the $T0_1'$, (0.0284 eV) phonon replicas of the I_2 exciton emission. Thomas, Dingle and Cuthbert (19) reported pair recombination associated with a band having a maximum at 4900 Å in crystals heavily doped with chlorine, bromine or iodine, which they suggested could be associated with a hole trapped at a neutral acceptor recombining with an electron trapped at a donor. Thomas et. al. suggested that the acceptor was a complex comprising a cadmium vacancy (double acceptor) next to a singly charged donor, such as a Cl atom, which would be at a nearest neighbour sulphur site. They suggested that isolated substitutional chlorine atoms provided the donors. The 4900 Å emission was the only band that Thomas et. al. have associated with pair recombination in the blue emission of CdS. Reynolds et. al. have recently demonstrated however, using Zeeman splitting, that the lines (in zero field) at 4907.15, 4908.7, 4912.4, 4915.32 and 4916.5 Å can be identified as the emission of photons, resulting from the annihilation of the I_5 and I_{2C} excitons bound to neutral donors, which had lost some of their recombination energy in exciting the neutralising electrons of the donors to their excited states. A donor ionisation energy of 0.026 eV provided the best fit to the calculated and experimentally determined ionisation energies of the I_5 and I_{2C} neutral donors, assuming a "hydrogenic donor" model.

This model provides a reasonable explanation of the maxima observed between 4900 and 4920 Å, see figure 4.9 and table 4.2. Thus the 4904.3 Å maximum in the I_2^* emission of figure 4.9 corresponds to the emission of photons following the annihilation of excitons which had been bound to the I_{2A} (4867 Å) neutral donor, but which had lost energy in exciting the neutralising electron from the ground state of

the donor (E_D eV below the conduction band) to the first excited state ($n=2$) of the donor. The energy lost is equal to $(1 - (\frac{1}{2})^2) E_D = \frac{3}{4} E_D$ eV. The value of 0.026 eV for E_D used by Reynolds et. al. provides a good fit to our 4902.6 and 4904.3 Å emission maxima, and can be assumed to account reasonably well for the remaining broader emission. The reason for the "merging" of the emission associated with the excitation of the electron to higher excited states into complex peaks is probably due to the higher temperature of 10°K ($kT = 0.001$ eV) at which our measurements were made compared with the 1.2°K temperature bath used by Reynolds et. al.

It is of interest to note that if a hydrogenic model could be used to describe the energy levels of the acceptor thought to be responsible for the I_1 bound exciton and the green edge emission, then the energy of the photon emitted associated with the I_1 exciton losing sufficient energy to raise the hole to its first excited state I_1^* ($n = 2$), would be $I_1 - \frac{3}{4} E_A$. Substituting the accepted values for I_1 and E_A of 2.53585 and 0.17 eV respectively, the I_1^* ($n = 2$) emission would have a maximum of 2.40835 eV, or 5147.3 Å. The I_1^* ($n=3$) emission maximum would be at $(I_1 - \frac{8}{9} E_A) = 2.38474$ eV or 5198.2 Å. The coincidence between these energies and those of the zero order phonon green emission peaks is remarkable. Hopfield (13) pointed out that, if exciton recombination in the field of an impurity is responsible for the green edge emission, a heavy carrier mass of about $5 m_0$ is required to raise the mean number of emitted phonons to the experimentally observed value of one. However the existence of strong phonon replicas of the I_1 exciton itself could well be thought to be sufficient evidence to indicate strong coupling of this exciton to the lattice. The binding energy of an exciton to a neutral acceptor was determined by Thomas and Hopfield (8). The value obtained, 0.018 eV, agreed remarkably

well with the simple extrapolation of the hydrogen-molecule binding energy for the appropriate configuration. The temperature at which $kT = 0.018$ eV is approximately 200°K , the temperature at which the intensity of the green edge emission is seen to be reduced rapidly.

There are numerous objections to the suggestion that I_1^* emission is responsible for the green edge emission.

- (1) The L.E.S. often dominates the green emission at liquid helium temperatures. If the model is correct, this would require the I_1^* ($n=3$) emission to be involved in preference to the I_1^* ($n=2$) emission.
- (2) The intensity of the I_1 bound exciton emission line is often less than the green emission intensity in certain crystals. This would require the I_1^* emission process to be a preferred process to the recombination of the simple I_1 bound exciton.
- (3) The observed width and shape of the green emission at low temperatures is due to acoustic lattice vibrations, and or lifetime broadening. Time resolved spectroscopy measurements, performed by Thomas, Dingle and Cuthbert (19), have shown a large shift of the L.E.S. to higher energies and a broadening of the emission in spectra observed at decreasing intervals after excitation. The zero order phonon maxima shifted to energies greater than 2.41 eV. The I_1^* emission cannot explain the shift or broadening of the L.E.S. green emission.
- (4) The green edge emission decays more slowly than the blue edge emission. The I_1^* model could not explain the large difference in decay time.
- (5) It seems unlikely that the I_1^* emission should have a weaker excitation intensity dependence than the I_1 bound exciton.

No doubt other objections could be raised against this model.

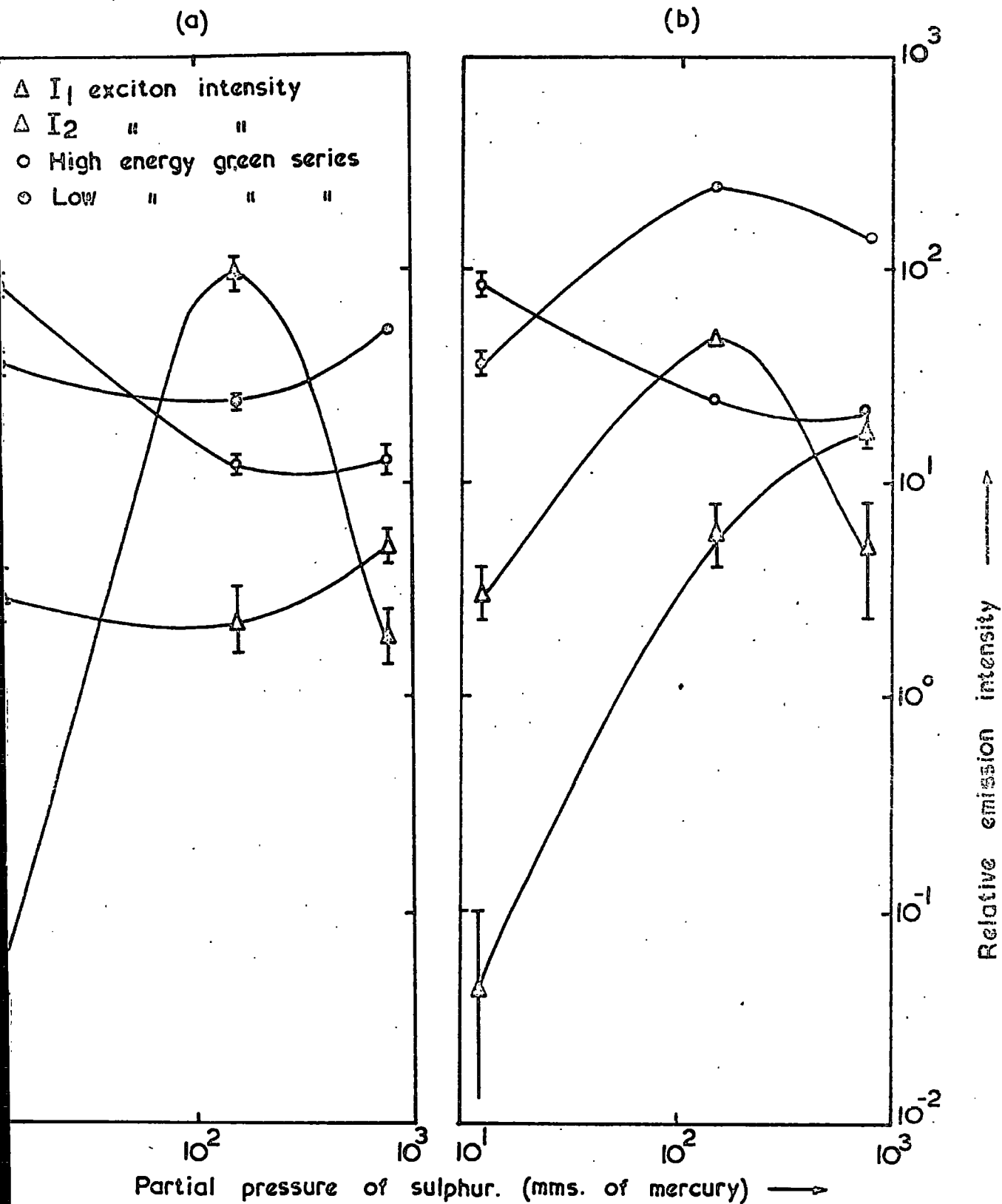
However this section serves to illustrate why the I_1^* emission may

not be observed. Even if the hydrogenic model of the acceptor must undergo strong perturbations, the maxima of the I_1^* emission probably lie in the region of the zero order phonon peak of the green edge emission. The acceptor responsible for the green edge emission is also thought to be the same as the acceptor associated with the I_1 exciton, see following section. Thus although the I_1^* emission cannot explain the green edge emission, the mechanism may still be operative. But because the green edge emission is also associated with the same acceptor, the I_1^* emission may be swamped by the green edge emission.

4.3.4 Dependence of the Intensities of the Edge Emission Components Upon Crystal Growth Parameters

Figure 4.11 shows the variations of the U.V. excited edge emission components in crystals grown under different partial pressures of sulphur with the upper CdS crystal growth chamber controlled at temperatures of (a) 1150°C and (b) 1125°C. Figure 4.12 shows the variations of the U.V. excited edge emission components in crystals grown under partial pressures of cadmium with the CdS at 1150°C. (Figures 4.11 and 4.12 are presented as a guide to assist the explanation of the trends observed and should not be taken too literally because of the small number of points and the difficulty of making absolute intensity measurements). Spectra measured on the Optica were used in the compilation of the results concerning the comparison of emission intensities throughout this section.

As the partial pressure of sulphur above the growing CdS was increased from crystal to crystal, the intensity of the I_1 component was observed to increase at first, reaching a maximum in figure 4.11 (b) when the sulphur reservoir temperature was 350°C. Figure 4.8 (a) shows the spectral distribution of the blue edge emission of the crystal grown with the CdS at 1125 °C under an excess pressure of about 150mm.



The dependence of the intensity of the components of the edge emission, excited by U.V. radiation, upon the partial pressure of sulphur during growth, with the CdS at (a) 1150°C and (b) 1125°C

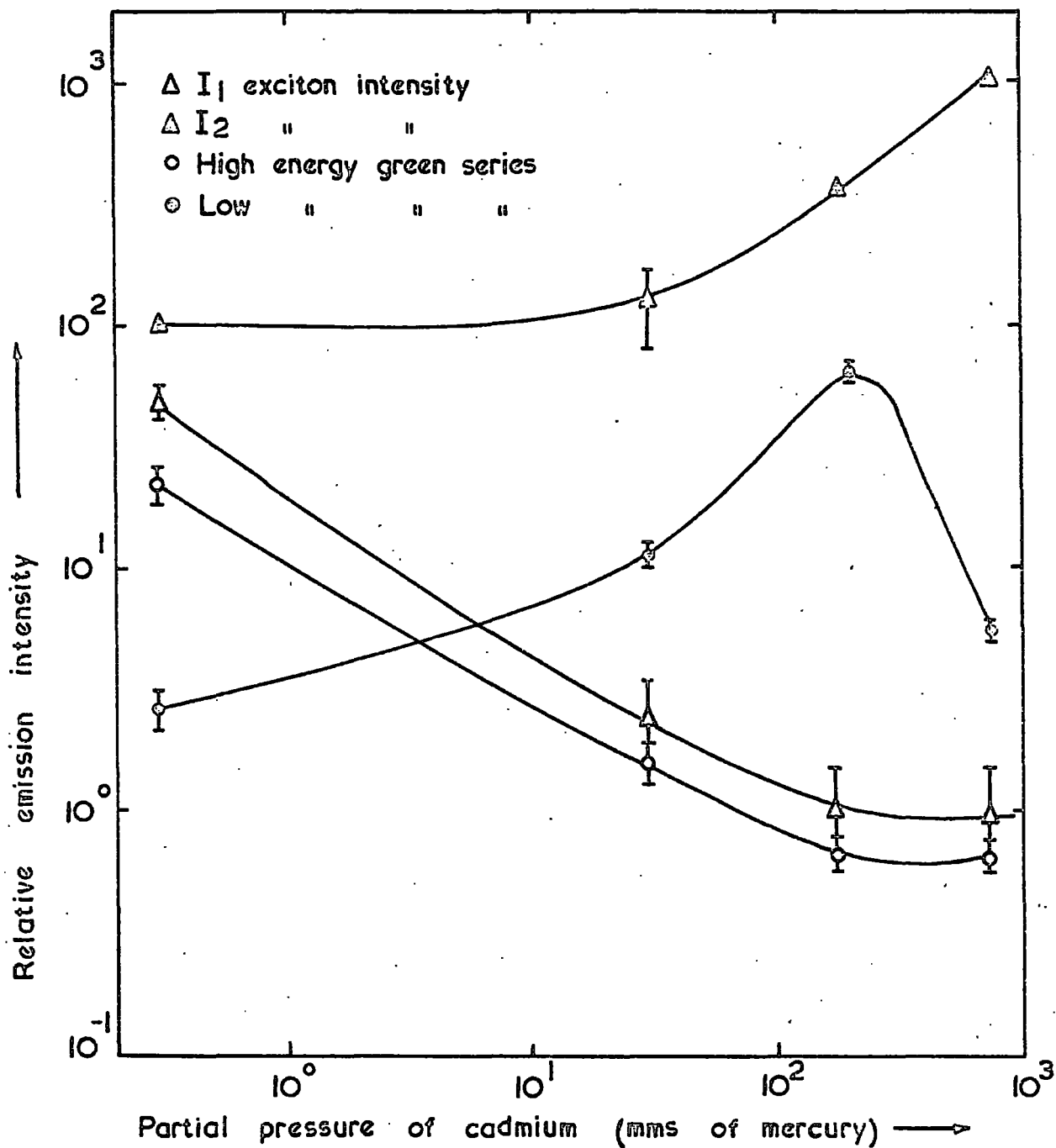


FIG. 4-12 The dependence of the intensity of the components of the edge emission, excited by U.V. radiation, upon the partial pressure of cadmium during growth, with the CdS at 1150°C.

The intensity of the I_1 component decreased as the partial pressure of the cadmium above the growing CdS was increased. These trends suggest that the acceptors to which the I_1 excitons are bound are associated with cadmium vacancies.

The most intense I_2 lines were found in crystals grown under high cadmium pressures. This suggests that the donors at which excitons recombine, to give at least a large part of the I_2 emission, are sulphur vacancies. Crystals grown under an equilibrium sulphur vapour pressure (such that the sulphur vapour pressure above the CdS at the growth temperature was approximately equal to that of the sulphur vapour pressure controlled by the tail temperature, i.e. of the order of tens of millimetres of mercury) did not exhibit the I_2 emission, which indicated a low donor concentration. Further increase in the sulphur partial pressure resulted in the unexpected reappearance of the I_2 emission. It is concluded that growth in a high pressure of sulphur vapour leads to a high acceptor concentration, as evidenced by the increased intensity of I_1 emission, but that at the same time an approximately equal concentration of donors is introduced. This automatic compensation mechanism which produced insulating (10^{10} - 10^{12} ohm. cm.), n - type crystals with poor photoconductive response, is discussed in the summary, section 4.4.

The intensity of the high energy green emission series (H.E.S.), arising from the recombination of free electrons with holes bound to acceptors, decreased as the excess vapour pressure of either cadmium or sulphur was increased. The intensity of the low energy green emission series (L.E.S.), arising from the recombination of electrons bound to donors with holes bound to acceptors, increased as the excess vapour pressure of either constituent was increased, reaching maxima when the crystal growth temperature was 1150°C , see figures 4.11 (b)

and 4.12. The increase in the intensity of the L.E.S. was probably due to the increase in the number of donors, which is illustrated by the increase in the intensity of the I_2 series. There is a correlation between the shapes of the L.E.S. and I_1 curves. For example in figure 4.11 (a), the L.E.S. curve continued to increase with increasing sulphur pressure at much the same rate as the I_1 exciton intensity. In figure 4.11 (b), the L.E.S. curve reached a maximum at the same pressure as the I_1 curve reached a maximum. The strong correlation between the magnitude of the intensity of the green emission and of the I_1 emission implies that the same acceptor is responsible for the green emission and the I_1 exciton emission. The L.E.S. also showed an interrelation with the intensity of the I_2 exciton emission, indicating that the donors associated with the I_2 emission are probably involved in the bound to bound recombination of the L.E.S..

Figure 4.13 shows the U.V. excited spectral emission distribution of a crystal (No. 171) grown at 1150°C under 180 mm excess cadmium pressure as recorded by the spectrograph. The major components of the " I_2 peak" were I_{2A} (4867 Å), I_{2B} or I_{2C} (4869 Å) and the Γ_6 free exciton (4857 Å). The remainder of the spectrum as presented, was recorded at about ten times the bandwidth used in the resolution of the I_2 emission, and as a result, the L.O. phonon replicas of the I_2 exciton and the I_2^* emission merged into a broad band. The green emission intensity was weak. A very broad red emission band dominated the emission spectrum. Similar red emission bands were found in other crystals grown under cadmium rich conditions. These crystals often luminesced bright orange on warming from liquid nitrogen temperatures. It was concluded that the presence of excess cadmium vapour pressure during growth:

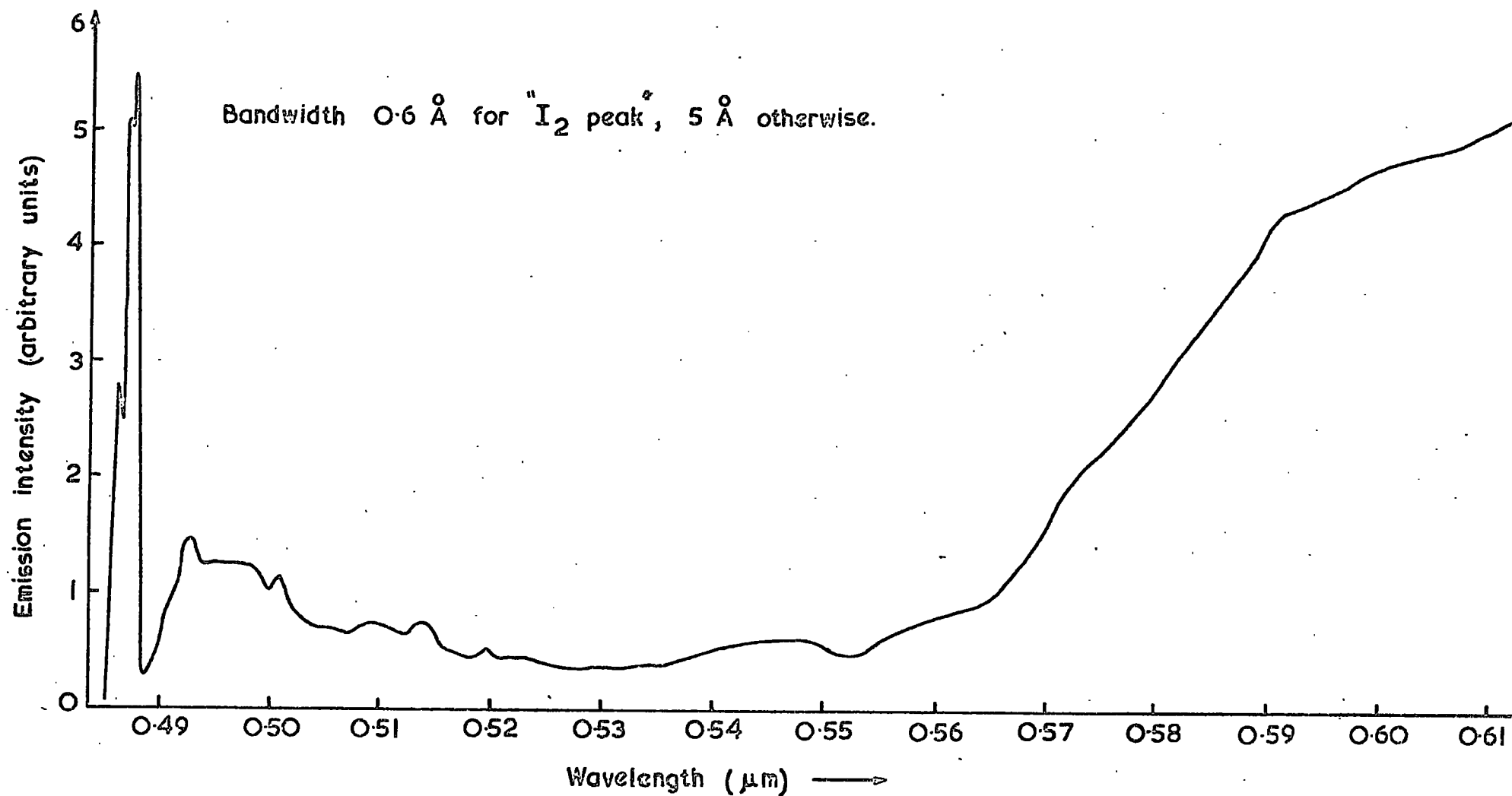


FIG.4.13 The SED of the UV. excited emission of a crystal grown under an excess pressure of cadmium, as recorded by the spectrograph.

- (1) encouraged the formation of donors as indicated by the intense I_2 emission,
- (2) inhibited the formation of acceptors as indicated by the relative absence of the I_1 exciton and green edge emission,
- (3) resulted in the increased efficiency of radiative recombination processes other than "band edge" processes.

Crystals grown under the same excess vapour pressure, but at different CdS growth temperatures, did not emit identical spectra. This may be seen by comparing figures 4.11 (a) and 4.11 (b), illustrating the variations of the components of the U.V. excited green edge emission, in crystals grown under different partial pressures of sulphur with the CdS controlled at (a) 1150°C and (b) 1125°C . The intensities of the various components were not equal in any two crystals grown at different temperatures but under the same excess partial pressure. (The experimental points at the lowest pressure in both figures were obtained from the same crystal (No. 77) which was grown at 1150°C). However the same trends, such as the increase in the intensity of the L.E.S. at the expense of the H.E.S. and the increase in the intensity of the I_2 component, were observed with increasing excess vapour pressure at both growth temperatures. The largest difference between the two curves was seen in the intensity of the excitons.

Consider the crystals grown under 150mm excess sulphur pressure, the emission of the 1150°C grown crystal (No. 80) was dominated by the " I_2 composite peak" with the I_1 exciton somewhat lost in the long wavelength edge of this peak. The emission of the crystal grown at 1125°C (No. 68) was dominated by the L.E.S. green emission, the photoexcited carriers associated with donors preferring to recombine via the green edge emission, with the I_1 emission dominating the blue emission. The spectrum of a third crystal (No. 174), grown at 1075°C

under 150 mm excess sulphur pressure, showed that the intensity of the green edge emission was approximately three times that of the exciton emission. The green edge emission, recorded by the Optica, is shown in figure 4.14 (a). By subtracting the anti-Stokes excited green emission (which only contains the L.E.S. - see chapter five) from the U.V. excited emission, it was possible to demonstrate that the U.V. excited emission contained both the L.E.S. and H.E.S. at approximately equal intensities. Spectrographic analysis of the blue emission, see figure 4.14 (b), showed maxima at 4867.6 \AA (I_{2A}) and at 4869.3 \AA (I_{2B} or I_5). (The width at half height of the I_{2A} emission was $6.3 \times 10^{-4} \text{ eV}$, which was greater than the bandwidth used in the measurement (0.6 \AA). This was probably due to the doublet nature of the I_{2A} emission). Comparing the emission characteristics of these three crystals illustrates the reduction in the intensity of the exciton emission, relative to the other emission with decreasing growth chamber control temperatures. In their search for CdS laser material, Thomas and Hopfield (20) preferred flow-grown platelets to large crystals because of the inability to grow large perfect crystals. The reduction in the intensity of the exciton emission with decreasing growth temperature observed in our experiments perhaps indicates a decrease in the crystalline quality of crystals grown at lower temperatures.

The characteristics of the exciton edge emission of three crystals supplied by A.E.I. Ltd. and one from Hull University were much the same as those of crystals grown at Durham. However, an interesting result was observed with the blue emission of a crystal grown by A.E.I. Ltd., crystal 578. Figure 4.15 shows the U.V. excited exciton emission of the crystal, which was semi-conducting (resistivity 10 ohm cm.) The intensity of the I_{2A} and I_{2B} emissions was small

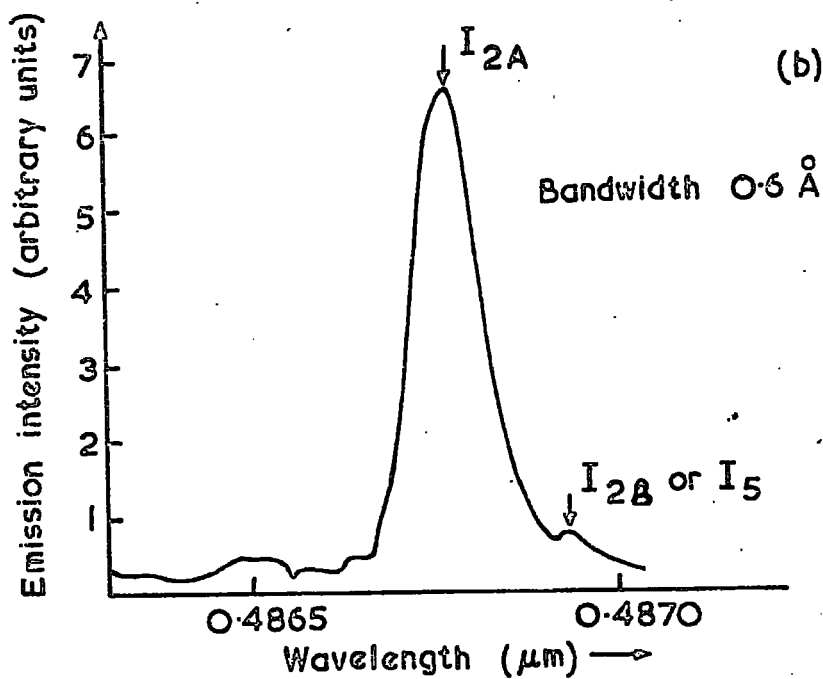
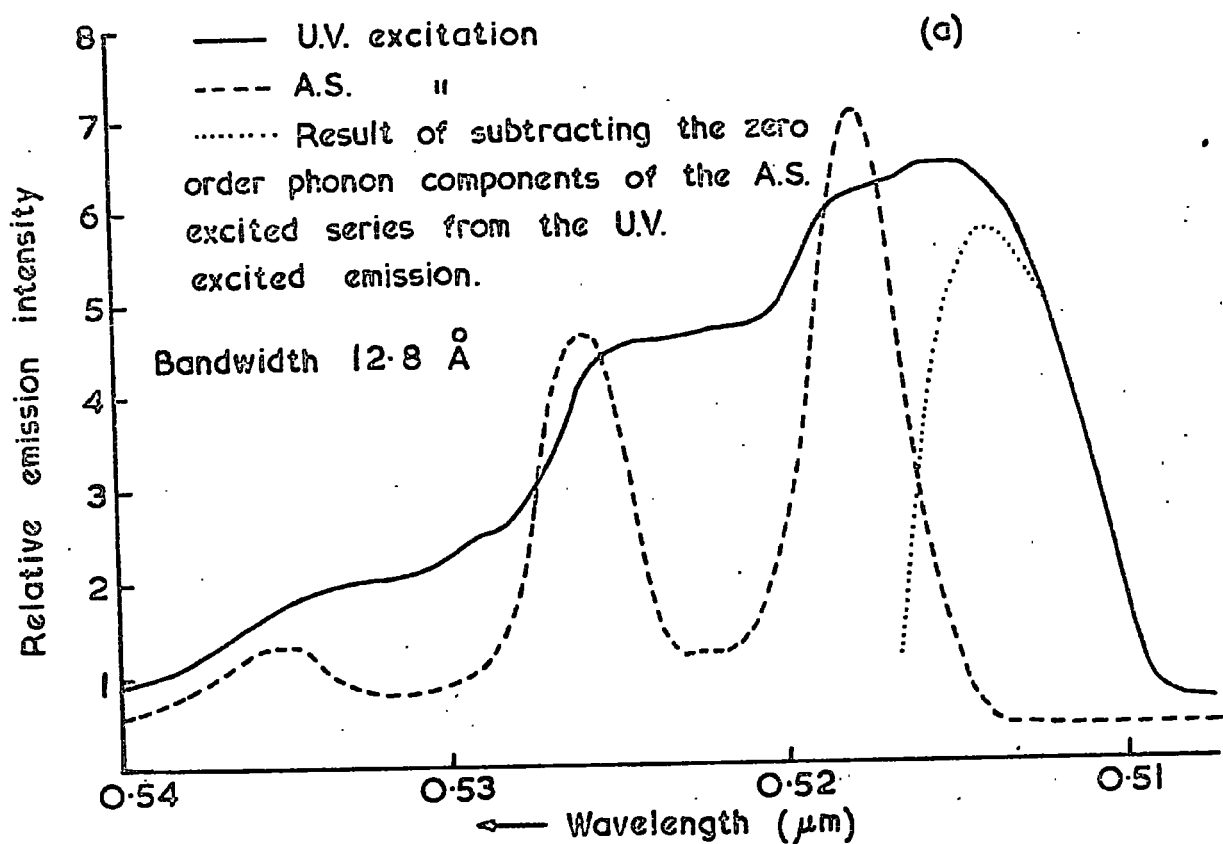


FIG. 4.14 The SED of (a) the green and (b) the blue emission, excited by UV. radiation, of a crystal grown under an excess pressure of sulphur.

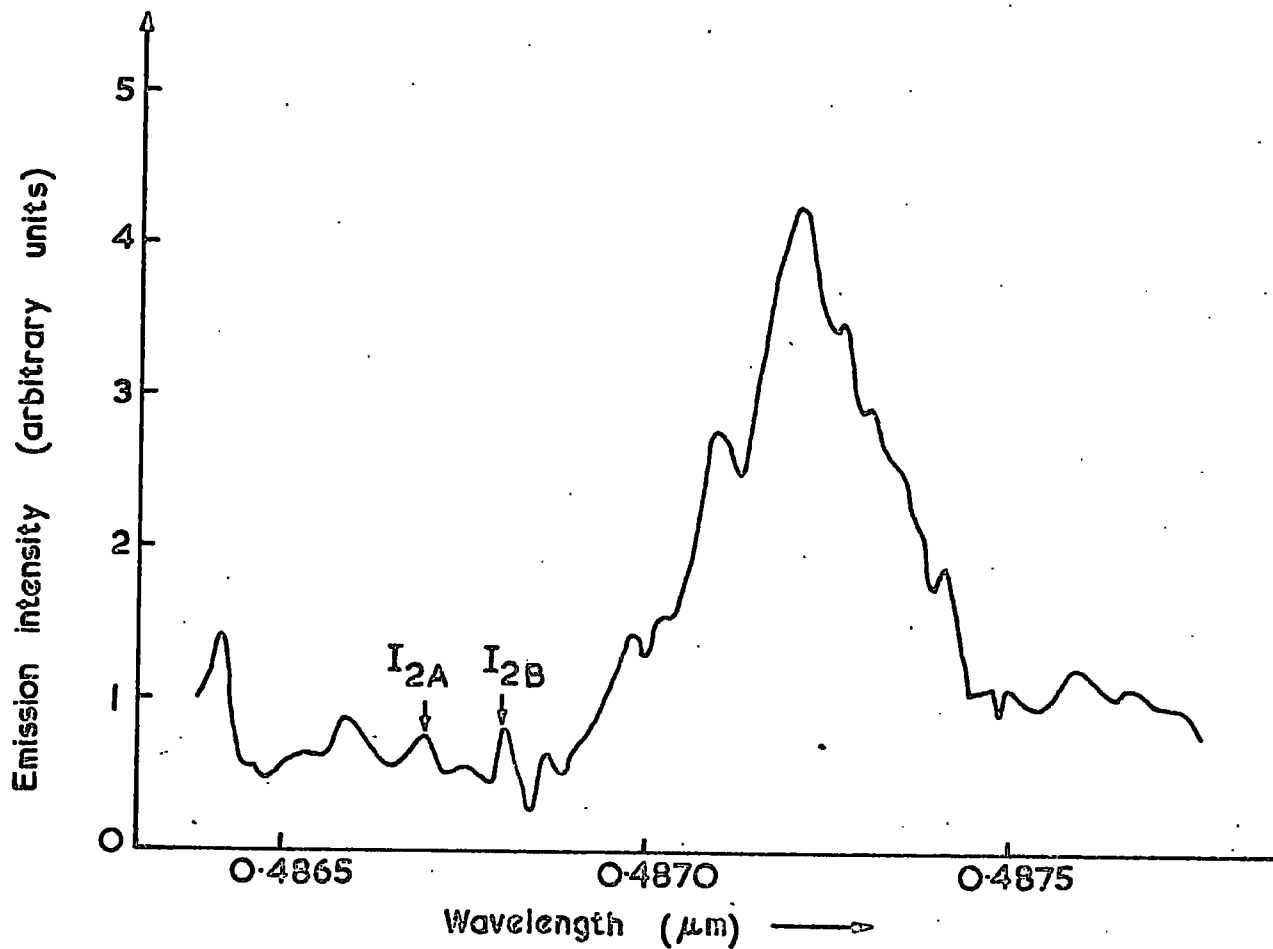


FIG.4.15 The SED of the 'donor bound' exciton emission, excited by U.V. radiation, of a crystal grown by A.E.I., as recorded by the spectrograph.

compared with the emission in the 4872 Å region, which was probably associated with some unidentified "donors". The donors were probably responsible for the low resistivity, and may have been associated with impurities.

4.4 Summary

The green edge emission of CdS crystals at liquid helium temperatures contains two L.O. phonon assisted series. The zero phonon component of the high energy series (H.E.S.) is due to the recombination of free electrons with holes trapped at acceptor levels some 0.17 eV above the valence band. The zero phonon component of the low energy series (L.E.S.) is due to the recombination of electrons bound to donors (some 0.03 eV below the conduction band) with holes bound to the same acceptor levels. The magnitude of the shift of the maxima of the L.E.S. to longer wavelengths as the excitation intensity was reduced, was used to calculate the mean separation between the donors and acceptors involved in the recombination. The separation was of the order of hundreds of Angstroms. The components of the blue emission spectra have been assigned to the phonon assisted recombination of free and bound excitons, and the excited states of donor bound excitons, by comparing the positions of the emission maxima with those of previous workers.

The observation of the emission associated with excitons bound to the neutral donors losing some of their recombination energy in raising the donor electron to an excited state of the donor, I_2^* emission, was used to evaluate a donor ionisation energy of 0.026 eV. The excitons were (a) I_{2A} , (b) I_{2B} (i.e. I_5) or perhaps I_{2C} (these two excitons were not resolved separately) and (c) perhaps the Γ_6 free exciton associated with the I_3 ionised donor or another exciton bound to a neutral donor, say I_{2D} , at 4865 Å. The donors which are responsible for a large part

of the "I₂ composite peak" are probably also involved in the L.E.S. recombination process, despite the slightly different ionisation energy ($E_D = 0.032$ eV) obtained. The E_D value obtained from the green edge emission measurements had been corrected for a Coulombic interaction. The correction applied was simply an order of magnitude correction obtained from the order of magnitude estimate of the donor-acceptor separation. Using the value of E_D of 0.026 eV and working back, the separation obtained is 174 \AA , once again in reasonable agreement with the values of Colbow (3).

The relative intensities of the major components of the edge emission were correlated with the excess partial pressures of the constituent elements under which the crystals had been grown. The variations led to the following conclusions:

- (1) The acceptor ~~is~~ responsible for the I₁ bound exciton emission is also involved in the green edge recombination processes. The acceptor is associated with a cadmium vacancy, even though other donor impurities may be juxtaposed with the vacancy (19).
- (2) The donors which are responsible for a large part of the I₂ bound exciton emission and the L.E.S. green emission are probably associated in some way with sulphur vacancies and/or cadmium interstitials. Sulphur vacancies have previously been suggested as possible centres for the recombination of excitons to produce the I_{2C} (4870.2 \AA) emission (9).
- (3) The I₂^{*} emission was observed in crystals showing an intense I₂ emission.
- (4) As the number of acceptor levels involved in the green edge emission was reduced by using excess cadmium pressures during growth, alternative radiative recombination processes became more obvious. Red emission was observed in many such crystals grown at Durham. The low resistivity crystal grown by A.E.I. Ltd.

appeared "white" under U.V. excitation due to the blue, green yellow and no doubt other recombination processes. The red emission centre may be associated in some way with the centre responsible for part of the I_2 emission. This possibility will be expanded in the discussion of the anti-Stokes excitation mechanism in the following chapters.

- (5) The appearance of I_2 emission in the U.V. excited spectra of crystals grown under high excess pressures of sulphur indicates that there is a strong tendency for an autocompensatory mechanism to operate in CdS. A possible system for the explanation of this effect is proposed in chapter eight.

Table 4.3 The features of the emission characteristics illustrated in the figures of Chapter 4.

Figure	Crystal	Growth Temp. °C	Excess	Pressure mms.	Features
1	180	1150	Cd	760	blue and green S.D.
2	H59	-	-	-	blue and green I vs J
3	AEI537	-	-	-	green S.D. dJ
4	AEI578	-	-	-	green S.D. dJ
5	68	1125	S	150	green S.D. dJ
6	"	"	"	"	" dE vs J
7	"	"	"	"	" I vs J
8(a)	"	"	"	"	blue S.D.
8(b)	172	1100	Cd	180	" "
9	"	"	"	"	" " (B & L)
10	80	1150	S	150	" I vs J
11	77	"	"	12	I(blue & Green) vs P _s
	80	"	"	150	"
	68	1125	"	"	"
	94	1150	"	760	"
	69	1125	"	"	"
12	78	1150	Cd	0.3	I(blue & green) vs P _{Cd}
	127	"	"	30	"
	129	"	"	180	"
	91	"	"	760	"
13	171	"	"	180	green, blue & red S.D.(B&L)
14(a)	174	1075	S	150	green S.D.
(b)	"	"	"	"	blue S.D. (B&L)
15	AEI578	-	-	-	"

S.D. spectral distribution, I emission intensity, J excitation intensity, B & L spectrographic record, P pressure of constituent.

CHAPTER 4

REFERENCES

1. D. C. Reynolds, C. W. Litton and T. C. Collins (1965), *Phys. Stat. Sol.* 12, 3.
2. L. S. Pedrotti and D. C. Reynolds (1960), *Phys. Rev.* 120, 1664.
3. K. Colbow (1966), *Phys. Rev.* 141, 742.
4. J. Voigt and F. Spiegelberg (1968), *Phys. Stat. Sol.* 30, 659.
5. M. Schön (1942), *Z. Phys.* 119, 463.
6. H. A. Klasens (1940), *Nature* 158, 306.
7. W. E. Spear and G. W. Bradberry (1965), *Phys. Stat. Sol.* 8, 649.
8. D. G. Thomas and J. J. Hopfield (1961), *Phys. Rev. Letters*, 7, 316.
D. G. Thomas and J. J. Hopfield (1962), *Phys. Rev.* 128, 2135.
9. E. T. Handelman and D. G. Thomas (1965), *J. Phys. Chem. Solids*, 26, 1261.
10. D. C. Reynolds, C. W. Litton and T. C. Collins (1968), *Phys. Rev.* 174, 845.
11. F. A. Kroger and H. J. G. Meyer (1954), *Physica* 20, 1149.
12. M. Balkanski, *Proc. Int. Conf. on Phys. of Semiconductors*, Paris 1964, p.1021.
13. J. J. Hopfield (1959), *J. Phys. Chem. Solids* 10, 110.
14. C. C. Klick (1951), *J. Opt. Soc. Amer.* 41, 816.
15. D. G. Thomas, J. J. Hopfield and W. M. Augustyniak (1965), *Phys. Rev.* 140, A202.
16. J. J. Hopfield and D. G. Thomas (1961), *Phys. Rev.* 122, 35.
17. D. Berlincourt, H. Jaffe and L. R. Shiozawa (1963), *Phys. Rev.* 129, 1009.
18. J. H. Yee and G. A. Condas (1967), *Solid State Electronics* 10, 257.
19. D. G. Thomas, R. Dingle and J. D. Cuthbert (1967), *Proc. of the Int. Conf. on II - VI Semiconducting Compounds*, Providence R.I.
20. D. G. Thomas and J. J. Hopfield (1962), *J. Appl. Phys.* 33, 3243.

CHAPTER 5

ANTI-STOKES EXCITED EDGE EMISSION OF UNDOPED CADMIUM SULPHIDE

5.1. Introduction

The edge emission of undoped cadmium sulphide excited by anti-Stokes radiation was studied at liquid nitrogen and liquid helium temperatures. The crystals were grown ^{under} controlled partial pressures of the constituent elements. At liquid nitrogen temperatures the green edge emission excited by anti-Stokes (A.S.) radiation was identical with that excited by U.V. radiation. At liquid helium temperatures, only one green edge series (L.E.S.) was observed under A.S. excitation. This was accompanied by weak exciton emission in some crystals.

The relationship between the crystal growth conditions and the intensity of the A.S. excited green emission at liquid helium temperatures was investigated. The Optica spectrophotometer was used to determine these basic trends, while the Bausch and Lomb spectrograph was used to determine the precise wavelength of the emission. In this chapter the characteristics of the A.S. excited edge emission at liquid nitrogen temperatures and liquid helium temperatures are described first. This is followed by an account of the way in which the edge emission at liquid helium temperatures varied depending on the conditions under which the crystal had been grown. Table 5.1. outlines the features of the emission illustrated in the figures of this chapter.

5.2. Edge emission characteristics at liquid nitrogen temperatures

No blue emission was observed in the A.S. excited emission spectra of CdS crystals at liquid nitrogen temperatures. The first maxima of the U.V. and A.S. excited green emissions were centred on

Table 5.1. The features of the emission characteristics illustrated in the figures of Chapter 5.

Figure	Crystal	Growth Temp. °C	Excess	Pressure mm.	Features
1	H59	-	-	-	U.V. & A.S. green S.D.
2	"	-	-	-	" " " " I vs J
3	77	1150	S	12	" " " " S.D.
4	68	1125	S	150	" " " " "
5	174	1075	S	150	" " " " " , dJ
6	H59	-	-	-	A.S. green S.D., dJ
7	215	1150	Cd	30	U.V. & A.S. green I vs J
8	216	1150	S	50	" " " " "
9	60	1075	S	-	" " " blue S.D.
10	77	1150	S	12	" " " " "
11	172	1100	Cd	180	" " " " "
12	See figures 4.11 and 4.12 and table 4.3, Chapter 4.				

S.D. spectral distribution, I emission intensity, J excitation intensity, dJ effect of the variation of J.

approximately the same wavelength. Both spectra indicated similar L.O. phonon assisted recombination. Figure 5.1. illustrates these features. The A.S. excited green emission was assigned to the same recombination process as the U.V. excited green emission at liquid nitrogen temperatures, that is a free electron recombining with a hole bound to an acceptor some 0.17 eV above the valence band.

Variation of the intensity of excitation, using neutral density filters, did not lead to any displacement in the wavelengths of the maxima of either the A.S. or U.V. excited green edge emission.

However the height of the zero phonon component of the green edge emission varied as I^n , where I is the excitation intensity and n was typically 0.93 ± 0.04 for the U.V. and 2.26 ± 0.06 for the A.S. excited emissions. These values refer to the same crystal, see figure 5.2. It was impossible to check the dependence of the A.S. excited emission intensity over several orders of intensity of excitation because of the strong intensity dependence and the weak emission intensity of the green edge emission. The linear dependence of the Stokes (U.V.) excited emission intensity compared with the square law dependence of the A.S. excited emission intensity implies that a two step excitation process was operating under A.S. excitation (1). This will be discussed more fully in chapter eight.

5.3.1. Anti-Stokes edge emission characteristics at liquid helium temperatures.

Green and blue emissions were observed in undoped CdS crystals at liquid helium temperatures under A.S. excitation. The green edge emission consisted of the L.E.S. alone, typical of the bound-to-bound recombination mechanism. The blue edge emission was not detected in all crystals, and was only recorded as a broad step

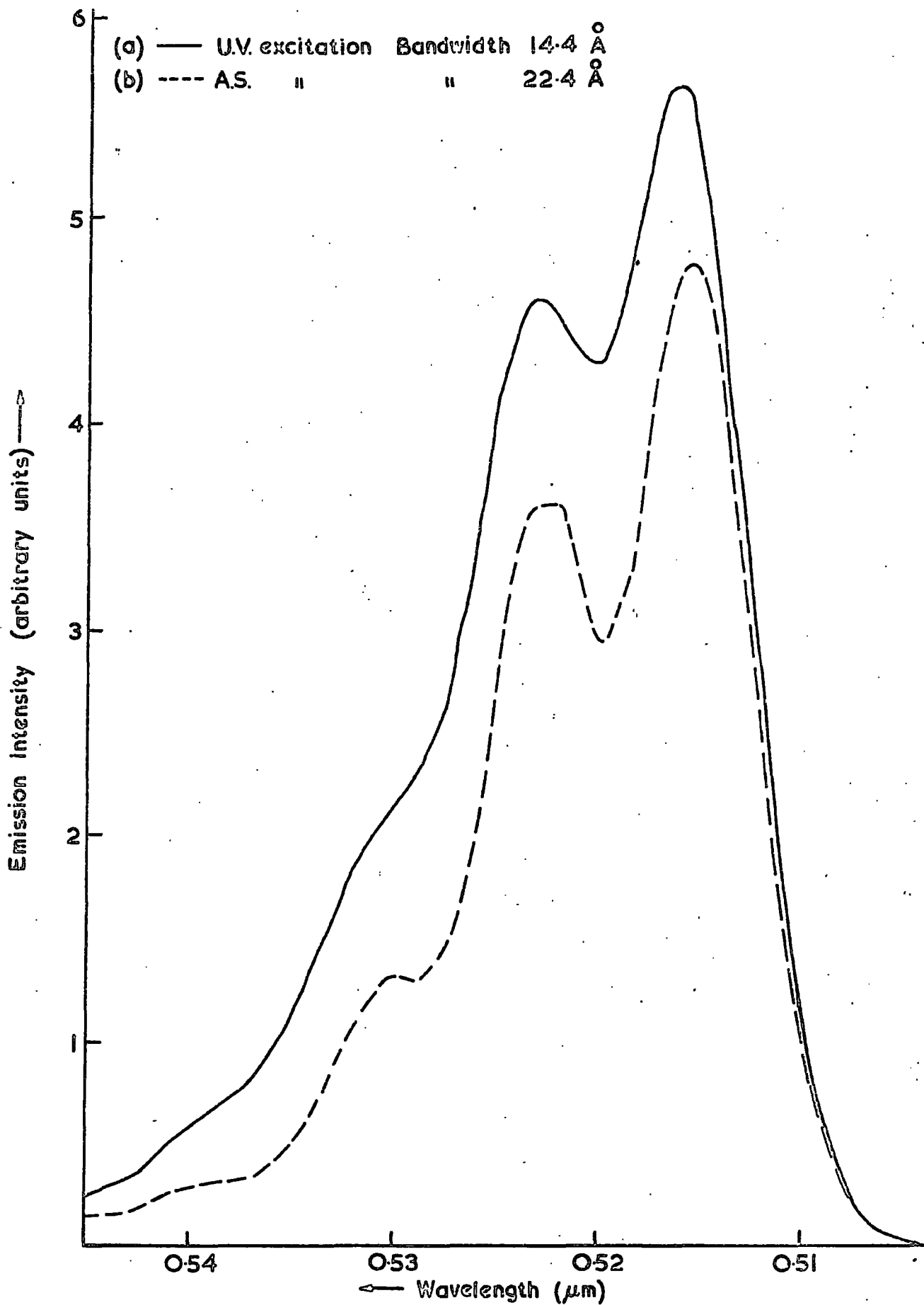


FIG 51. The S.E.D. of the green emission of CdS at 80°K excited by (a) U.V. and (b) A.S. radiation.

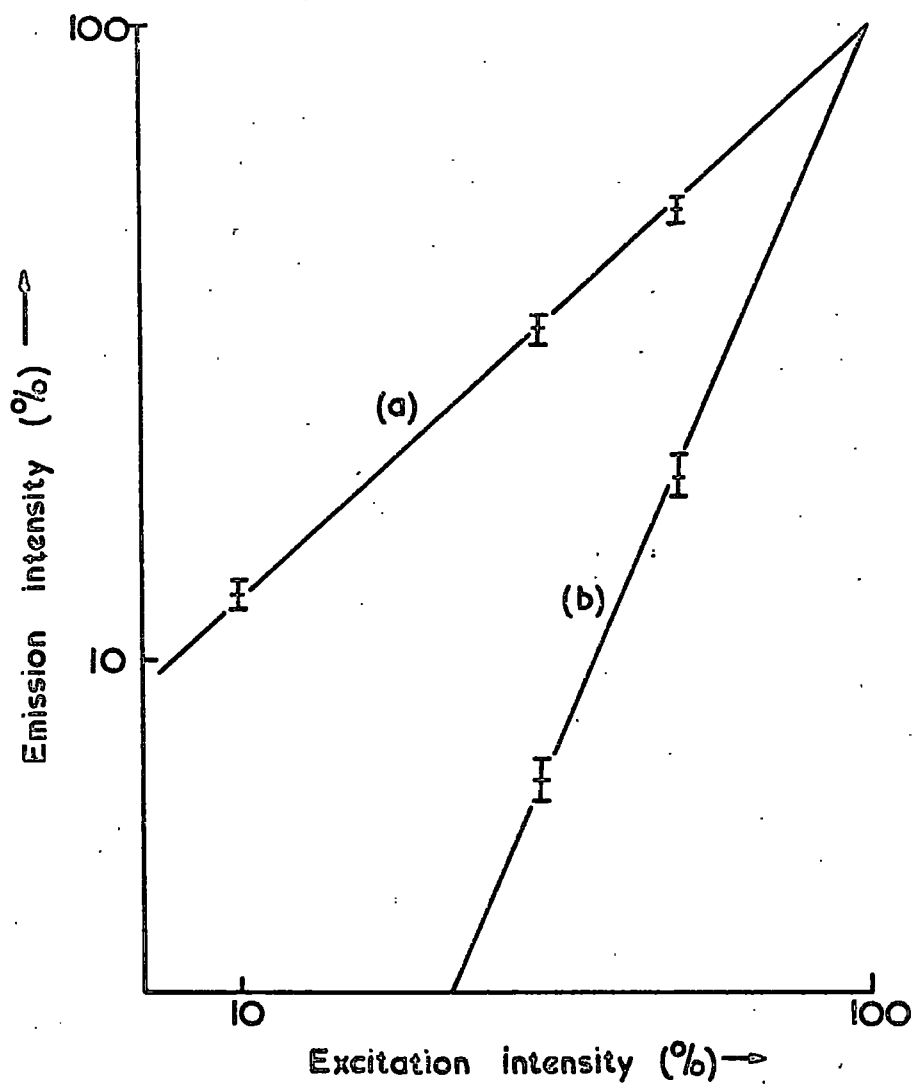


FIG.5-2. The dependence of the intensity of the green emission of CdS at 80°K upon the intensity of (a) the U.V. and (b) the A.S. radiation.

leading to the rising edge of the green emission in many crystals. (This was due to the large slit widths which had to be employed to detect the radiation.) Although no sharp "exciton-like" lines were recorded, the position of maxima, which were resolved in three crystals (see 5.5.3.), indicated that the blue emission was due to the L.O. phonon assisted emission of photons, resulting from the annihilation of excitons bound to neutral donors, which had lost some of their recombining energy in exciting the neutralising electrons of the donors to their lower excited states. The resulting emission is that which has been denoted I_2^* earlier. Phonon replicas of I_2^* as well as I_2 are possibly superimposed in the observed spectra. The assignment of the emission to the I_2^* excitons was made on the basis that the positions of the maxima recorded by the Optica were similar to those observed under U.V. excitation. This assignment is rather tentative.

5.3.2. Green edge emission

The anti-Stokes excited green edge emission of all undoped CdS crystals at liquid helium temperatures consisted of the low energy series (L.E.S.) alone, even in some crystals which preferentially emitted the shorter wavelength series (H.E.S.) under U.V. excitation. Figure 5.3. shows the green edge emission spectra excited by A.S. and U.V. radiation of a crystal in which the U.V. excited emission was dominated by the H.E.S. The asymmetry of the component bands of the U.V. excited emission indicated that there was some L.E.S. present. As can be seen in figure 5.3, the A.S. excited emission consisted of a sharp, L.O. phonon assisted series, with its maxima corresponding to those of the U.V. excited L.E.S. observed in other crystals. Figure 5.4. shows the U.V. and A.S. excited

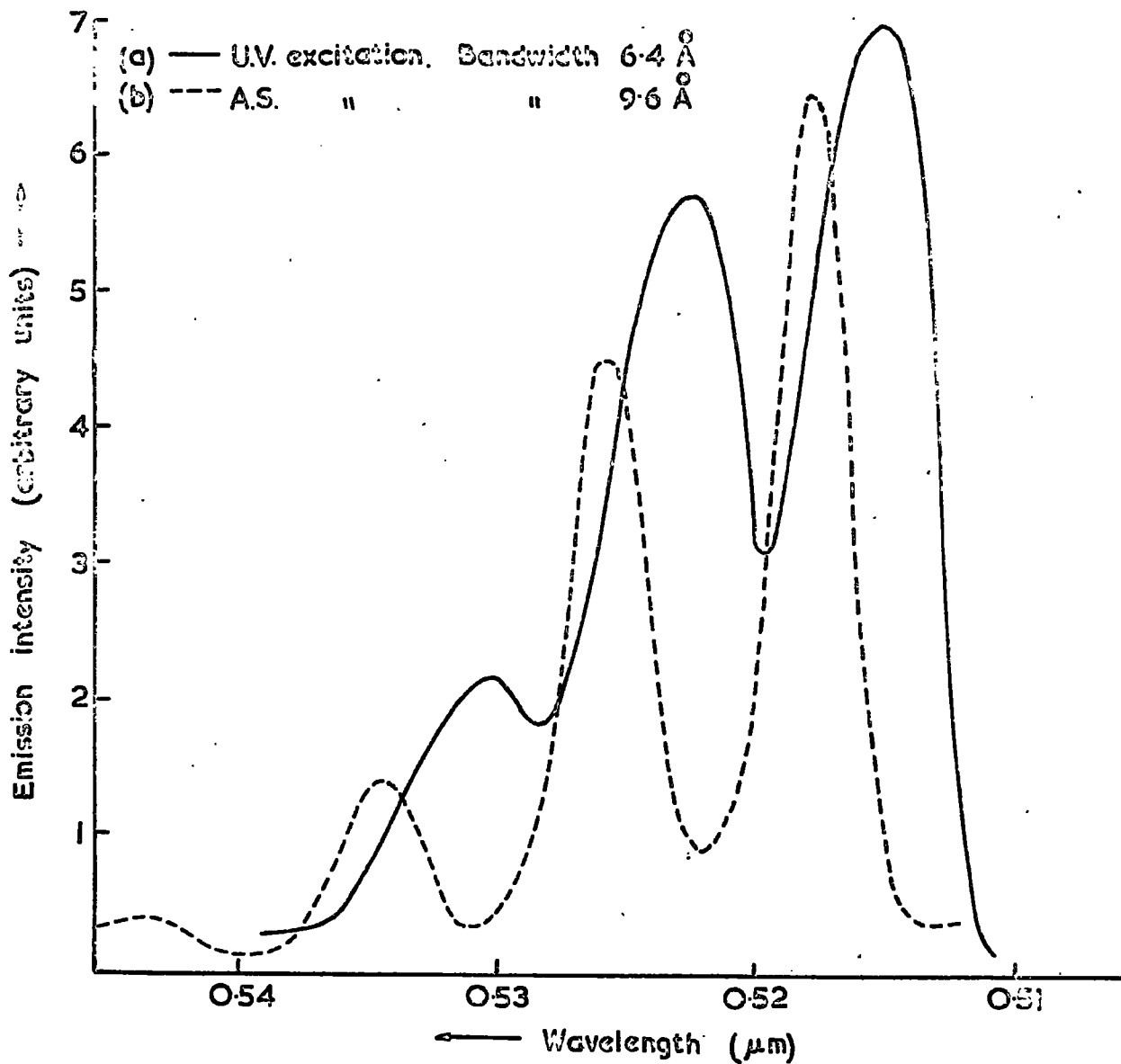


FIG. 5-3. The S.E.D. of the green emission excited by (a) U.V. and (b) A.S. radiation.

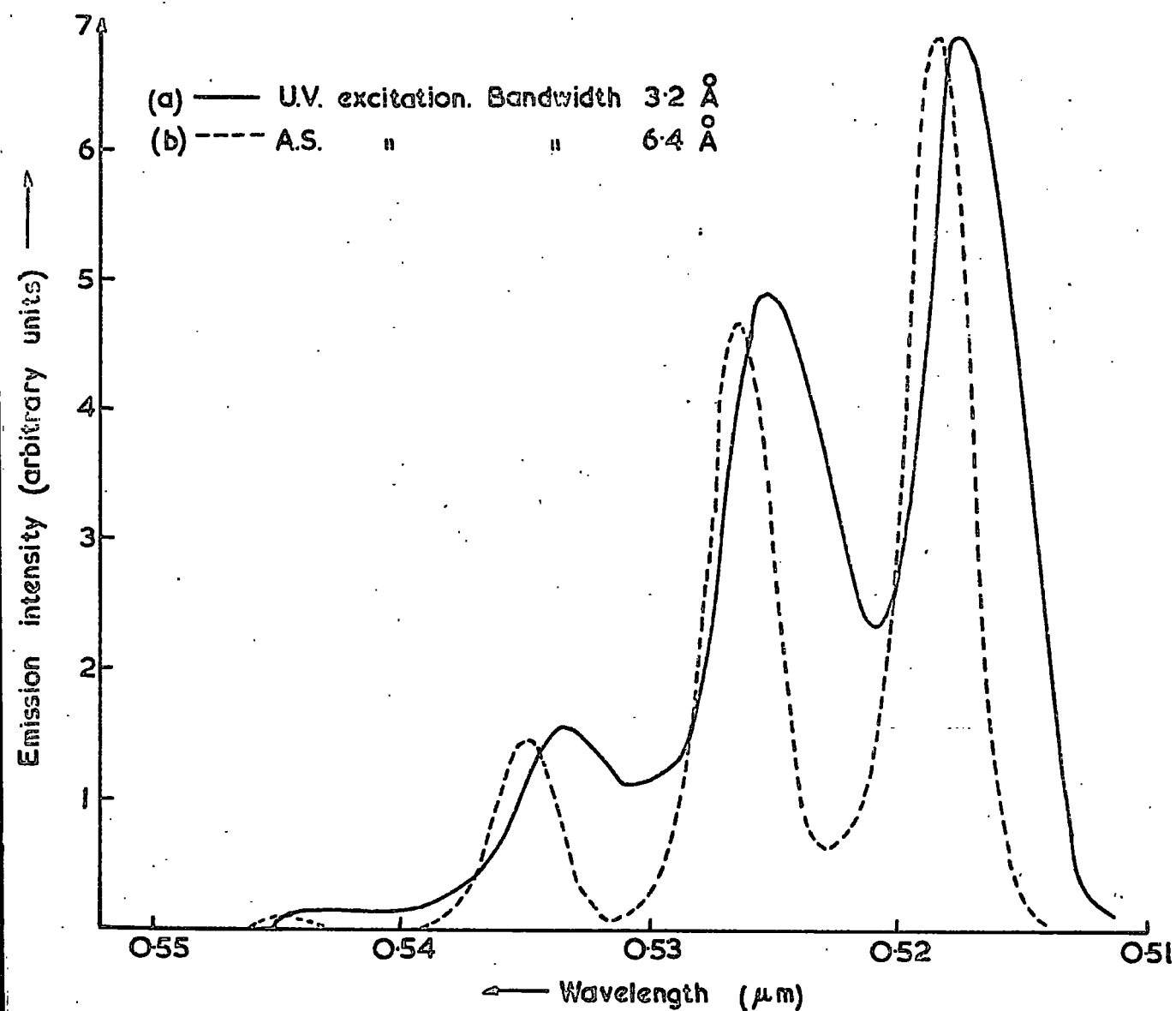


FIG.5.4. The S.E.D. of the green emission excited by (a) U.V. and (b) A.S. radiation

green edge emission of a crystal in which the U.V. excited emission was dominated by the L.E.S. The slight shift of the A.S. excited series to longer wavelengths compared with the U.V. excited L.E.S., the narrowness and bottoming of the A.S. excited series were typical characteristics of the A.S. emission. This figure also demonstrates that the L.O. phonon energy involved was the same for both methods of excitation, and that the distribution of the phonon components of the A.S. excited emission could also be described by a Poisson distribution with the same mean number of emitted phonons as the U.V. excited emission. Figure 5.5a illustrates how the subtraction of the zero order phonon components of the green edge emission of the A.S. excited series from the U.V. excited spectrum can be used to establish the existence of the H.E.S., when both L.E.S. and H.E.S. were approximately equal intensities in the U.V. excited emission.

The effects of varying the intensity of the U.V. and A.S. excitations is well demonstrated by comparing figures 5.5a and 5.5b. The intensity of the U.V. excited emission is directly comparable with the intensity of the A.S. excited emission for both the 100 % excitation intensity, figure 5.5a, and the 10 % excitation intensity, figure 5.5b, emission spectra. However the emission intensities of figure 5.5a are not directly comparable with those of figure 5.5b. The reduction in the intensity of excitation resulted in the shift of the A.S. excited series to longer wavelengths. In figure 5.5 the shift of the maximum of the zero phonon component of the A.S. excited emission was from 5180 to 5190 \AA as the excitation intensity was reduced by an order of magnitude. The shift, observed in the emission of another crystal, is illustrated more clearly in figure 5.6.. The shift indicates that the recombination mechanism which was

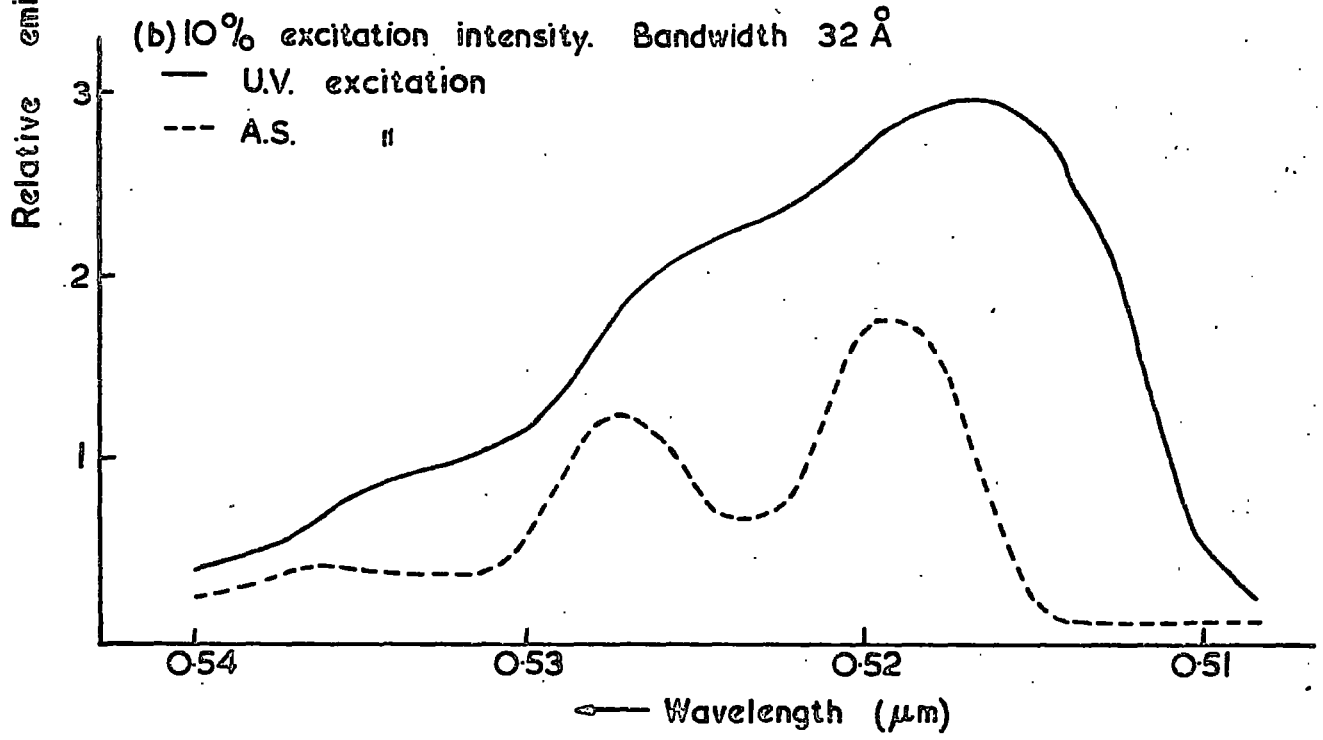
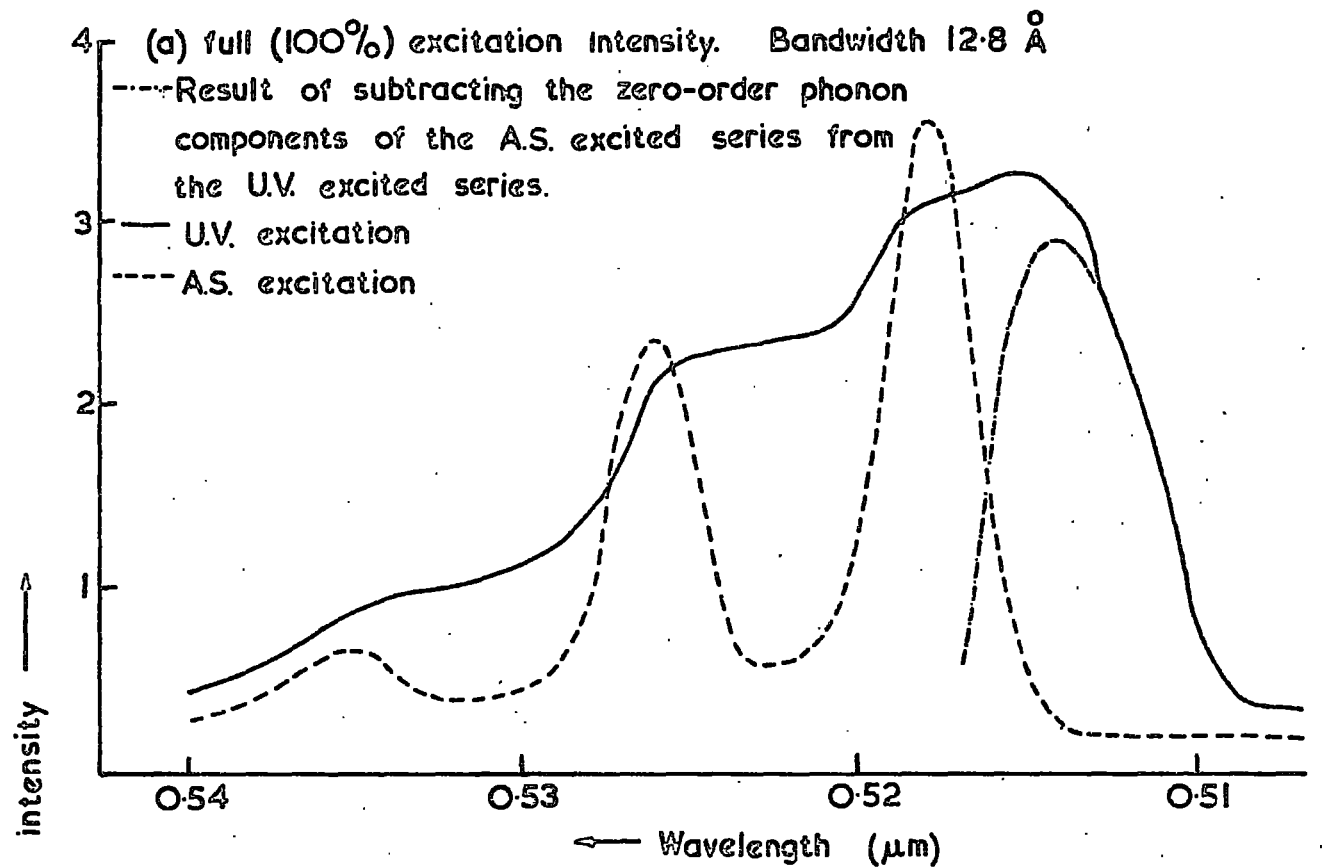


FIG.5.5. The SED of the green emission excited by (a) 100% and (b) 10% intensity U.V. and A.S. radiation.

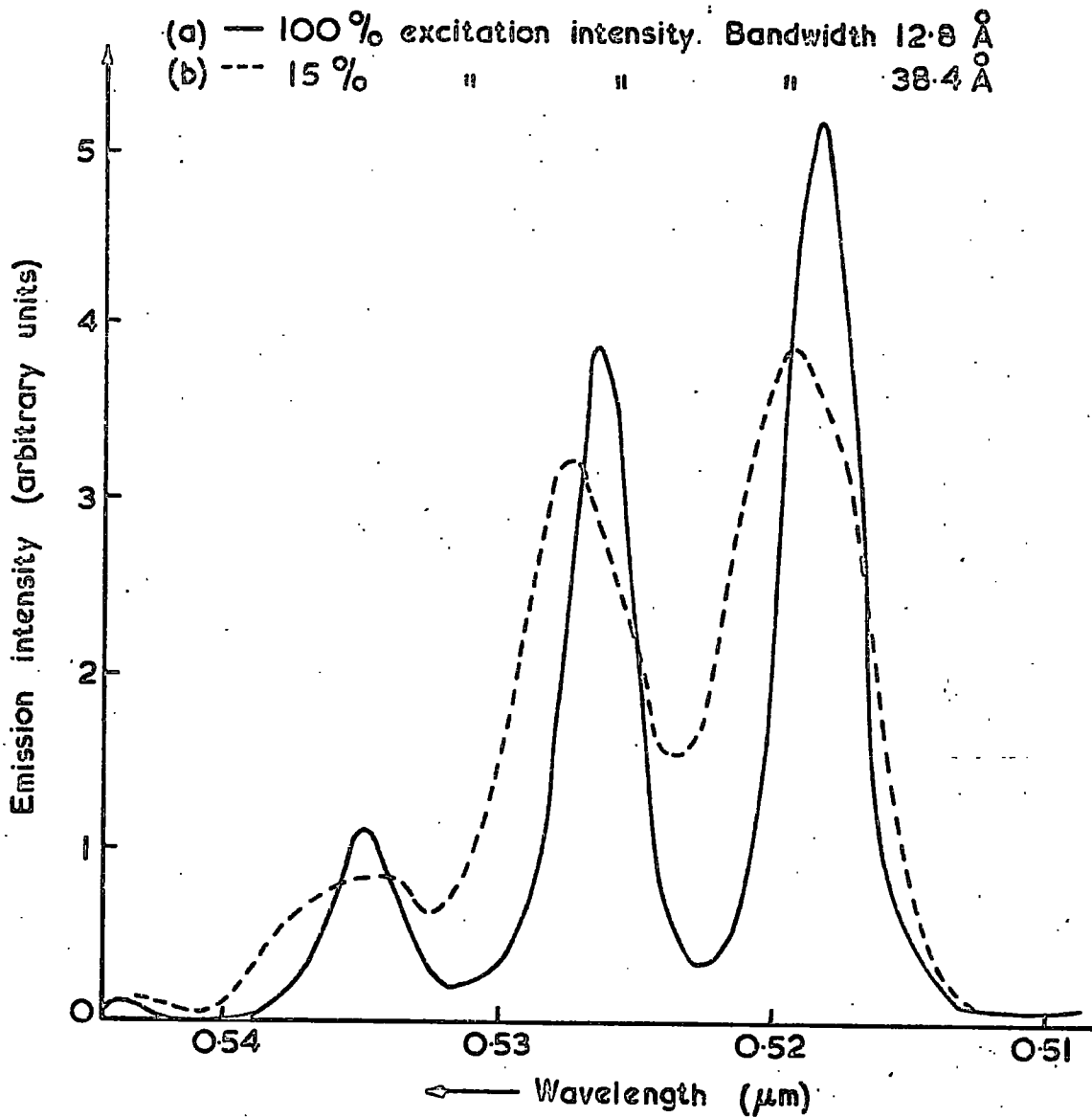


FIG. 5-6. The S.E.D. of the green emission excited by (a) 100% and (b) 15% intensity A.S. radiation.

responsible for the A.S. excited series is the same as that responsible for the U.V. excited L.E.S.. However, the energy shift of the zero phonon maxima per order of magnitude change in the excitation intensity was approximately 10 to 100% larger than the shift observed under U.V. excitation. In figure 5.5, the intensities of the 100% U.V. excited and 100% A.S. excited emissions were approximately equal. At 10% excitation intensity the U.V. excited series was more intense than the A.S. excited emission, indicating a difference in the excitation intensity dependence of the two series. A typical example of the excitation intensity dependence of the peak height of the zero-order phonon component of the A.S. excited series compared with that of the U.V. excited dependence is shown in figure 5.7. The intensity dependence indices of the U.V. and A.S. excited emissions of this crystal were 0.82 ± 0.03 and 1.2 ± 0.2 respectively. Averaged over four crystals the indices were 0.95 ± 0.05 and 1.23 ± 0.04 for the U.V. and A.S. excited emissions respectively. One "unusual" crystal showed an intensity dependence which was stronger than that observed in other crystals. Curves "a" and "b" of figure 5.8. show the dependence of the height of the zero phonon component of the U.V. and A.S. excited emissions, respectively. The indices obtained were $n(AS) = 1.89 \pm 0.09$ and $n(UV) = 1.12 \pm 0.07$. The results "c" were obtained by measuring the "total edge emission output" at low intensities of excitation, using two OR2 plus two HAL filters in the exciting beam. The "total edge emission output" was the signal produced as a result of the A.S. excited emission passing through a three inch cell containing a saturated solution of copper sulphate before falling on a photomultiplier. The copper sulphate cell was capable of absorbing

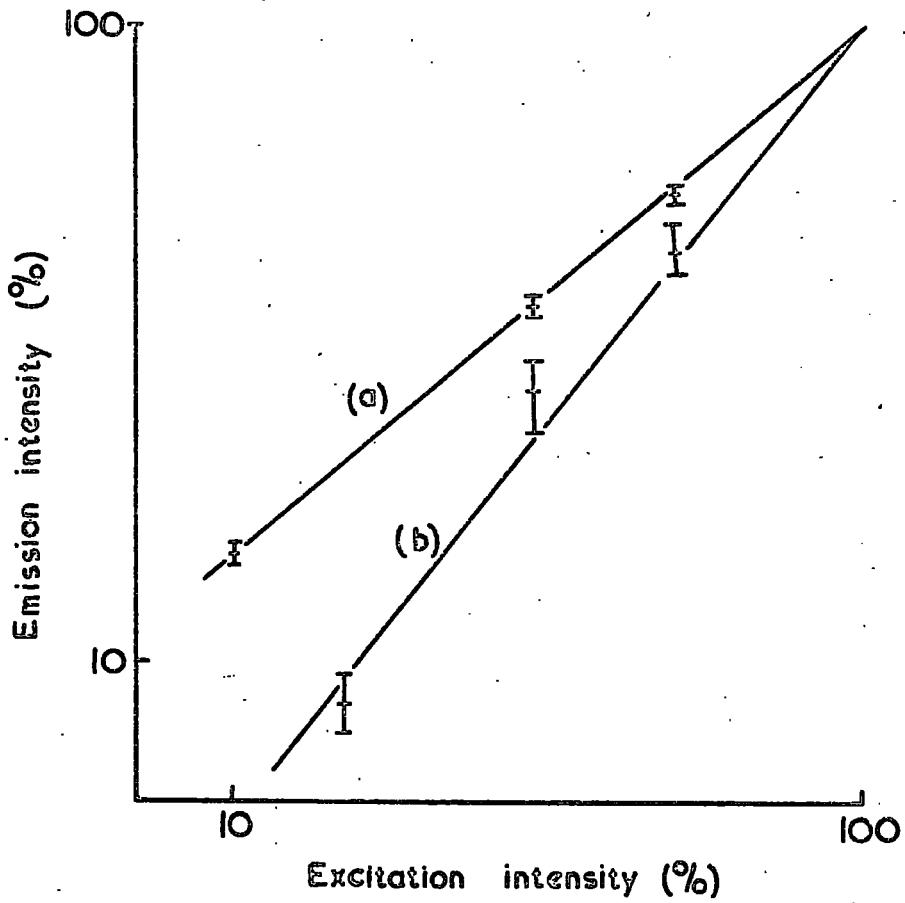


FIG.5-7. The dependence of the intensity of the green emission upon the intensity of (a) the UV and (b) the AS radiation.

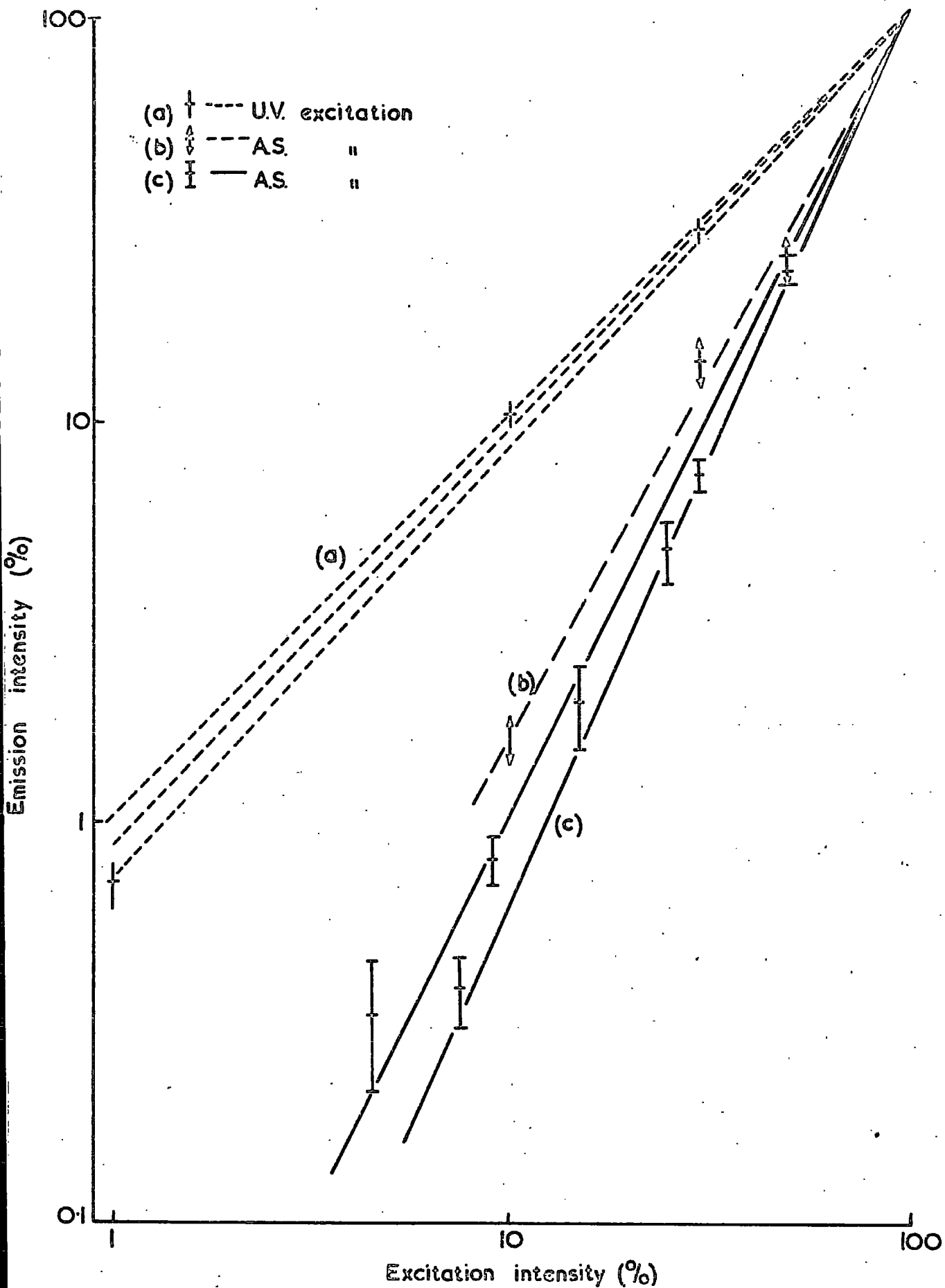


FIG. 58. The dependence of the intensity of the green emission upon the intensity of (c) the U.V. and (b)(c) the A.S. radiation, for an "unusual" crystal.

all the exciting beam, whilst allowing sufficient green radiation through to allow the measurement of a variation of three orders of magnitude change in light intensity. The index obtained from this measurement was $n(\text{AS}) = 2.08 \pm 0.04$, in good agreement with the value obtained by the conventional peak height method, and which was performed at a higher excitation intensity and included infra-red radiation in the exciting beam.

Discussion

The shift of the A.S. excited green emission spectrum to longer wavelengths as the intensity of the excitation was reduced indicates that the recombination process is the same as that in the U.V. excited L.E.S., namely the bound-to-bound transition. As in the case of the U.V. excited emission, the position of the maximum of the zero-phonon component varied from crystal to crystal. However, the variation in the position of the maximum in different crystals cannot be taken as an indication of a variation in the donor or acceptor ionisation energy for the following reasons :

- (a) the bound to bound nature of the recombination results in the variation of the position of the maximum with the intensity of excitation,
- (b) the variation of the ratio of the intensities of the U.V. to A.S. excited emissions from crystal to crystal indicates a variation in the efficiency of the excitation process - (this is described in section 5.4.)

The larger shift of the zero phonon maximum per order of magnitude change in excitation intensity, the lower energy of the zero phonon maximum and the narrower nature of the emission components of the A.S. excited emission compared with the U.V. excited emission are consistent with the recombination having taken place between donors and acceptors with a greater separation than those involved in the

U.V. excited L.E.S. recombination process. It was concluded that the same donors and acceptors are involved in the U.V. and A.S. excited L.E.S. recombination processes, but that the separation of the pairs of the recombination are greater in the A.S. excited process. Thus a larger volume of the crystal was probably involved in the A.S. excited recombination, which is consistent with the fact that the "red" exciting radiation would be able to penetrate the CdS crystal to a much greater depth than the U.V. excitation before being absorbed. The absorption coefficients corresponding to "red" and "band gap" excitation are of the order of 1 and 10^5 respectively (2,3).

A crude theory of a two step excitation process requires that the intensity dependence of the A.S. excited emission should follow a square law. An intensity dependence index of two was observed in an "unusual" crystal, however the index normally observed was approximately 1.2. This suggests that more than one excitation mechanism may be operative in the majority of crystals. The possible transition involved in the excitation, and possible reasons for the appearance of only the L.E.S. under A.S. excitation will be proposed in chapter eight.

5.3.3. Blue Edge Emission

Blue edge emission was observed in several undoped crystals at liquid helium temperatures under A.S. excitation. The intensity of the emission was weak, and it was necessary to increase the bandwidth of the Optica in order to obtain a reasonable spectrum. As a result, no sharp exciton-like lines were observed. Similar difficulties were experienced with the U.V. excited blue emission at low excitation intensities. The A.S. excited blue emission observed in some crystals was not resolved into meaningful maxima,

but consisted of a broad step running into the rising edge of the green emission. The emission observed in three other crystals showed distinct maxima and will be described more fully.

Figure 5.9. shows the U.V. and A.S. excited blue emission spectra of a crystal grown at 1075°C with a "sulphur tail temperature" of 50°C . The partial pressure due to the tail temperature was less than that due to sulphur over the growing CdS. The U.V. excited blue emission spectrum contained both the I_1 and I_2 bound exciton emissions. The principal maxima of the A.S. excited blue emission were at approximately 4920 and 5010\AA . Similar A.S. blue emission maxima, figure 5.10, were observed in a crystal grown at 1150°C under a sulphur pressure of 12mm., approximately less than or equal to the sulphur partial pressure over the growing CdS. The U.V. excited blue emission of this crystal was dominated by the I_1 bound exciton emission. The U.V. excited green emission spectra of the crystals of figures 5.9. and 5.10. were both dominated by the H.E.S. emission, however the asymmetry of the components indicated the presence of L.E.S. emission. In both crystals, the intensity of the A.S. excited blue emission was approximately two orders of magnitude less intense than the A.S. excited green emission.

Figure 5.11. shows the U.V. and A.S. excited blue emission spectra of a crystal grown at 1100°C under an excess cadmium pressure of 180mm.. The U.V. excited emission was completely dominated by I_2 emission. The U.V. excited exciton emission of this crystal was resolved using the spectrograph, see chapter four, and contained peaks designated I_2^* and $I_2^* + \text{L.O.}$. The corresponding maxima were located at approximately 4916 and 4990\AA as determined with the

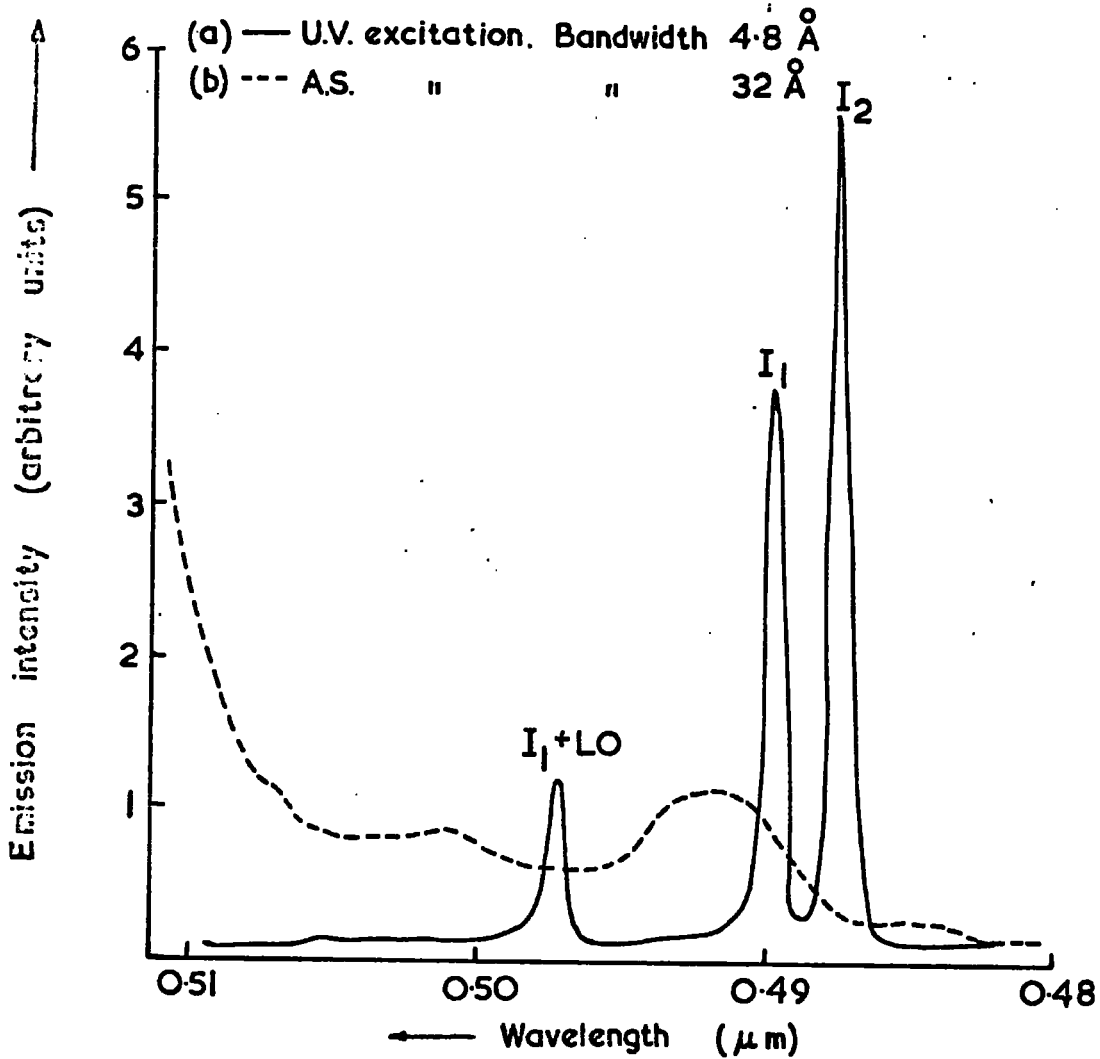


FIG.5.9 The S.E.D. of the blue emission excited by (a) U.V. and (b) A.S. radiation.

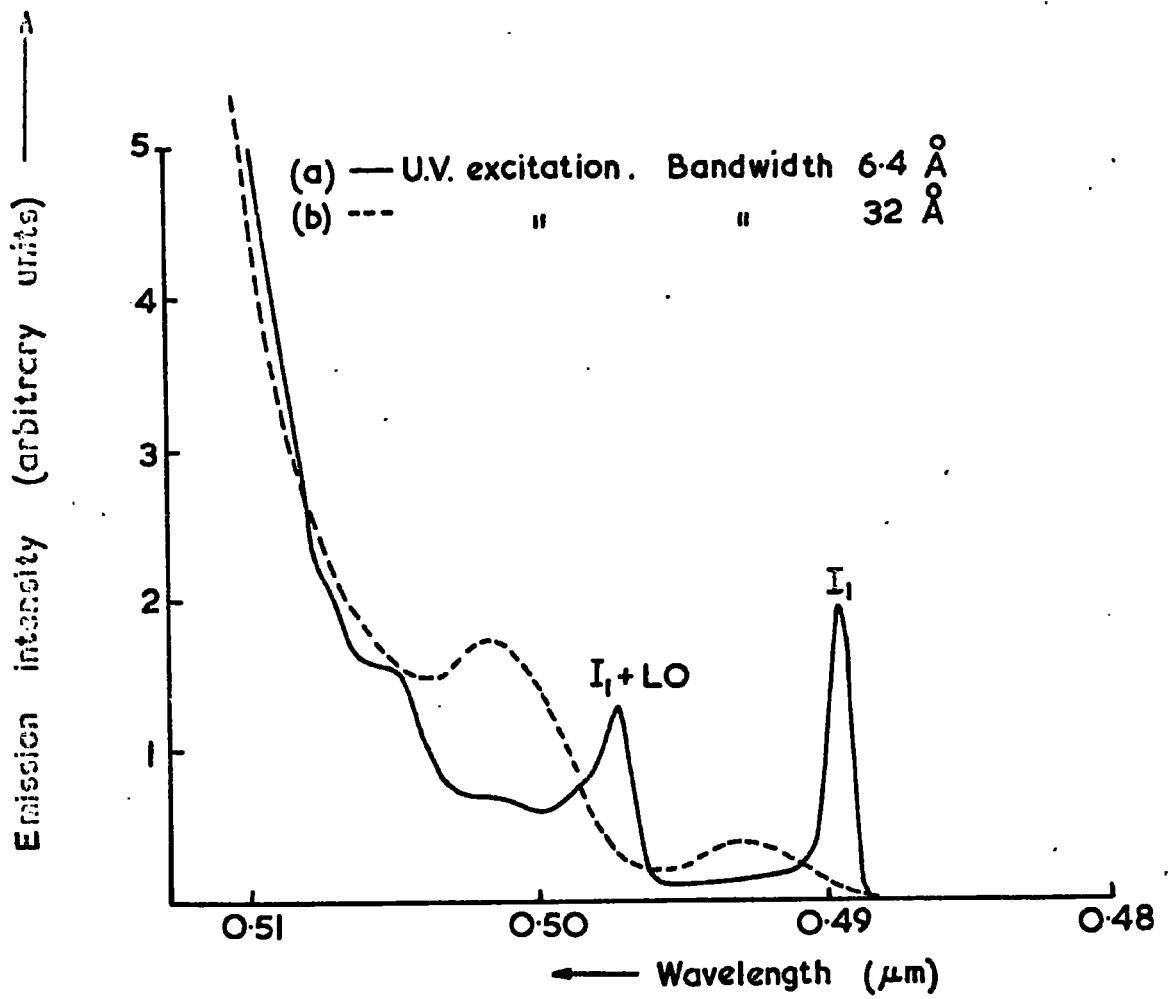


FIG. 5. The S.E.D. of the blue emission excited by (a) U.V. and (b) A.S. radiation.

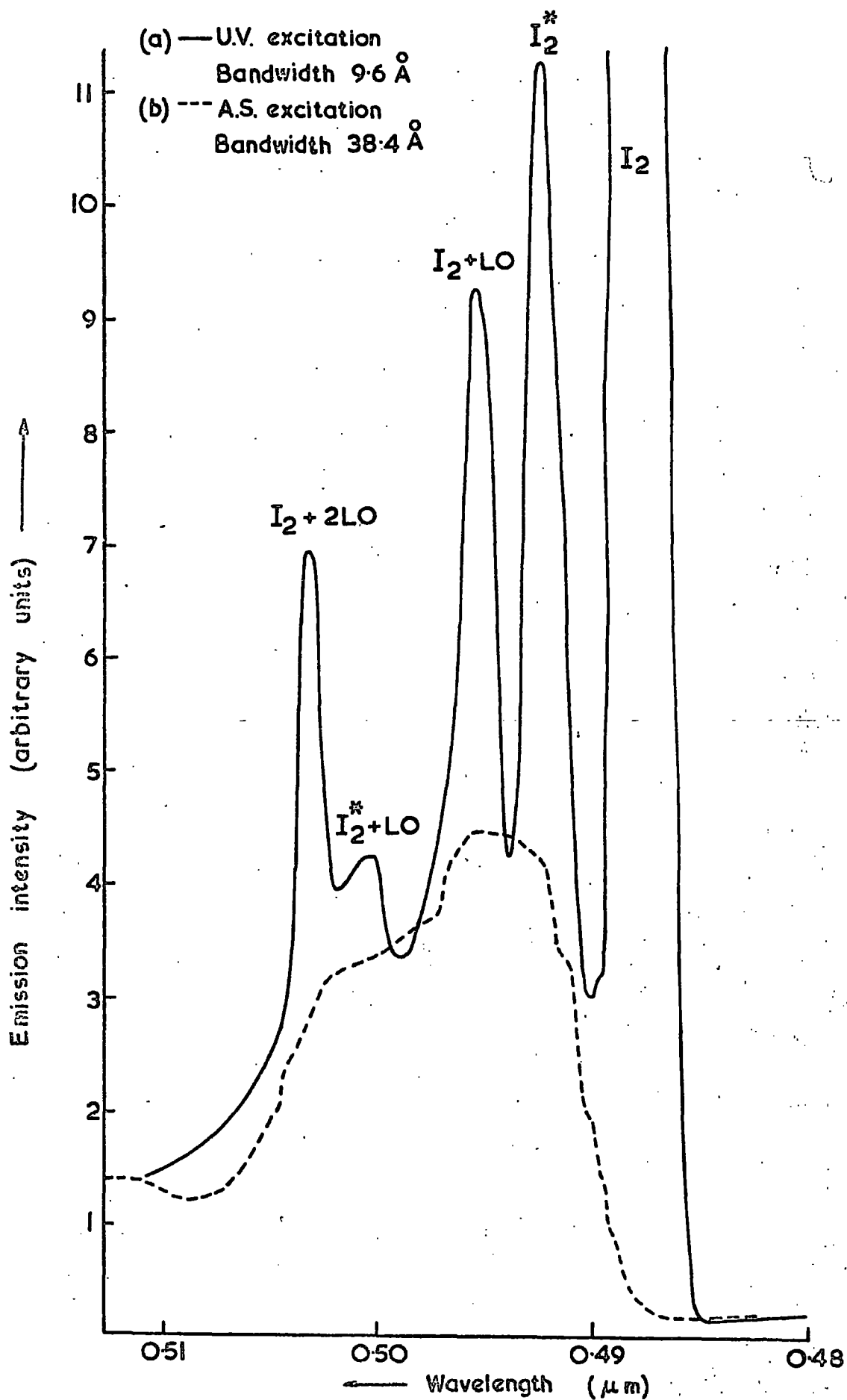


FIG. 511. The S.E.D. of the blue emission excited by (a) U.V. and (b) A.S. radiation.

spectrograph, and at approximately 4920 and 5000 \AA as recorded by the spectrophotometer. The intensity of the U.V. excited green emission of this crystal was very low. The intensities of the A.S. excited green and blue emissions were approximately equal.

Discussion

Comparing the spectra of figure 5.11. it appears that the A.S. excited emission of this crystal may be associated with the I_2^* and $I_2^* + L.O.$ emissions, and possibly the first and second L.O. phonon replicas of the I_2 exciton. Similarly the emission maxima at approximately 4920 and 5000 \AA in figures 5.9. and 5.10. are probably associated with I_2^* and $I_2^* + L.O.$ emission. The spectrographic analysis of the U.V. excited emission showed that the I_2^* "peak" consisted of several maxima which could be assigned to the emission of photons which had resulted from excitons bound to the neutral donors losing some of their recombination energy in raising the donor electron to different excited states of the donor. Because of the broad nature of the recorded maxima of the A.S. excited emission, and the absence of a spectrographic recording of the emission, these assignments are rather tentative.

It is significant that the intensity of the L.E.S. of the U.V. excited emission was low compared with that associated with other recombination processes in all the three crystals in which excitons were observed in the A.S. excited emissions. The intensity ratio of the H.E.S. to L.E.S. of the U.V. excited green emission of the two crystals whose spectra are illustrated in figures 5.9. and 5.10. was approximately two. In contrast, the intensity of the U.V. excited I_2 exciton emission was approximately two orders of magnitude greater than the intensity of the first component of the U.V. excited

L.E.S. It was concluded, therefore, that A.S. excited blue emission is only observed in crystals in which the normal L.E.S. recombination process is inefficient compared with the H.E.S. or exciton recombination processes. Because of the low intensity of the emission, no intensity dependence measurements could be obtained.

5.4. Effects of crystal growth conditions upon A.S. excited emission

Figure 5.12. illustrates the way in which the relative intensities of the U.V. and A.S. excited green edge emissions varied in undoped crystals grown under different partial pressures of cadmium and sulphur. The ratio of the intensities of the A.S. to U.V. excited L.E.S. is also shown. The intensities of the A.S. excited emission followed reasonably closely the same trends as the U.V. excited L.E.S.... However, the plots of the ratio of the A.S. to U.V. excited L.E.S. intensities were not straight horizontal lines. As the excess sulphur pressure was increased above 100mms., the A.S. to U.V. ratio decreased. For excess cadmium pressures above about 10mms., the A.S. to U.V. ratio decreased. Although there were differences in the actual intensities of the components of crystals grown under excess sulphur pressure in which the CdS was maintained at 1150 and 1125°C during growth, the same trend was observed in the ratio of the A.S. to U.V. excited L.E.S. intensities.

The crystals grown with the CdS held at 1075°C, one under 180mm. cadmium pressure, the other under 150mm. sulphur excess pressure, showed higher A.S. to U.V. intensity ratios than the crystals which had been grown under the same excess pressures, but with the CdS at higher temperatures. However, the U.V. excited emission of both 1075°C crystals showed a very weak exciton emission compared to those grown at the higher temperatures. This is the reverse of the

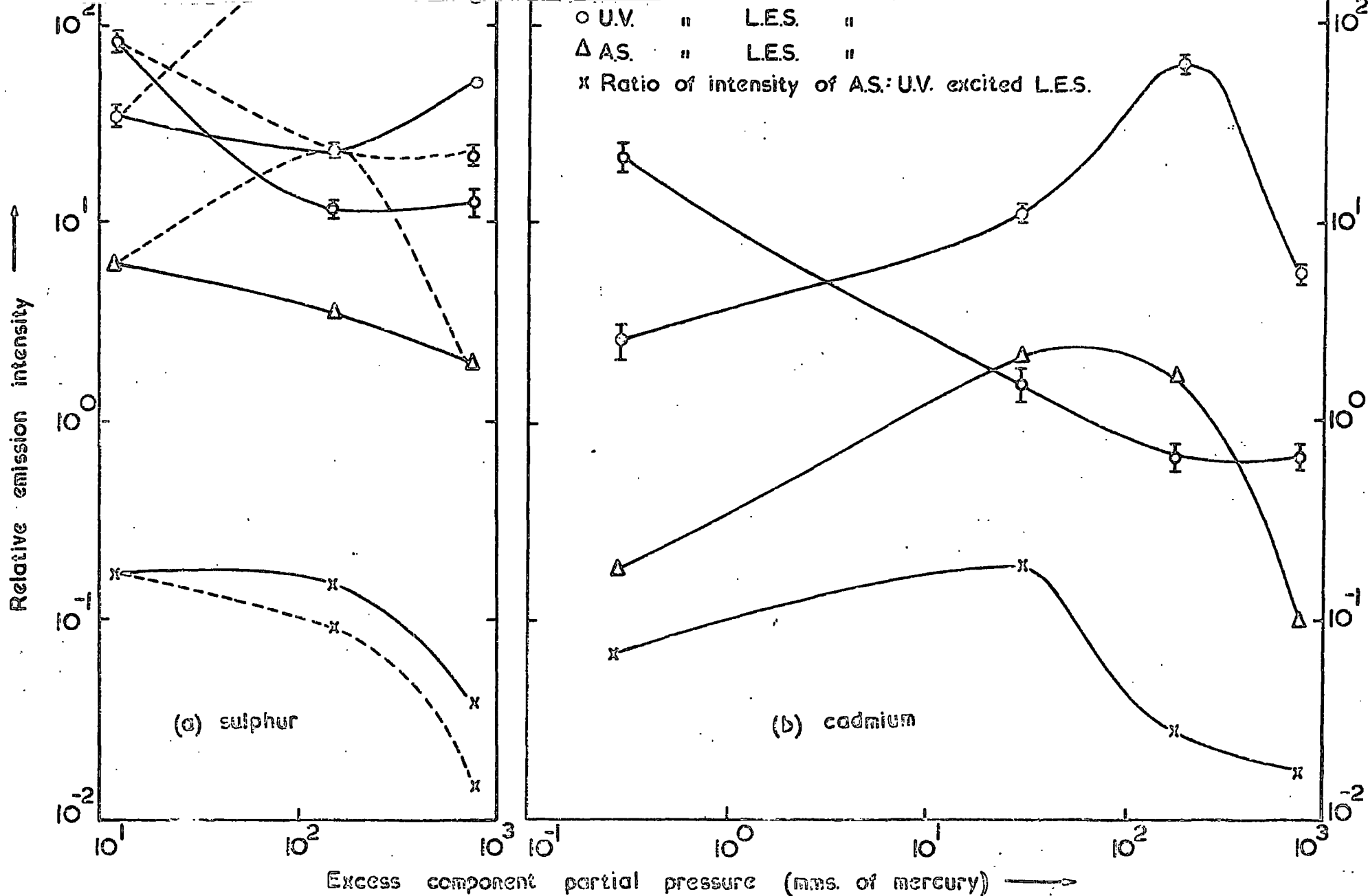


FIG.5-12. The dependence of the intensity of the green emission excited by U.V. and A.S. radiation upon the partial pressure of the excess constituent during growth. — CdS at 1150°C ---- CdS at 1125°C.

effect mentioned in the preceding section, where A.S. excited exciton emission probably appeared because the L.E.S. recombination process was so inefficient compared with exciton recombination. The crystal grown under 12mm. sulphur pressure, which showed A.S. excited blue emission, was one of those used in the compilation of figure 5.12. If the A.S. excited carriers had recombined via the bound to bound rather than the exciton process, the A.S. to U.V. intensity ratio may have shown a more emphasised decrease with increasing sulphur pressure.

Anti-Stokes excited green edge emission was detected in the crystals supplied by A.E.I.Ltd. and Hull University. The intensity of the A.S. excited emission was almost the same as that of the U.V. excited L.E.S. emission in two crystals. The emission characteristics were the same as those of crystals grown at Durham, and some A.S. excited blue emission was detected in one crystal. These observations indicated that the A.S. excitation of edge emission is an effect observable in CdS crystals other than those grown at Durham, possibly involving a native defect. This was further supported by the increase of the A.S. to U.V. excited L.E.S. emission intensity ratio by at least two orders of magnitude in a Durham crystal, initially grown under a high excess cadmium pressure, which had subsequently been treated at 800°C for three hours under a pressure of sulphur of 180 torr.

Discussion

The decrease in the A.S. to U.V. excited L.E.S. intensity ratio with increasing pressure of either cadmium ^{or} sulphur may be explained in terms of a reduction in the overall efficiency of the excitation process, or an increase in the number of alternative

recombination mechanisms. It appears that the alternative green edge recombination process, the free to bound transition, is in some way "forbidden" under A.S. excitation or requires higher input powers than were available. The observation of the I_2^* emission in the absence of the bound exciton (I_2) emission itself implies that complex recombination selection rules may be operating in the blue emission excited by A.S. radiation. The efficiency of this recombination process is certainly very low judging by the absence of A.S. excited blue emission in crystals which had intense U.V. excited blue emission. Recombination via mechanisms other than band edge processes, either radiative or non-radiative, may certainly be effected by growth conditions. For example, the drop in the A.S. to U.V. ratio above about 10mm. excess cadmium pressure is probably due to the onset of the red (2.0 eV, 0.62 microns) recombination process observed in the U.V. excited emission of "cadmium rich" crystals reported in the preceding chapter. A donor-acceptor associate (DAA) model has been suggested to describe the emission and absorption processes in the 2.0 eV region (4,2). Goede (4) observed two emission bands, one was ascribed to cadmium vacancies with donors substituted on nearest neighbour sites forming singly ionisable acceptors $(V_{Cd} D)'$, the other to cadmium interstitials with acceptors substituting on nearest neighbour sites forming singly ionisable donors $(Cd_i A)^\bullet$. To explain the results of the variation of the A.S. excited green emission intensity with crystal growth conditions, a model involving a donor acceptor associate level will be used, see chapter eight.

5.5. Summary

The single green edge emission series of CdS crystals at

liquid helium temperatures observed under A.S. excitation is attributed to the L.O. phonon assisted recombination of electrons bound to donors some 0.03 eV below the conduction band with holes bound to acceptors some 0.17 eV above the valence band. The recombination process is similar to that observed in the U.V. excited L.E.S. emission except that the separation of the donor-acceptor pairs is assumed to be slightly larger in the A.S. than the U.V. excited emission, probably as a result of the higher absorption coefficient at the shorter wavelengths. Evidence for the greater separation is the larger energy shift per order of magnitude change in excitation intensity, the lower energy of the zero phonon maximum and the narrower nature of the emission components of the A.S. excited emission compared with the U.V. excited emission.

The blue edge emission observed in several crystals is attributed, by comparison of U.V. and A.S. excited emission spectra, to the emission of photons which have lost some of their energy in exciting the neutralising electrons of the donors to which they were bound. This assignment is rather tentative. However, since the H.E.S. was never observed, it seems highly probable that the same donor levels are involved in both green and blue edge emissions.

The variation of the ratio of the intensities of the zero phonon components of the A.S. to U.V. excited L.E.S. emission with the conditions under which the crystals had been grown indicated that there was a dependence upon the constituent pressures. The effects and mechanism of other competing recombination processes must not be forgotten when considering the excitation mechanisms. This will be discussed in later chapters.

The green emission excited by A.S. radiation may be observed

from a suitable CdS crystal immersed in liquid nitrogen and irradiated by an OR2 filtered microscope lamp. The green can be resolved from the red by the naked eye generally, however an auxiliary copper sulphate filter was helpful occasionally. The incorporation of suitable dopants increased the "efficiency" of the process, as described in the next chapter. The external efficiency, which relates the number of photons incident and the number emitted, of Durham grown crystals was determined by Brown et al. (5), at Christchurch, to be some one percent. The H.E.S. was observed in the A.S. excited emission of several CdS crystals at liquid helium temperatures by the workers at Christchurch. They suggested that these crystals were more pure than those in which the L.E.S. emission was the more intense emission.

CHAPTER 5

REFERENCES

1. I. Broser and R. Broser-Warminsky, Luminescence of Organic and Inorganic Materials, H.P. Kallmann and G.M. Spruch, Eds. (J. Wiley and Sons, Inc., New York, 1962), p. 402.
2. R. Boyn (1968) Phys. Stat. Sol. 29, 307.
3. B. Segall and D.T.F. Marple (1967) "The Physics and Chemistry of II-VI Compounds" Chapter 7.
4. O. Goede (1968) Phys. Stat. Sol. 28, K 167.
5. M.R. Brown, A.F.J. Cox, D.S. Orr, J.M. Williams, and J. Woods (to be published).

CHAPTER 6

EDGE EMISSION OF DOPED CADMIUM SULPHIDE CRYSTALS

6.1. Introduction

The U.V. and A.S. excited edge emissions of aluminium, antimony, chlorine, copper and sodium doped cadmium sulphide crystals measured at liquid helium temperatures are described in this chapter. The dopant, in suitable form, was added to the cadmium sulphide charge prior to the growth of the boule. The materials used were aluminium, antimony, cadmium chloride, cuprous sulphide, sodium and sodium sulphide. The effects upon the edge emission of maintaining excess pressures of cadmium or sulphur during crystal growth were compared for aluminium, chlorine and copper doped crystals. Unless otherwise specified, the crystals were all grown with the upper furnace control set at 1150°C.

The edge emission characteristics of deliberately doped cadmium sulphide crystals were essentially the same as those of undoped crystals. There were changes in individual components in certain cases. For example, the green emission of sodium doped crystals was much broader than the emission of undoped crystals grown under similar conditions. The exciton emission of doped crystals was often so weak that it could not be resolved into individual components. However, some doped crystals showed well resolved exciton emission, so that absence of exciton emission in particular crystals probably indicated poor crystal quality. The intensities of the components of the A.S. and U.V. excited edge emission of doped crystals differed from those of undoped crystals grown under the same conditions. This indicated that the dopant was incorporated in the crystals.

The relative intensities of the peak heights of the major components of the U.V. and A.S. excited edge emission of doped crystals are compared with those of undoped crystals grown under similar conditions in Table 6.1. The table, which was compiled from the recordings of the spectrophotometer, provides the quantitative basis of this chapter. The emission characteristics are described and discussed in sections which deal with the individual dopants. In order to facilitate the presentation, the crystals will be referred to as (X,Y) and "undoped", where X was the dopant element, Y the element of the excess pressure during growth and "undoped" refers to the crystal or crystals grown under similar conditions without the addition of any deliberate dopant.

6.2. Aluminium doped crystals

Two aluminium doped crystals were studied, the (Al,Cd) sample was grown under a low pressure of cadmium, and the (Al,S) one under a high pressure of sulphur. It was hoped that these growth conditions would allow the aluminium to substitute for cadmium, and form a donor. The U.V. excited emission spectra of these two crystals were different from one another, and their undoped counterparts. The presence of the H.E.S. was more obvious in the (Al,Cd) crystal than in the (Al,S) crystal, although the two L.E.S. emission peaks were approximately equal. The blue edge emission of the (Al,Cd) crystal was dominated by I_2 exciton emission, with the first longitudinal optical (L.O.) phonon replica of the I_1 exciton rising above the broad background emission. This background was probably due to the I_1 exciton, the I_2^* emission and L.O. phonon assisted I_2 emission. The exciton emission of the (Al,S) crystal, which was a broad peak at 4900\AA (30\AA wide at half height), was not resolved

Table 6.1. A comparison of the emission intensities of doped and undoped cadmium sulphide crystals. (The dopant concentration, in p.p.m. atomic, was that calculated from the proportions by weight of the dopant element to the CdS charge. - - 0.07- - indicates a broad emission band with a maximum emission intensity of 0.07)

P _{Cd} or P _S mm. of Hg (crystal no.)	Dopant p.p.m.	U.V. Excited emission					A.S. Excited	
		I ₁	I ₂	I ₂ *	H.E.S.	L.E.S.	L.E.S.	Blue
S 12 (77)	- -	3.0	0.05	-	85	26	6.3	0.08
S 12 (179)	Cu 180	0.3	132	0.3	2.7	22.6	9.8	0.05
S 150 (80)	- -	1.6	100	1.6	12	24	3.7	-
S 150 (155)	Cu 36	- -	0.16-	-	3.7	25.8	45.8	-
S 150 (153)	Cl 13	- -	0.02-	-	5	126	85	-
S 760 (94)	- -	5	1.9	-	13	52	2.0	-
S 760 (104)	Al 3500	- -	0.62-	-	3.6	21.9	6.0	-
S 760 (135)	Sb 714	-	-	-	2	19.3	16.7	-
S 760 (120)	Na 1850	- -	0.02-	-	13	82	2	-
Cd 0.3 (78)	- -	48	100	2.6	22	2.6	0.17	-
Cd 4.5 (109)	Al 3000	0.2	3.7	0.2	11	22	0.42	-
Cd 30 (127)	- -	2.4	130	1.2	1.6	11.2	2.1	-
Cd 180 (129)	- -	1	480	1	0.65	65	1.8	-
Cd 180 (154)	Cl 13	- -	0.07-	-	0.35	7.7	141	-
Cd 180 (152)	Cu 22	- -	0.1	-	0.3	14	29	-
Cd 180 (177)	Cu 180	1	168	7.3	0.11	2.0	0.42	0.14

into components because of its weak intensity. The emission was probably largely due to I_1 exciton recombination, although only a weak first L.O. phonon replica was observed. The intensity of the A.S. excited L.E.S. of the (Al,S) crystal was approximately ten times that of the (Al,Cd) crystal. There was no A.S. excited blue edge emission detected from either of the aluminium doped crystals.

No measurements were made upon an undoped crystal grown under exactly similar growth conditions to the (Al,Cd) crystal. However, in comparison with those grown under comparably low cadmium pressures, the intensity of the U.V. excited exciton emission was lower, and probably as a consequence, the green emission intensity was higher in the doped crystal. The A.S. to U.V. excited L.E.S. emission intensity ratio of the (Al,Cd) crystal was less than that of the undoped crystals. (This was the only case recorded where the addition of a deliberate dopant to the starting charge had a possible adverse effect upon the A.S. to U.V. intensity ratio.) The intensity of the A.S. excited emission of the (Al,S) crystal was approximately three times that of the undoped crystal. The A.S. to U.V. intensity ratio was increased by approximately an order of magnitude as a result of the addition of the dopant.

6.3. Antimony doped crystal

Only one antimony doped crystal was studied, which was grown under an excess sulphur pressure, (Sb,S). If antimony substitutes for cadmium, it would probably be trivalent and act as a single donor, using two of its three 5p electrons to satisfy lattice bonding requirements. The two 5s electrons would remain ineffective. The crystal was a brownish-yellow colour, having a resistivity of the order of 10^3 ohm.cm.. No blue emission was detected in either the

U.V. or A.S. excited spectra. This was probably a result of poor crystal quality, as will be discussed in the summary at the end of this chapter.

Figure 6.1. shows the relative intensities of the A.S. and U.V. excited green emission of the (Sb,S) crystal. The L.E.S. dominated the U.V. excited emission, which was sharper than the A.S. excited emission although the A.S. excited emission was clearly shifted to longer wavelengths. This is unusual. Figure 6.2. shows the shift of the A.S. excited green emission series to longer wavelengths with reduced excitation intensity. The shift to lower energy of the zero phonon peak of the green emission per order of magnitude decrease in excitation intensity was 2.9 meV under U.V. and 5.3 meV under A.S. excitation. The larger shift under A.S. excitation indicates that recombination was associated with distant pairs having a greater separation than those under U.V. excitation. The unusual feature that the A.S. excited series was broader than the U.V. excited series, despite the larger shift of the A.S. series, may have been associated with a change in the coulombic nature of the donor under A.S. excitation, as discussed in the summary. The intensity dependence indices (n) for the U.V. and A.S. excited zero phonon peaks were 0.96 ± 0.01 and 1.21 ± 0.04 , respectively.

The intensity of the U.V. excited green emission of the undoped crystal grown under corresponding conditions was approximately three times the intensity of the (Sb,S) crystal. The intensity of the A.S. excited emission of the doped crystal was approximately eight times that of the undoped crystal. This indicated that the addition of antimony to the starting charge of the growth system had improved the A.S. to U.V. intensity ratio by a factor of

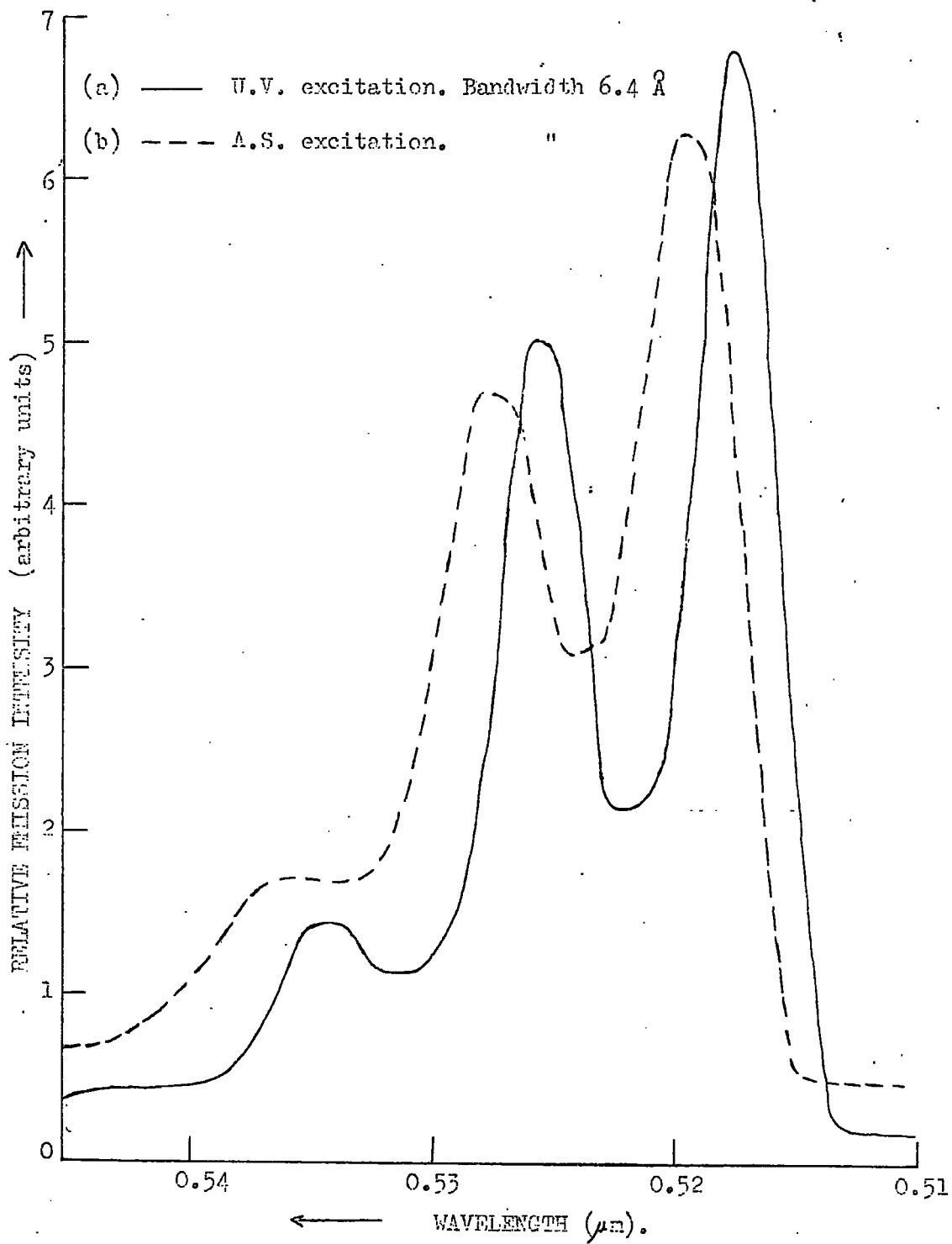


Figure 6.1. The S.F.D. of the green emission of the antimony doped crystal, no. 135, excited by (a) U.V. and (b) A.S. radiation.

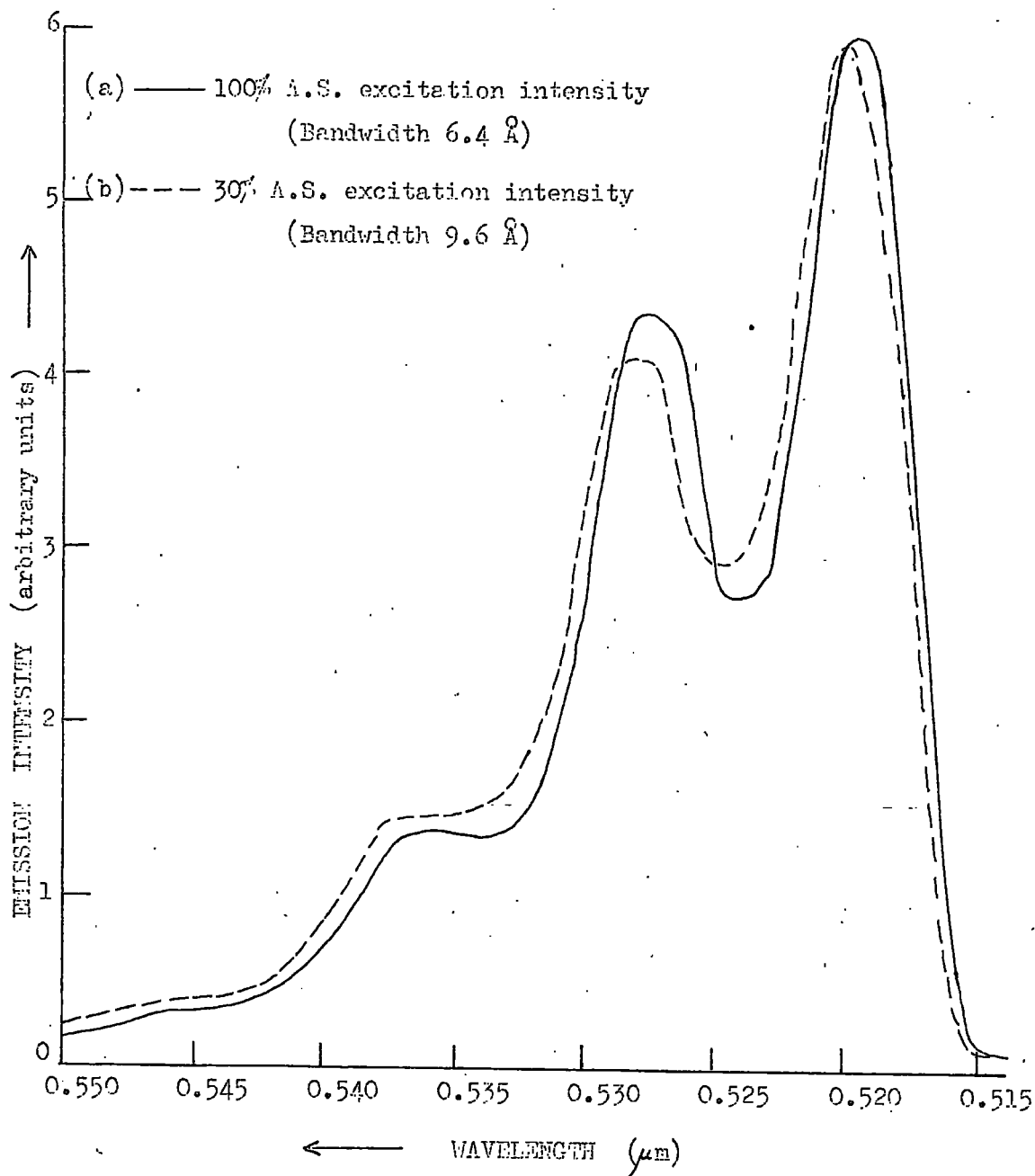


Figure 6.2. The S.E.D. of the green emission of the antimony doped crystal, no. 135, excited by (a) 100 % and (b) 30 % A.S. excitation radiation.

approximately twenty.

6.4. Chlorine doped crystals

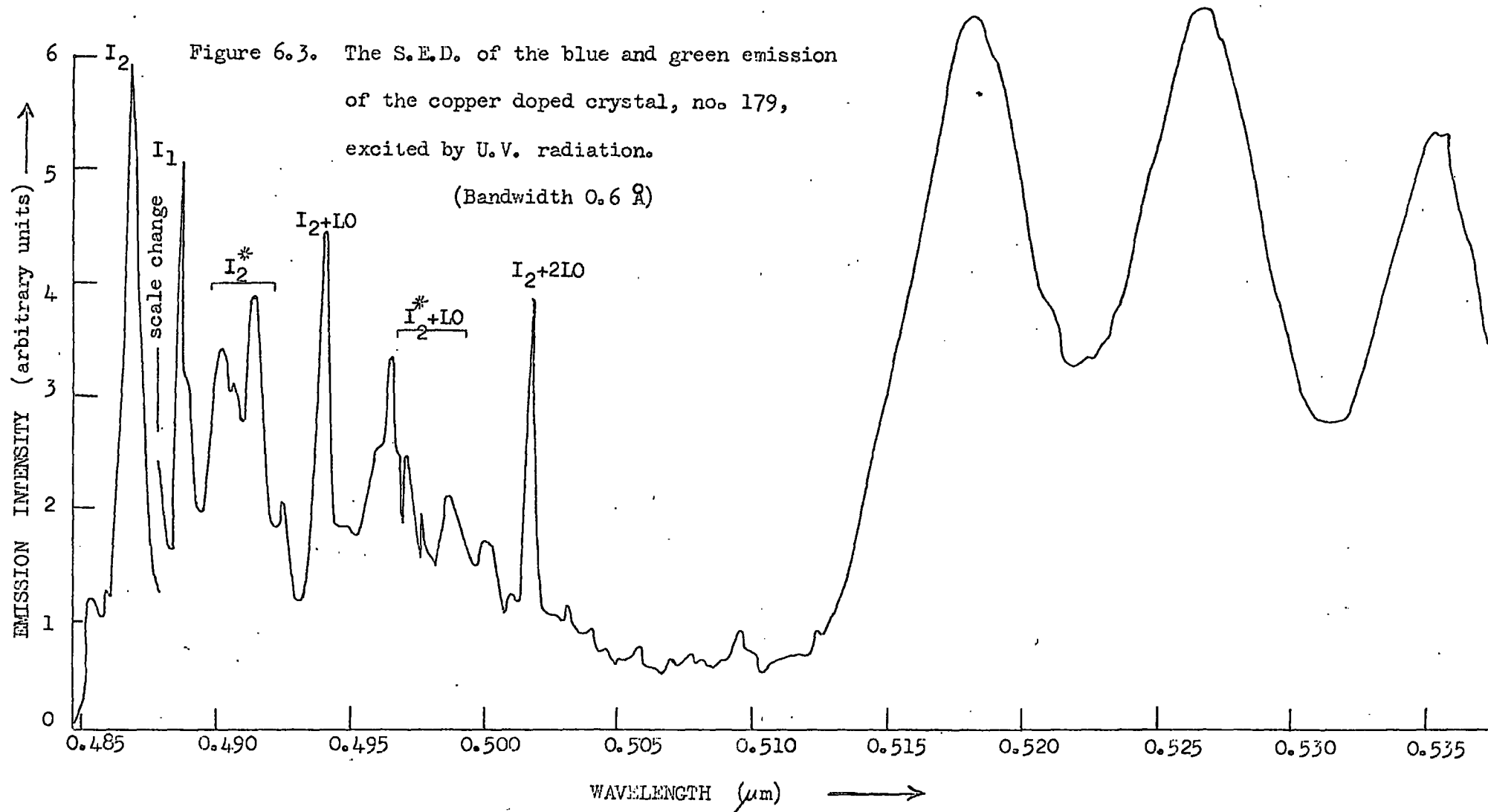
Two chlorine doped crystals were studied, (Cl,Cd) and (Cl,S), grown under excess pressures of approximately 180 and 150 mm. of cadmium and sulphur respectively. The U.V. excited blue emission of both crystals was weak. The blue emission of the (Cl,Cd) crystal was the most intense, and was recorded as a broad band (40\AA at half height) centred at approximately 4885\AA . The green emission of both crystals was dominated by the L.E.S., although the zero order phonon peaks of the (Cl,Cd) and (Cl,S) crystals were observed to be at approximately 5189 and 5174\AA , respectively while the A.S. excited peaks were at 5188 and 5177\AA respectively. However such small differences in the position of the maxima of continuously excited photoluminescent spectra cannot be taken as positive variations in the ionisation energy of a carrier as has been mentioned in preceding chapters.

The intensity of the U.V. excited green emission of the (Cl,S) crystal was greater than that of the undoped and (Cl,Cd) crystals, see table 6.1. The intensity of the U.V. excited green emission of the (Cl,Cd) crystal was less than that of the undoped crystal. However, the intensity of the A.S. excited emission of the (Cl,Cd) crystal was about twenty times the intensity of the U.V. excited emission, and more intense than the U.V. excited emission intensity of the (Cl,S) crystal. This implies that the cadmium atmosphere had assisted the incorporation of chlorine on sulphur sites, and that the resultant donors are closely associated in some way with the level responsible for the A.S. excitation mechanism.

6.5. Copper doped crystals

Two sets of crystals were studied which had been deliberately doped with different concentrations of copper. The low concentration set (30 p.p.m.) will be considered firstly. The U.V. excited blue emission consisted of broad, low intensity bands centred at 4885 and 4890Å for the (Cu,Cd) (No.152) and (Cu,S) (No.155) crystals respectively. There was no blue emission detected under A.S. excitation. The L.E.S. dominated all green edge emission spectra. The intensity of the U.V. excited green emission of the (Cu,Cd) crystal was less than that of the undoped crystal, whereas the intensities of the (Cu,S) and undoped crystals were comparable. (This was probably due to the tendency of the cadmium atmosphere to inhibit the formation of native acceptors). The intensity of the A.S. excited green emission of the doped crystals was at least an order of magnitude greater than that of the undoped crystals. Thus the A.S. to U.V. ratio was considerably improved by light copper doping, and was slightly higher in the (Cu,Cd) crystal, probably due to the growth conditions favouring the autocompensatory formation of donors, see chapter eight.

The U.V. excited emission spectra of both heavily doped crystals were dominated by I_2 exciton emission, see figures 6.3 and 6.4(a). The (Cu,S) crystal (No.179) was grown under a sulphur pressure which was less than the sulphur partial pressure above the CdS charge. The pressure, 12mm, was probably insufficient to prevent the autocompensatory formation of donors (I_2), resulting from the introduction of the large number of copper acceptors. The I_1 emission line of the (Cu,S) crystal, figure 6.3, was more intense than that of the (Cu,Cd) (No.177) crystal, figure 6.4(a). I_2^* emission



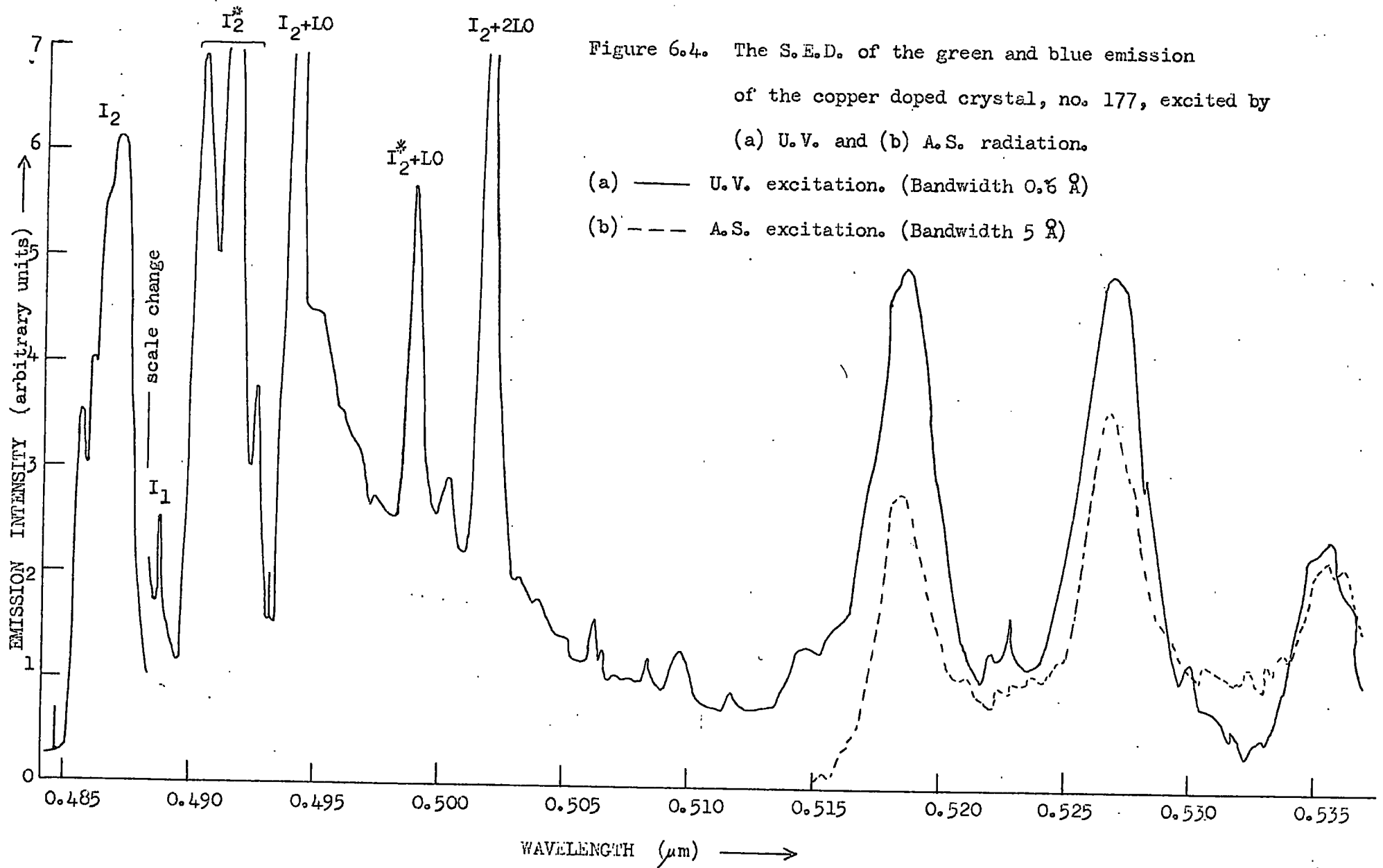
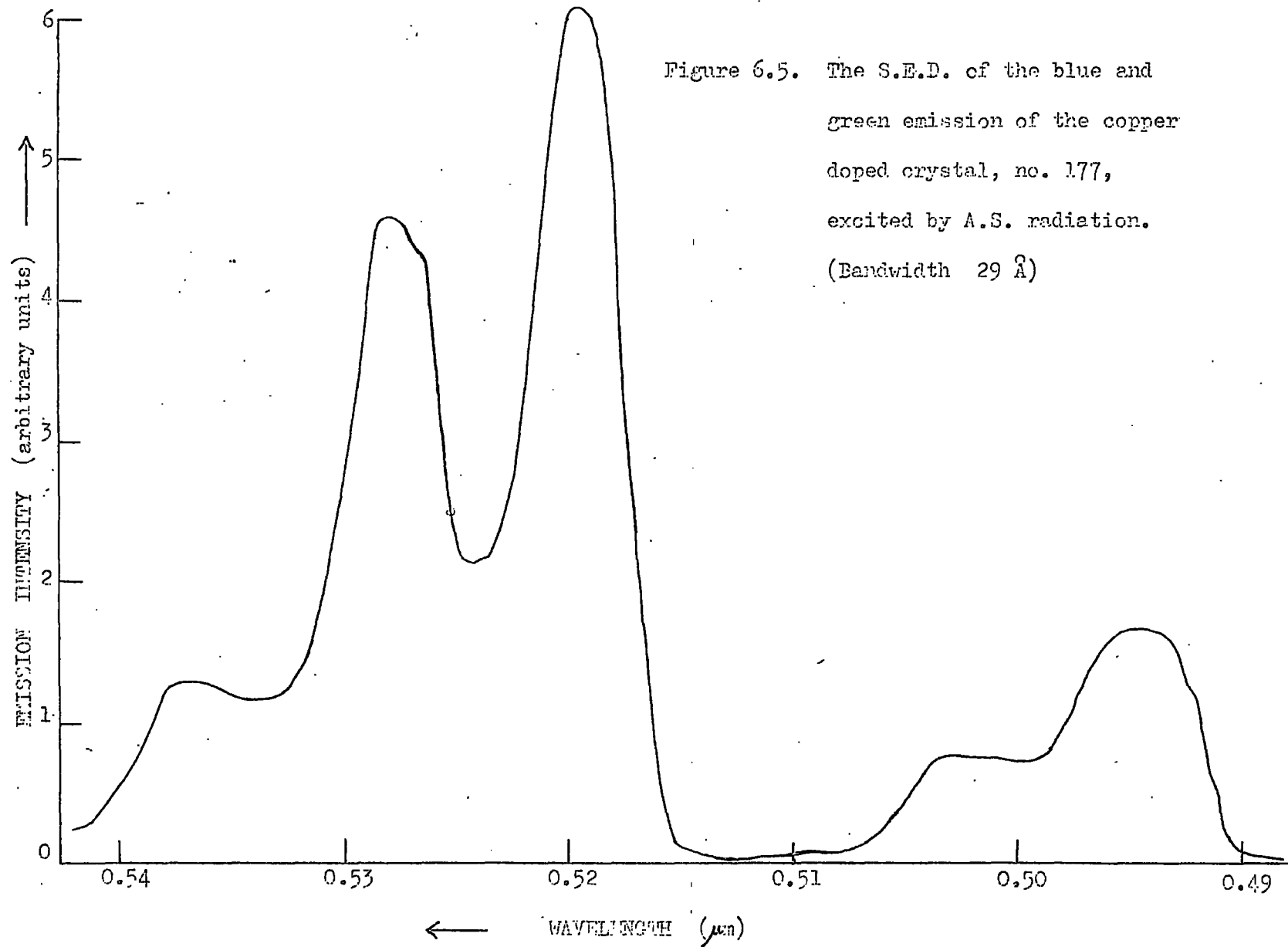


Figure 6.4. The S.E.D. of the green and blue emission of the copper doped crystal, no. 177, excited by (a) U.V. and (b) A.S. radiation.

- (a) — U.V. excitation. (Bandwidth 0.6 Å)
- (b) - - - A.S. excitation. (Bandwidth 5 Å)

maxima were resolved in the microdensitometer recordings of the spectra from both crystals. The I_2 and I_2^* emission intensities were more intense in the (Cu,Cd) crystal. The U.V. excited green emission spectra of both doped crystals were dominated by the L.E.S., with the H.E.S. being more obvious in the (Cu,S) crystal. The intensities of the U.V. excited green emission spectra of the doped crystals were less intense than those of the undoped crystals. No difference was observed in the positions of the blue or green components of the copper doped crystals compared with those of undoped crystals.

The A.S. excited emission spectra of both of the heavily doped crystals showed both green and blue edge emission. Figure 6.4(b) shows the A.S. excited green emission of the (Cu,Cd) (No.177) crystal, as recorded by the spectrograph. The complete spectrum, as recorded by the spectrophotometer, is shown in figure 6.5. The emission spectrum of the (Cu,S) (No.179) crystal was similar, however the intensity of the blue edge emission was weaker while that of the green emission was stronger than the respective intensities of the emission of the (Cu,Cd) crystal. As with the blue emission of undoped crystals excited by A.S. radiation, the intensity was too weak to enable the precise nature of the emission to be resolved, and the maxima have been assigned to I_2^* and $I_2^* + L.O.$ emission by comparison of the spectra obtained under the two different excitation conditions. This tentative assignment is supported by the fact that the exciton emission was more intense in the (Cu,Cd) than the (Cu,S) crystal, which is consistent with the fact that, under U.V. excitation, the I_2^* emission was most readily observed in undoped crystals grown under excess pressures of cadmium vapour.



Because the blue emission provides a competitive recombination process for the A.S. excited electrons and holes, the A.S. to U.V. excited emission intensity ratio was lower in the heavier doped crystals compared with that in the more lightly doped samples. At both doping levels, the most intense U.V. and A.S. excited green emission was observed in the crystals which had been grown under an excess pressure of sulphur. The intensities of the U.V. excited green emission of both the (Cu,S) crystals were approximately equal to those of the corresponding undoped crystals. In contrast, the intensities of the U.V. excited green emission of both of the (Cu,Cd) were less than those of the undoped crystals. The A.S. to U.V. intensity ratio was increased by copper doping. The largest ratios were obtained in the crystals with the lower doping concentrations, which were of poorer crystalline quality which reduced the efficiency of the potentially competitive exciton recombination processes.

6.6. Sodium doped crystals

It was found that the silica growth tubes were very easily attacked by sodium during the course of a growth run. To minimise the attack and possibility of oxidation, growth was carried out very rapidly and consequently the resultant "boules" were small. Three sodium doped crystals were studied which had been obtained using the normal growth technique, while a fourth was post-treated in sodium vapour. The characteristics of the emission described below and recorded in table 6.1. are typical of those observed in all four crystals. The particular crystal described was grown under an excess sulphur pressure of approximately one atmosphere.

The blue edge emission excited by U.V. radiation was weak and



broad. No blue emission was detected under A.S. excitation. Figure 6.6. shows the spectral emission distribution of the U.V. and A.S. excited green edge emission of the sodium doped crystal. The most unusual feature of the edge emission of sodium doped crystals of cadmium sulphide was the broad nature of the A.S. excited emission. Similar broad spectra were observed in other crystals when it was necessary to increase the bandwidth of the instrument to obtain a reasonable recording. However the emission intensity of the sodium doped crystals was sufficient to allow a relatively narrow bandwidth to be employed. The shape of the spectrum is not unlike the form of the green edge emission of CdS at liquid nitrogen temperatures. Thus the sodium doped crystals appear to interact with acoustic phonons more strongly under A.S. excitation than under U.V. excitation; since the U.V. excited spectra were not in any way so unusual.

The intensity of the green edge emission excited by U.V. radiation for the sodium doped crystals was greater than that of the corresponding undoped crystals. The intensity of the A.S. excited emission of the doped crystal was approximately equal to that of the undoped crystal. Thus the A.S. to U.V. emission intensity ratio was not increased by doping with sodium. This fact and the unusual shape of the A.S. excited spectra support the hypothesis that the sodium ion, substituting on a cadmium site, reduces the number of cadmium vacancies, but at the same time can create an acceptor. The result is that (1) the intensity of the U.V. excited green edge is only slightly modified, since new acceptors replace the old, (2) the efficiency of the A.S. excitation is reduced since the concentration of cadmium vacancies (which are believed to be

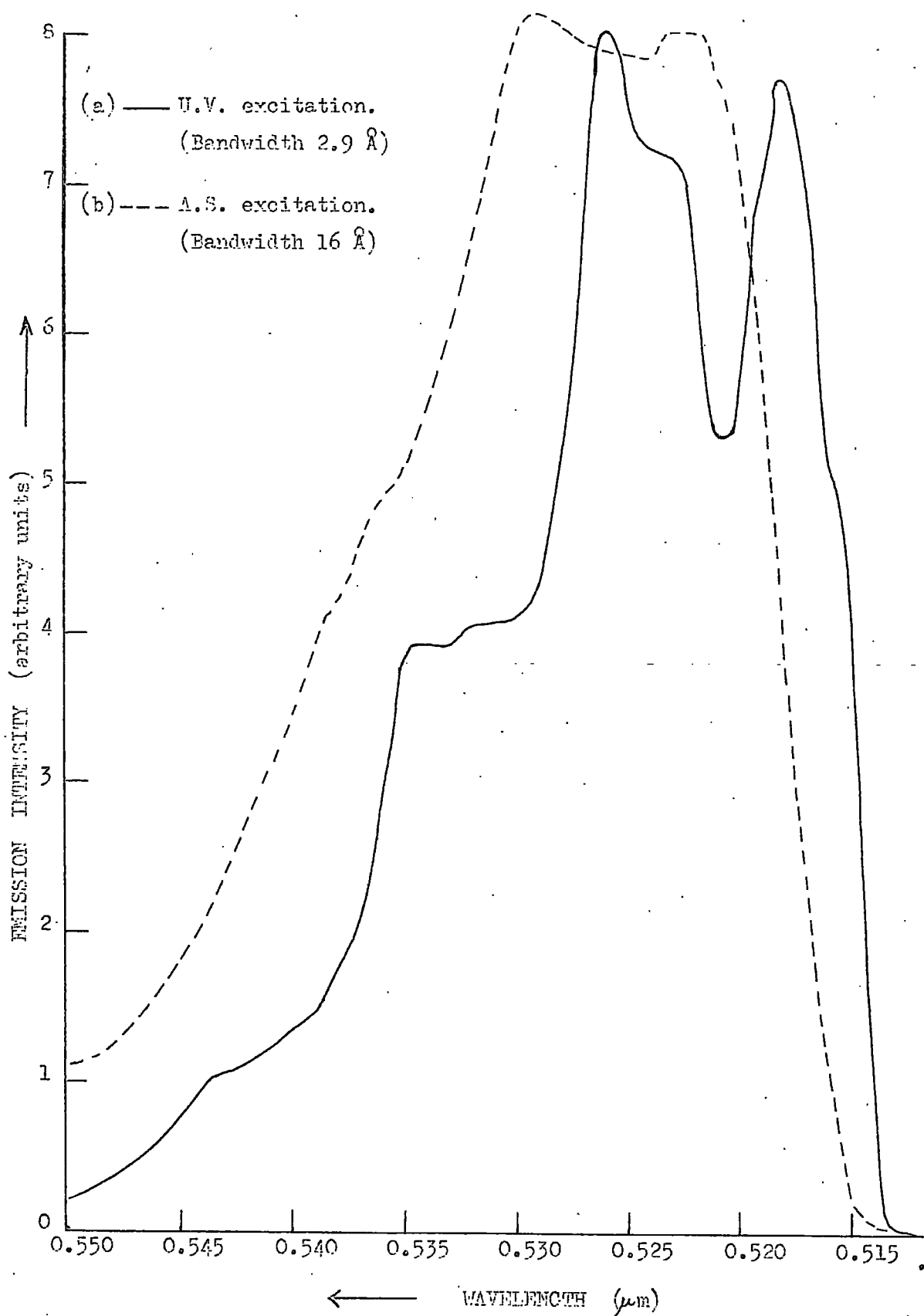


Figure 6.6. The S.E.D. of the green emission of the sodium doped crystal, no. 120, excited by (a) U.V. and (b) A.S. radiation.

associated with the excitation mechanism) is reduced.

6.7. Further properties of the crystals

This section describes some interesting results obtained by my colleagues in the Department of Applied Physics. The results appertain to doped and undoped crystals. Table 6.2. shows the pertinent results of the mass spectrometer analysis of four doped crystals, work performed outside the University. The level of the particular element of the deliberate dopant was significantly greater than the level found for that element in other doped (and undoped) crystals, for example see the antimony doped crystal. The results regarding other "difficult" elements must be viewed with caution, for example the level of chlorine in the four crystals. The silicon content was also alarming in certain crystals, however in the case of the antimony doped sample, the result was probably due to the fact that the crystal was small and the sample for analysis came from close to the wall of the growth tube.

The resistivity of crystals grown from material which contained aluminium, chlorine and antimony as deliberate dopants was less than or of the order of 10^3 ohm.cm.. Copper doping resulted in photoconductive crystals. Sodium doped crystals were less photosensitive and had a high dark resistivity compared with the copper doped crystals. Infra-red emission bands having maxima at 2.04 and 2.35 microns were observed from sodium doped crystals, which also showed unusual thermally stimulated current curves suggesting a continuum of traps from 0.2 to 0.8 eV below the conduction band.

The comparison of the intensity of the exciton emission with the magnitude of the Hall and drift mobilities of three, nominally

Table 6.2. The results of a mass spectrometer analysis of four doped CdS crystals, concentrations in p.p.m.. Not all the elements listed in the original table have been included.

Element detected	Deliberate dopant and crystal number			
	COPPER(182)	ANTIMONY(134)	SODIUM(121)	CHLORINE(154)
Na	0.4	0.4	1.8	0.1
Al	0.2	< 0.2	0.3	< 0.2
Si	4	600	< 3	< 2
P	0.06	0.6	0.12	0.02
Cl	0.6	3	1.5	1
K	0.1	0.4	< 0.03	< 0.02
Cu	0.8	0.2	0.03	0.02
Zn	< 4	< 4	9	< 4
Ga	< 0.04	0.6	< 0.1	1
In	< 0.2	2	0.09	< 0.06
Sb	< 0.04	1.2	< 0.06	< 0.04

undoped, A.E.I. crystals suggested a correlation between these quantities. The mobility decreased as the intensity of the exciton emission, relative to the standard settings of the spectrophotometer, decreased. Similarly a low drift mobility was observed in a copper doped crystal (no.155) having a relatively low intensity exciton emission. The possible correlation, which needs further experimental verification, may indicate that a decrease in the crystal quality was responsible for the decrease in these measured values.

6.8. Summary and Conclusion

The comparison of the relative intensities of the components of the edge emission of the doped crystals with those of undoped crystals, table 6.1., and the mass spectrometer analysis, table 6.2., indicates that the deliberate addition of a dopant to the starting charge of the boule growth system resulted in the incorporation of the dopant in the resultant crystal. The resistivity of the doped crystals supports this conclusion.

The exciton excited by U.V. radiation was resolved in three doped crystals only, two with copper and one with aluminium as the dopant elements. The blue spectrum of these crystals was dominated by the I_2 and I_2^* emissions. The donors, associated with I_2 and I_2^* , probably originated from the autocompensation of the copper impurities and from the substitution of aluminium ions on cadmium lattice sites. There were no observable differences in the positions or shapes of the U.V. excited exciton emission of the doped crystals compared with that of the undoped crystals. The exciton emission of other doped crystals excited by U.V. radiation consisted of a broad unresolved band. The absence of resolvable exciton emission was regarded as indicating poor crystal quality. Exciton emission, assigned

tentatively to the I_2^* process, was observed in both the copper doped crystals under A.S. excitation.

The intensity of the green edge emission of doped crystals excited by U.V. radiation was on the whole less than that of undoped crystals, with the following exceptions.

(1) The chlorine doped crystal grown under an excess pressure of sulphur vapour, which probably favoured the formation of the cadmium vacancy-chlorine donor complex. It will be proposed in chapter eight that this donor-acceptor associate, which occurs as a singly ionisable acceptor, is the acceptor associated with the I_1 exciton and the green edge emission. If this proposition is correct, an increase in the intensity of the green edge emission of this doped crystal would be expected.

(2) The aluminium doped crystal grown under a pressure of cadmium which was less than the pressure of cadmium above the CdS in the growth chamber. These growth conditions probably favoured the formation of cadmium vacancy-aluminium donor complexes, which would act as singly ionisable acceptors and may also be associated with the green emission as suggested above.

(3) The sodium doped crystals were also efficient emitters of green edge emission. A sodium ion substituting on a cadmium site acts as a singly ionisable acceptor which may be associated with the increase in the efficiency of the green edge emission. The L.E.S. was always present in the green emission which indicates that some donors may have been introduced into the crystal by the autocompensation mechanism. The suggestion that sodium impurities give rise to a new acceptor which is involved in the green emission may explain the unusual nature of the green emission excited by A.S. radiation

in the sodium doped crystals. Stronger acoustic phonon cooperation associated with the sodium acceptor is also a possible explanation.

There were no observed differences in the shapes or positions of the U.V. and A.S. excited green emission of the doped crystals compared with the emission of the undoped crystals with the exception of the sodium doped crystal, just mentioned, and the antimony doped crystal. The unusual feature of the antimony doped crystal was that the components of the green emission spectrum excited by A.S. radiation were broader than those excited by U.V. radiation. An explanation of this effect could have been that the separation of the donor and acceptors involved in the recombination was smaller in the case of the A.S. excited emission than in the U.V. excited emission, were it not for the fact that the maxima of the A.S. excited series were to the long wavelength side of the maxima of the U.V. excited series which indicates that the separation is larger. Bearing in mind the unusual nature of the core of the proposed antimony donor, it is possible that the A.S. excitation modifies the coulombic nature of the donor compared with its state under U.V. excitation, thus the shape of the emission components is slightly altered. Additional acoustic phonon cooperation seems an unlikely explanation since it would probably have broadened the U.V. excited emission also.

The deliberate introduction of chlorine, copper and antimony impurities resulted in an increase in the ratio of the intensities of the U.V. to A.S. excited emission compared with the ratio observed in undoped crystals. The ratio was also increased in the case of the aluminium doped crystal grown under an excess pressure of sulphur. Comparing the A.S. to U.V. intensity ratio of doped

crystals grown under excess pressures of sulphur vapour with those grown under cadmium pressures, it was concluded that (a) excess sulphur pressure permitted aluminium ions to substitute for cadmium to form donors, (b) excess cadmium pressure permitted chlorine ions to substitute for sulphur to form donors, (c) excess sulphur pressure permitted copper ions to substitute for cadmium to form acceptors. The fact that the intensity of the A.S. excited emission was greater than the intensity of the U.V. excited emission in two copper doped and in a chlorine doped sample may indicate that the centre responsible for the A.S. excitation mechanism is also associated with the recombination process. The nature of the centre is changed by the incident radiation in such a way that the recombination process becomes apparently more efficient under A.S. excitation.

Visible green emission was excited by infra-red radiation incident upon the antimony doped crystal at liquid helium temperatures. This effect and other infra-red effects observed in doped crystals are described in the next chapter.

CHAPTER 7

ANTI-STOKES EXCITATION SPECTROSCOPY

7.1. Introduction.

The intensity of the edge emission varied according to whether the tungsten lamp excitation radiation was passed through the OR1, OR2 or 7700Å interference filter. It was also observed that certain crystals emitted green radiation when excited by infra-red radiation. In order to establish the energy of the photons responsible for the A.S. excitation of green edge emission, the measurements described in this chapter were made.

The effects of infra-red radiation upon the intensity of the green edge emission, measured using the Optica spectrophotometer, are described first. This is followed by a description of the experimental apparatus used to observe the excitation spectra, and the results obtained from the measurements.

7.2. Single and double beam effects.

The edge emission excited by A.S. radiation, provided by a tungsten lamp filtered by an OR2 filter, has been described in the two preceding chapters. The same emission was observed using an OR1 filter, however the emission intensity was reduced by approximately 10% using this excitation. The emission intensity was reduced by a factor of the order of one hundred when the 7700Å interference filter replaced the OR2 filter. This meant that the luminescence was below the limit of detection in some crystals. The chlorine doped crystal grown under an excess pressure of cadmium, when irradiated by infra-red only; using either the silicon, 0.953 or 1.205 micron interference filters, emitted visible green luminescence. The most intense emission was obtained when the

0.953 micron filter was used. A Bellingham and Stanley monochromator was used as the source of excitation for the emission spectrum in an attempt to establish the excitation spectrum. The results were inconclusive because the intensity of the emission was too low to produce a measurable spectrum on the Optica. However the monochromator could be used as a source of primary excitation in the double beam experiments.

In the case of the chlorine doped sample grown under excess cadmium pressure and a copper doped sample grown under excess sulphur pressure, the green edge emission produced by a primary excitation of 6700\AA from the monochromator was enhanced by some 50% when auxiliary infra-red was focussed onto the crystal. The 0.953 micron filter produced the largest effect on the chlorine doped sample, and the silicon filter was most effective on the copper doped crystal. The green emission of the chlorine doped sample grown under excess sulphur pressure also showed infra-red enhancement effects. The 7700\AA filter produced luminescence which was increased slowly by 10% when 0.953 micron radiation was added.

The A.S. emission produced by the 7700\AA excitation of two sodium doped crystals grown with a low reservoir temperature, was increased by some 125% by the addition of any of the three auxiliary infra-red filters. The only other crystal which showed this 7700\AA plus infra-red enhancement was "undoped", but grown, under similar growth conditions, from a starting material in which the preparative conditions employed by the manufacturers may have produced sodium and phosphorus contamination. The 30% enhancement observed, confirmed the suspicion that the starting material was contaminated in this case. The enhancement is shown in the two superimposed

spectra in figure 7.1. However in the majority of cases, where the 7700Å excited emission was detectable, the signal was reduced by some 50% by the addition of infra-red radiation.

The emission intensity produced by OR1 and OR2 excitation was never increased by the addition of auxiliary infra-red radiation. It was generally unaffected, but decreased slowly by about some 10% in some samples, however this may have been a heating effect. The removal of infra-red from the exciting radiation of OR1 and OR2, by the introduction of one Chance glass heat absorbing (HAL) filter, increased the intensity of the emission. Addition of further HAL's tended to reduce the intensity of the emission since the absorption of red by the HAL then became more significant than the effect of removing further infra-red radiation. It was concluded that the effect was largely associated with the infra-red causing the temperature of the crystal to increase. This was confirmed by the decrease in the intensity of the emission, excited by say the OR2 filtered lamp, to a steady level after initial illumination. The emission quenching effect of additional infra-red from the auxiliary source was approximately doubled when HAL's were used in conjunction with OR1 or OR2.

Resistance measurements were made on several crystals. Red excitation, provided by OR1 and OR2 filtered sources, reduced the dark resistivity to approximately the same level as that observed under U.V. excitation. Removal of the infra-red from these sources, by HAL filters, increased the resistivity. Simultaneous irradiation of the OR+ HAL excited crystal with auxiliary infra-red reduced the resistivity again, however only slightly.

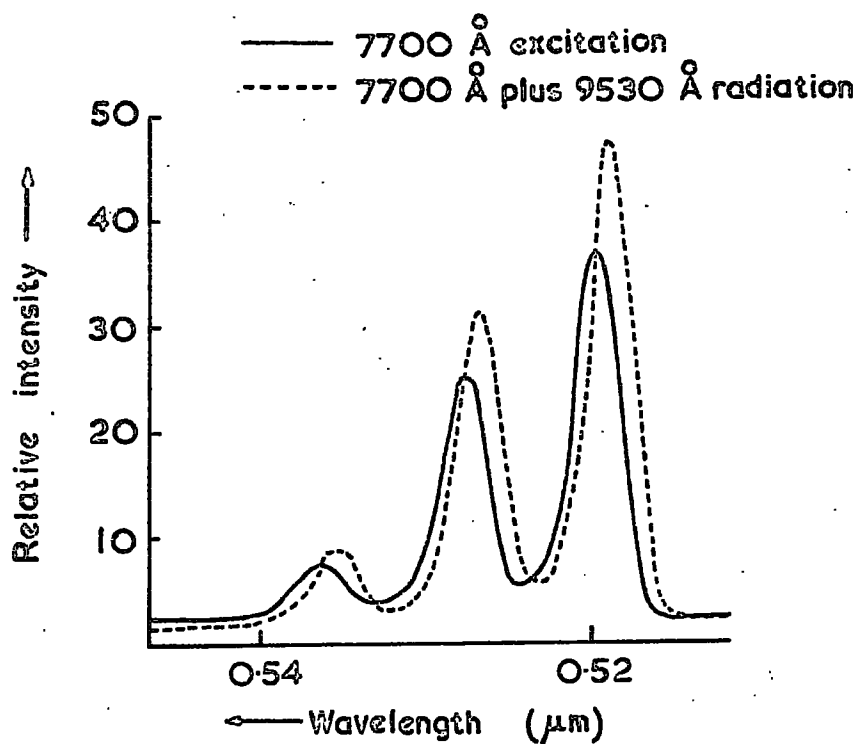


Figure 7-i. The spectral distribution of the green edge emission of a CdS crystal at liquid helium temperatures excited by 7700 Å and 7700 Å plus 9530 Å radiation, illustrating the infra red enhancement of the emission intensity.

7.3.1. The measurement of A.S. excitation spectra

The Optica spectrophotometer is essentially a two component instrument consisting of a grating monochromator and a double beam detection system. The monochromator of the Optica was used as the input of the excitation measurement system. The 75 watt tungsten lamp incorporated in the Optica monochromator was replaced by a 500 watt, 240 volt, tungsten projector lamp, underrun at about 220 volts (400 watts), focussed onto the input aperture of the monochromator. The arrangement of the experimental apparatus is demonstrated diagrammatically in figure 7.2.

The output of the monochromator was focussed, using a 10cm. focal length bi-convex lens, down a telescopic tube (A), through the cryostat window (number one) onto the crystal. The same metal helium cryostat was used, as in the emission measurements. The radiation passing through window number two was focussed, using the telescope-lens system B, through a 12" diameter, 8 blade chopper (C) and a three inch cell containing a saturated solution of copper sulphate (E) onto the photomultiplier (P.M.). The copper sulphate cell absorbed the reflected exciting radiation, except for a small breakthrough band at 1.05 microns, and transmitted in the green and blue regions of the spectrum, see figure 3.3. Thus the cell acted as a broad band filter transmitting the edge emission of CdS. Dry batteries, in a screened box, were used as the power supply for the EMI type 6094 B photomultiplier. The series resistor R_1 (10^6 ohms) made the arrangement less lethal. The photomultiplier current was passed through the resistor R_2 (10^4 ohms), and the voltage developed fed through the 0.47 microfarad capacitor into the phase sensitive detector (P.S.D.).

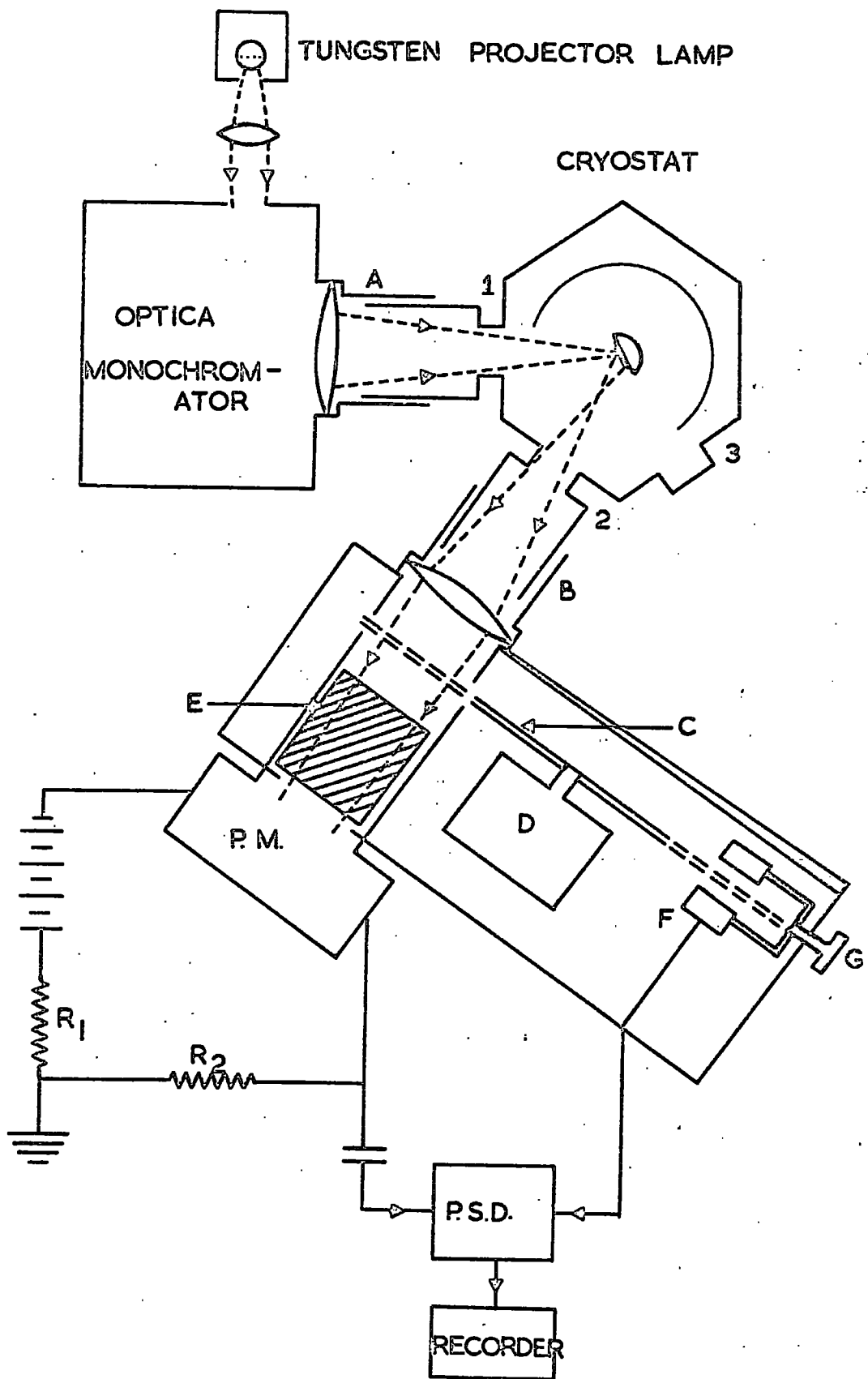


Figure 7-2. Scheme for excitation spectroscopy.

A and B : telescope tubes, incorporating 10cm focal length lenses

C : 12" diameter, 8 blade chopper

D : Synchronous motor and gearbox drive

E : 3" long cell containing a saturated solution of copper sulphate

F : Source and Detector supplying reference signal to P.S.D.

G : Screw adjustment of phase

P.M. : Photomultiplier

P.S.D. : Phase sensitive detector

1, 2 and 3 : Windows of cryostat

The reference signal for the P.S.D. was provided by means of a small lamp and a photoconductive detector (F) which were placed on opposite sides of the chopper blade. The source and detector were mounted on an adjustable platform, such that the phase of the reference and signal inputs could be varied by means of the screw G. The synchronous motor was geared down so that the drive (D) rotated the chopper at 66 revolutions per second. The P.S.D. consisted of a Brookdeal (model MS 320) meter unit/phase shifter used in conjunction with a Brookdeal (model FL355) lock-in amplifier. The time constant of the system was set at zero. The output of the P.S.D. was displayed on a Honeywell Electronik class 19 recorder, 10mV full scale deflection.

The crystals were cooled down to liquid helium temperatures in the dark. The wavelength of the exciting radiation was set at 1 micron, and the crystal illuminated. The crystal was illuminated with this radiation for the time required for the recorder chart to travel one inch, i.e. 20 seconds, and then the wavelength was adjusted manually, to 0.99 microns. This process was repeated down to 0.60 microns in 0.01 micron steps every 20 seconds, to complete a run. The mean of the recorded trace, ignoring the first and last tenths of the trace, was taken as the signal corresponding to a particular wavelength setting in any run.

It was necessary to correct the results obtained for the spectral response of the exciting radiation. It was assumed that the output of the detection system was uniform with respect to incident intensity. To determine the response of the excitation system, a linear vacuum thermopile replaced the cryostat at the end of the telescope tube A. The output of the thermopile was fed into a

Hilger and Watts FA1 photo-electric relay, which produced a signal that could be displayed on a galvanometer. In order to correct for the intensity dependence of the green edge emission excited by A.S. radiation the galvanometer deflection was raised to the power n , where n is the intensity dependence index. No measurement of the spectral dependence of n was possible because of the lack of sensitivity of the apparatus. However it had been reported that there was no intensity dependence to be observed on similar crystals (1). Multiplying the corrected intensity by a factor $(\text{wavelength})^3 \div (1.24)^2$ converted the intensity of emission into "number of photons emitted per unit energy interval". The error bars employed in the graphs displaying the results arise from the errors involved in correcting for the intensity of the exciting radiation. The scatter of the points was taken as an indication of the errors of measurement.

7.3.2. The A.S. excitation spectra obtained

Figure 7.3 shows the A.S. excitation spectra obtained for the 36 p.p.m. copper doped crystal grown under an excess pressure of sulphur (crystal no. 155). The curves (a) and (b) were obtained with the crystal maintained at liquid helium and liquid nitrogen temperatures respectively. The spectra are those obtained without the crystal having previously been illuminated. The "lift-off" points occurred at approximately the same photon energy at both temperatures, i.e. 1.65 eV.

The spectra presented in figures 7.4, 7.5. and 7.6. were obtained with the crystals maintained at liquid helium temperatures.

The spectra denoted (a) were those obtained without the crystal having previously been illuminated. The spectra denoted (b) were those obtained after the crystal had been irradiated with shorter

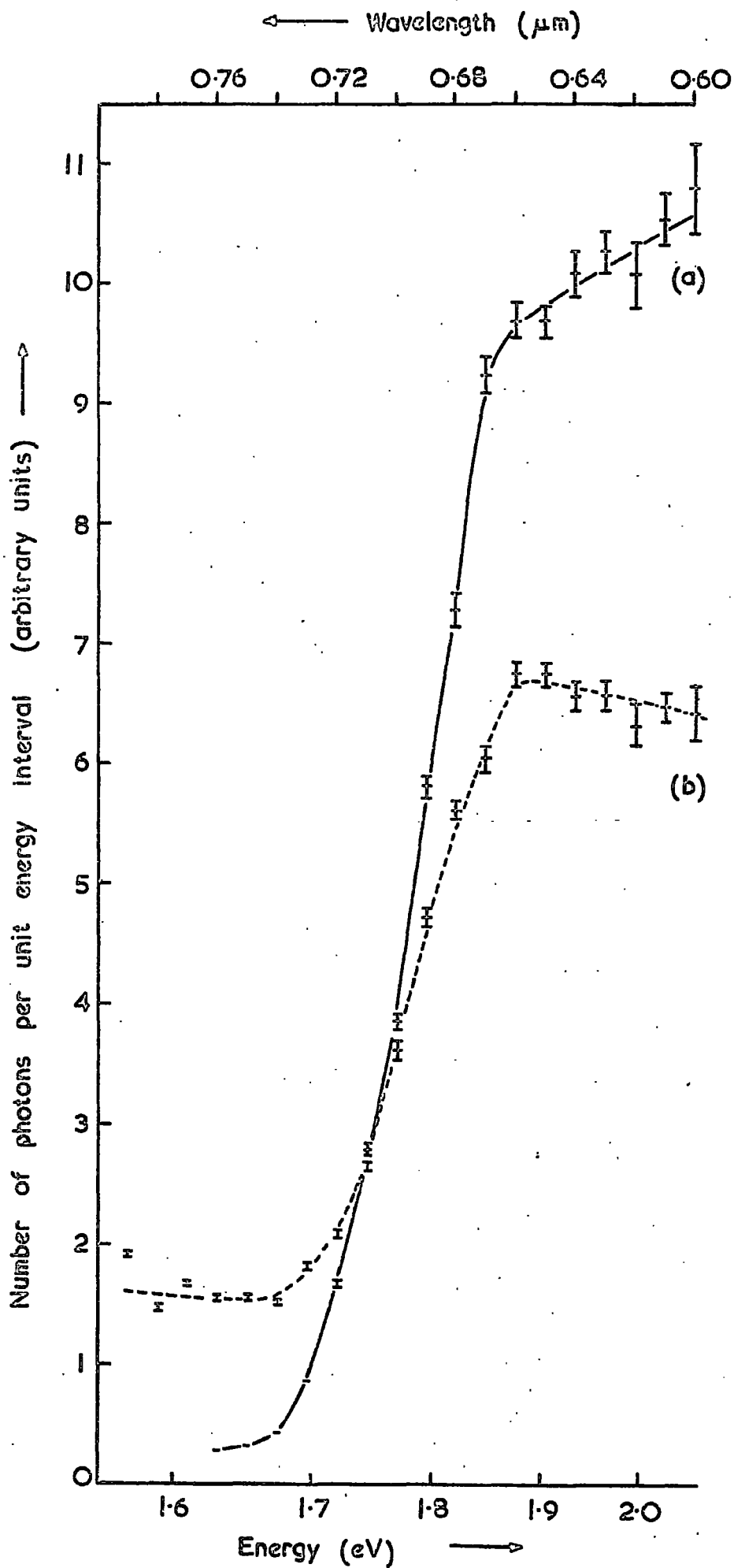


Figure 7-3. A. S. excitation spectra of crystal no. 155 at a) liquid helium and b) liquid nitrogen temperatures.

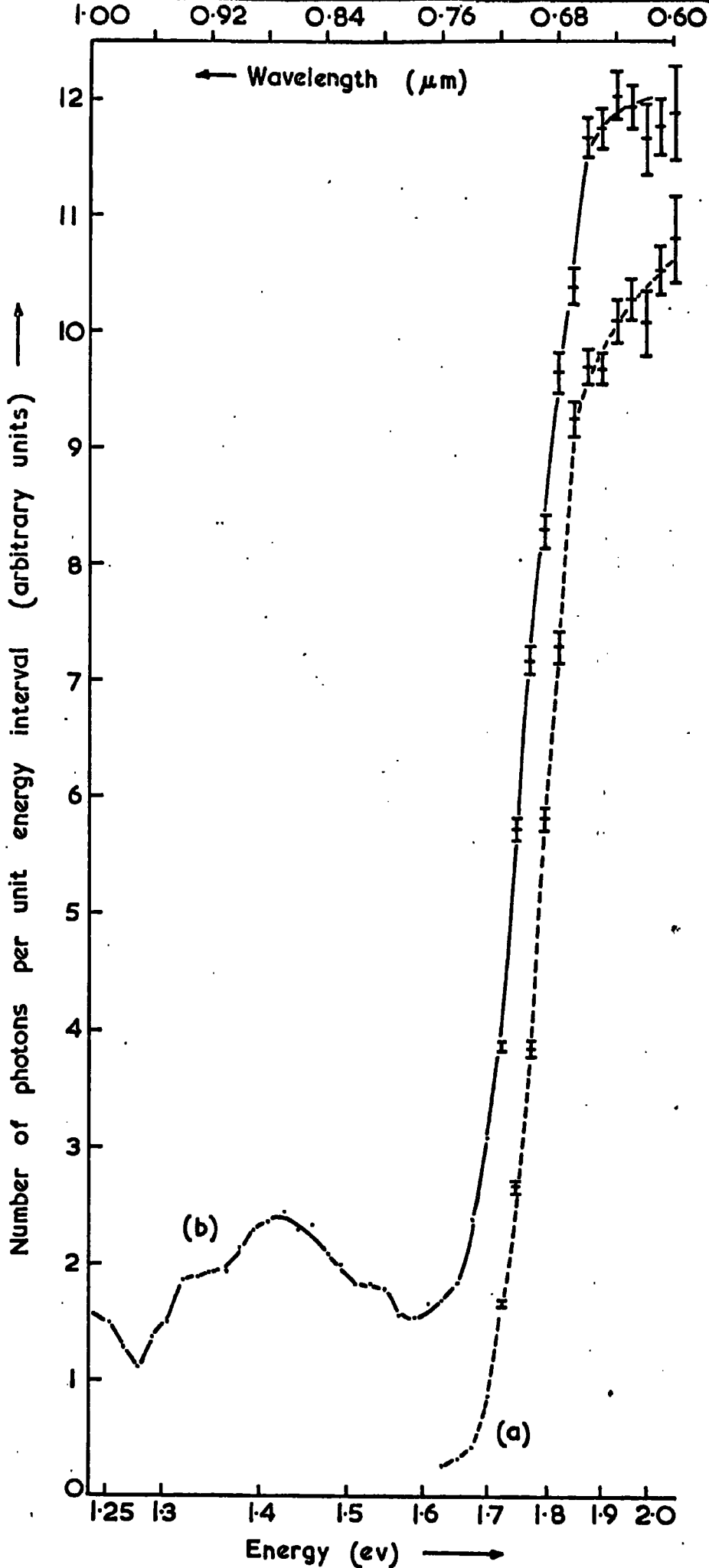


Figure 7.4. A.S. excitation spectra of crystal no. 155 at liquid helium temperatures a) initial run b) previously irradiated.

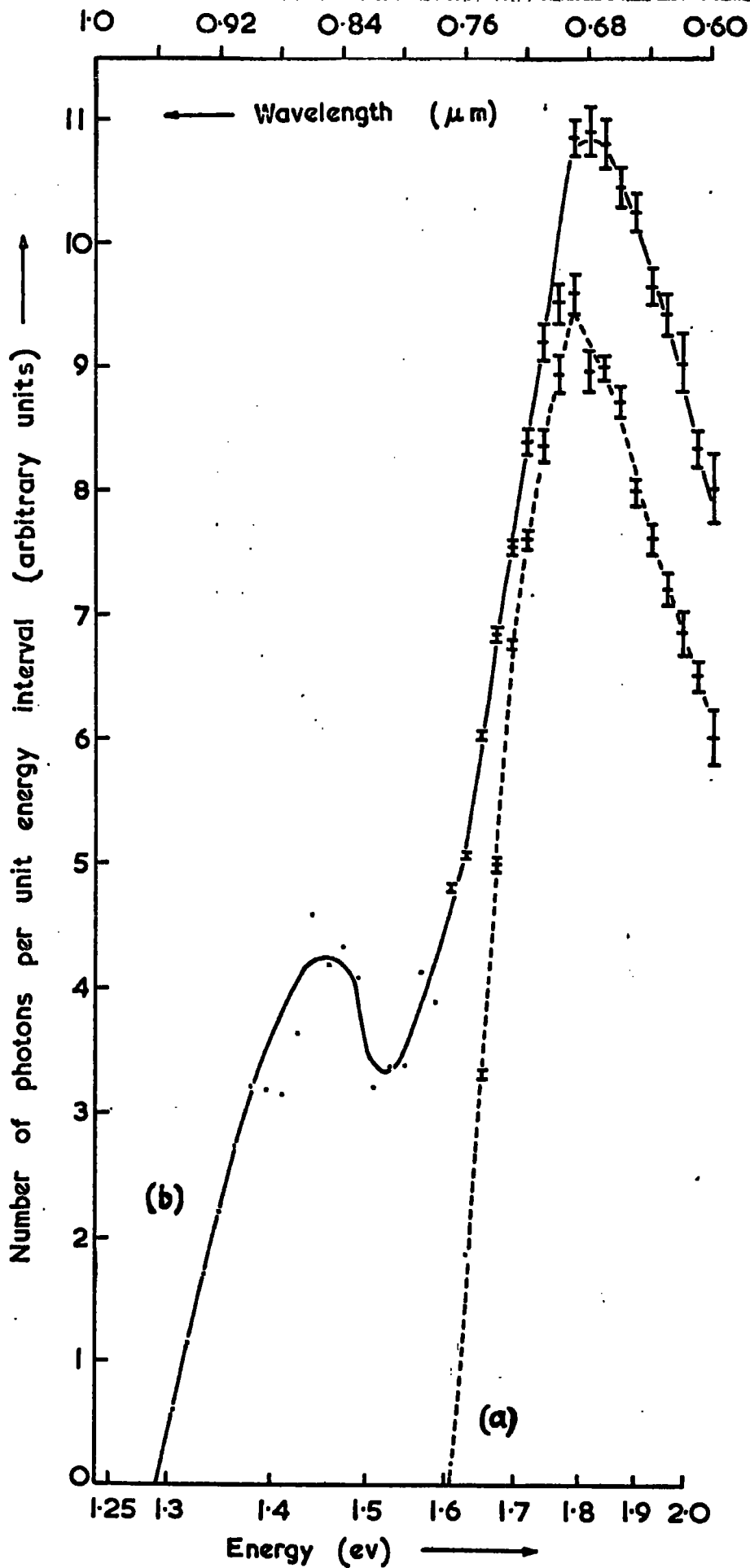


Figure 7.5. A.S. excitation spectra of crystal 135 at liquid helium temperatures a) initial run b) previously irradiated.

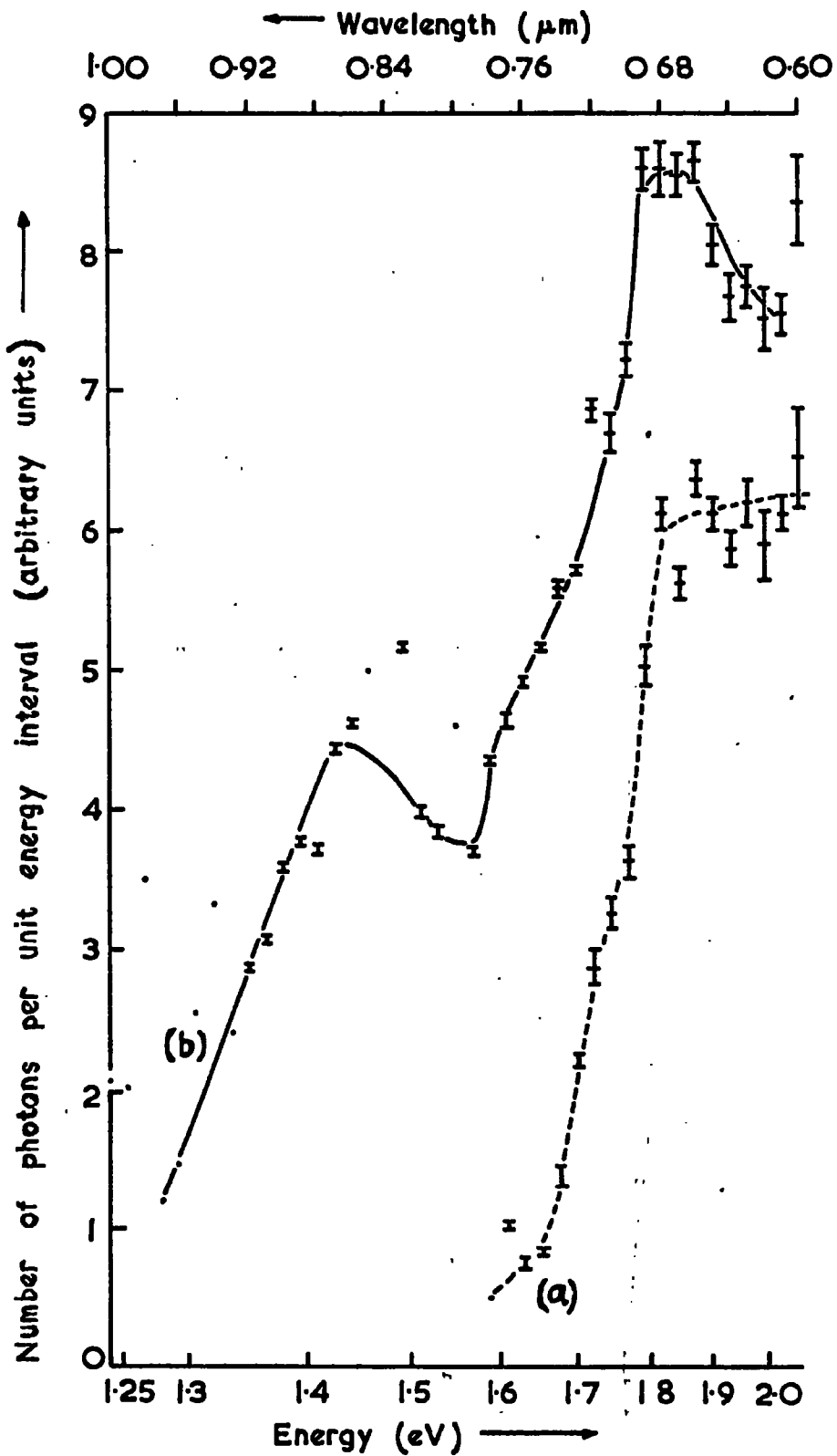


Figure 7.6. A.S. excitation spectra of crystal 153 at liquid helium temperatures. a) initial run b) previously illuminated.

wavelength excitation. Figure 7.4. shows the spectra for crystal 155, copper doped, as in figure 7.3. Figure 7.5. shows the spectra for crystal 135, the antimony doped crystal, and figure 7.6. for crystal 153, the chlorine doped crystal grown under an excess pressure of sulphur. Thresholds within the range 1.63 ± 0.05 eV were observed in all the spectra obtained without the crystals having previously been illuminated. A second threshold at 1.29 ± 0.03 eV was observed in the curves obtained after the first run.

The "b" curves rose from the second threshold to a maximum at approximately 1.4 eV, then went through a minimum before following the shape of the "a" curves at higher photon energies. The curves of figure 7.6. indicate that there may be some structure in the high energy peak. However, more sensitive apparatus, and more sophisticated measurement and correction techniques are required to confirm this suggestion.

Because of the breakthrough of the copper sulphate filter at about 1.05 microns, see figure 3.3, a narrow band 5200\AA interference filter was added to the detection system in an attempt to determine a double beam excitation spectrum. A standing level was obtained using a tungsten lamp filtered by two OR1 plus two HAL filters, and the monochromator scanned to the long wavelength side of one micron. Unfortunately, no additional signal was observed.

7.4. Discussion

The second threshold at 1.29 ± 0.05 eV was not observed in the excitation spectra unless the crystal had been previously illuminated. This indicates that higher energy photons are necessary to create the required state for the excitation process involving the 1.29 eV photons. It may be that the carriers which were placed in excited

energy levels by the ~~1.6 eV~~^{>1.6 eV} photons are liberated, by the 1.29 eV photons, to levels which permit radiative recombination. It is probably no more than remarkable that the energy 1.29 eV is approximately half the accepted band gap energy of CdS at liquid helium temperatures. Two photon excitation involving an intermediate phonon state requires the very much greater incident flux densities of pulsed lasers (2).

The principal excitation threshold for the A.S. excitation of band edge emission was observed to be 1.63 ± 0.05 eV in three crystals grown with three different dopants. An attempt to determine the threshold for an undoped sample was unsuccessful because of the lack of sensitivity. However, since the threshold remained remarkably unchanged despite the variety of the dopants, it was concluded that the threshold indicated that the level involved in the excitation was probably closely associated with native defects.

Thresholds of 1.52 ± 0.02 eV for single beam excitation and 1.19 ± 0.02 eV for double beam excitation have been reported (1). These measurements were made at S.R.D.E., Christchurch. The correspondence between the 1.63 and 1.29 eV thresholds reported here indicate perhaps

- (a) that the 1.29 eV threshold corresponds to the double beam threshold and hence requires previous higher energy excitation, and
- (b) that the discrepancy may arise from the zero employed in determining the lift off.

CHAPTER 7

REFERENCES

1. M. R. Brown, A. F. J. Cox, D. S. Orr, J. M. Williams and J. Woods
(to be published).
2. B. M. Ashkinadze and I. D. Yaroshetskii (1968) Sov. Phys.
Semiconductors, 1, 1413.

CHAPTER 8

CONCLUSION AND DISCUSSION

8.1. Introduction

It has been suggested in preceding chapters that the appearance of I_2 exciton emission in the U.V. excited emission spectra of crystals grown under excess partial pressures of sulphur vapour indicates that there is a strong tendency for an automatic or self-compensatory mechanism to operate in CdS. In this chapter the model of the acceptor associated with the I_1 exciton and the measured energy values for the "new halogen band" at 4900\AA proposed and reported by Thomas, Dingle and Cuthbert (1) have been developed to obtain an estimate of the binding energies of the acceptor levels involved. A donor-acceptor associate (D.A.A.) model has also been used to explain donor levels which include native defects. Then, the D.A.A. model coupled with the concepts of auto-compensation have been employed to explain the observed trends of the components of the edge emission with growth conditions. The model has also been used to explain the mechanisms of the anti-Stokes excitation and emission processes.

8.2.1. The singly ionisable acceptor complex

Thomas et al. (1) suggested that the line at 4888.75\AA was due to the emission associated with the recombination of an exciton bound to a neutral acceptor, and that the acceptor was an associated pair composed of a cadmium vacancy and a chlorine ion substituted on a nearest neighbour (N.N.) sulphur site. They also observed a line at 4888.40\AA which they suggested was associated with the recombination of an exciton bound to a neutral acceptor composed of a cadmium vacancy and an aluminium ion at a neighbouring cadmium site. The

centre has a strong tendency to bind a hole. The neutral form of the complex will be denoted $[\ominus \oplus +]$.

Thomas et al. also reported a new halogen band at 4900\AA . The emission was associated with the recombination of a hole bound to a neutral acceptor, i.e. the complex centre described above, with an electron bound to a chlorine donor. Since one of the constituents, the acceptor, has a neutral ground state, little or no coulombic interaction would be involved. This was confirmed by the very small shift of the maximum of the emission with variation of the intensity of the excitation. The binding energy of the chlorine donor (E_D) was quoted as 0.024 eV.

These results are used here to find the binding energy of the hole to the neutral acceptor, E_A , using the simple equation for the energy of the 4900\AA recombination transition, E_T ,

$$E_T = E_G - (E_A + E_D) .$$

The band gap energy, E_G , is 2.5826 eV (2), thus we find $E_A = 0.0772$ eV.

E_A is the energy which binds the hole to the neutral acceptor and is denoted as $E[\ominus \oplus +]$. This state may be reasonably considered analogous to the hydrogen atom binding an electron to itself and forming an H^- ion. Comparing the ionisation energy of the neutral state with the electron attachment energy of the charged state of the hydrogen analogy and the present complex (3), we may write the equation

$$\frac{E[\ominus \oplus +] + 0.75}{E[\ominus \oplus +]} = \frac{13.6}{13.6} = 0.055$$

Thus $E[\ominus \oplus +] = 1.4036$ eV.

This value for the binding energy of the first hole to the acceptor is in close agreement with the value of 1.3 eV which Morigaki and Hoshina (4) used to explain their E.S.R. studies in CdS. They

ascribed the centre to a simple cadmium vacancy, however there was no experimental evidence to support this model as opposed to a complex centre (see chapter one). It is assumed here that the level is associated with the complex of a cadmium vacancy with a chlorine ion substituted on a sulphur N.N. site, denoted (V_{Cd}, Cl_S) and that the approximations which were used in the calculation of the binding energy of the first hole to the complex were reasonable. The next problem is to find the ionisation energy which is associated with a simple cadmium vacancy.

8.2.2. The cadmium vacancy - a double acceptor

In order to find the ionisation energy of the first hole bound to this double acceptor we consider the formation of the complex acceptor described in the previous section. Assume that the binding energy of the acceptor complex is the sum of the binding energy of the double acceptor, $E_{[\ominus \oplus]}$, the donor binding energy, $E_{[\oplus -]}$ or E_D , and the work done in bringing the chlorine donor from infinity to the N.N. position through the medium of the cadmium sulphide. This work done, W.D., is approximately equal to $(+2e) \cdot (-e) / 4\pi\epsilon\epsilon_0 r$ which equals $-2.78/r$. r is the separation of the donor and acceptor in Å, the work done is in eV and $\epsilon = 10.33$ (5). The energy required to remove the sulphur ion to allow the chlorine ion substitution is assumed to be negligible compared with the other energies because the substitution takes place during the growth of the crystal, when it is supposed that the native elements will be sufficiently mobile to move about readily; whilst foreign elements are more affected by the environment of cadmium and sulphur. Thus we obtain the equation

$$E_{[\ominus \oplus \oplus]} = E_{[\ominus \oplus]} + E_{[\oplus -]} + W.D.$$

For CdS the nearest neighbour separation is 2.52\AA , thus
 $W.D. = -1.1031\text{ eV}$, and $E_{[\ominus\ddagger]} = 1.4036 - (-1.1031 + 0.024) = 2.4827\text{ eV}$.
 This is the ionisation energy of the first hole of the doubly
 charged acceptor arising from an isolated cadmium vacancy. This
 corresponds to an acceptor level some 0.10 eV below the conduction
 band, a value in remarkable agreement with that of 0.09 eV reported
 by Lorenz and Woodbury (6) to explain some of their electrical
 measurements.

8.2.3. The singly ionisable donor complex

The donors associated with the I_2 exciton emission are
 thought to be singly ionisable (7). In this section, the same
 principles used in the previous section are applied to a sulphur
 vacancy - acceptor pair complex. The complex investigated consists of
 a sulphur vacancy with an impurity ion acting as a singly ionisable
 acceptor substituted on a N.N. cadmium site. It is assumed that

(a) 0.026 eV is a reasonable value for the binding energy of the
 second electron to the double donor, $E_{[\oplus=]}$, formed by the isolated
 sulphur vacancy as proposed by Morigaki and Hoshina (4),

(b) the binding energy of the complex, $E_{[\oplus\ominus]}$, is some 0.03 eV as
 determined from the bound exciton and green edge emission as reported
 earlier in this thesis and elsewhere,

(c) the work done in bringing the donor and the acceptor together
 is the same as in the double acceptor-chlorine donor case, i.e. -1.1 eV ,

(d) the energy required to remove the cadmium ion to allow
 substitution may be neglected, as assumed previously. Then using the
 equation

$$E_{[\oplus\ominus]} = E_{[\oplus=]} + E_{[\ominus+]} + W.D.,$$

the binding energy of the impurity ion required to form the complex is 0.87 eV. This is the magnitude of the binding energy associated with impurities, such as copper, acting as singly ionisable acceptors in CdS. See figure 8.1.

8.3. Substitution on next nearest neighbour sites

It has been shown that the substitution of a chlorine ion on a N.N. sulphur site will reduce the binding energy of the first hole to a cadmium vacancy by

$$E_{\left[\ominus \oplus \right]} - E_{\left[\ominus \oplus \oplus \right]} = 2.48 - 1.40 = 1.08 \text{ eV,}$$

and produce a singly rather than a doubly ionisable vacancy. The substitution of a copper ion on a N.N. cadmium site will reduce the binding energy of the first electron to a sulphur vacancy by

$$E_{\left[\oplus = \right]} - E_{\left[\oplus \ominus - \right]} = 0.26 - 0.03 = 0.23 \text{ eV,}$$

and produce a singly rather than a doubly ionisable donor complex, denoted (V_S, Cu_{Cd}) .

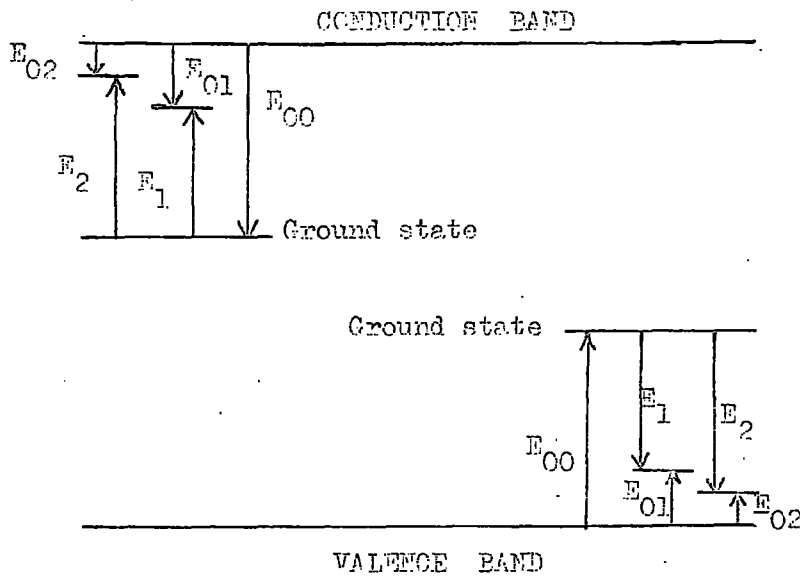
Similarly, reductions in the binding energy and changes to the singly ionisable state may be effected by substituting impurities on next nearest neighbour (N.N.N.) sites which would act as singly ionisable donors or acceptors as appropriate. For example, in the substitution of aluminium ions which associate with a cadmium vacancy (V_{Cd}, Al_{Cd}) , the separation would be 4.14\AA so that the work done in bringing the impurity to the site is only about 0.663 eV. Then the binding energy of the complex for a hole is approximately 1.85 eV, and the substitution of the aluminium ion reduces the binding energy of the first hole of a cadmium vacancy some 0.63 eV. Similarly, substitution of a group Vb impurity ion (N,P,...) on a N.N.N. sulphur site would be expected to reduce the binding energy of the first electron of a sulphur vacancy, forming a (V_S, N_S) complex.

However, unless the binding energy of the acceptor is less than or equal to 0.43 eV, the binding energy of the (V_S, N_S) complex will be greater than that of the (V_S, Cu_{Cd}) complex.

Two points arise in the comparison of the complexes formed by N.N. substitution with those formed by N.N.N. substitution. Firstly, in the case of the complexes arising from the cadmium vacancy, the calculated differences in the binding energies of the (V_{Cd}, Cl_S) and (V_{Cd}, Al_{Cd}) systems are very large compared with the change in the position of the two emission maxima associated with the recombination of excitons bound to the complexes (1). Obviously the models used to evaluate the binding energies of the complexes and the isolated cadmium vacancy are primitive and in the case of the (V_{Cd}, Al_{Cd}) complex no allowance was made for any screening of the V_{Cd} centre by sulphur ions. However, it seems more probable that there is a larger difference in the binding energies of the two complexes than might be inferred from the difference in the position of the emission of the excitons, on the assumption that the exciton is bound to the neutral acceptor in its ground state. However, if one considers the excited states of these complexes, the differences in the "binding energy" of the hole become less striking. Table 8.1. shows the energies associated with the excited states of the complexes assuming a simple hydrogenic model. The energy required to ionise the hole from the n^{th} state is denoted E_{On} , where $n = 0$ for the ground state. Even for $n = 1$, the values of E_{On} of the two complexes are more nearly equal, and the difference decreases as n increases. The E_{On} values are also nearer to the accepted values, 0.14 to 0.17 eV, for the binding energy of the acceptor thought to be associated with the green emission as well as the I_1 emission. It is suggested, from

Table 8.1. The energies of the ground and excited states of the donor-acceptor-associates of CdS. (Energies in electron.volts)

Complex State	$V_{Cd,ClS}$	$V_{Cd,AlCd}$	$V_{S,CuCd}$
Ground, E_{00}	1.40(36)	1.85	0.030
1st excited, E_1	1.05(27)	1.39	0.023
" , E_{01}	0.35(09)	0.46	0.007
2nd excited, E_2	1.15(88)	1.64	0.027
" , E_{02}	0.24(48)	0.21	0.003
3rd excited, E_3	1.31(59)	1.73	0.028
" , E_{03}	0.08(77)	0.12	0.002



from this rather crude theory, that the hole is in an excited state of the acceptor complex which is involved in these edge emission processes.

Secondly, there is a greater gain of energy in the formation of a complex composed of a N.N. associated pair (i.e. (V_{Cd}, Cl_S) and (V_S, Cu_{Cd})) than the formation of a N.N.N. associated complex (i.e. (V_{Cd}, Al_{Cd}) and (V_S, N_S)). Thus it appears that the N.N. pair would be formed in preference to the N.N.N. pair given identical concentrations of the respective impurities.

8.4. Auto-compensation and complex formation

The introduction of electrically active impurities into a semiconductor host lattice induces the formation of electrically active native defects, vacancies, interstitials et cetera, which tend at least to partially compensate the electrical activity of the impurity (8). This auto- or self-compensation may be analysed simply in terms of an energy balance equation. That is, if the energy gained by compensation, i.e. the energy of recombination of the carriers from the impurity centres with those of the native defect, exceeds the energy required to be supplied by the crystal to form the compensating defect, the defect will form and compensate the impurity centre. Thus only insulating crystals will be grown under equilibrium processes. Clearly, if the energy of defect formation is large compared with the energy gained by compensation, very little auto-compensation will take place.

In the case of cadmium sulphide, with the possibility of the formation of complex pairs of donor-acceptor associates, there are essentially two alternative auto-compensation mechanisms. For example, to compensate a donor impurity either a cadmium vacancy (a doubly ionisable acceptor) or a complex of a cadmium vacancy in association

with a singly ionisable donor (a singly ionisable acceptor complex) may be formed. It has been shown that the binding energy of the complex is some one electron volt less than that of the simple native defect, thus it is more probable that the complex would be formed in preference to the simple defect whenever possible, i.e. whenever the donors comprising the complex are available. Similarly, it is more probable that any complex involving cadmium or sulphur vacancies or interstitials would be formed in preference to the simple defect, since the energy gained by the compensation process is larger.

8.5. Explanation of results

The variation of the intensities of the components of the U.V. and A.S. excited edge emission with the conditions under which the crystals were grown may be explained in terms of native defects as described in the following sections.

8.5.1. Donor centres

The crystals studied during the course of this research were generally grown under excess partial pressures of the constituent elements, so that the compensatory processes were controlled to some extent by the excess pressures. The appearance of the emission associated with the I_2 (neutral donor) bound excitons in the U.V. excited emission spectra of crystals which had been grown under high excess partial pressures of sulphur may be explained in the following manner. Under high partial pressures of sulphur, the native defects most likely to be formed are cadmium vacancies and sulphur interstitials. As the crystal grows, donor impurities may be expected to be "dragged in" to compensate for the acceptors induced by the ambient. It is reasonable to suppose that at low excess pressures, less than about 100 torr, cadmium vacancies have a higher probability

of being formed than sulphur interstitials, whilst as the pressure increases above this range the probability of sulphur interstitial formation will increase. Interstitial migration at room temperature is rapid (9), and it is expected that the interstitials formed during the growth of the crystal will migrate to the surface, to sulphur vacancies or to defect clusters during the period between the removal of the crystal from the growth tube and the observation of the emission characteristics. As a result, there would be a number of donor impurities remaining in the crystal which had been introduced during the growth to compensate the sulphur interstitials. These donors may be the centres which are associated with the unexpected " I_2 " exciton emission of these crystals.

There appear to be several excitons bound to neutral and ionised donors in the emission spectra of CdS. The values obtained for the binding energy of the I_2 and I_5 neutral donor excitons are approximately equal to those of the donors involved in the distant pair recombination process of the green emission. Therefore it appears that the same centres are involved in both processes. Both native and impurity defects have been suggested as possible centres for the processes (1,10), and the impurity donor has already been used to explain some of the " I_2 " emission observed. Using the ideas discussed in chapters one and two and the results of this thesis, it is suggested that sulphur vacancies are involved to some extent in these donors. The results of ionic bombardment also indicate that the appearance of excitons bound to neutral donors may be attributed to the creation of sulphur vacancies (11). In order to explain the singly ionisable nature of these centres, it is necessary to postulate that there are singly ionisable acceptors

associated with these vacancies so that complexes are formed.

8.5.2. Acceptor centres

The exciton bound to a neutral acceptor, I_1 , has been assigned to the recombination of an exciton bound to a singly ionisable acceptor composed of a cadmium vacancy and a neighbouring singly ionisable donor forming a donor-acceptor complex (1). The correlation between the intensity of this exciton and the intensity of the green edge emission observed in crystals grown under controlled conditions indicates that the same acceptor is involved in both mechanisms. In order to obtain a reasonable correlation between the binding energy of the acceptor observed experimentally and that derived for the complex earlier in this chapter, it is necessary to postulate that the hole is in an excited state of the acceptor complex.

It is of interest to consider, once again, the energy of the photon that would be emitted if the I_1 exciton lost sufficient energy to raise the neutralising hole (a) from its ground state to the first excited state, (b) from its first excited state to the second and (c) from its second excited state to the third. Considering the case of the (V_{Cd}, Cl_S) complex, the values of the energy lost in exciting the hole will be (a) 1.0527, (b) 0.1061 and (c) 0.1572 eV, see table 8.1.. The energy of the I_1 exciton maximum is 2.53585 eV, thus the photon would have an energy of 1.4832, 2.4299 and 2.3787 eV for a, b and c respectively. The corresponding wavelengths are about 8350, 5100 and 5296Å, respectively. The spectral region of 8350Å was not examined in the experiments performed during the course of this research. An emission maximum at 5296Å would probably have been swamped by the green edge emission. Emission bands having maxima at about 5100Å have been observed in the emission of several

crystals, however the third longitudinal optical phonon replica of the I_2 emission also occurs at about this wavelength. Therefore it is difficult to positively identify the maximum as the I_1^* emission.

8.5.3. A.S. excitation and emission mechanisms

The cadmium vacancy-donor impurity complex may be used to explain the phenomena of the A.S. excitation and emission spectra. The binding energies of the complexes involving cadmium vacancies are very similar to the threshold energy of the A.S. excitation spectrum observed without the crystal having previously been illuminated, namely 1.63 ± 0.05 eV. The second threshold, at 1.29 ± 0.03 eV observed after the crystal had been illuminated at that temperature, may correspond to (1) the energy required to excite a hole in the complex to an excited state of the complex so that recombination may take place, or to (2) the energy required to excite an electron from the complex to a state from which it may recombine. The excitation processes described in this section are illustrated diagrammatically in figure 8.2..

In the model of the excitation process, it is desirable to be able to explain the strong tendency for the distant pair, bound-to-bound, recombination process to be so dominant in the emission spectra excited by A.S. radiation. The creation of excitons in some crystals under A.S. excitation conditions must also be explained. There are always a large number of donors in CdS, with ionisation energies of some 0.024 eV. The radius of these donors is given by $1.39/2E_D = 30\text{\AA}$. With such a large "sphere of influence", the donors which are associated with the acceptor complex and those electrically independent of the complex will very probably capture the electron before it has the opportunity of recombining with a bound hole to

Centre A : $[\oplus -]$, e.g. (Cl_S) , or $[\oplus \ominus -]$.

Centre B : probably $[\oplus \ominus -]$ e.g. (V_S, Cu_{Cd}) .

Centre C : $[\ominus \oplus +]$, e.g. (V_{Cd}, Cl_S) .

Centre C' : excited state of centre C.

Centre D : (Cu_{Cd}) .

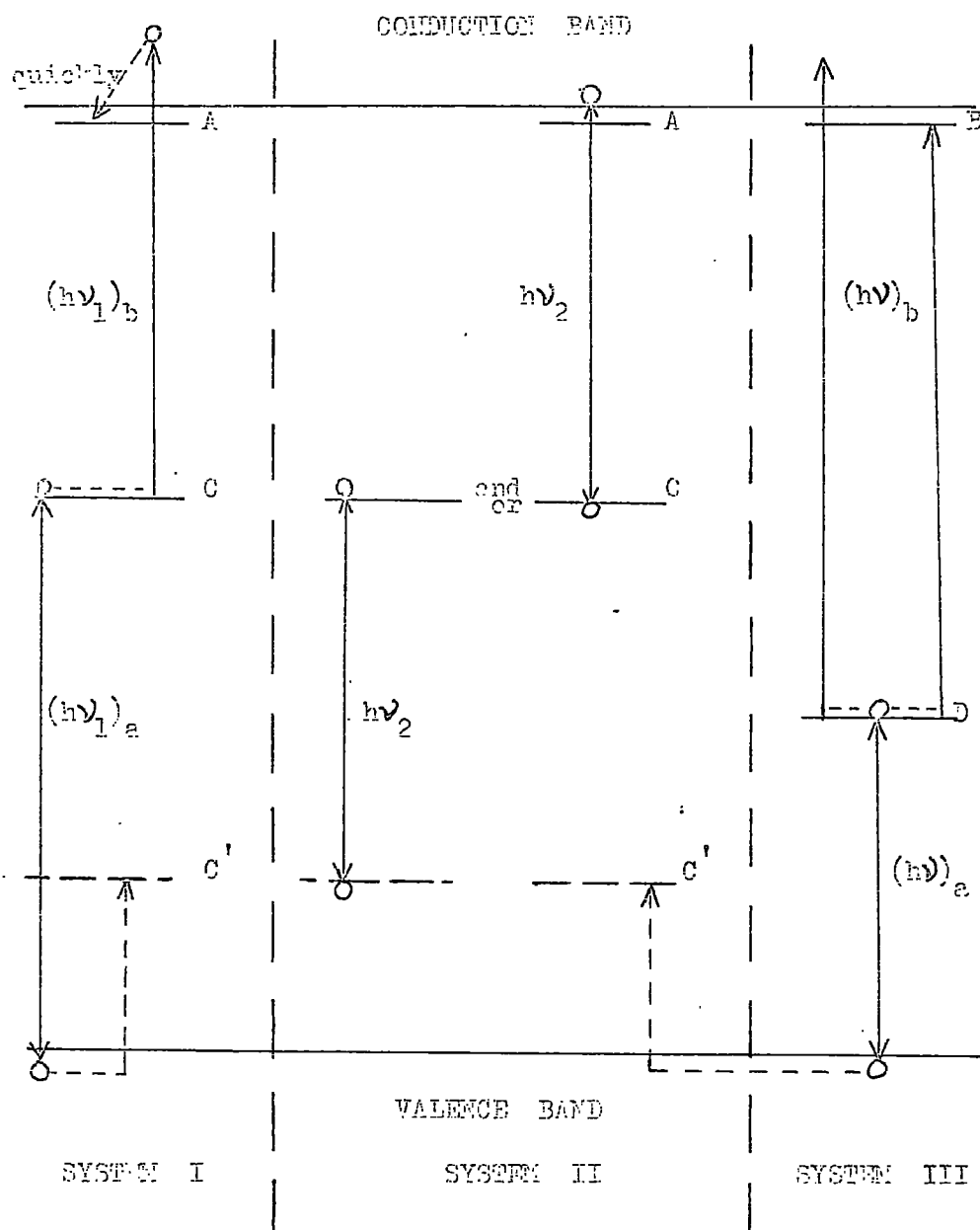


Figure 6.2. The centres involved in the anti-Stokes excitation mechanisms of CdS proposed in this thesis.

System I, corresponding to the first excitation threshold observed, $h\nu_1 = 1.63$ eV. System II, corresponding to the second, post-irradiation threshold, $h\nu_2 = 1.29$ eV. System III, excitation via a centre involving a copper impurity ion.

produce the free-to-bound, high energy series. It is therefore tentatively suggested that the donors associated with the complex through which the electron is excited may capture the photoexcited electron before it has sufficient time to recombine.

The observation of excitons in the emission spectra excited by A.S. radiation indicates that free carriers must be created. The U.V. excited emission of this type of crystal showed very intense I_2 and I_2^* exciton emission, with very weak green emission. It is suggested that the blue emission excited by A.S. radiation is due to I_2^* and or L.O. phonon assisted I_2 annihilation. (Further experiments are required to positively identify this emission. A.F.J. Cox, in a private communication, has suggested that such emission is largely due to the phonon assisted annihilation of free excitons, which he has observed at higher temperatures, however he does not ignore the possibility of excitons bound to neutral donors being involved in the low temperature emissions). No doubt the appearance of excitons in the A.S. excited emission spectrum of these crystals is due to the fact that the potentially competitive green edge recombination processes were relatively inefficient, as evidenced by the U.V. excited emission. If there were fewer donors than acceptors in a crystal, one might expect to see an A.S. excited high energy series emission as the hole bound to the acceptor recombines with a free electron.

From the observation of the distant pair, L.E.S., emission process exclusively under A.S. excitation, it was concluded that the centre involved in the excitation process is closely associated with the donors involved in the recombination process. It is suggested that this centre consists of a cadmium vacancy with a

singly ionisable donor in a neighbouring substitutional position. The variations of the ratio of the intensities of the A.S. to U.V. excited emission with the growth conditions of the crystal confirm this suggestion. Crystals grown under increasingly high cadmium pressures showed a gradual reduction in the ratio of the intensities. If the probability of forming sulphur interstitials rather than cadmium vacancies is higher for excess partial pressures of sulphur above 100 torr, and if the interstitials do migrate from active to inactive positions as assumed in section 8.5.1., then the number of cadmium vacancies in crystals grown under excess sulphur pressures above about 100torr might be expected to saturate and possibly decrease. The intensity ratio of these crystals was found to decrease with increasing sulphur pressure.

The changes in the intensities and observable features of the emission following the deliberate addition of dopants to the starting charge of the growth system tend to confirm the correctness of the model proposed for the centres involved in the emission and excitation processes. For example, the addition of chlorine dramatically increased the efficiency of the A.S. excited emission process, supporting the suggestion that the (V_{Cd}, Cl_S) centre takes part in the A.S. excitation mechanism. There was also a large increase in the efficiency of the copper doped crystals. This latter may have been due to the formation of native, sulphur vacancy, donors in association with copper ions, where the impurity acceptor acted as the centre responsible for the two-step excitation process and the donor-acceptor associate was responsible for the donor involved in the recombination process.

The model described above is similar to that presented by Brown et al. (12). They suggest that some form of centre involving a cadmium vacancy, in association with other defects or alone, is responsible for the excitation mechanism of the A.S. excited emission. It is further suggested that, in the recombination processes of the green edge emission of CdS, the hole is probably bound in an excited state of the acceptor formed by a cadmium vacancy. The donor acceptor associate model presented here appears to explain the results of this work more fully.

8.6. Conclusion

The edge emission and exciton recombination spectra of a number of cadmium sulphide crystals at liquid nitrogen and liquid helium temperatures have been observed. The spectra obtained with the crystals at liquid helium temperatures contained more interesting components which were more easily resolved and thus were of primary concern. It was possible to excite visible emission using radiation with photon energies greater than the band gap, i.e. U.V. excitation, and less than the band gap, i.e. A.S. excitation.

The crystals were grown under controlled partial pressures of the constituent elements. The variation of the relative intensities of the emission components was related to the growth conditions of the crystal. This variation and the analysis of the emission characteristics indicated that the recombination mechanisms involved donors and acceptors of native origin. A theory based upon cadmium and sulphur vacancies associated with impurity ions was used to explain the results. It is further suggested that the impurity ions associated with the vacancies, lying on neighbouring substitutional sites, take part in the recombination

processes. This is supported by the effects observed in the intensity and characteristics of the emission following the introduction of impurities to the starting charge of the crystal growth system.

Further investigation of the somewhat unexpected emission of excitons excited by A.S. radiation is required in order positively to identify the recombination process. A systematic programme of observing the emission of crystals grown under various pressures of cadmium and sulphur from charges containing a variety of dopants would provide a useful determination of the precise nature of the centres involved and may lead to a useful device. Anti-Stokes excitation spectra of these crystals, obtained using more sensitive apparatus, would indicate the location of the centres within the band gap. Precise monitoring of the electrical resistance during the excitation measurements would provide information on whether free carriers are created. Double beam excitation measurements would, under these conditions, prove very useful. Zeeman effect measurements of the U.V. and A.S. excited exciton emission of doped and undoped crystals is an essential extension of this work, providing verification of the assignments of all the bound excitons and the I_2^* emission. It may also be possible to observe differences in the Zeeman splitting of an exciton line according to which dopant element is associated with the complex to which the exciton is bound. If the proposed model is correct, it ought to be possible to correlate the components of the edge emission with those of the red and infra-red emissions.

CHAPTER 8

REFERENCES

1. D. G. Thomas, R. Dingle and J. D. Cuthbert (1967) Proc. of Int. Conf. on II-VI Semiconducting Compounds, p.863.
2. J. J. Hopfield and D. G. Thomas (1961) Phys. Rev. 122, 35.
3. R. E. Halsted (1967) "Phys. and Chem. of II-VI Compounds" Chapter 8 (N. Holland).
4. K. Morigaki and T. Hoshina (1968) J. Phys. Soc. Japan, 24, 120.
5. D. Berlincourt, H. Jaffe and L. R. Shiozawa (1963) Phys. Rev. 129, 1009.
6. M. R. Lorenz and H. H. Woodbury (1963) Phys. Rev. Letters, 10, 215.
7. D. G. Thomas and J. J. Hopfield (1962) Phys. Rev. 128, 2135.
8. G. Mandel (1964) Phys. Rev. 134, A1073, see also 136, A300 and 136, A826.
9. A. B. Lidiard (1968) Sci. Prog., Oxf. 56, 103.
10. E. T. Handelman and D. G. Thomas (1965) J. Phys. Chem. Solids, 26, 1261.
11. K. F. LIDER and B. V. Novikov (1967) Optics & Spectroscopy, 23, 611.
12. M. R. Brown, A. F. J. Cox, D. S. Orr, J. M. Williams and J. Woods (to be published).

